

Online ISSN: 1920-3853

Vol. 6, No. 2, June 2012

Print ISSN : 1715-9997

Canadian Journal of pure & applied sciences

an International Journal

SENRA
Academic Publishers
Burnaby, British Columbia

EDITORIAL STAFF

Jasen Nelson
Walter Leung
Sara Ali
Hao-Feng (howie) Lai
Ben Shieh
Alvin Louie

MANAGING DIRECTOR

Mak, SENRA Academic Publishers
Burnaby, British Columbia, Canada

The Canadian Journal of Pure and Applied Sciences (CJPAS-ISSN 1715-9997) is a peer reviewed multi-disciplinary specialist journal aimed at promoting research worldwide in Agricultural Sciences, Biological Sciences, Chemical Sciences, Computer and Mathematical Sciences, Engineering, Environmental Sciences, Medicine and Physics (all subjects).

Every effort is made by the editors, board of editorial advisors and publishers to see that no inaccurate or misleading data, opinions, or statements appear in this journal, they wish to make clear that data and opinions appearing in the articles are the sole responsibility of the contributor concerned. The CJPAS accept no responsibility for the misleading data, opinion or statements.

CJPAS is Abstracted/Index in:
EBSCO, Ulrich's Periodicals Directory, Scirus, CiteSeerX, Index Copernicus, Directory of Open Access Journals, Google Scholar, CABI, Chemical Abstracts, Zoological Records, Biblioteca Central, The Intute Consortium, WorldCat. CJPAS has received Index Copemicus Journals Evaluation for 2010 = 4.98

Frequency: 3 times per year
Feb., June, Oct.

Editorial Office
E-mail: editor@cjpas.ca
: editor@cjpas.net

SENRA Academic Publishers
7845 15th Street Burnaby
British Columbia V3N 3A3 Canada
www.cjpas.net
E-mail: senra@cjpas.ca

CANADIAN JOURNAL OF PURE AND APPLIED SCIENCES

Board of Editorial Advisors

- Richard Callaghan
University of Calgary, AB, Canada
David T Cramb
University of Calgary, AB, Canada
Matthew Cooper
Grand Valley State University, AWRI, Muskegon, MI, USA
Anatoly S Borisov
Kazan State University, Tatarstan, Russia
Ron Coley
Coley Water Resource & Environment Consultants, MB, Canada
Chia-Chu Chiang
University of Arkansas at Little Rock, Arkansas, USA
Michael J Dreslik
Illinois Natural History, Champaign, IL, USA
David Feder
University of Calgary, AB, Canada
David M Gardiner
University of California, Irvine, CA, USA
Geoffrey J Hay
University of Calgary, AB, Canada
Chen Haoan
Guangdong Institute for drug control, Guangzhou, China
Hiroyoshi Ariga
Hokkaido University, Japan
Gongzhu Hu
Central Michigan University, Mount Pleasant, MI, USA
Moshe Inbar
University of Haifa at Qranim, Tivon, Israel
SA Isiorho
Indiana University - Purdue University, (IPFW), IN, USA
Bor-Luh Lin
University of Iowa, IA, USA
Jinfei Li
Guangdong Coastal Institute for Drug Control, Guangzhou, China
Collen Kelly
Victoria University of Wellington, New Zealand
Hamid M.K.AL-Naimiy
University of Sharjah, UAE
Eric L Peters
Chicago State University, Chicago, IL, USA
Roustam Latypov
Kazan State University, Kazan, Russia
Frances CP Law
Simon Fraser University, Burnaby, BC, Canada
Guangchun Lei
Ramsar Convention Secretariat, Switzerland
Atif M Memon
University of Maryland, MD, USA
SR Nasirov
Kazan State University, Kazan, Russia
Russell A Nicholson
Simon Fraser University, Burnaby, BC, Canada
Borislava Gutarts
California State University, CA, USA
Sally Power
Imperial College London, UK
Gordon McGregor Reid
North of England Zoological Society, UK
Pratim K Chattaraj
Indian Institute of Technology, Kharagpur, India
Andrew Alek Tuen
Institute of Biodiversity, Universiti Malaysia Sarawak, Malaysia
Dale Wrubleski
Institute for Wetland and Waterfowl Research, Stonewall, MB, Canada
Dietrich Schmidt-Vogt
Asian Institute of Technology, Thailand
Diganta Goswami
Indian Institute of Technology Guwahati, Assam, India
M Iqbal Choudhary
HEJ Research Institute of Chemistry, Karachi, Pakistan
Daniel Z Sui
Texas A&M University, TX, USA
SS Alam
Indian Institute of Technology Kharagpur, India
Biagio Ricceri
University of Catania, Italy
Zhang Heming
Chemistry & Environment College, Normal University, China
C Visvanathan
Asian Institute of Technology, Thailand
Indraneil Das
Universiti Malaysia, Sarawak, Malaysia
Gopal Das
Indian Institute of Technology, Guwahati, India
Melanie LJ Stiassny
American Museum of Natural History, New York, NY, USA
Kumlesh K Dev
Bio-Sciences Research Institute, University College Cork, Ireland.
Shakeel A Khan
University of Karachi, Karachi, Pakistan
Xiaobin Shen
University of Melbourne, Australia
Maria V Klevitch
Robert Morris University, PA, USA
Xing Jin
Hong Kong University of Science & Tech.
Leszek Czuchajowski
University of Idaho, ID, USA
Basem S Attili
UAE University, UAE
David K Chiu
University of Guelph, Ontario, Canada
Gustavo Davico
University of Idaho, ID, USA
Andrew V Sills
Georgia Southern University Statesboro, GA, USA
Charles S. Wong
University of Alberta, Canada
Greg Gaston
University of North Alabama, USA
XiuJun (James) Li
The University of Texas at El Paso, TX, USA



CONTENTS

LIFE SCIENCES

Ibtisam M Ababutain, Zeinab K Abdul Aziz and Nijla A. AL-Meshhen Lincomycin Antibiotic Biosynthesis Produced by <i>Streptomyces</i> sp. Isolated from Saudi Arabia Soil II - Extraction, Separation and Purification of Lincomycin	1905
M Zaheer Khan, Abeda Begum, Syed Ali Ghalib, Abdur Razzaq Khan, Rehana Yasmeen, Tanveer Fatima Siddiqui, Afsheen Zehra, Darakhshan Abbas, Fouzia Tabassum, Saima Siddiqui, Tanveer Jabeen and Babar Hussain Effects of Environmental Pollutants on Aquatic Vertebrate Biodiversity and Inventory of Hub Dam: Ramsar Site.....	1913
Mahmoud AbdEl-Mongy Regulation of <i>Eurotium repens</i> Reproduction and Secondary Metabolite Production.....	1937
Felix Kutsanedzie, George NK Rockson, Elias D Aklaku, Charles Quansah and Ato Bart-Plange Survival of Compost Microbial Community in Two Composting Systems.....	1945
Matilda Iyayi Ikhataua and Abiodun Falodun The Essential Oil Components of <i>Irvingia gabonensis</i> and <i>Irvingia wombolu</i> from Southern Nigeria	1955
WM Kpikpi and I Sackey <i>Gliricidia sepium</i> (Jacq.) Walp.: Hardwood with Potential for Pulp and Paper-Making	1961
Mbatchou V Chi and Sachyere P Apiah Toxic and Feeding Deterrent Effects of <i>Hyptis suaveolens</i> and <i>Hyptis spicigera</i> Extracts on Cowpea Weavils (<i>Callosobrucus maculatus</i>)	1967
CA Loto and A P I Popoola Plants Extracts Corrosion Inhibition of Aluminium Alloy in H ₂ SO ₄	1973

PHYSICAL SCIENCES

Mohammed Farfour, Wang Jung Yoon and Youngeun Jo Spectral Decomposition in Illuminating thin Sand Channel Reservoir, Alberta, Canada	1981
CK G Piyadasa Will Rising Water Droplets Change Science?	1991
Gouda Mohamed, Magdi Ibrahim, Ali Abu El ezz, Mahmoud Adly and Ali Khatab Analysis of the Effects of the Sample Inclination on Results of Vickers Hardness Testing	1999
JT Nwabanne and PK Igbokwe Breakthrough Curve Studies for the Removal of Heavy Metals in a Fixed Bed Column	2009
Sherin A Saraireh, Abdul-Wali Ajlouni, Mashhoor Al-Wardat and Hatim Al-Amairyean Radiation Absorbed Dose Rates in the Dead Sea Region, Jordan.....	2017
AJ Anifowose, L Lajide, SH Awojide and KA Fayemiwo Comparative Studies of Extracted Resin from Plantain Peels as a Potential Binder and Co-Binder with Cement in Particleboard Production.....	2023

SHORT COMMUNICATIONS**Maher MH Marzuq**A Note on Linear Functional in A^P Space 2029**Parviz Nasiri, Saman Hosseini and Masoud Yarmohammadi**

A New Approach to Statistical Inference for Exponential Distribution Based on Record Values 2033

JI Mbegbu, E Akpeli and FO Chete

Statistical Analysis of Medical Data on Anorexia Nervosa Patients 2039

Nishteman N Suliman and Abdul-Rahman H MajeedOn Dependent Elements and Free action of Derivations in Semiprime Γ -Rings 2043**Okiwelu AA, Evans UF, Ekanem CH and Etim VB**Shallow Resistivity Survey for Protection of Submerged Fuel Tanks from External Corrosion in a Coastal Environment,
Southeastern, Nigeria 2049

LINCOMYCIN ANTIBIOTIC BIOSYNTHESIS PRODUCED BY *STREPTOMYCES* sp. ISOLATED FROM SAUDI ARABIA SOIL II - EXTRACTION, SEPARATION AND PURIFICATION OF LINCOMYCIN

*Ibtisam M Ababutain¹, Zeinab K Abdul Aziz² and Nijla A. AL-Meshhen¹

¹Department of Biology, Faculty of Science, Girls College of Science
University of Dammam, Kingdom of Saudi Arabia

²Botany and Microbiology Department, Faculty of Science
Girl's branch, Al-Azhar University, Cairo, Egypt

ABSTRACT

The most potent actinomycete isolates which was previously identified as *Streptomyces* sp. MS-266 Dm4 was selected for the biosynthesis of the active metabolite having biodiversal activities. The active metabolite was extracted by diethyl ether at pH 7.0. The organic phase was collected and evaporated under reduced pressure using a rotary evaporator. The extract was concentrated and treated with petroleum ether (b.p. 60-80°C) for precipitation process, where only one fraction was obtained in the form of yellowish brown viscous texture. The purification process was performed using both thin layer (TLC) and column chromatography (CC) techniques. The active compound under study was tested for its physicochemical characteristics, where the results revealed that the compound melting point is 155°C; and soluble in chloroform, n-butanol, methanol, acetone, ethanol, ethyl acetate and isopropyl alcohol but insoluble in petroleum ether, hexane and water. The elemental analysis of the active compound suggested the empirical formula of: (C₁₀ H₂₀ N₂ O₁₆). The spectroscopic characteristics of active compound revealed the presence of the maximum absorption peak in UV at 269 nm, infrared absorption spectrum represented by nine peaks in addition to Mass- spectrum suggests the molecular weight of the active compound as 447 Dalton. The purified antimicrobial agent was suggestive of being belonging to Lincomycin antibiotic. The Minimum Inhibitory Concentration (MIC) of the antimicrobial agent was also determined which was found to have a bacteriostatic activity.

Keywords: *Streptomyces* sp., purification, lincomycin.

INTRODUCTION

Since almost antibiotics are made by aerobic fermentation processes, a number of similarities in the processes used in their production exist. The general outline of these methods is fairly well known although the industrial concerns producing antibiotics have been reluctant to publish details of their processes. Extraction, Separation, Purification and Identification of the antimicrobial agent which produced by different actinomycetes had been done by many researchers (Enomoto *et al.*, 2000; Pandey *et al.*, 2004; Ilić *et al.*, 2005; Kim *et al.*, 2005; Jeong *et al.*, 2006; Ahmed, 2007; Xie *et al.*, 2007; Igarashi *et al.*, 2008; Malik *et al.*, 2008).

The (MIC) of the active substance produces by different streptomycete isolates were investigated by many researchers. Pandey *et al.* (2004) estimated the MIC of the active substance produced by *Streptomyces* spp and *Saccharopolyspora* spp against *Staph aureus* and it was 5, 1.25 mg/ml respectively. Mukai *et al.* (2006) studied the MIC of transvalencin Z antibiotic and they estimated the MIC value against gram positive

bacteria by less than (4.0mg/ml) and against gram negative bacteria by (0.25mg/ml). Xie *et al.* (2007) found that the MIC of sansanmycin antibiotic against the *Mycobacterium tuberculosis* H37 and *Pseudomonas aeruginosa* was (10.0 and 12.5mg/ml), respectively.

In the course of our continuing search for new antibiotics produced by microorganisms (Abd El- Aziz *et al.*, 1997; Ghazal *et al.*, 2001, 2002), a culture of streptomycetes which identified as *Streptomyces* sp. MS-266 Dm4 (Ababutain *et al.*, 2012) was found to produce an lincomycin antibiotic. This antibiotic exhibited antibacterial and insecticidal activities against gram positive, gram negative bacteria and *Culex pipiens* mosquito. The objective of this study was to separate, purified and identifies the active compounds.

MATERIALS AND METHODS

Microorganism

Streptomyces sp. MS-266 Dm4 (Ababutain *et al.*, 2012) isolated from soil sample collected from Dammam governorate, Saudi Arabia was used for antibiotic production.

*Corresponding author email: dr.king2007@hotmail.com

Fermentation

The isolate Dm4, was inoculated into yeast extract glucose broth at pH7, and incubated under aerobic conditions using incubator shaker at 200 rpm/ mint at 30°C for three days. One ml of these cultures has been used to inoculate the production medium (Starch-nitrate broth). The flasks were incubated on incubator shaker at 200rpm at 30°C for 7 days. A twenty liter total volume was filtered through Whatman No.1 filter paper and followed by centrifugation at 5000rpm for 20 minutes.

Extraction

The clear filtrate was adjusted at different pH values (4 to 9) and extraction process was carried out using diethyl ether solvent at the level of 1:1 (v/v). The organic phase was concentrated to dryness under vacuum using a rotary evaporator at a temperature not exceeding 50°C yielding a yellowish brown viscous texture.

Precipitation

The precipitation process of the crude compound was carried out using petroleum ether (b.p 60-80°C) followed by centrifugation at 5000rpm for 15 min.

Purification by TLC

Separation of the antimicrobial compound into its individual components was conducted by thin layer chromatography using chloroform and methanol (24:1, v/v) as a solvent system.

Purification by Column Chromatography

The purification of the antimicrobial compound was carried out using silica gel column (2.5X50) chromatography. Chloroform and Methanol 95:5 (v/v) (Guangying *et al.*, 2005) was used as an eluting solvent. The column was left overnight until the silica gel (Prolabo) was completely settled. One-ml crude extract to be fractionated was added on the silica gel column surface and the extract was adsorbed on top of silica gel. Fifty fractions were collected (each of 5ml) and tested for their antimicrobial activities.

Bioautography

It is conducted by preparing nutrient agar medium, seeded by *Bacillus cereus* as a test organism, flooded over the glass sheet of the tray and left to cool under aseptic conditions. The developed whatman No. 1 chromatographic strips containing the antibiotic material and flooded over the agar plate, left for half an hour in a refrigerator for diffusion and then incubated at 37°C for 18 hours (Weinstein and Wagman, 1978) which indicates the purity of the active substance under study.

Physicochemical Properties and Spectroscopic analysis

Physical and chemical properties of the purified active substance such as solubility in organic solvents, behavior towards acids and alkalis and melting point were studied.

- 1- Elemental analysis: The elemental analysis C, H, O, N, and S was carried out at the micro-analytical center, Cairo University, Egypt.
- 2- Spectroscopic analysis: The IR, UV, Mass spectrum and NMR spectrum were determined at the micro analytical center of Cairo University, Egypt.
- 3- Biological activity of the antimicrobial agent: The Minimum Inhibitory Concentration (MIC) has been determined by using the agar plate dilution technique (Betina, 1983).
- 4- Characterization of the antimicrobial agent: The antibiotic produced by *Streptomyces* sp. MS-266 Dm4 was identified according to the recommended international references of (Umezawa, 1977; Berdy 1980 a, b, c).

RESULTS

Fermentation, Extraction and Purification

The fermentation process was carried out for seven days at 30°C using liquid starch nitrate as production medium. Twenty-liter total volume filtered was conducted followed by centrifugation at 5000rpm for 20 minutes. The clear filtrates containing the active metabolite (20liters) was adjusted to pH 7.0 then extraction was carried out using diethyl ether at the level of 1:1 (v/v). The organic phase was collected and evaporated under reduced pressure using rotary evaporator. The extract was concentrated and treated with petroleum ether (b.p. 60-80°C) for precipitation process, where only one fraction was obtained in the form of yellowish brown viscous syrup. The purification process was carried out through a column chromatography packed with silica gel, where one definite inhibition zone was detected using *B. cereus* as a test organism, indicating that the metabolite under study is composed of one compound (Table 1, Fig. 1).

Table 1. Bioautographic mobility of the antimicrobial agent produced by *Streptomyces* sp. MS-266 Dm₄.

No.	Developing solvent	R _f
1	Diethyl ether	0.95
2	Ethyl acetate	0.85
3	Chloroform / Ethyl acetate (1:1)	0.85
4	Alkaline chloroform	0.84
5	Chloroform	0.80
6	Acetone	0.77
7	Acidic chloroform	0.75
8	Ethyl alcohol	0.69
9	Methyl alcohol	0.60
10	Alkaline diethyl ether	0.60
11	Acidic diethyl ether	0.50
12	Petroleum ether	0.0
13	n – Hexane	0.0
14	Water	0.0

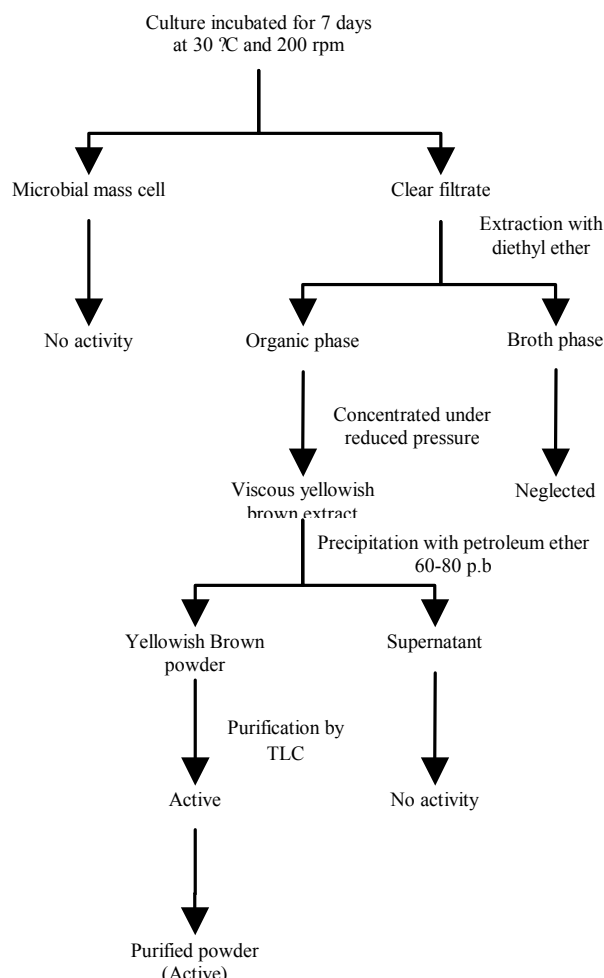


Fig. 1. Dichotomous scheme for production and purification of the antimicrobial agent produced by *Streptomyces* sp. MS-266 Dm₄.

Physicochemical Characteristics

The purified antimicrobial agent produced by *Streptomyces* sp. MS-266 Dm₄ produces characteristic odor, their melting points are 155°C. The compound is freely soluble in chloroform, ethyl acetate, acetone, ethyl alcohol, diethyl ether but insoluble in petroleum ether, n-hexane and water.

Elemental Analysis

The elemental analytical data of the antimicrobial agent produced by *Streptomyces* sp. MS-266 Dm₄ showed the following: C=29.46; H=4.42; N=3.86; and O=60.76, from which the empirical formula is calculated to be: C₁₀H₂₀N₂O₁₆.

Spectroscopic Characteristics

Mass spectrometry analysis of the active substance (Mass spectrum), gave an account for the molecular weight (447) Dalton (Fig. 2). The ultra violet absorption spectrum of the active substance exhibits maximum absorption band at 269 nm (Fig. 3). The infrared

absorption spectrum of the active substance gave nine values of absorption (3414.4, 2924.5, 2858.0, 2355.6, 1742.4, 1634.4, 1451.2, 1028.8 and 607.5) nm (Fig. 4). H-Nuclear Magnetic Resonance (H-NMR) illustrated in (Fig. 5).

Identification of the purified active antimicrobial agent

The study concluded that the active substance contains the effective hard-core, which is a pyrrolidine with a percentage of similarity with lincomycin antibiotic (Fig. 6).

Screening for the Antimicrobial Activities

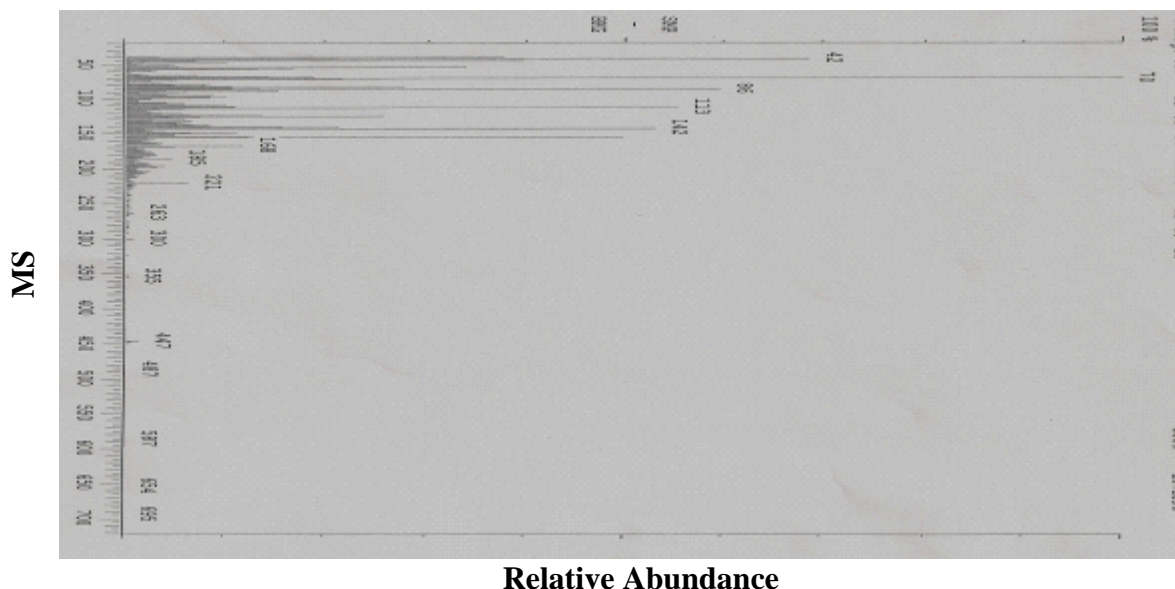
The active metabolite produced by actinomycete culture, *Streptomyces* sp. MS-266 Dm₄ exhibited various degrees of activities against gram positive and gram negative bacteria. The MIC was found to be 31.25 µg/ml against the tested microorganisms, except for *E. coli* was found to be 15.62 µg/ml, (Table 2). The effect of the active substance on the organisms tested was bacteriostatic.

Table. 2. Minimum Inhibitory Concentration (MIC) of *Streptomyces* sp. MS-266 Dm₄ against test microorganisms

Test organisms	MIC ($\mu\text{g/ml}$) concentration
<i>Bacillus cereus</i> ATCC 14579	31.25
<i>Bacillus subtilis</i> ATCC 6633	31.25
<i>Staphylococcus aureus</i> ATCC6538P	31.25
<i>E. coli</i> ATCC 7839	15.62
<i>Pseudomonas aeruginosa</i> ATCC9027	31.25
<i>Candida albicans</i> ATCC 10231	31.25

DISCUSSION

The most potent actinomycete isolates which was identified as *Streptomyces* sp. MS-266 Dm₄ (Ababutain *et al.*, 2012) was selected for the biosynthesis of the active metabolite having biodiversal activities. For this reason *Streptomyces* sp. MS-266 Dm₄ was inoculated in nutrient broth media under favorable environmental and nutritional conditions. At the end of the incubation time, the active metabolite was extracted by diethyl ether at pH 7.0. The organic phase was collected and evaporated under reduced pressure using a rotary evaporator. The extract was concentrated and treated with petroleum ether



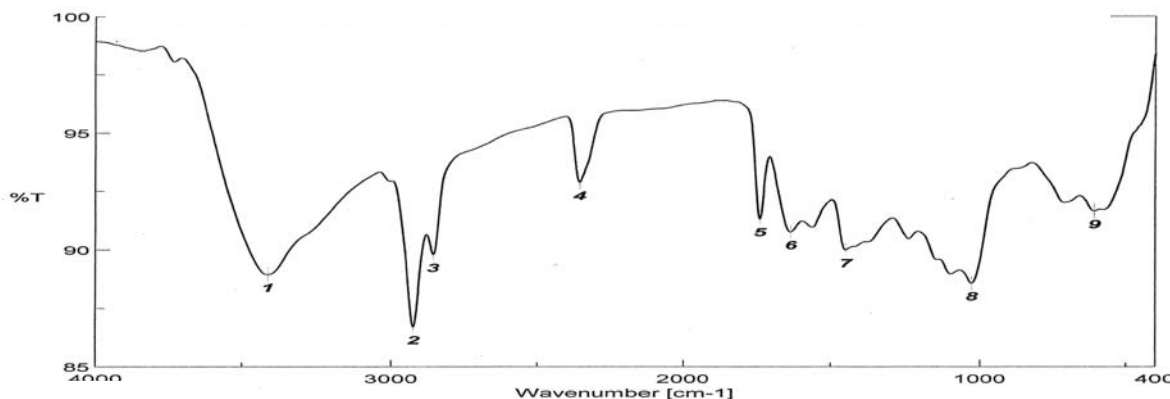


Fig. 4. IR – spectrum bands of the purified active substance produced by *Streptomyces* sp. MS-266 Dm₄

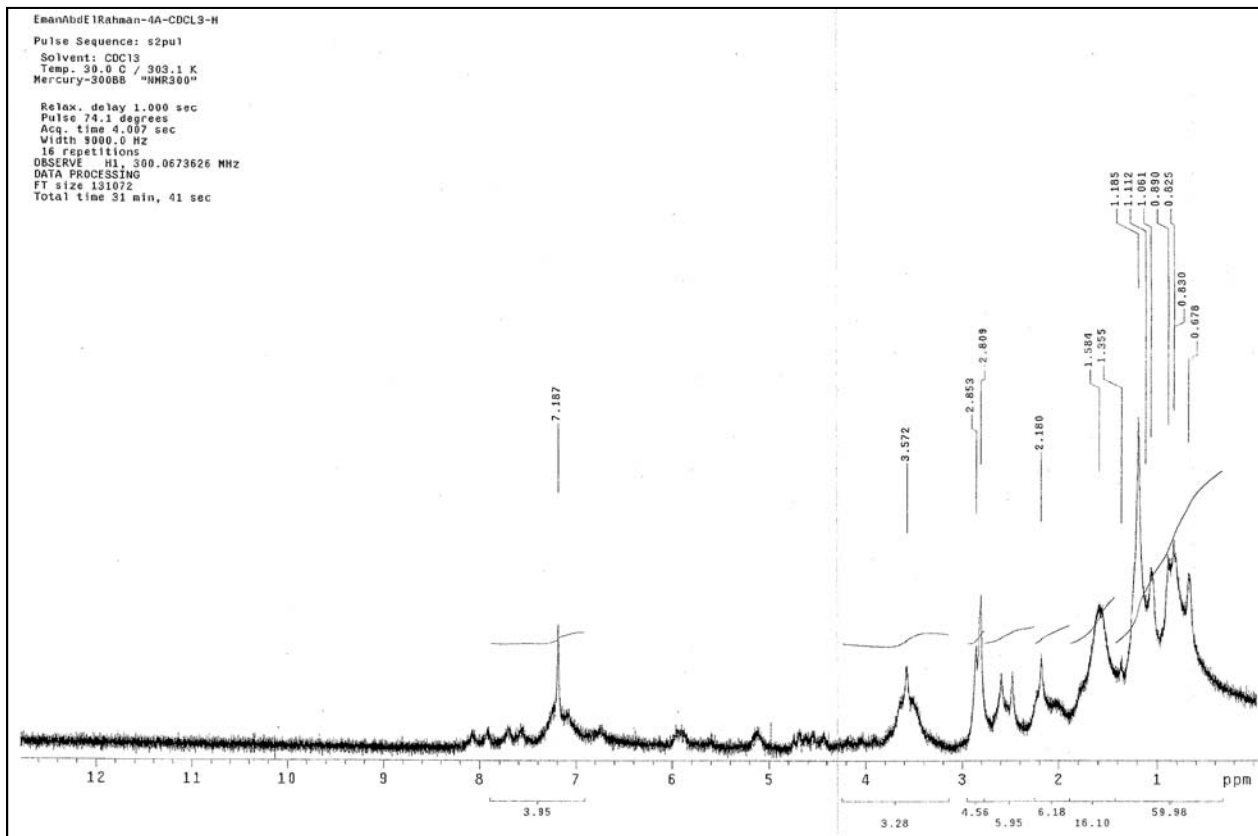


Fig. 5. H. NMR – spectrum peaks of the purified active substance produced by *Streptomyces* sp. MS-266 Dm₄

(b.p. 60-80°C) for precipitation process, where only one fraction was obtained in the form of yellowish brown viscous texture. The purification process was carried out through a column chromatography packed with silica gel, where one definite inhibition zone was detected using *B. cereus* as a test organism, indicating that the metabolite under study is in pure form. The active compound under

study was tested for its physical and chemical characteristics, where the results revealed that the compound melting point is 155°C and soluble in chloroform, n-butanol, methanol, acetone, ethanol, ethyl acetate and isopropyl alcohol but insoluble in petroleum ether, n- hexane and water.

The elemental analysis of the active compound revealed the detection of the following elements (%): C, (29.46); H, (4.42); N, (3.86) and O, (60.76) which give the empirical formula of: (C₁₀ H₂₀ N₂ O₁₆). The spectroscopic characteristics of active compound revealed the presence of the maximum absorption peak in UV at 269 nm, infrared absorption spectrum represented by nine peaks in addition to Mass- spectrum suggests the molecular weight of the active compound as 447 Dalton. In addition, H-Nuclear Magnetic Resonance was determined (Pandey *et al.*, 2004; Ilic' *et al.*, 2005; Jeong *et al.*, 2006; Ahmed, 2007; Xie *et al.*, 2007).

On the basis of comparative study of the recorded chemical composition and physical properties of the active substance produced by *Streptomyces* sp. MS-266 Dm4 and by consulting the recommended identification keys of antibiotics such as (Umezawa, 1977; Berdy, 1980 a, b, c) it could be stated that the compound contains an effective hard-core Pyrrolidine and have high similarity with Lincomycin antibiotic. The obtained active substance was investigated for (MIC) by using various microbial test organisms; it was found that the active substance has antimicrobial activity against gram positive, gram negative bacteria this result agree with several researchers (Pandey *et al.*, 2004; Mukai *et al.*, 2006; Xie *et al.*, 2007).

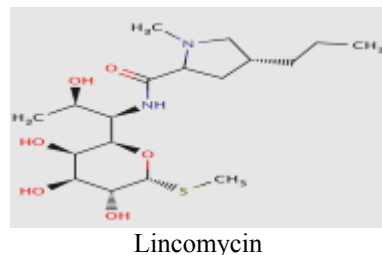
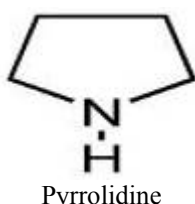


Fig. 6. The identification of the purified active antimicrobial agent produced by *Streptomyces* sp. MS-266 Dm₄

REFERENCES

- Ababutain, IM., Abdul Aziz, ZA. and AL-Meshhen NA. 2012. Lincomycin Antibiotic Biosynthesis Produced by *Streptomyces* Sp. Isolated from Saudi Arabia Soil: I-Taxonomical, antimicrobial and insecticidal studies on the producing organism. Canadian Journal of Pure and Applied Sciences. 6(1):1739-1748.
- Abd El-Aziz, ZK., Ghazal, SA. and Abd El- Fattah, ME. 1997. Antibiotics produced by *Kibdelosporangium* species. Isolation, purification and characterization. Egypt J. Biotechnol. 1:81-100.
- Ahmed, AA. 2007. Production of antimicrobial agent by *Streptomyces rochei rochei*.The International conference on the Arabian Oryx in the Arabian Peninsula. The 23 Meeting of the Saudi Biological Society.
- Berdy, J. 1980^a. Recent advances in and prospects of antibiotics research. Proc. Biochem. 15:28-35.
- Berdy, J. 1980^b. CRC Handbook of antibiotic compounds. Vol. I.
- Berdy, J. 1980^c. CRC Handbook of Antibiotic Compounds. Vol. II.
- Betina, V. 1983. The Chemistry and Biology of Antibiotics. Elsevier Scientific Publishing Company Inc, Amsterdam, New York, USA.
- Enomoto, Y., Shiomi, K., Matsumoto, A., Takahashi,Y., Iwai, Y., Harder, A., KÖLBL, H., Woodruff, HB. and Ōmura, S. 2000. Isolation of a New Antibiotic OligomycinG produced by *Streptomyces* sp. WK-6150. J. Antibiot. 54(3):308-313.
- Ghazal, SA. and Abd El- Aziz, ZK. 2002. Sporangial forming actinomycete genera as antibiotic producers from Arabian soils. Xth International Congress of Bacteriology and Applied Microbiology, Paris.
- Ghazal, SA., Bream, A., Abd El-Aziz, Z. and Ibrahim, S. 2001. Preliminary Studies on Insecticidal Activities of Actinomycete Strains Propagated on Solid and Broth Media using *Musca domestica* (Diptera: Muscidae). Meded Rijksuniv Gent Fak Landbouwkde Toegep Biol. Wet. 66(26):559-570.
- Guangying, C., Birun L., Yongcheng, L., Fengchun, X., Wen, L. and Wang-Fun, F. 2005. A New Fungicide Produced by a *Streptomyces* sp. GAAS7310. J. Antibiot. 58(8):519-522.
- Igarashi, M., Sawa, R., Kinoshita, N., Hashizume, H., Nakagawa, N., Homma, Y., Nishimura, Y. and Akamatsu, Y. 2008. Pargamycin A, A Novel Cyclic Peptide Antibiotic from *Amycolatopsis* sp. J. Antibiot. 61(6):387-393.
- Ilic', SB., Konstantinovic', SS. and Todorovic, ZB. 2005. UV/VIS Analysis and Antimicrobial Activity of *Streptomyces* Isolates. Medicine and Biology. 12(1):44-46.
- Jeong, SY., Shin, HJ., Kim, TS., Lee, HS., Park, SK. and Kim, HM. 2006. Streptokordin, A New Cytotoxic Compound of the Methyl Pyridine Class from a Marine-derived *Streptomyces* sp. KORDI- 3238. J. of Antibiotic, Japan.
- Kim, BS., Oh, H., Kim, SY., Park, JA., Yoon, YJ., Lee, SK., Kim, BY. and Ahn, JS. 2005. Identification and Antibacterial Activity of a New Oleandomycin Derivative from *Streptomyces antibioticus*. J. Antibiot. 58(3):196-201.
- Malik, H., Sur, B., Singhal, N. and Bihari, V. 2008. Antimicrobial Protein from *Streptomyces fulvissimus*

- Inhibitory to Methicillin Resistant *Staphylococcus aureus*. Indian J. Exp. Biol. 46:254-257.
- Mukai, A., Fukai, T., Matsumoto, Y., Ishikawa, J., Hoshino, Y., Yazawa, K., Harada, K-I. and Mikami, Y. 2006. Transvalencin Z, A New Antimicrobial Compound with Salicylic acid Residue from *Nocardia transvalensis* IFM 10065. J. Antibiot. 59(6):366-369.
- Pandey, B., Ghimire, P. and Agrawal, VP. 2004. Studies on the Antibacterial Activity of the Actinomycetes Isolated from the Khumbu Region of Nepal. J. Biol. Sci. 23:44-53.
- Umezawa, H. 1977. Recent Advances in Bioactive Microbial Secondary Metabolites. Jep. J. Antibiotic. Suppl. 30:138-163.
- Weinstein, MJ. and Wagman, GH. 1978. Antibiotics, Isolation, Separation and Purification. Elsevier Scientific Publishing Co. New York, USA.
- Xie, Y., Chen, R., Si, S., Sun, CH. and Xu, H. 2007. A New Nucleosidyl-peptide Antibiotic, Sansanmycin. J. Antibiot. 60(2):158-161.

Received: March 30, 2012; Accepted: April 24, 2012

EFFECTS OF ENVIRONMENTAL POLLUTANTS ON AQUATIC VERTEBRATE BIODIVERSITY AND INVENTORY OF HUB DAM: RAMSAR SITE

*M Zaheer Khan¹, Abeda Begum¹, Syed Ali Ghalib¹, Abdur Razzaq Khan¹, Rehana Yasmeen¹, Tanveer Fatima Siddiqui², Afsheen Zehra¹, Darakhshan Abbas¹, Fouzia Tabassum¹, Saima Siddiqui², Tanveer Jabeen¹ and Babar Hussain¹

¹Department of Zoology, Faculty of Science, University of Karachi, Karachi-75270

²Department of Zoology, Federal Govt Urdu University of Arts, Science and Technology, Karachi.

ABSTRACT

In the present study, the effects of environmental pollution on aquatic vertebrate biodiversity were studied and inventory of vertebrate fauna of Hub Dam was prepared. The water samples taken from four sampling sites from the study areas viz. Main Dam, Spill way, Hub Canal and shallow water area were analyzed for physico-chemical parameters viz temperature in air, temperature in water, color, pH, TDS, COD, BOD, alkalinity, salinity, conductivity, hardness, Phosphate, Nitrate, Bicarbonates, Sulphate, Chloride, Carbon dioxide, Dissolved Oxygen, Turbidity and Fluoride, Cations (Ca^+ , Na^+ , Mg^+ , K^+) and some selected heavy metals (Cr, Fe, Ni, Cu, Zn, As, Cd, Pb, and Hg). The seasonal and yearly variations in selected physico chemical parameters and trace metals were determined with respect to the amount of annual rainfall and contamination factors involved. During the study, no adverse effects of environmental pollution were found on the aquatic biodiversity except for some minor toxic effects due to trace metals in water. All the physico – chemical parameters' values were observed as per limits of World Health Organization standard. Microbial analysis was carried out and water samples of Hub Dam did not meet the microbiological standard set by WHO. After suitable treatment the water may be supplied for domestic use. As many as 16 species of mammals, 160 species of birds, 23 species of reptiles, 03 species of amphibians, 29 species of fishes, and 25 species of plants were recorded from the Hub Dam area. There are no serious effects of pollution on the vertebrate biodiversity of the wetland. The population of the waterbirds has declined significantly in recent years mainly due to disturbances and commercial fishing activities in the reservoir area.

Keywords: Hub dam, environmental pollution, vertebrate biodiversity.

INTRODUCTION

Hub dam ($25^{\circ} 15' \text{N}$ $67^{\circ} 07' \text{E}$) constructed across Hub River in 1981, at a distance of 56 km North of Karachi falls in the provinces of Sindh and Balochistan (Fig. 1). Main Dam is 15,640 m long whereas 5,400 m lies in Balochistan and 10,240 m in Sindh.

Hub Dam (Fig. 3) has also been declared as a Wildlife Sanctuary in Sindh and was established in 1972 for the preservation of waterbirds and the fish Mahsheer. It falls under Category IV of IUCN as Habitat / Species Management Area under the IUCN Protected Area Category System.

The dam is situated in an area of semi arid and desert with sedimentary rocks. The hills which run around on three sides are yellow with many shades of brown and grey. There are a few small islands in the midst of the reservoir. The Hub River rises in Kirthar Range of eastern Balochistan and enters the Arabian Sea just west of Karachi. The water level in the reservoir fluctuates widely

according to rainfall in the water catchment area which extends over 3410 sq.miles. The topography of the upper catchment is sub – mountainous to hilly and plain. The area is generally barren with sparse vegetation at certain locations. The catchment of the Hub reservoir is wholly rain fed. The dam is relatively shallow with maximum depth of 9.6 m. The water has relatively high concentration of dissolved salts of sulphates, sodium and chloride and dissolved oxygen which results into much greater primary and secondary production (Sohail Siddiqi, pers. comm.).

The Hub Dam Canal system consists of the Main Canal, Karachi Water Supply Canal, Lasbella Canal and the Bund Murad Minor (Fig. 2). The water supply canal is 14 miles long lined with concrete tiles to supply 100 MGD to Karachi Water and Sewerage Board.

The Lasbella branch canal, 20 miles long lined with concrete tiles to supply water for irrigation of 21,000 acres of land and 15 MGD water for industries in Lasbella district.

*Corresponding author email: zaheerkhan67@yahoo.ca



Fig.1. Map of Pakistan showing the location of Hub Dam.

Table 1. List of Ramsar Sites in Pakistan.

S. No.	Name	Location	Area
01	Astola (Haft Talar) Island	Balochistan	5,000ha
02	Chashma Barrage	Punjab	34,099 ha
03	Deh Akro	Sindh	20243 ha
04	Drigh Lake	Sindh	164 ha
05	Haleji Lake	Sindh	1,704 ha
06	Hub Dam	Sindh, Balochistan	27,000 ha
07	Indus Delta	Sindh	472,800 ha
08	Indus Dolphin Reserve	Sindh	125,000 ha
09	Jiwani Coastal Wetland	Balochistan	4,600 ha
10	Jabho Lagoon	Sindh	706 ha
11	Keenjhar Lake	Sindh	13,468 ha
12	Miani Hor	Balochistan	55,000 ha
13	Nurri Lagoon	Sindh	2,540 ha
14	Ormara Turtle Beaches	Balochistan	2,400 ha
15	Rann of Kutch	Sindh	566,375 ha
16	Tanda Dam	Khyber Pakhtoonkhah	405 ha
17	Taunsa Barrage	Punjab	6,756 ha
18	Thanedar Wala,	Khyber Pakhtoonkhah	40,47 ha
19	Uchhali Complex (including Khabbaki, Uchhali and Jahlar lakes),	Punjab	1,243 ha

The climate of the area tends to be very arid and average annual rainfall is less than 200 mm. The temperature often exceeds 36°C during the summer.

The water level in the dam depends on the amount of rainfall in the water catchment area. The maximum depth is 45 m and the average drawdown 19m. There has been no ample rain for the last five years and the water level in the reservoir has decreased significantly, posing a problem for the drinking water supply to Karachi West.

This site is an important staging and wintering area for waterbirds including Grebes, Pelicans, Flamingos, Anatids, Coots and Cranes. It regularly supported over 45,000 water birds (in the past, but does not anymore) including Black-necked Grebe (*Podiceps nigricollis*), Little Cormorant (*Phalacrocorax niger*), Tufted Duck (*Aythya fuligula*), Common Pochard (*Aythya ferina*), Dalmatian Pelican (*Pelecanus crispus*), White Pelican (*Pelecanus onocrotalus*), Coot (*Fulica atra*), and Little Tern (*Sterna albifrons*). The site is a breeding site for

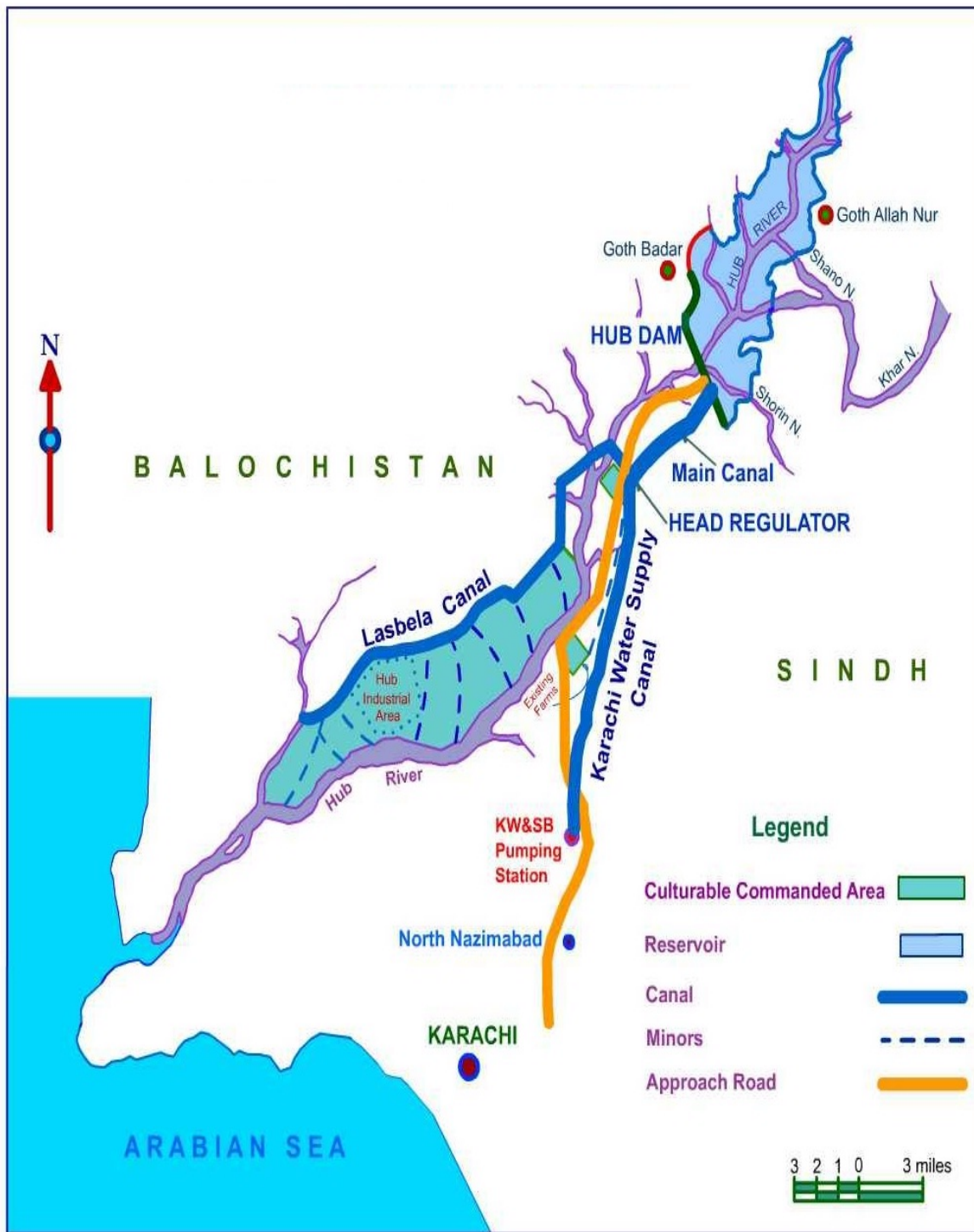


Fig. 2. Map showing location of Hub Dam.

Little Tern (*Sterna albifrons*) and Painted Snipe (*Rostratula benghalensis*). Marsh Crocodile or Mugger (*Crocodylus palustris*) is now found in the Hub Reservoir. The reservoir is an important spawning ground for a large number of fishes including some exotic fishes such as *Labeo rohita*, *Cyprinus carpio* and *Tilapia mossambica*,

while the Mahsheer (*Tor putitora*) is the most important fish of this reservoir.

During 1986, the Fisheries Directorate, WAPDA started development of fisheries at Hub Dam according to National Fisheries Management Program to meet the



Fig. 3. View of Hub Dam.

protein demand of the growing population of the country. In order to develop and promote fisheries in Hub reservoir, a medium sized hatchery and a rearing farm were established in 1990 located in front of WAPDA colony on the right bank of Hub Dam Canal, 500 meter downstream of the Dam. (Muhammad Aslam, pers. comm.).

Commercial fishing was allowed in the Dam in 1988. Since 1989, hatchery and rearing farm were utilized to produce fish seeds of the following species:

Rohu (*Labeo rohita*)
 Mori (*Cirrihinus mrigala*)
 Gulfam (*Cyprinus carpio*)
 Silver carp (*Hypophthalmichthys molitrix*)
 Grass carp (*Ctenopharyngodon idella*)

An area of 27,192ha on the eastern shore and south of dam in the Sindh province has been declared as a Wildlife Sanctuary but the greater part of the reservoir in Balochistan province remains unprotected.

There are social impacts due to the presence of the many villages around such as Haji Muhammad Bux Goth, Usman Qalandria Goth, Dado Bandeejah Goth, Robo Goth, and Safar Goth. Raho Khaskeli Goth is the largest one having a population of almost 3000 people.

The objective of the present study was to identify the environmental factors and their effect on the aquatic vertebrate biodiversity and to prepare the inventory of vertebrate biodiversity of Hub Dam with a view to make recommendations for its conservation and management.

MATERIALS AND METHODS

The reservoir and adjoining areas were regularly visited during summer and winter seasons from 2007 to 2010. Quarterly surveys of three weeks duration were undertaken each year in the area for the collection of data with regard to the occurrence, distribution and habitats of the biodiversity of the area i.e birds, mammals, reptiles, fishes, amphibians and plants.

The avifauna of Hub Dam consists of resident as well as migratory species. Water bird census was undertaken in January and the data for the annual Waterbird Census were collected.

On the basis of baseline study, sites such as Spill way area, Main Hub dam, Main Sampling Point, Agriculture Land, Khar Centre, Usman Qalandria Goth, Hub Canal, Raho Khaskheli Goth, Robo Goth, Safar Goth, Rest House, Plantation Area and Bund Murad were selected for data collection with respect to mammals, resident and migratory birds, reptiles, amphibians, fishes and plants (Fig. 4, Table 2).

A. PARAMETERS FOR WATER QUALITY ANALYSIS

(i) Preparation of water samples and sampling sites

For the study of physico-chemical parameters, composition of trace metal and microbial analysis, four different sites viz. Main Dam, Spill way, Hub Canal, and shallow water were selected. Rainfall data were collected from Metrology department.

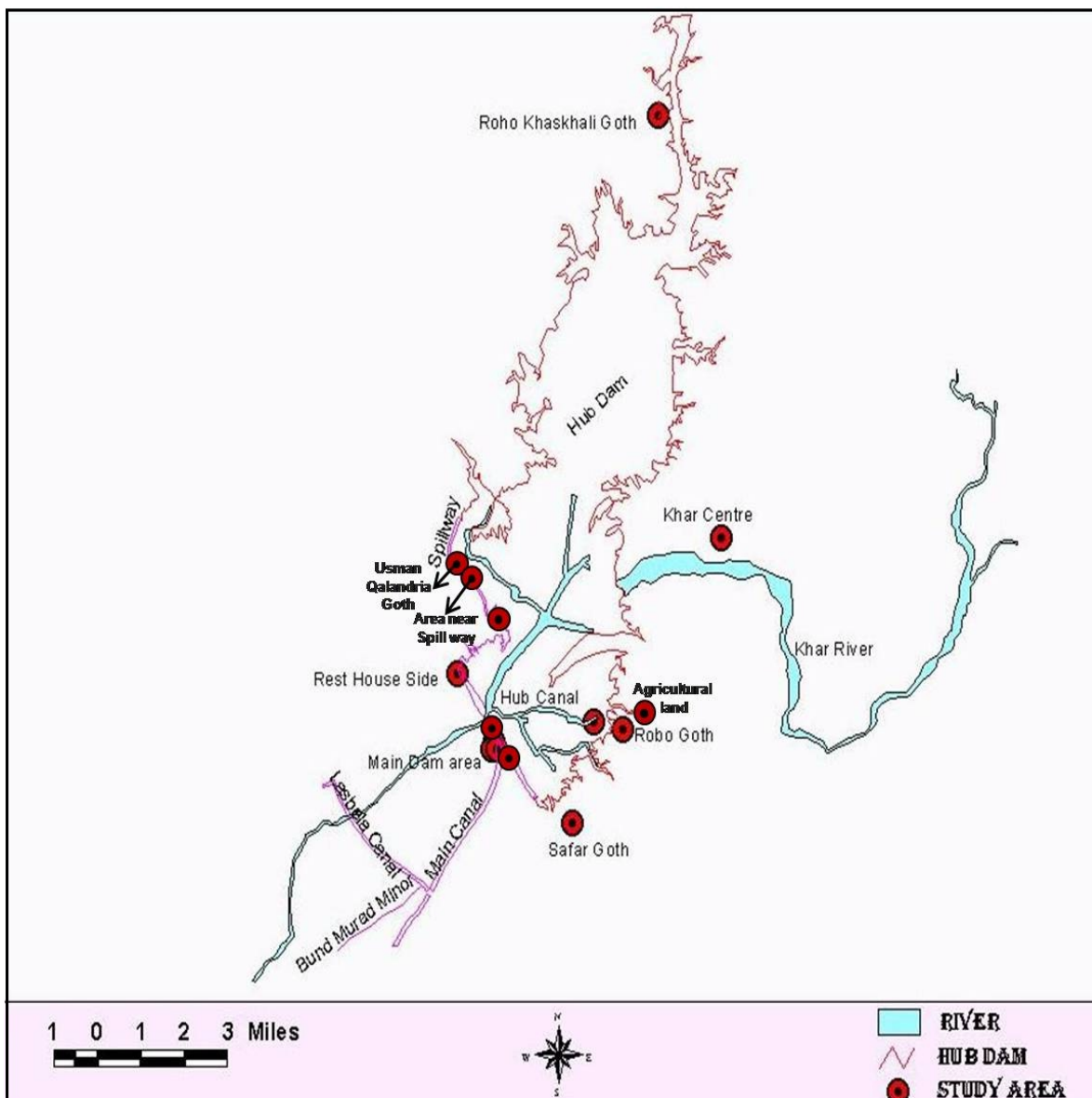


Fig. 4. Map showing the study areas.

During the study period 2007 – 2010, most of the samples were collected in 1000 ml polyethylene screw – cap bottles in order to obtain the water of the required depth. Bottles were cleaned sequentially, tap water rinse, 24 hour soak in 1% HNO₃ and several distilled water rinse. Dried at 100°C for 1 hour, cooled at room temperature, capped and labeled. After collecting the samples, 10 ml HNO₃ (1 ml acid / 100 ml) was added to the samples which were useful for the estimation of concentration of trace metals.

(ii) Digestion of the samples

A very crucial step to analyze the samples was the transformation of a sample into an analytic solution. For this purpose a complete digestion of the samples was required. Decomposition procedures were dry ashing and

wet oxidation (Gorsuch, 1976; Santa *et al.*, 1986). In present investigation nitric acid based digestion method was carried out.

(iii) Methodology

For the preparation of reagents, Analytical Grade (AR) chemicals were used. For the determination of water quality parameters, standard analytical methods were carried out.

(a) Physico Chemical Analysis of Samples

Temperature measured at the spot by using Mercury Thermometer, pH was recorded with Orion 420 pH meter. Alkalinity was measured by titration method with 0.02 M hydrochloric acid (Electrometric method No.15 WHO,

Table 2. Study areas of Hub Dam.

S. No.	Study Area	Co-ordinates	Habitat
01	Area near Spill Way (Balochistan)	N 25° 17' 23.2 E 67° 05' 55.6	Rocky slopes with sparse vegetation, reservoir area
02	Main Dam area	N 25° 14' 35.5 E 67° 06' 45.8	Wetland
03	Main sampling point (on dam)	N 25° 14' 42.9 E 67° 06' 40.1	Wetland
04	Agriculture land / Shallow water area towards Khar Centre	N 25° 14' 55.3 E 67° 08' 56.3	Agriculture land, Rocky area and marshes
05	Khar Centre	N 25° 18' 03.2 E 67° 11' 40.9	Hilly, Rocky area and Agricultural plain area
06	Usman Qalandria Goth	N 25° 17' 38.5 E 67° 05' 94.2	Rocky area, Agricultural land and Plain area
07	Hub Canal	N 25° 14' 26.6 E 67° 06' 48.6	Rocky and Plain area
08	Roho Khaskheli Goth	N 25° 17' 48.4 E 67° 10' 12.2	Rocky and Flat Plain area
09	Robo Goth	N 25° 14' 48.1 E 67° 09' 32.5	Rocky and Plain area
10	Safar Goth	N 25° 13' 15.6 E 67° 08' 31.2	Rocky area, Agricultural land and Plain area
11	Rest House Side	N 25° 15' 40.1 E 67° 05' 54.8	Wetland and Rocky area
12	Plantation Area	N 25° 16' 32.3 E 67° 06' 39.1	Forest / Wetland and Rocky area
13	Bund Murad	N 26° 05' 77.4 E 69° 09' 39.0	Wetland and Rocky area

1982). Conductivity was measured by light and dark bottles method (Welch, 1952). The turbidity of water was estimated with the help of Secchi disk while free Carbon Dioxide was measured as describe by APHA (1998). By gravimetric methods Sulphate and TDS were determined, Chloride by argentometric method, Nitrate was measured by employing a specific ion analyzer Orion -710, Calcium and Magnesium were determined by EDTA titration method, Sodium and Potassium were measured by flame photometer. The Chemical Oxygen Demand (COD) was measured by Method No. 16.4 (WHO, 1982), BOD, Fluoride, Bicarbonate, Salinity and Colour were measured by using standard method APHA (1998). Phosphate was measured using pectrophoto-metric method (Jones *et al.*, 1983), Hardness were analyzed by titration with 0.01m EDTA (Ethylene Diamine Tetra Acetic Acid, Method No. 103 WHO, 1982). Dissolved Oxygen was analyzed by standard procedure mentioned in APHA (1998).

(b) Chemical Analysis of Trace Metals

To give aqueous phase the acidified water samples were treated with reagent and trace metal analyzed by Flame Atomic Absorption (Mastoi *et al.*, 1997). Digested liquid wastes were used to analyze Cr by Graphite Furnace

method, Fe by Flame Atomic Absorption Spectrophotometer, Ni by Graphite Furnace method, Cu and Zn by Flame Atomic Absorption Spectrophotometer, As by Hydrate Generation method, Cd and Pb by Graphite Furnace method, Na and K by Flame Photometer method, Ca and Mg by titration method and Hg by Hydrate Generation method. The instrument (Perkin Elmer Model No. A analysts 700) was using different techniques such as Flame atomic absorption spectrometer, Graphite and hydrates system to analyze the chemicals. Determination for each metal was taken out in triplicate for getting representative results.

(c) Microbial Analysis of the samples

For microbial analysis, samples were collected in Brown Nelson Bottles and immediately transferred to lab. Microbial characteristic of the water samples were determined such as HPC, Total Coliforms and Faecal Coliforms by using multiple fermentation technique and membrane filter techniques described by standard method APHA (1998).

B. Survey Techniques and Counting Methods for the Biodiversity

Following direct and indirect observation methods have been applied during the surveys.

Large Mammals

The mammals were indentified by Roberts (1997, 2005a, b).

1. Roadside Counts

In this method, motor vehicles have been used along the road trails while the sighted number of individuals of the species being estimated is tallied and related to the number of kilometers travelled (Brower *et al.*, 1990). Roadside counts method has some advantages such as: travelling on vehicle does not disturb the animals and there is a chance to observe the animals along the road / track from a few meters distance. Another advantage of this method is that large areas can be covered in short time using only two persons and a vehicle, but in this method there are chances of some species being overlooked.

2. Track Counts

A track count is another method used for locating and observing the presence of nocturnal and secretive animals.

3. Pellet Counts

This technique involves removing all pellet groups from plots and then estimating from subsequent observations on those plots the number of groups per hectare to compare animal use of area between sampling periods.

Small Mammals

One effective way to survey small mammals is active searching, particularly during the day time. This method is equally applicable to both nocturnal and diurnal species in potential and suitable microhabitats along the banks, open plains, particularly in bushy areas and agriculture fields. Active searching is very effective for inventory of Gerbils, Jirds, Porcupine, and Hedgehogs. To investigate nocturnal species, night surveys are conducted in exposed areas of potential habitats on the ground. This methodology involves the use of a powerful torch light, sticks, long boots, gloves etc.

A mixture of different food grains mixed with fragrant seeds may be used as bait for the attraction of the small mammals. Wheat and rice are used as food grain while peanut butter, corriander, oats and onion are used for fragrance. This bait is found to be highly successful in the study area probably due to the overall shortage of food and fragrance.

Traps and trapping procedure

Sherman traps are used to collect the live specimens. Fifty traps are set at specific areas on a line approximately 500 m long and approximately 10 m apart. Each trap is marked by a colorful ribbon to locate the traps easily. The

traps are set in the afternoon and checked early in the morning. The specimens are transferred into polythene bags, identified in the field and released.

Birds

Birds are identified using spottingscopes and binoculars and making use of the field identification guides such as Grimmett (1998) and Snobe *et al.* (1993). Each major habitat type in the study area was identified and surveyed to record the species of birds found in each discreet habitat such as marshes, forest, agriculture fields, vicinity of human habitation and fallow lands. The number of birds observed in each habitat type was also recorded with particular emphasis on the key species and to relate the data to other components of the study area such as vegetation, water and soil etc.

The most commonly used field method in birds surveying is the "Line Transect method". It is based on recording birds continually along a predefined route within a predefined survey unit.

Line Transects are suitable for extensive, open and uniform habitats and for large and conspicuous species. Double counting of birds becomes a minor issue as the observer is continually on the move. Line Transects are suited to situations where access is good and these are very useful for bird-habitat studies (Khan *et al.*, 2010b).

In the present studies, each sample area was transversed/examined by 2 observers separately; birds were searched on each side of the strip for 150m so that each study strip was 300m wide.

To evaluate the numbers of water birds the entire reservoir area, associated marshes, rocky and plain areas, and agriculture land were surveyed.

Reptiles and Amphibians

Various survey techniques have been employed to record the reptiles and amphibians (Khan *et al.*, 2010a).

A: Direct Counting:

1. Plot Searching

This consists of searching approximately 20 ha. (with 250 meter radius of sampling points) for one hour and recording the number of individuals of each species seen. Similarly night survey is done with the help of search lights and torches.

2. Pitfall Traps

Reptiles and amphibians are also detected using a line or pitfall traps. Each pitfall line consists of 30 meter of low, flexible nylon fencing pinned to the ground to divert the movements of small ground dwelling animals mainly reptiles with six 3-liter meter bucket buried in the ground with its lips at ground level along and below the fence, so

that the fence straddled each bucket. The use of pitfall lines are restricted to sites where the ground surface is soft enough to dig or sandy areas. Pitfall lines are set for one night only. Team members reach early in the morning before sunrise and record the total number of reptiles of each species found in the bucket.

3. Turning of Stones, Rocks and Rotten Trees Process

Nocturnal reptiles and amphibians take shelter or rest hiding themselves under the space of stones or rocks. Therefore, in the day time survey, stones or rocks or rotten fallen trees are turned to locate and record the animals.

4. Study of Basking Behavior

This method of sighting or locating Crocodiles is the most suitable but it can be applied mostly in winter season. In winter, the temperature of the water becomes very low. Crocodiles come outside the lake to enjoying the sunshine and keep warm. Thus, counting of crocodiles becomes very easy at particular areas during this season.

B: Indirect Counting

Presence of signs like fecal pellets, tracks, den or tunnels (egg laying excavation)

Evidences from the impression of finger or footprints, or tail, presence of fecal pellets, tracks and existence of tunnels (egg laying excavation) are collected to record the occurrence of various reptiles.

Fishes

Samples of fishes were collected through gill netting and cast netting. The data collected through these two methods were pooled and this formed the representative sampling of the study site.

RESULTS AND DISCUSSION

In the present study, water quality parameters were analyzed to assess the impact of environmental pollution on aquatic biodiversity, while inventory of vertebrate fauna of Hub Dam was also prepared.

A: Water Quality

Physico – chemical Parameters

The water of the reservoir was found to be clear, odourless and tasteless. During the study period, Air Temperature, Water Temperature, Color, pH, Total Dissolved Solids, COD, BOD, Alkalinity, Salinity, Conductivity, Hardness, Phosphate, Nitrate, Bicarbonate, Sulfate, Chloride, Carbon Dioxide, Dissolved Oxygen, Turbidity, Calcium, Magnesium, Sodium, Potassium and Fluoride along with a few trace metals were recorded viz. Chromium, Iron, Nickel, Copper, Zinc, Cadmium, Lead, Mercury and Arsenic at the Main Dam, Spill Way, Hub Canal and in shallow water.

The results of all selected physico – chemical parameters and trace metals were compared with the given WHO standard values.

Total amount of annual rainfall recorded in 2007 was, 465.6 mm, in 2008, 121.6 mm, in 2009, 279.9 mm and in 2010, 372.9 mm.

Results of all the physico-chemical and trace metals are shown in tables 3 and 4. All the physico – chemical and biological properties are dependant on the temperature as it is essential for aquatic environment. Temperature is important for the aquatic environment, the growth and death of aquatic life depends on maximum and minimum temperatures that fluctuate during summer and winter season. The minimum temperature of water was recorded at 17°C in November and 29°C in June. The maximum temperature in June indicates the season of extreme summer before rain when the DO declines and concentration of salt becomes higher and disturbs the aquatic life. The value of color of water body as per WHO Standard is 6 Hazen and the observed value during present study is under the limits set by WHO. In a previous study Beg *et al.* (1988) the color was recorded in the range 3-6. The mean value of water color observed during 2007 – 2010 in Hazen scale shown in table 4, a slight fluctuation was noted in summer and winter season in all the sampling sites. The pH which is approximately neutral is an indication of unpolluted water (Fakoyode, 2005), here pH of Hub Dam water were 6.8 to 7.5 in all sampling sites which is best for the survival of aquatic organisms, WHO recommended the value of pH 6.5 - 9.0, while Beg *et al.* (1988) reported 7.2 to 8.0. The mean of TDS was observed shown in table 4, these values are under WHO limits, while Beg *et al.* (1988) recorded range 1176 - 1309 mg/l. High value of BOD means decline in DO that could create trouble for survival of the fish and other aquatic organisms. Chemical Oxygen Demand and Biochemical Oxygen Demand were not detected during present investigation. No detection of COD and BOD indicated that no industrial effluent comes in the water body. Higher value of Alkalinity causes higher level of pollution in the water, recorded values of Alkalinity shown in table 4. Alkalinity was previously recorded between 60-90 mg/l (Beg *et al.*, 1988) all recorded values are under the permissible value of WHO standard limits i.e. 50 - 500 mg/l. The mean salinity of all sampling sites was recorded having no adverse impact on aquatic biodiversity. Higher value of Salinity presented during summer may be due to evaporation and low value was recorded during rainy season. Conductivity indicates the level of the soluble salts that are present in water body. Higher value of conductivity indicates highly polluted water not fit for drinking and for supplying but in the present study the results show that the water is not polluted having no adverse effect on aquatic life. The hardness was observed to be within the prescribed value

of WHO standard i.e. 200 – 500 mg/l and estimated value indicates that there is no pollution in water body. Mean value of Nitrate was recorded. The maximum value of Nitrate was recorded in shallow water 0.518 mg/l near plantation area, it slightly exceeded in shallow water because of agricultural land near by this site and water drainage during rains on this site that indicated a slightly exceeded value as compared to other site but its value did not indeed exceed the limit of WHO Standard limits (40 mg/l). Phosphate was not detected during the present study. No concentration of phosphate was recorded in all sampling sites which indicate that water is unpolluted and safe for aquatic biodiversity. Bicarbonate was found to have the higher values than the Sulphate and Chloride in all sampling sites. The mean value of Bicarbonate, Sulphate and Chloride were estimated. In a previous study the bicarbonates were measured ranging between 98-154 mg/l during 1978 – 1985 (Beg *et al.*, 1988). Carbon Dioxide was observed to be very low. In the present study, low level of Carbon dioxide in water as compared to DO indicated favourable conditions for fish. The recorded value of Carbon Dioxide indicates that there is no adverse effect of CO₂ on aquatic organisms. DO were recorded as a high value in rainy period in all sampling sites and lower value were measured after rainy period in winter. These values of DO in all sites are under the limit of WHO Standard that indicates the safe site for aquatic biodiversity survival. In present study, turbidity values were also within acceptable range in all sites. Highest level of turbidity has an adverse effect on aquatic life and high value of turbidity could be due to the discharge of untreated effluent so in the present investigation no such untreated effluents were found. Fluoride is an important constituent for drinking water and for aquatic organisms, if a higher value of Fluoride is present in water it is caused by pollution. Recorded value of Fluoride indicated no adverse effect on aquatic biodiversity and the level of Fluoride is lower than the prescribed value of WHO standards (1.5 mg/l). Calcium plays an important role in aquatic environment. The concentration of Ca was recorded at higher value during summer; minimum concentration was recorded in rainy period due to dilution of Dam water. The higher value of Ca may adversely affect quality of water. The mean value of Magnesium was estimated at 14.189 mg/l. Sodium is an important element in drinking water. During study period the measured value of Sodium is in range 51.192 – 51.305 mg/l. Physiological problems may be produced in water for flora and fauna in aquatic environment due to higher value of Sodium and Potassium (Khuwar and Mastoi, 1996). In the present study, the mean recorded value of K and Na in all sampling sites ranged between 5.37 – 5.52 mg/l. The concentration of cations during present study were estimated in Ca > Na > Mg > K while in previous study the concentration was recorded in this order Na > Ca > Mg > K.

(ii) Trace Metal Analysis

Trace metals get access into aquatic environment from anthropogenic sources and get distributed in water, suspended solids and sediments from the course of their transportation (Olajre and Imeo Kparia, 2000). The mean concentrations of trace metals of Hub Dam were recorded from all sampling sites (Table 4). The concentrations of trace metals are widely found in all samples and with values comparatively higher as per limits of WHO Standard. The Variation in values of trace metals were measured during summer, rainy season and winter. The recorded values of trace metal in water of Hub Dam indicated a little pollution caused due to drainage of water, human waste and other human activities. The recorded value of Cr in present study indicates a higher value as compared to the set limit of WHO Standard i.e. 0.05 mg/l. Fe is a most abundant metal found in natural water body within the range of 0.5 – 50 mg/l (WHO, 1993). The recommended value of WHO standard is 0.3 mg/l and estimated value slightly exceeds the limit of WHO standard. In the present study, Fe level does not have high adverse effect on biodiversity as it is under acceptable limits. Some micro organisms convert ferrous into ferric hydroxide by taking dissolved iron as an energy source (Trivedi, 1993). Nickel is normally found in water bodies by the drainage of sewage water. The WHO Guidline value is 0.02 mg/l and our observed value of Ni was found to exceed the WHO limit. The concentration of Ni was generally found in low level. The level of copper indicated a higher value as per WHO standard i.e. 2.0 mg/l but observed value is acceptable having no adverse effect on aquatic biodiversity. Recorded value of Zn indicates the acceptable range in all sites and did not exceed the WHO limit of 3.0 mg/l. Cadmium toxicity affects kidney, heart and liver (Mench *et al.*, 1997), and even the low concentration of Cd affects aquatic life. In the present study, the mean value of Cd of all sampling sites was slightly higher than WHO Standard i.e. 0.003 mg/l. It can affect aquatic biodiversity and human health. Pb is a normally toxic and cumulative poisonous metal present in water bodies. Pb value was significantly higher than the prescribed value of WHO standard i.e. 0.01 mg/l during present study. Mercury is a highly toxic metal and yearly mean was recorded. Arsenic is a highly toxic metal and it affects the digestive tract, abdominal cavity and muscle tissue in fish with highly adverse effects but in the present investigation no traces of arsenic were observed in sampling sites.

Based on chemical examination, the water of this reservoir was fit for drinking purposes. But there are some agriculture lands near the margins which may in the long run affect the water quality of the reservoir. There are few social impacts like washing of clothes and grazing of cattle. These social impacts may affect and pollute the water but not to a great extent.

(iii) Microbial Analysis

The range of bacteria is determined by heterotrophic count (HPC) in any environment (EPA, 2002). In all water samples, the total bacterial counts were exceeded the limits of WHO standard 1998, of heterotrophic count which is 100 cfu / dl. The microbiological analysis of the reservoir was taken for HPC, total coliforms and faecal coliforms. In year 2007, HPC 1.7×10^3 cfu/ml, total coliforms 6.3×10^1 cfu/ml, and faecal coliforms 6.0×10^1 cfu/ml. In year 2008, HPC $1.6^3 \times 10$ cfu/ml, total

coliforms 7.1×10^1 cfu/ml, and faecal coliforms 5.2×10^1 cfu/ml. In year 2009, HPC 1.5×10^3 cfu/ml, total coliforms 7.2×10^1 cfu/ml, and faecal coliforms 5.0×10^1 cfu/ml, and in year 2010, HPC 1.6×10^3 cfu/ml, total coliforms 6.9×10^1 cfu/ml, and faecal coliforms 4.9×10^1 cfu/ml were measured. The present investigation indicated that the water is microbiologically unfit for drinking purpose as per limit of WHO guideline and needs to be treated before supplying.

Table 3. Mean Composition of Physico-chemical Analysis of all Sampling Sites during 2007-2010.

Parameters	Main Dam	Spill Way	Hub Canal	Shallow Water	WHO's Stand.
Temperature in air (°c)	25.07	25.36	25.1	25.27	-
Temperature in water (°c)	22.315	21.86	21.93	22.2	-
Color (Hazen Scale)	2.65	2.56	2.575	2.55	6 Hazen Scale
pH	7.18	7.1	7.125	7.07	6.5 - 9.0
TDS (mg/l)	514.9	515.84	515.69	516.09	-
COD	ND	ND	ND	ND	-
BOD	ND	ND	ND	ND	-
Alkalinity (mg/l)	74.43	74.52	74.45	74.91	30 - 500 mg / 1
Salinity (mg/l)	0.364	0.346	0.343	0.348	-
Conductivity ($\mu\text{s}/\text{cm}$)	564.21	564.68	560.21	528.41	NS (No standard)
Hardness (mg/l)	177.9	177.51	177.44	177.9	100 - 200 mg / 1
Phosphate	ND	ND	ND	ND	-
Nitrate (mg/l)	0.414	0.416	0.409	0.518	50.0 mg / 1
Bicarbonate (mg/l)	122.96	125.32	123.6	129.6	-
Sulphate (mg/l)	74.28	74.28	73.95	73.97	250 mg / 1
Chloride (mg/l)	97.3	96.83	97.25	97.237	250 mg / 1
Carbon Dioxide (mg/l)	1.41	1.392	1.421	1.41	-
Dissolved Oxygen (mg/l)	4.145	4.162	4.268	4.198	-
Turbidity (NTU)	1.341	1.334	1.4	1.382	5 NTU
Fluoride (mg/l)	0.397	0.394	0.384	0.393	1.5 mg / 1
Calcium (mg/l)	56.08	52.105	52.16	52.555	-
Magnesium (mg/l)	14.189	14.313	14.2	14.4	-
Sodium (mg/l)	51.27	51.302	51.305	51.192	200 mg / 1
Potassium (mg/l)	5.37	5.487	5.383	5.52	-

ND: Not Detected in mg/l

Table 4. Mean Composition of Trace Metal Analysis of all Sampling Sites during 2007-2010.

Metals	Main Dam	Spill Way	Hub Canal	Shallow Water	WHO's Standards
Chromium (mg / l)	0.0825	0.077	0.072	0.085	0.05 mg / 1
Iron (mg / l)	0.759	0.727	0.746	0.74	0.3 mg / 1
Nickel (mg / l)	0.0625	0.07	0.075	0.071	0.02 mg / 1
Copper (mg / l)	2.567	2.621	2.608	2.677	2.0 mg / 1
Zinc (mg / l)	1.208	1.151	1.137	1.242	3.0 mg / 1
Cadmium (mg / l)	0.097	0.09	0.079	0.086	0.003 mg / 1
Lead (mg / l)	0.199	0.187	0.188	0.26	0.01 mg / 1
Mercury (mg / l)	0.015	0.017	0.015	0.016	0.001 mg /
Arsenic (mg / l)	BDL	BDL	BDL	BDL	0.01 mg / 1

BDL = Below Detection Limit

B: Current Inventory

During the study, 16 species of mammals, 160 species of birds, 23 species of reptiles, 3 species of amphibians, 19 species of fishes, and 25 species of plants were recorded from Hub Dam and surrounding areas.

Mammals

Sixteen species of mammals belonging to 6 orders and 10 families were recorded (Table 5).

Asiatic Jackal (*Canis aureus*), Red Fox (*Vulpes vulpes*), Grey Mongoose (*Herpestes edwardsi*), Small Indian Mongoose (*Herpestes javanicus*), House Mouse (*Mus musculus*), Desert Jird (*Meriones hurrianae*), Indian Porcupine (*Hystrix indica*), Five-striped Palm Squirrel (*Funambulus pennantii*), Desert Hedgehog (*Hemiechinus collaris*) and Roof Rat / House Rat (*Rattus rattus*) were recorded as common.

Indian Fox (*Vulpes bengalensis*), Red Fox (*Vulpes vulpes*), Jungle Cat (*Felis chaus*), Small Mongoose (*Herpestes javanicus*) and Grey Mongoose (*Herpestes edwardsi*), Pangolin (*Manis crassicaudata*), Porcupine (*Hystrix indica*), Cairo Spiny Mouse (*Acomys cahirinus*) and Indian Hare (*Lepus nigricollis*) are the important mammals of the area.

Birds

Out of the total of 197 species of birds recorded so far (Table 6), 68 species were new findings and 37 species reported earlier were not recorded during the present study (Table 6).

There are 79 resident species, 72 winter visitors, 03 summer breeding visitors, 01 summer visitor and 06 passage migrants.

Waterbirds form the largest group of the birds recorded

comprising of 71 species, while there are 41 species of passerines, 27 species of birds of prey, 07 species of game birds and 14 species of other birds recorded during the present study.

Garganey, Demoiselle Crane, Kentish Plover, Yellow Wagtail, and Black – headed Bunting were recorded as passage migrants. Common Swift and Blue-cheeked Bee-eater were recorded as summer breeding visitors, while Common Tern was recorded as a summer visitor.

The most common birds of the area include Little Grebe, Large Cormorant, Grey Heron, Pond Heron, Large Egret, Little Egret, Pintail, Shoveller, Common Pochard, Black Kite, Marsh Harrier, Black Headed Gull, Little Tern, Ring Dove, House Swift and Indian Pied Kingfisher.

WATER BIRD CENSUS

The winter visitors are mainly water birds which migrate to Pakistan along the Central Asian / Indus Flyway during the migratory season ranging from October to April. January is the peak season for these birds. Annual Waterbird Censuses have been undertaken on Hub Dam during 2000 to 2004 and in 2010, while from 2005 to 2009 the censuses were not undertaken (Fig.6).

The population of the waterbirds has declined drastically during recent years as compared to earlier records mainly due to disturbances and commercial fishing activities in the reservoir.

Reptiles

Twenty three species of reptiles were recorded. The common species of reptiles of the area include Spotted Indian House Gecko (*Hemidactylus leschnaultii*), Yellow-bellied House Gecko (*Hemidactylus flaviviridis*), Common Tree Lizard (*Calotes versicolor*) and Indian

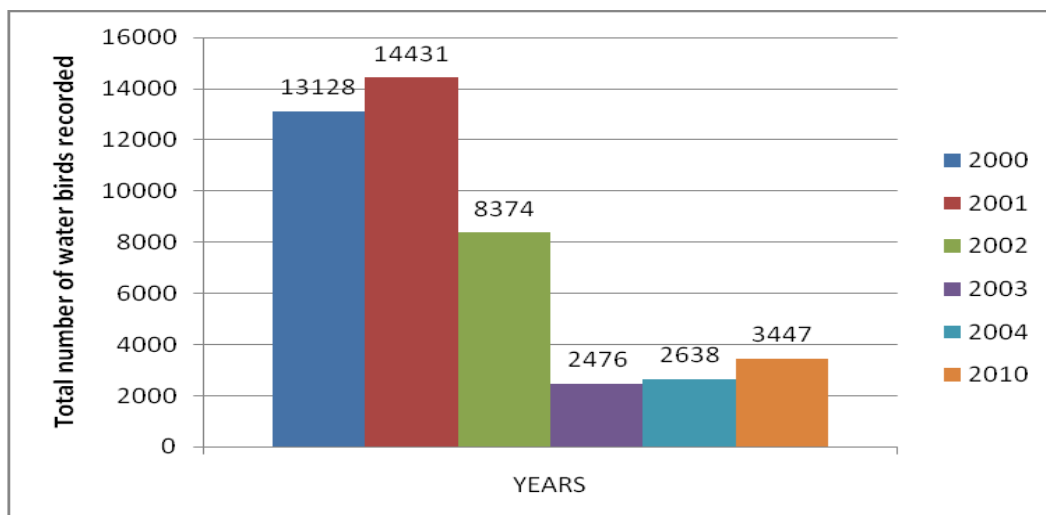


Fig. 6. Graph showing results of annual Waterbird census at Hub Dam.

Fringed-toad Lizard (*Acanthodactylus cantoris*) (Table 7). Marsh Crocodile (*Crocodylus palustris*), Brilliant Agama (*Trapelus agilis*), Indian Spiny – tailed Lizard (*Saura hardwickii*), Indian Monitor Lizard (*Varanus bengalensis*), Indian Cobra (*Naja naja*), Indian Fringed toed Lizard (*Acanthodactylus cantoris*), Indian Desert Monitor (*Varanus griseus*) Indian Sand Boa (*Eryx johnii*), Common Krait (*Bungarus caeruleus*) and Saw Scaled

Viper (*Echis carinatus*) are the important species of reptiles of the area.

Amphibians

Three species of amphibians were recorded viz. Indus Valley Toad (*Bufo stomaticus*), Skittering Frog (*Euphlyctis cyanophlyctis*) and Burrowing Frog (*Sphaerotheca breviceps*) (Table 8).

Table 5. List of Mammals Recorded from Hub Dam.

S. No.	Order	Family	Scientific Name	Common Name	Status
01	Insectivora	Erinaceidae	<i>Hemiechinus collaris</i>	Long eared or Desert Hedge hog	C
02	Chiroptera	Pteropidae	<i>Rousettus egypciacus</i>	Egyptain Bat	L/c
03	Carnivora	Canidae	<i>Canis aureus</i>	Asiatic Jackal	C
04	Carnivora	Canidae	<i>Vulpes bengalensis</i>	Indian Fox	L/c
05	Carnivora	Canidae	<i>Vulpes vulpes</i>	Red fox	C
06	Carnivora	Herpestidae	<i>Herpestes edwardsi</i>	Grey Mongoose	C
07	Carnivora	Herpestidae	<i>Herpestes javanicus</i>	Small Indian Mongoose	C
08	Carnivora	Felidae	<i>Felis chaus</i>	Jungle Cat	R
09	Lagomorpha	Leporidae	<i>Lepus nigricollis</i>	Indian Hare	L/c
10	Pholidota	Manidae	<i>Manis crassicaudata</i>	Indian Pangolin	R
11	Rodentia	Sciuridae	<i>Funambulus pennanti</i>	Five striped Palm Squirrel	C
12	Rodentia	Hystricidae	<i>Hystrix indica</i>	Indian Porcupine	C
13	Rodentia	Muridae	<i>Rattus rattus</i>	Roof Rat / House Rat	L/c
14	Rodentia	Muridae	<i>Mus musculus</i>	House mouse	C
15	Rodentia	Muridae	<i>Acomys cahirinus</i>	Cairo Spiny Mouse	L/c
16	Rodentia	Muridae	<i>Meriones hurrianae</i>	Desert Jird	C

Status: L / c = Less common C = Common R= Rare

Table 6. Consolidated List of Birds recorded from the Hub Dam.

S. No.	Order	Family	Scientific Name	Common Name	Occurrence	Status	Recorded earlier (Ghalib et al., 2000)	Recorded during present study (2007-2010)
1	Podicipediformes	Podicipedidae	<i>Podiceps cristatus</i>	Great Crested Grebe	WV	L/c	+	+
2	Podicipediformes	Podicipedidae	<i>Podiceps grisegena</i>	Red necked Grebe	WV	Ra	+	-
3	Podicipediformes	Podicipedidae	<i>Podiceps nigricollis</i>	Black necked Grebe	WV	L / c	+	+
4	Podicipediformes	Podicipedidae	<i>Tachybaptus ruficollis</i>	Little Grebe	R	C	+	+
5	Pelecaniformes	Pelecanidae	<i>Pelecanus onocrotalus</i>	Great White Pelican	WV	L / c	+	+
6	Pelecaniformes	Pelecanidae	<i>Pelecanus crispus</i>	Dalmatian Pelican	WV	Ra	+	+
7	Pelecaniformes	Phalacrocoracidae	<i>Phalacrocorax carbo</i>	Large Cormorant	WV	C	+	+
8	Pelecaniformes	Phalacrocoracidae	<i>Phalacrocorax niger</i>	Little Cormorant	R	C	+	+
9	Pelecaniformes	Anhingidae	<i>Anhinga rufa</i>	Indian Darter	R	L / c	-	+
10	Ciconiiformes	Ardeidae	<i>Ardea cinerea</i>	Grey Heron	WV	C	+	+

Continued...

Table 7. Continue...

S. No.	Order	Family	Scientific Name	Common Name	Occurrence	Status	Recorded earlier (Ghalib et al., 2000)	Recorded during present study (2007-2010)
11	Ciconiiformes	Ardeidae	<i>Ardea purpurea</i>	Purple Heron	R	L / c	+	+
12	Ciconiiformes	Ardeidae	<i>Ardeola grayii</i>	Pond Heron	R	C	+	+
13	Ciconiiformes	Ardeidae	<i>Egretta alba</i>	Large Egret	WV/R	C	+	+
14	Ciconiiformes	Ardeidae	<i>Egretta intermedia</i>	Median Egret	R	L/c	+	-
15	Ciconiiformes	Ardeidae	<i>Egretta garzetta</i>	Little Egret	R	C	+	+
16	Ciconiiformes	Ardeidae	<i>Egretta gularis</i>	Indian Reef Heron	R	L / c	-	+
17	Ciconiiformes	Ardeidae	<i>Ixobrychus minutus</i>	Little Bittern	R	L/c	+	-
18	Ciconiiformes	Ardeidae	<i>Dupetor flavicollis</i>	Black Bittern	R	Ra	+	-
19	Ciconiiformes	Threskiornithidae	<i>Plegadis falcinellus</i>	Glossy Ibis	R/WV	L / c	+	+
20	Ciconiiformes	Threskiornithidae	<i>Platalea leucorodia</i>	Spoonbill	WV/R	L / c	+	+
21	Ciconiiformes	Phoenicopteridae	<i>Phoenicopterus ruber</i>	Great Flamingo	NBR	L / c	+	+
22	Anseriformes	Anatidae	<i>Anser anser</i>	Greylag Goose	WV	Ra	+	-
23	Anseriformes	Anatidae	<i>Tadorna tadorna</i>	Common Shelduck	WV	L / c	+	+
24	Anseriformes	Anatidae	<i>Anas angustirostris</i>	Marbled t\Teal	WV	Ra	+	-
25	Anseriformes	Anatidae	<i>Anas acuta</i>	Pintail	WV	C	+	+
26	Anseriformes	Anatidae	<i>Anas crecca</i>	Common Teal	WV	C	+	+
27	Anseriformes	Anatidae	<i>Anas platyrhynchos</i>	Mallard	WV	L / c	+	+
28	Anseriformes	Anatidae	<i>Anas strepera</i>	Gadwall	WV	L / c	+	+
29	Anseriformes	Anatidae	<i>Anas penelope</i>	Wigeon	WV	L / c	+	+
30	Anseriformes	Anatidae	<i>Anas querquedula</i>	Garganey	PM	Ra	+	+
31	Anseriformes	Anatidae	<i>Anas clypeata</i>	Shoveller	WV	C	+	+
32	Anseriformes	Anatidae	<i>Netta rufina</i>	Red Crested Pochard	WV	Ra	+	+
33	Anseriformes	Anatidae	<i>Aythya ferina</i>	Common Pochard	WV	C	+	+
34	Anseriformes	Anatidae	<i>Aythya nyroca</i>	Ferruginous Duck	WV	Ra	+	+
35	Anseriformes	Anatidae	<i>Aythya fuligula</i>	Tufted Duck	WV	L / c	+	+
36	Falconiformes	Accipitridae	<i>Elanus caeruleus</i>	Black winged Kite	R	L / c	+	+
37	Falconiformes	Accipitridae	<i>Milvus migrans</i>	Black Kite	R	C	+	+

Continued...

Table 7. Continue...

S. No.	Order	Family	Scientific Name	Common Name	Occurrence	Status	Recorded earlier (Ghalib et al., 2000)	Recorded during present study (2007-2010)
38	Falconiformes	Accipitridae	<i>Haliastur indus</i>	Brahminy Kite	R	L / c	-	+
39	Falconiformes	Accipitridae	<i>Accipiter badius</i>	Central Asian Shikra	R	L/c	+	+
40	Falconiformes	Accipitridae	<i>Buteo rufinus</i>	Long legged Buzzard	WV	L / c	-	+
41	Falconiformes	Accipitridae	<i>Hieraetus pennatus</i>	Booted Hawk-Eagle	WV	L / c	-	+
42	Falconiformes	Accipitridae	<i>Aquila heliaca</i>	Imperial Eagle	WV	L / c	+	+
43	Falconiformes	Accipitridae	<i>Aquila rapax</i>	Tawny Eagle	R	L / c	-	+
44	Falconiformes	Accipitridae	<i>Aquila nipalensis</i>	Steppe Eagle	WV	L / c	-	+
45	Falconiformes	Accipitridae	<i>Hieraetus fasciatus</i>	Bonelli's Eagle	R	Ra	+	-
46	Falconiformes	Accipitridae	<i>Aquila clanga</i>	Greater Spotted Eagle	WV	L / c	-	+
47	Falconiformes	Accipitridae	<i>Haliaeetus leucoryphus</i>	Pallas's Fishing Eagle	R	L / c	-	+
48	Falconiformes	Accipitridae	<i>Aegypius monachus</i>	Black Vulture / Cinereous Vulture	R	L/c	+	-
49	Falconiformes	Accipitridae	<i>Gyps fulvus</i>	Griffon Vulture	R	L/c	+	+
50	Falconiformes	Accipitridae	<i>Gyps bengalensis</i>	White backed Vulture	R	Ra	+	-
51	Falconiformes	Accipitridae	<i>Neophron percnopterus</i>	Egyptian Vulture	R & B	L/c	+	+
52	Falconiformes	Accipitridae	<i>Circus cyaneus</i>	Hen Harrier	WV	L / c	-	+
53	Falconiformes	Accipitridae	<i>Circus macrourus</i>	Pallid Harrier	WV	L/c	+	+
54	Falconiformes	Accipitridae	<i>Circus pygargus</i>	Montagu's Harrier	WV	L / c	-	+
55	Falconiformes	Accipitridae	<i>Circus aeruginosus</i>	Marsh Harrier	WV	C	+	+
56	Falconiformes	Accipitridae	<i>Circaetus gallicus</i>	Short-toed Eagle	R	L / c	+	+
57	Falconiformes	Pandionidae	<i>Pandion haliaetus</i>	Osprey	WV	L / c	+	+
58	Falconiformes	Falconidae	<i>Falco jugger</i>	Lagger Falcon	R	L / c	-	+
59	Falconiformes	Falconidae	<i>Falco columbarius</i>	Pallid Merlin	WV	L / c	-	+
60	Falconiformes	Falconidae	<i>Falco tinnunculus</i>	Common Kestrel	R/WV	L / c	-	+
61	Galliformes	Phasianidae	<i>Francolinus francolinus</i>	Black Partridge	R	Ra	-	+
62	Galliformes	Phasianidae	<i>Francolinus pondicerianus</i>	Grey Partridge	R	L / c	-	+

Continued...

Table 7. Continue...

S. No.	Order	Family	Scientific Name	Common Name	Occurrence	Status	Recorded earlier (Ghalib et al., 2000)	Recorded during present study (2007-2010)
63	Gruiformes	Gruidae	<i>Grus grus</i>	Common Crane	M	L / c	+	+
64	Gruiformes	Gruidae	<i>Anthropoides virgo</i>	Demoiselle Crane	PM	L / c	+	+
65	Gruiformes	Rallidae	<i>Rallus aquaticus</i>	Water Rail	WV	L / c	-	+
66	Gruiformes	Rallidae	<i>Amaurornis phoenicurus</i>	White-breasted Water Hen	R	C	-	+
67	Gruiformes	Rallidae	<i>Gallinula chloropus</i>	Indian Moorhen	R	C	-	+
68	Gruiformes	Rallidae	<i>Fulica atra</i>	Coot	WV	C	+	+
69	Charadriiformes	Jacanidae	<i>Hydrophasianus chirurgus</i>	Pheasant Tailed Jacana	R	L/c	+	+
70	Charadriiformes	Charadriidae	<i>Vanellus leucurus</i>	White-tailed Lapwing	WV	L / c	+	+
71	Charadriiformes	Charadriidae	<i>Vanellus gregarius</i>	Sociable Lapwing	WV	Ra	+	-
72	Charadriiformes	Charadriidae	<i>Vanellus vanellus</i>	Lapwing	WV	Ra	+	-
73	Charadriiformes	Charadriidae	<i>Vanellus indicus</i>	Red wattled Lapwing	R	C	+	+
74	Charadriiformes	Charadriidae	<i>Vanellus malabaricus</i>	Yellow-wattled Lapwing	SBV	L / c	+	+
75	Charadriiformes	Charadriidae	<i>Charadrius leschenaultii</i>	Large Sand Plover	WV	L / c	+	+
76	Charadriiformes	Charadriidae	<i>Charadrius hiaticula</i>	Ringed Plover	WV	L / c	+	+
77	Charadriiformes	Charadriidae	<i>Charadrius dubius</i>	Little Ringed Plover	R	L / c	+	+
78	Charadriiformes	Charadriidae	<i>Charadrius alexandrinus</i>	Kentish Plover	SBV/W V/PM	L / c	-	+
79	Charadriiformes	Charadriidae	<i>Charadrius mongolus</i>	Lesser Sand Plover	WV	L / c	-	+
80	Charadriiformes	Scolopacidae	<i>Numenius phaeopus</i>	Whimbrel	WV	L / c	-	+
81	Charadriiformes	Scolopacidae	<i>Numenius arquata</i>	Curlew	WV	L / c	-	+
82	Charadriiformes	Scolopacidae	<i>Limosa limosa</i>	Black Tailed Godwit	WV	L / c	+	+
83	Charadriiformes	Scolopacidae	<i>Limosa lapponica</i>	Bartailed Godwit	WV	L / c	-	+
84	Charadriiformes	Scolopacidae	<i>Tringa totanus</i>	Common Redshank	WV	L / c	+	+
85	Charadriiformes	Scolopacidae	<i>Tringa stagnatilis</i>	Marsh Sandpiper	WV	L / c	-	+
86	Charadriiformes	Scolopacidae	<i>Tringa nebularia</i>	Green Shank	WV	L / c	-	+
87	Charadriiformes	Scolopacidae	<i>Tringa hypoleucos</i>	Common Sandpiper	WV	C	+	+
88	Charadriiformes	Scolopacidae	<i>Arenaria interpres</i>	Turn Stone	WV	L/c	+	-

Continued...

Table 7. Continue...

S. No.	Order	Family	Scientific Name	Common Name	Occurrence	Status	Recorded earlier (Ghalib et al., 2000)	Recorded during present study (2007-2010)
89	Charadriiformes	Scolopacidae	<i>Calidris minutus</i>	Little Stint	WV	C	—	+
90	Charadriiformes	Scolopacidae	<i>Calidris temminckii</i>	Temminck's Stint	WV	L / c	—	+
91	Charadriiformes	Scolopacidae	<i>Philomachus pugnax</i>	Ruff	WV	L / c	—	+
92	Charadriiformes	Rostratulidae	<i>Rostratula benghalensis</i>	Painted Snipe	R	L/c	—	+
93	Charadriiformes	Recurvirostridae	<i>Himantopus himantopus</i>	Black winged Stilt	R	C	+	+
94	Charadriiformes	Burhinidae	<i>Burhinus oedicnemus</i>	Stone Curlew	R	Ra	+	—
95	Charadriiformes	Glareolidae	<i>Cursorius cursor</i>	Cream Coloured Courser	R	L / c	+	+
96	Charadriiformes	Laridae	<i>Larus argentatus</i>	Herring Gull	WV	L / c	+	+
97	Charadriiformes	Laridae	<i>Larus fuscus</i>	Lesser Black backed Gull	WV	L / c	—	+
98	Charadriiformes	Laridae	<i>Larus ichthyaetus</i>	Great Black headed Gull	WV	L / c	—	+
99	Charadriiformes	Laridae	<i>Larus brunnicephalus</i>	Brown Headed Gull	WV	L / c	—	+
100	Charadriiformes	Laridae	<i>Larus ridibundus</i>	Black Headed Gull	WV	C	+	+
101	Charadriiformes	Laridae	<i>Larus canus</i>	Common Gull	WV	L / c	—	+
102	Charadriiformes	Sternidae	<i>Chlidonias hybrida</i>	Indian Whiskered Tern	M	L / c	+	+
103	Charadriiformes	Sternidae	<i>Chlidonias leucopterus</i>	White – winged Black Tern	PM	L / c	—	+
104	Charadriiformes	Sternidae	<i>Gelochelidon nilotica</i>	Gull bellied Tern	WV	Ra	+	+
105	Charadriiformes	Sternidae	<i>Sterna aurantia</i>	Indian River Tern	R	L / c	—	+
106	Charadriiformes	Sternidae	<i>Sterna hirundo</i>	Common Tern	SV	L / c	—	+
107	Charadriiformes	Sternidae	<i>Sterna acuticauda</i>	Black – bellied Tern	R	L / c	—	+
108	Charadriiformes	Sternidae	<i>Sterna albifrons</i>	Little Tern	R	C	+	+
109	Charadriiformes	Sternidae	<i>Sterna sandvicensis</i>	Sandwich Tern	M	L / c	—	+
110	Columbiformes	Pteroclidae	<i>Pterocles exustus</i>	Chestnut-bellied Sandgrouse	R	Ra	—	+
111	Columbiformes	Pteroclidae	<i>Pterocles alchata</i>	Painted Sandgrouse	R	Ra	—	+
112	Columbiformes	Columbidae	<i>Columba livia</i>	Blue Rock Pigeon	R	C	—	+
113	Columbiformes	Columbidae	<i>Streptopelia decaocto</i>	Ring Dove	R	C	+	+

Continued...

Table 7. Continue...

S. No.	Order	Family	Scientific Name	Common Name	Occurrence	Status	Recorded earlier (Ghalib et al., 2000)	Recorded during present study (2007-2010)
114	Columbiformes	Columbidae	<i>Streptopelia senegalensis</i>	Little Brown or Senegal Dove	R	C	—	+
115	Psittaciformes	Psittacidae	<i>Psittacula krameri</i>	Rose ringed Parakeet	R	L / c	+	+
116	Cuculiformes	Cuculidae	<i>Eudynamys scolopacea</i>	Indian Koel	R	L / c	+	+
117	Strigiformes	Tytonidae	<i>Tyto alba</i>	Indian Barn Owl	R	L / c	—	+
118	Strigiformes	Strigidae	<i>Bubo bubo</i>	Eagle Owl	R	L / c	+	+
119	Strigiformes	Strigidae	<i>Bubo coromandus</i>	Dusky Eagle or Horned Owl	WV	Ra	—	+
120	Strigiformes	Strigidae	<i>Athene brama</i>	Spotted Owlet	R	L / c	+	+
121	Strigiformes	Strigidae	<i>Asio otus</i>	Long eared Owl	WV	L / c	—	+
122	Caprimulgiformes	Caprimulgidae	<i>Caprimulgus europaeus</i>	European Nightjar	R	Ra	+	+
123	Caprimulgiformes	Caprimulgidae	<i>Caprimulgus mahrattensis</i>	Syke's Nightjar	R	L / c	+	—
124	Caprimulgiformes	Caprimulgidae	<i>Caprimulgus asiaticus</i>	Indian Nightjar	R	L/c	+	+
125	Apodiformes	Apodidae	<i>Apus apus</i>	Common Swift	SBV	L/c	+	—
126	Apodiformes	Apodidae	<i>Tachymarptis melba</i>	Alpine Swift	M	L / c	+	—
127	Apodiformes	Apodidae	<i>Apus affinis</i>	House Swift	SV	Ra	—	+
128	Coraciiformes	Alcedinidae	<i>Ceryle rudis</i>	Indian Pied Kingfisher	R	C	+	+
129	Coraciiformes	Alcedinidae	<i>Alcedo atthis</i>	Indian Small Blue Kingfisher	R	L / c	+	+
130	Coraciiformes	Alcedinidae	<i>Halcyon smyrnensis</i>	White breasted Kingfisher	R	C	—	+
131	Coraciiformes	Meropidae	<i>Merops persicus</i>	Blue Cheeked Bee-eater	SBV/P M	L / c	+	+
132	Coraciiformes	Meropidae	<i>Merops orientalis</i>	Common Bee-eater	R	L/c	+	—
133	Coraciiformes	Coraciidae	<i>Coracias benghalensis</i>	Roller or Blue Jay	R	C	+	+
134	Coraciiformes	Upupidae	<i>Upupa epops</i>	Hoopoe	WV	C	—	+
135	Piciformes	Picidae	<i>Dinopium benghalense</i>	Sind Golden Backed Woodpecker	R	L / c	—	+
136	Piciformes	Picidae	<i>Dendrocopos assimilis</i>	Sind pied Woodpecker	R	C	+	+
137	Passeriformes	Alaudidae	<i>Mirafra erythroptera</i>	Indian Bush Lark / Sind Redwinged Bush Lark	R	L/c	+	+
138	Passeriformes	Alaudidae	<i>Eremopterix grisea</i>	Ashy Crowned Finch-Lark	R	C	+	+

Continued...

Table 7. Continue...

S. No.	Order	Family	Scientific Name	Common Name	Occurrence	Status	Recorded earlier (Ghalib <i>et al.</i> , 2000)	Recorded during present study (2007-2010)
139	Passeriformes	Alaudidae	<i>Eremopterix nigriceps</i>	Black Crowned Finch Lark	R	C	+	+
140	Passeriformes	Alaudidae	<i>Ammomanes desertri</i>	Desert Finch Lark	R	C	-	+
141	Passeriformes	Alaudidae	<i>Alaemon alaudipes</i>	Greater Hoopoe Lark	R	R	+	-
142	Passeriformes	Alaudidae	<i>Calandrella rufescens</i>	Lesser Short-Toed Lark	WV	L / c	-	+
143	Passeriformes	Alaudidae	<i>Galerida cristata</i>	Crested Lark	R	C	+	+
144	Passeriformes	Hirundinidae	<i>Riparia riparia</i>	Collared Sand Martin	WV	C	-	+
145	Passeriformes	Hirundinidae	<i>Hirundo concolor</i>	Dusky Crag Martin	R	L / c	-	+
146	Passeriformes	Hirundinidae	<i>Hirundo rupestris</i>	Crag Martin	R	L/c	+	-
147	Passeriformes	Hirundinidae	<i>Hirundo fuligula</i>	Pale Crag or Rock Martin	R	L/c	+	-
148	Passeriformes	Hirundinidae	<i>Hirundo smithi</i>	Wire-tailed Swallow	R	L / c	-	+
149	Passeriformes	Hirundinidae	<i>Hirundo daurica</i>	Redrumped Swallow	R	L/c	+	-
150	Passeriformes	Laniidae	<i>Lanius isabellinus</i>	Isabelline Shrike	PM	L/c	+	-
151	Passeriformes	Laniidae	<i>Lanius excubitor</i>	Grey Shrike	R	L / c	+	+
152	Passeriformes	Laniidae	<i>Lanius vittatus</i>	Bay backed Shrike	R	C	-	+
153	Passeriformes	Laniidae	<i>Lanius schach</i>	Rufous-backed Shrike	R	L / c	-	+
154	Passeriformes	Dicruridae	<i>Dicrurus adsimilis</i>	King Crow / Black Drongo	R	C	+	+
155	Passeriformes	Sturnidae	<i>Acridotheres tristis</i>	Common Myna	R	C	+	-
156	Passeriformes	Sturnidae	<i>Acridotheres ginginianus</i>	Bank Myna	R	C	+	+
157	Passeriformes	Sturnidae	<i>Sturnus roseus</i>	Rosy Starling	WV	L/c	+	+
158	Passeriformes	Corvidae	<i>Dendrocitta vagabunda</i>	Indian Tree - pie	R	L/c	+	-
159	Passeriformes	Corvidae	<i>Corvus splendens</i>	Sindh House Crow	R	C	+	+
160	Passeriformes	Bombycillidae	<i>Hypocolius ampelinus</i>	Grey Hypocolius	WV	Ra	+	-
161	Passeriformes	Campephagidae	<i>Tephrodornis pondicerianus</i>	Common Wood Shrike	R	L / c	+	+
162	Passeriformes	Campephagidae	<i>Pericrocotus cinnamomeus</i>	Small Minivet	R	L/c	+	-
163	Passeriformes	Pyconotidae	<i>Pycnonotus leucogenys</i>	White Cheeked Bulbul	R	C	+	+

Continued...

Table 7. Continue...

S. No.	Order	Family	Scientific Name	Common Name	Occurrence	Status	Recorded earlier (Ghalib et al., 2000)	Recorded during present study (2007-2010)
164	Passeriformes	Pyconotidae	<i>Pycnonotus cafer</i>	Red-vented Bulbul	R	C	-	+
165	Passeriformes	Timaliidae	<i>Turdoides caudatus</i>	Common Babbler	R	C	+	-
166	Passeriformes	Timaliidae	<i>Turdoides striatus</i>	Sind Jungle Babbler	R	C	-	+
167	Passeriformes	Sylviidae	<i>Prinia buchanani</i>	Rufous Fronted Wren Warbler	WV	L / c	+	+
168	Passeriformes	Sylviidae	<i>Prinia burnesii</i>	Long tailed Grass Warbler	R	L / c	-	+
169	Passeriformes	Sylviidae	<i>Sylvia curruca</i>	Lesser Whitethroat	WV	L / c	-	+
170	Passeriformes	Sylviidae	<i>Sylvia nana</i>	Desert Warbler	WV	C	-	+
171	Passeriformes	Sylviidae	<i>Phylloscopus sindianus</i>	Sind Chiffchaff	WV	C	-	+
172	Passeriformes	Sylviidae	<i>Phylloscopus neglectus</i>	Plain Willow Warbler	WV	Ra	+	-
173	Passeriformes	Sylviidae	<i>Acrocephalus dumetorum</i>	Blyth's Reed Warbler	PM	L/c	+	-
174	Passeriformes	Sylviidae	<i>Scotocerca inquieta</i>	Streaked Scrub Warbler	R	L/c	+	+
175	Passeriformes	Turdidae	<i>Saxicola caprata</i>	Pied Bush Chat	R	C	-	+
176	Passeriformes	Turdidae	<i>Oenanthe isabellina</i>	Isabelline Wheatear	WV	L/c	+	+
177	Passeriformes	Turdidae	<i>Oenanthe xanthoprymnna</i>	Red tailed Wheatear	WV	L/c	+	-
178	Passeriformes	Turdidae	<i>Oenanthe deserti</i>	Desert Wheatear	WV	L / c	+	+
179	Passeriformes	Turdidae	<i>Oenanthe picata</i>	Eastern Pied Wheatear	WV	L/c	+	+
180	Passeriformes	Turdidae	<i>Oenanthe albomiger</i>	Hume's Wheatear	R	L/c	+	+
181	Passeriformes	Turdidae	<i>Saxicoloides fulicata</i>	Indian Robin	R	C	-	+
182	Passeriformes	Turdidae	<i>Turdus philomelos</i>	Song Thrush	WV	Ra	+	-
183	Passeriformes	Motacillidae	<i>Anthus similis</i>	Long billed Pipit	R	Ra	+	-
184	Passeriformes	Motacillidae	<i>Motacilla flava</i>	Yellow Wagtail	PM	C	+	+
185	Passeriformes	Motacillidae	<i>Motacilla alba</i>	White or Pied Wagtail	WV	C	-	+
186	Passeriformes	Motacillidae	<i>Motacilla cinerea</i>	Grey Wagtail	WV	L / c	-	+
187	Passeriformes	Motacillidae	<i>Motacilla citreola</i>	Citrine Wagtail	WV	Ra	+	-
188	Passeriformes	Nectariniidae	<i>Nectarinia asiatica</i>	Purple Sunbird	R	C	+	+
189	Passeriformes	Passeridae	<i>Passer domesticus</i>	House Sparrow	R	C	-	+

Continued...

Table 7. Continue...

S. No.	Order	Family	Scientific Name	Common Name	Occurrence	Status	Recorded earlier (Ghalib et al., 2000)	Recorded during present study (2007-2010)
190	Passeriformes	Passeridae	<i>Passer hispaniolensis</i>	Spanish Sparrow	R	L/c	+	-
191	Passeriformes	Passeridae	<i>Passer pyrrhonotus</i>	Sind Jungle Sparrow	R	C	-	+
192	Passeriformes	Passeridae	<i>Petronia xanthocollis</i>	Yellow throated Sparrow	R	C	+	+
193	Passeriformes	Estrildidae	<i>Lonchura malabarica</i>	White throated Munia	R	L / c	+	+
194	Passeriformes	Fringillidae	<i>Bucanetes githagineus</i>	Trumpeter Finch	R	L/c	+	-
195	Passeriformes	Emberizidae	<i>Emberiza melanocephala</i>	Black-headed Bunting	PM	L / c	+	+
196	Passeriformes	Emberizidae	<i>Emberiza buchanani</i>	Grey – necked Bunting	WV	L/c	+	-
197	Passeriformes	Emberizidae	<i>Emberiza striolata</i>	House Bunting	R	L/c	+	-

Numbers of birds recorded

Total species of birds recorded (years 2000 +2010) =197, Total species of birds recorded in the present study = 160

Total species of birds recorded previously (year 2000) = 128

Total No. of species of birds recorded during the previous studies but not recorded during present study =37, New findings = 68

Legend:

Occurrence: R = Resident WV = Winter visitor SBV = Summer Breading Visitor PM = Passage migrant SV = Summer Visitor

Status: L / c = Less common C = Common Ra= Rare

Table 7. List of Reptiles Recorded from Hub Dam.

S. No.	Order	Family	Scientific Name	Common Name	Status
01	Chelonia	Emydidae	<i>Hardella thurjii</i>	Brahminy River Turtle	L/c
02	Crocodylia	Crocodylidae	<i>Crocodylus palustris</i>	Marsh Crocodile	R
03	Squamata	Gekkonidae	<i>Eublepharus maculatus</i>	Fat tailed Gecko	L/c
04	Squamata	Gekkonidae	<i>Hemidactylus brooki</i>	Spotted Indian House Gecko	C
05	Squamata	Gekkonidae	<i>Hemidactylus leschnaultii</i>	Bark Gecko	L/c
06	Squamata	Gekkonidae	<i>Hemidactylus flaviviridis</i>	Yellow-bellied House Gecko	C
07	Squamata	Agamidae	<i>Trapelus megalonyx</i>	Afghan Ground Agama	L/c
08	Squamata	Agamidae	<i>Trapelus agilis</i>	Brilliant Agama	L/c
09	Squamata	Agamidae	<i>Laudakia nupta</i>	Yellow-headed Agama	L/c
10	Squamata	Agamidae	<i>Calotes versicolor</i>	Common Tree Lizard	C
11	Squamata	Agamidae	<i>Nouveumeces blythianus</i>	Orange tail Skink	L/c
12	Squamata	Uromastycidae	<i>Uromastix hardwickii</i>	Indian Spiny-tailed Lizard	L/c
13	Squamata	Varanidae	<i>Varanus bengalensis</i>	Indian Monitor Lizard	L/c
14	Squamata	Varanidae	<i>Varanus griseus</i>	Indian Desert Monitor	L/c
15	Squamata	Lacertidae	<i>Acanthodactylus cantoris</i>	Indian Fringed-toed Lizard	C
16	Squamata	Typhlopidae	<i>Typhlops porrectus</i>	Slender Blind Snake	L/c
17	Squamata	Boidae	<i>Eryx johnii</i>	Indian Sand Boa	L/c
18	Squamata	Boidae	<i>Psammophis candanura</i>	Indian Sand Snake	L/c
19	Squamata	Colubridae	<i>Platyceps rhodorachis</i>	Cliff Racer	L/c
20	Squamata	Colubridae	<i>Platyceps vertromaculatus</i>	Glossy bellied Racer	L/c
21	Squamata	Elapidae	<i>Naja naja</i>	Indian Cobra	L/c
22	Squamata	Elapidae	<i>Bungarus caeruleus</i>	Common Krait	R
23	Squamata	Viperidae	<i>Echis carinatus</i>	Saw Scaled Viper	L/c

Status: L / c = Less common

C = Common

Ra = Rare

Table 8. List of Amphibians Recorded from Hub Dam

S. No.	Order	Family	Scientific Name	Common Name	Status
01	Anura	Bufonidae	<i>Bufo stomaticus</i>	Indus Valley Toad	L/c
02	Anura	Ranidae	<i>Euphlyctis cyanophlyctis</i>	Skittering Frog	C
03	Anura	Ranidae	<i>Sphaerotheca breviceps</i>	Burrowing Frog	L/c

Status: L / c = Less common C = Common R= Rare

Table 9. List of Fishes Recorded from Hub Dam.

S. No.	Order	Family	Scientific Name
01	Clupeiformes	Clupeidae	<i>Gadusia chapra</i>
02	Osteoglossiformes	Notopteridae	<i>Notopterus chitala</i>
03	Osteoglossiformes	Notopteridae	<i>Notopterus notopterus</i>
04	Cypriniformes	Cyprinidae	<i>Salmostoma bacaila</i>
05	Cypriniformes	Cyprinidae	<i>Barbodes sarana</i>
06	Cypriniformes	Cyprinidae	<i>Catla catla</i>
07	Cypriniformes	Cyprinidae	<i>Cirrhinus mrigala</i>
08	Cypriniformes	Cyprinidae	<i>Cirrhinus reba</i>
09	Cypriniformes	Cyprinidae	<i>Labeo dyocheilus</i>
10	Cypriniformes	Cyprinidae	<i>Labeo gonius</i>
11	Cypriniformes	Cyprinidae	<i>Labeo rohita</i>
12	Cypriniformes	Cyprinidae	<i>Labeo calbasu</i>
13	Cypriniformes	Cyprinidae	<i>Labeo sindensis</i>
14	Cypriniformes	Cyprinidae	<i>Labeo diplostomus</i>
15	Cypriniformes	Cyprinidae	<i>Cheila bacaila</i>
16	Cypriniformes	Cyprinidae	<i>Cheila laubuca</i>
17	Cypriniformes	Cyprinidae	<i>Danio devario</i>
18	Cypriniformes	Cyprinidae	<i>Tor putitora</i>
19	Cypriniformes	Cyprinidae	<i>Barbus ticto</i>
20	Cypriniformes	Cyprinidae	<i>Barbus sarana</i>
21	Cypriniformes	Cyprinidae	<i>Ctenopharyngodon idella</i>
22	Cypriniformes	Cyprinidae	<i>Cyprinus carpio</i>
23	Siluriformes	Siluridae	<i>Wallago attu</i>
24	Siluriformes	Siluridae	<i>Mystus seenghala</i>
25	Channiformes	Channidae	<i>Channa marulia</i>
26	Perciformes	Gobidae	<i>Glossogobius giuris</i>
27	Perciformes	Cichlidae	<i>Oreochromis mossambicus</i>
28	Symbranchiiformes	Mastacembelidae	<i>Mastacembelus armatus</i>
29	Chiocephalioformes	Ophicephalidae	<i>Ophicephalus</i>

Fishes

Twenty nine species of fishes were recorded viz. *Gadusia chapra*, *Notopterus chitala*, *Notopterus notopterus*, *Salmostoma bacaila*, *Barbodes sarana*, *Catla catla*, *Cirrhinus mrigala*, *Cirrhinus reba*, *Labeo dyocheilus*, *Labeo gonius*, *Labeo rohita*, *Labeo calbasu*, *Labeo sindensis*, *Labeo diplostomus*, *Cheila bacaila*, *Cheila laubuca*, *Danio devario*, *Tor putitora*, *Barbus ticto*, *Barbus sarana*, *Ctenopharyngodon idella*, *Cyprinus carpio*, *Wallago attu*, *Mystus seenghala*, *Channa marulia*, *Glossogobius giuris*, *Oreochromis mossambicus*, *Mastacembelus armatus*, and *Ophicephalus* (Table 9).

The most important edible fishes are *Cyprinus carpio*, *Tor putitora*, *Barbus ticto* and *Barbus sarana*.

Flora

Twenty five species of flora were recorded (Table 10). The dominant species were viz. *Acacia jacquemontii*, *Acacia nilotica*, *Aerva javanica*, *Acacia senegal*, *Alhaji maurorum*, *Azadirachta indica*, *Calotropis procera*, *Capparis decidua*, *Cassia italica*, *Cymbopogon jwarancusa*, *Cymbopogon schoenanthus*, *Eleusine compressa*, *Euphorbia caducifolia*, *Eucalyptus sp.*, *Ficus religiosa*, *Lasiurus hirsutus*, *Leptadenia pyrotechnica*, *Olea ferruginea*, *Prosopis glandulosa*, *Prosopis juliflora*, *Rhazia stricta*, *Tamarix aphylla*, *Typha elephantiana*, *Zizyphus mauritiana* and *Zizyphus nummularia*.

Table 10. List of Flora Recorded from Hub Dam.

S. No.	Scientific Name
01	<i>Acacia jacquemontii</i>
02	<i>Acacia nilotica</i>
03	<i>Aerva javanica</i>
04	<i>Acacia senegal</i>
05	<i>Alhagi maurorum</i>
06	<i>Azadirachta indica</i>
07	<i>Calotropis procera</i>
08	<i>Capparis decidua</i>
09	<i>Cassia italica</i>
10	<i>Cymbopogon jwarancusa</i>
11	<i>Cymbopogon schoenanthus</i>
12	<i>Eleusine compressa</i>
13	<i>Euphorbia caducifolia</i>
14	<i>Eucalyptus sp.</i>
15	<i>Ficus religiosa</i>
16	<i>Lasiusurus hirsutus</i>
17	<i>Leptadenia pyrotechnica</i>
18	<i>Olea ferruginea</i>
19	<i>Prosopis glandulosa</i>
20	<i>Prosopis juliflora</i>
21	<i>Rhazia stricta</i>
22	<i>Tamarix aphylla</i>
23	<i>Typha elephantiana</i>
24	<i>Zizyphus mauritiana</i>
25	<i>Zizyphus nummularia</i>

CONCLUSION

Regarding the effects of environmental pollution, there are no serious effects on the aquatic biodiversity of the wetland. There is a serious decline in waterbird population but these are mainly due to social disturbances. Areas near spillway, main dam area, agriculture land/ shallow water, and Hub Canal are the prime habitats of birds in the wetland.

During the study no adverse effect of environment pollution was found on the aquatic biodiversity except for slightly higher concentrations of some trace metals in water. All the physico – chemical parameters were recorded as per limits of WHO Standard. The present investigation indicates that all the physico-chemical parameters are not exceeding the limits significantly for aquatic life of the Dam and no significant excessive concentration of heavy metals were recorded during the present study. Therefore the water of Hub Dam is chemically safe and fit for human consumption, irrigation supply and for the growth of aquatic flora and aquatic biodiversity.

It was also found that the Dam Water is polluted with microbial infestation and the assessed value is higher than

the set limits of WHO Standard. Therefore the water must be treated periodically before supplying particularly for domestic use.

There was not an observed correlation or significant differences between selected physico – chemical parameters and the different sites. The significant differences found between the metals will assist in the selection of an appropriate treatment method to minimize the contamination of the water of Hub Dam.

There are no serious threats to the biodiversity of the area. Hunting of wildlife has been controlled to a great extent.

RECOMMENDATIONS

- To maintain the water quality of Hub Dam, long-term monitoring program may be undertaken and regular environmental assessment must be made to ensure the safety of this wildlife sanctuary, Ramsar Site and its aquatic life.
- It is concluded that the area is rich in biodiversity. It is suggested that the management plan of the reservoir should be implemented in its true letter and spirit.
- Studies on the migration of water birds may be undertaken and ringing/ banding programmes may be started.
- Steps for the development of fisheries may be taken up, as the reservoir is an important area for fishes, particularly the Mahseer.
- Public awareness programmes may be taken up for the conservation and sustainable utilization of the natural resources.

REFERENCES

- APHA. 1998. Standard Methods for the Examination of Water and Waste Water (20th ed.). America Public Health Association. New York, USA.
- Beg, MAA., Mehmood, SN., Naeem, S. and Yousuf zai, AHK. 1988. Characterization of waters Part II. Chemical Composition of Hub Dam water and its Variations. Pak. J. Sci. Ind. Res. 31(3).
- Brower, J., Zar, J. and Ende, C. 1990. Field and Laboratory Methods for General Ecology. Wm. C. Brown Publishers. 2460 Kerper Boulevard, Dubuque. A 52001.
- EPA. 2002. US Environment Protection Agency: Safe Drinking Water Act Ammdement. www. Epa. Gov/safe water / mcl.Html
- Fakayode, SO. 2005. Impact Assessment of Industrial Effluent on Water Quality of the Receiving Alaro River in Ibadan Nigeria. Ajean Henry 10:1-13.

- Ghalib, SA., Hasnain, SA. and Khursheed, SN. 2000. Observations on the Avifauna of Hub Dam. Pak.J. Zool. 32(1):27-32.
- Gorsuch, TT. 1976. Accuracy in Trace Analysis: Sample Handing and Graphite Furnace AAS. Anal: Chem. 55:981.
- Grimmett, R., Inskip, C. and Inskip, T. 1998. Birds of the Indian Subcontinent. Oxford University Press, Delhi. pp890.
- Jones, MH., PFA. Vander and GK. Alaman. 1983. Analysis Scheme for the Determination of Phosphate in Water. Anal. Chem. 15:58.
- Khan, MZ., Hussain, B., Ghalib, SA., Zehra, A. and Mahmood, N. 2010^a. Distribution, Population Status and Environmental Impacts on Reptiles in Manora, Sandspit, Hawkesbay and Cape Monze areas of Karachi Coast. Canadian Journal of Pure and Applied Sciences. 4(1):1053-1071.
- Khan, MZ., Ghalib, SA., Zehra, A. and Hussain. B. 2010^b. Bioecology and Conservation of the Birds of Hingol National Park, Balochistan. Journal of Basic and Applied Sciences. 6 (2):175-184.
- Khuwar, MY. and Mastoi, GM. 1996. Metal Pollution in Fresh water. Science International Lahore. 8:327.
- Mastoi, GM., Khahawar, MY. and Bozdar, RB. 1997. Some Studies on Jamshoro and Lakhra Power Stations Liquid Effluents. Proc. NSMTCC 97 Env. Pollut., Islamabad, Pakistan. 45-51.
- Mench, M., Baize, D. and Mocquot, B. 1997. Level of Metals in Water. Env. Pollut. 95:93-10.
- Olajire, AA. and Imeo, K. 2000. A Study of the Water Quality of the Osun River: Metal Monitoring and Geochemistry. Bull. Chem. Soc. Ethio. 14:1-8.
- Roberts, TJ. 1997. The Mammals of Pakistan (Revised edition), Oxford University Press Karachi, Pakistan. pp525.
- Roberts, TJ. 2005. Field Guide to the Large and Medium Sized Mammals of Pakistan. Oxford University Press, Karachi, Pakistan. pp259.
- Roberst, TJ. 2005. Field guide to Small Mammals of Pakistan, Oxford University Press, Karachi.
- Santa, MM., Gonzalez. W. and Lara, O. 1986. A Rsenic Levels in Chilean Marine Species. Bull. Env. Contam. Toxical. 32:635-639.
- Snobe, K. and Usui. (eds.). 1993. A Field Guide to the Water Birds of Asia. Wild Birds Society of Japan, Tokyo. pp228.
- Trivedi, RN. 1993. Environmental Science. Anmol Publ., New Delhi. pp202.
- Welch, PS. 1952. Limnology (2nd ed.). Mc Graw Hill Book Comp., New York, USA.
- WHO. 1982. Examination of Water for Pollution Control. World Health Organization, Regional Office for Europe: 203-204.
- WHO. 1993. Guidline for Drinking Water Quality. World Health Organization. Geneva, Switzerland.

Received: Nov 4, 2011; Revised: Jan 4, 2012; Accepted: Feb 22, 2012

REGULATION OF *EUROTIUM REPENS* REPRODUCTION AND SECONDARY METABOLITE PRODUCTION

Mahmoud AbdEl-Mongy

Microbial Biotechnology Department, Genetic Engineering and Biotechnology Research Institute
Minoufiya University, Sadat City, Egypt

ABSTRACT

Eurotium repens (Anamorph *Aspergillus repens*) was isolated from spoiled fruit. It reproduced sexually at different sucrose concentrations up to 50% (w/v); water activity, 0.79. It reproduced asexually at high sucrose concentration 60% (w/v) water activity, 0.75. The concentrations of all detected amino acids were higher in the teleomorph than the anamorph stage except that of glycine, while α -amino adipic acid and alanine were detected in teleomorph only. The extracellular secondary metabolites produced by the teleomorph and anamorph stages were variable and different except epoxysuccinic acid and 2-pyruvylamino benzamide which were produced by both stages. Glycine, arginine and calcium chloride unlike glutamic acid, aspartic acid and alanine, are important in the induction of teleomorph stage formation at high sucrose concentration 60 % (w/v).

Keywords: *Aspergillus repens*, reproduction, fungi, amino acids, sucrose.

INTRODUCTION

Eurotium species often dominate the fungal population in stored grain and are responsible for spoilage of jams, dried foods, dried salted fish and sponge cake (Abellana *et al.*, 1999; Bluhm *et al.*, 2005). *Eurotium repens* sexually reproduces as an ascomycete (telomorph) whereas asexual conidial reproduction of the same fungus (Anamorph) is classified as *Aspergillus repens*.

Water activity (a_w) measurements estimate the proportion of the available water in a system, i.e. the water available for biological (biochemical) and chemical reaction. Water activity can be controlled through water removal or solute addition; solutes that can be used for this purpose are polyols, salts and sugars (Rose, 1983). Xerophilic fungi are characterized as being capable of growing below a_w of 0.85, and are most commonly associated with intermediate moisture foods, including cereals, nuts species and several dried food stuffs (Hocking, 1988). The majority of xerotolerant fungi belongs to the genera *Aspergillus* and *Penicillium* or are perfect forms of *Aspergillus* such as *Eurotium* and *Emericella*. One of the principal factors controlling the growth of these organisms in food is a_w ; the effective growth range can be as low as 0.61 (Corry, 1987; Jay, 1992).

Low a_w significantly reduced spores germination of *Aspergillus spp* (Nesci *et al.*, 2003; Ni and Streett, 2005). The spores only germinated on a medium with high a_w values; 0.982 and 0.937, while the spores did not germinate with a_w values 0.747 and 0.809.

Fungi reproduce asexually under favorable condition and sexually under stress conditions (Griffin, 1994). Bluhm *et al.* (2005) reported that *Aspergillus nidulans* and *Aspergillus flavus* strains grew only at 0.98 a_w . At 0.86 a_w . No growth of *Aspergillus nidulans* or *Aspergillus flavus* was visible after 8 days. At 0.83 a_w , *Aspergillus nidulans* was not observed, nor were sclerotia produced by *Aspergillus flavus*.

Secondary metabolites are low-molecular-weight natural products generated by filamentous fungi, plants, algae, bacteria, and animals in response to environmental abiotic and biotic stimuli. Secondary metabolites have a strong impact on humankind via their application in health, medicine, agriculture, and industry; they include useful (e.g. antibiotics) and detrimental compounds (e.g. mycotoxins). These metabolites are frequently associated with asexual and sexual development (Chang *et al.*, 2001; Wilkinson, *et al.*, 2004). Adams *et al.* (1998) and Pena *et al.* (1998) found a positive correlation between cleistothecial formation and secondary metabolites production in wild type and mutant strains of *Emericella nidulans*.

Aspergillus spp. produce an array of secondary metabolites including aflatoxin, cyclopiazonic acid, aflatrem, patulin, penicillin, kojic acid, lovastatin, carotenoids, and spore pigments; novel secondary metabolites have also been discovered that are synthesized from so called silent gene clusters in *A. nidulans*, such as terrequinone.

A, monodictyphenone, emodins, and polyketides (Bok *et al.*, 2009).

Some ascomycetes may require exogenous vitamins, minerals, or other natural materials for ascocarp production that are often not duplicated in synthetic media (Moore – Landecker, 1992). *Venturia inaequalis* produced large number of ascocarps with glycine but no ascocarps were produced with ammonium tartrate (Roos and Bremner, 1971). Engelkes *et al.* (1997) found that the tyrosine was one of the better nitrogen sources for production of *Taloromyces flavus* ascospores. Also, fatty acids or related lipids are important for sexual development of filamentous fungi (Nukina *et al.*, 1981; Goodrich – Tanrikulu *et al.*, 1998). The objectives of this study was to assess the metabolic regulation through stress conditions on growth, reproduction and secondary metabolites biosynthesis of *Eurotium repens* which cause spoilage of fruits.

MATERIALS AND METHODS

Fungal strain

The fungal isolate was isolated from spoiled fruit and identified as *Eurotium repens* according to Rapper and Fennel (1965).

Media

Dox's agar medium (sucrose, 20g; NaNO₃, 2g; KH₂PO₄, 1g; KCl, 0.5g; MgSO₄. 7H₂O, 0.5g; Fe SO₄. 7H₂O, 0.001 g; agar 20 g and distilled water, 1L) and Malt extract agar medium (malt extract, 20g; peptone, 1g; dextrose, 20g; agar, 20g and distilled water, 1L) were used for isolation, cultivation and identification of the fungal isolate.

Growth and culture conditions

Dox's agar medium was supplemented with different sucrose concentrations; 2, 30, 40, 50, 60, 70 and 80% (w/v) to adjust the water activity (a_w) 0.99 , 0.86, 0.82, 0.79 , 0.75 , 0.72 and 0.70, respectively according to Hefnawy, 1993. A plug of inoculum from the loading edge of a colony growing on an agar plate was either inoculated in the center of another plate contain the above medium (for growth and detection of the anamorph and teleomorph stages) or transferred to 500 ml conical flask (s) for detection of amino acids, secondary metabolites, metals and antimicrobial activity. Dox's agar medium supplemented with different sucrose concentrations and pHs, were inoculated and incubated were at different temperatures for 8 days to study their effects on anamorph and teleomorph stages formation.

Nitrogen free Dox's agar medium supplemented with different sucrose concentrations was amended with selected amino acids in equivalent weigh to N of NaNO₃ and certain metals; calcium chloride and aluminum chloride, (0.01mg/100ml medium) for metabolic

regulation of anamorph and teleomorph stages formation. The percentage of teleomorph and anamorph forms, as represented by the presence of cleistothecia and conidial heads, respectively was calculated by using a hemacytometer.

Secondary metabolites detection

Secondary metabolites were determined by the method described by Paterson and Bridge (1994) as follows the fungal mat of *Eurotium repens* was harvested and the fungal growth medium was filtered and extracted with equal volume of chloroform : methanol (2 :1, v/v), left to evaporate till dryness and then dissolved in 1 ml of extraction solvent.

The extraction concentrates were spotted on a pre-coated thin layer chromatography (TLC) plate (20 × 20 cm aluminum sheet silica gel 60, layer thickness 0.2 mm) along with griseofulvin as a standard reference. The metabolites were eluted using toluene: ethyl acetate: 90% formic acid (5:4: 1, v/v/v). The developed secondary metabolites spots were visualized for their colour and R_f under white, UV (365 nm), UV (254 nm) and back under UV (365 nm) light respectively. The plate was then sprayed with 0.5 % (w/v) ρ -anisaldehyde in methanol: acetic acid: concentrated sulphuric acid (17:2:1, v/v/v) and visualized under white light. The plat was heated for 8 minutes at 105°C and reexamined under white, UV (365 nm) and UV (254 nm) light respectively.

Amino acids analysis

Cell free extracts was prepared by grinding the fresh fungal mycelium (5gm) in sterile mortar with 70% ethanol (v/v). The slurry was centrifuged at 600 rpm for 10 minutes, and the supernatant was concentrated using a vacuum desiccators. The concentrated cell free extract was analyzed for amino acids qualitatively and quantitatively with a full automated Amino Acid analyzer: Model Lc 3000 (Eppendorf-Biotronik, Germany) at the Regional Center for Mycology and Biotechnology Al-Azhar University.

Metals analysis

Dry fungal mycelium (0.5gm) was ground and analyzed for metals with a Fei QUANTA 200 Environmental scanning electron microscope with Edex Unit Microanalysis.

Antimicrobial activity

The antimicrobial activity of extra-and intracellular secondary metabolites were determined by the filter paper disc method (Nester *et al.*, 1983). The filter paper discs, 6 mm in diameter were separately soaked in the extracts and transferred onto the surface of the growth medium seeded with the test organism after the incubation period, the diameter of the inhibited growth area around the disc (s) was measured.

RESULTS

As showing in table 1, growth of *Eurotium repens* increased with increasing sucrose concentration up to 40% reflect a decreasing water activity (a_w , 0.82), but then decreased slightly, and failed to grow at 80% sucrose concentration (a_w 0.70). The percentage of teleomorph and anamorph stages formation detected as shown in figure 1a and 1b, decreased and increased respectively, with increasing sucrose concentration up to 50%. At 60 and 70% sucrose concentration, the fungus failed to reproduce sexually (Table 1).

The percentage of teleomorph and anamorph stages formation at stress temperatures (20 & 40°C) and pHs (4 & 8) was relatively similar to those of control (30°C & pH6) at the same sucrose concentrations (Tables 2, 3) but among the conditions compared, the optimum-growth temperature and pH were 30°C and pH 6.

Secondary metabolites

The extracellular secondary metabolites produced by teleomorph and anamorph stages of *Eurotium repens* were different except for two metabolites; epoxy succinic acid and 2-pyruvylaminobenzamid (Table 4). The number of extracellular secondary metabolites produced by teleomorph stage was more than that produced by anamorph stage.

Table 1. Teleomorph and anamorph stages formation at different sucrose concentrations.

Sucrose concentration % (w/v)	Colony radius (cm)	Percentage (%) of the formation of	
		Teleomorph	Anamorph
2	3.2	95	5
30	3.5	90	10
40	4.3	87	13
50	3.9	80	20
60	2.5	0.0	100
70	1.6	0.0	100
80	0.0	0.0	0.0

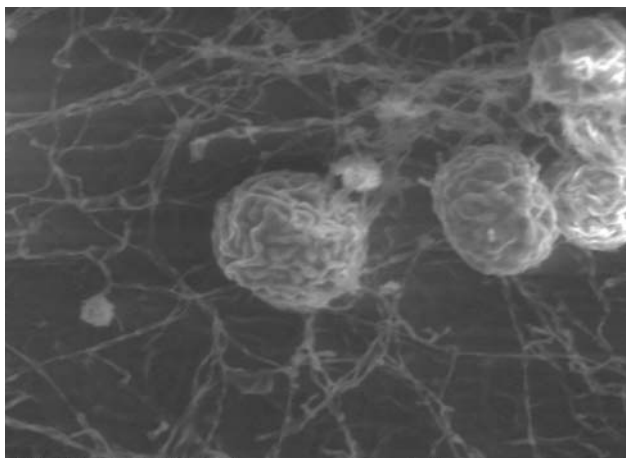


Fig. 1a. Teleomorph stage represented by cleistothecia.

Antimicrobial activity

The intra- and extracellular secondary metabolites of the teleomorph stage exhibited antimicrobial activity against *Bacillus subtilis*, *Escherichia coli* and *Pseudomonas aeruginosa*, while the intracellular secondary metabolites of the anamorph stage exhibited antimicrobial activity against *E. coli* and *B. subtilis* (Table 5a).

Amino acids

The free amino acids in teleomorph and anamorph stages were varied (Table 5b). Although, the level of all detected free amino acids except glycine was higher in teleomorph than anamorph stage. Alanine and the secondary amino acid α -amino adipic acid were detected only in the teleomorph stage. The concentration of glutamic acid, alanine, phosphoethanol amine and aspartic acid were considerable higher in teleomorph stage (253. 93, 61.88, 61.79 and 40. 50 μ g/ml, respectively) than other detected amino acids in the same stage. On the other hand, glutamic acid and glycine concentrations (82.79 and 31.97 μ g/ml, respectively) were higher than other detected amino acids in anamorph stage.

Metals analysis

There was considerable variation among the teleomorph and anamorph stages in their elemental analysis (Table 6). Most of the detected elements in anamorph stage were

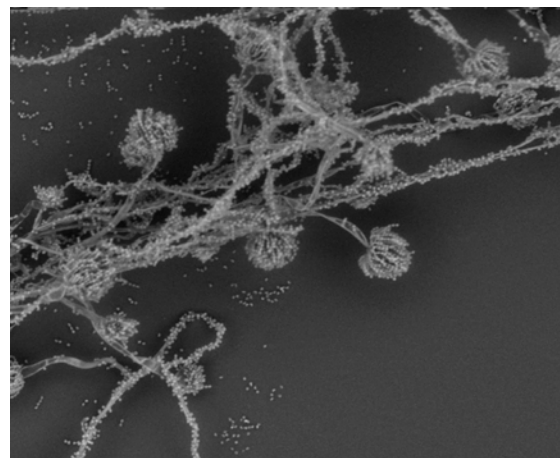


Fig. 1b. Anamorph stage represented by conidial heads.

Table 2. Effect of temperature on growth, teleomorph and anamorph stages formation of *Eurotium repens* at different sucrose concentrations % (w/v).

Sucrose % (w/v)	Temperature (°C)														
	10			20			30			40			45		
	Cr (cm)	T (%)	A (%)	Cr (cm)	T (%)	A (%)	Cr (cm)	T (%)	A (%)	Cr (cm)	T (%)	A (%)	Cr (cm)	T (%)	A (%)
2	0.0	0.0	0.0	2.2	95	5	3.1	96	4	1.1	96	4	0.0	0.0	0.0
30	0.0	0.0	0.0	2.8	88	12	3.5	90	10	2.4	87	13	0.0	0.0	0.0
40	0.0	0.0	0.0	2.9	84	16	4.2	85	15	2.6	82	18	0.0	0.0	0.0
50	0.0	0.0	0.0	0.0	0.0	0.0	3.7	81	19	1.1	81	19	0.0	0.0	0.0
60	0.0	0.0	0.0	0.0	0.0	0.0	2.3	0.0	100	0.0	0.0	0.0	0.0	0.0	0.0
70	0.0	0.0	0.0	0.0	0.0	0.0	1.2	0.0	10	0.0	0.0	0.0	0.0	0.0	0.0
80	0.0	0.0	0.0	0.0	0.0	0.0	0.0	0.0	0.0	0.0	0.0	0.0	0.0	0.0	0.0

Cr, colony radius; T, teleomorph stage; A, anamorph stage

Table 3. Effect of pH on growth, teleomorph and anamorph stages formation of *Eurotium repens* at different sucrose concentrations % (w/v).

Sucrose concentration % (w/v)	pH														
	4			5			6			7			8		
	Cr(cm)	T (%)	A (%)												
2	2.1	90	10	2.3	93	7	2.9	94	6	2	88	12	0.9	89	11
30	2.5	88	12	2.9	88	12	3.2	89	11	2.2	90	10	2.1	92	8
40	2.6	85	15	2.8	84	16	4.0	86	14	2.6	83	17	2.4	90	10
50	2.0	79	21	3	80	20	3.5	80	20	3.1	79	21	1.9	80	20
60	1.6	0.0	10.0	1.7	0.0	100	2.1	0.0	100	1.9	0.0	100	1.5	0.0	100
70	0.0	0.0	0.0	0.0	0.0	0.0	1.1	0.	10	0.9	0.0	10	0.0	0.0	0.0
80	0.0	0.0	0.0	0.0	0.0	0.0	0.0	0.0	0.0	0.0	0.0	0.0	0.0	0.0	0.0

Cr, colony radius; T, teleomorph stage; A, anamorph stage

Table 4. Extracellular secondary metabolites production by teleomorph and anamorph stages.

Secondary metabolites produced by	
Teleomorph	Anamorph
* Epoxysuccinic acid	* Epoxysuccinic acid
* 2-pyruoylaminobenzamide	* 2-pyruoyl aminobenzamide
* Lapisin	* Kojic acid
* Wartmannin	*2-carboxy-3,5, dihydroxyphenyl acetyl- carbinol
* Gensisyl alcohol	* Unknown (2)
* (-) Flavoskyrin	* Unknown (3)
* Compactin	
* Unknown (1)	

present in higher concentration than teleomorph stage except for potassium. Silicon and copper were not detected in teleomorph stage. On the other hand iron and calcium were not detected in anamorph stage.

(70 % w/v), the fungus failed to grow on medium amended with alanine and aluminum chloride.

DISCUSSION

In this study the high sucrose concentration 80% (w/v), (a_w 0.70) inhibit the growth of *Eurotium repens*. Pitt (1975) showed that the lower a_w limit for growth of *Eurotium* species is approximately 0.70. Fungi reproduce asexually under favorable condition and sexually under stress condition (Griffin, 1994). However *Eurotium repens* did not reproduce sexually under stress of low water activity 0.75 and 0.72 adjusted by sucrose

Regulation of reproduction by amino acids and metals
Alanine and arginine unlike aspartic acid, glutamic acid and glycine, exhibited stimulatory effect on growth of *Eurotium repens* at low sucrose concentration (2% w/v), while glycine and arginine exhibited stimulatory effect on growth and teleomorph stage formation at high sucrose concentrations (Table 7). At high sucrose concentration

Table 5a. Antimicrobial activity of *Eurotium repens*.

Test organism	Intracellular secondary metabolites inhibition zone (mm)		Extracellular secondary Metabolites inhibition zone (mm)	
	Anamorph	Teleomorph	Anamorph	Teleomorph
<i>Fusarium oxysporum</i>	0	0	0	0
<i>Aspergillus terreus</i>	0	0	0	0
<i>Candida albicans</i>	0	0	0	0
<i>Cunninghamella sp</i>	0	0	0	0
<i>Escherichia coli</i>	2.2	22	0	24
<i>Bacillus subtilis</i>	27	23	18	25
<i>Pseudomonas aeruginosa</i>	0	17	0	20
<i>Salmonella typhi</i>	0	0	0	0

0, Inhibition zone not detected.

Table 5b. Amino acids pool analysis of teleomorph and anamorph stages.

Amino acids	Concentration ($\mu\text{g/ml}$) of amino acids in	
	Teleomorph	Anamorph
Phosphoserine	23.42	5.22
Taurine	14.50	7.72
Phosphoethanol amine	61.79	20.72
Aspartic acid	40.50	15.21
Threonine	14.60	6.83
Serine	30.32	18.09
Glutamic acid	253.93	82.79
α -Aminoadipic acid	14.54	0.0
Glycine	9.76	31.97
Alanine	61.88	0.0
α -Aminobutyric acid	10.25	7.56
Methionine	8.69	5.58
Isoleucine	9.80	8.04
Leucine	6.72	3.20
Tyrosine	11.39	7.43
Phenylalanine	7.53	2.01
3-Methylhistidine	6.64	5.38
Carnosine	29.48	27.75
Ornithine	7.36	4.84
Lysine	34.99	11.19
Arginine	18.91	1.89

0.0, Amino acid not detected.

concentration 60% (w/v) and 70% (w/v) respectively. Recently, Bluhm *et al.* (2005) found that the conidial heads of *Eurotium rubrum* were visible after 6 days at 0.98 a_w . Cleistothecia were produced only at 0.98 a_w , however mature ascospores were not detected until 10 days.

From the current study there is indirect relationship between the low a_w and reproduction in *Eurotium repens* where at low a_w certain amino acids were produced while others not produced. Generally the free amino acids are known to play an important role in the regulation of synthesis of some enzymes, on secondary metabolites production and osmoregulation. The unusual amino acid α amino adipic acid and alanine were not detected when

the *Eurotium repens* reproduce asexually (anamorph). On the other hand, glycine was only detected in higher concentration in teleomorph than in anamorph. These amino acids may be involved in the regulation of *Eurotium repens* reproduction. Mc Alpin and Wicklow (2005) stated that high nitrate (0.3% - 0.6% NaNO_3) and high sucrose (10 – 20 %) concentrations were optimal for stromata development. No stromata were produced by *Petromyces alliaceus* (Anamorph *Aspergillus alliaceus*) on media in which cystine or ammonium sulphate represented the only source of nitrogen, while the percentage of stromata containing ascocarps was the greatest with ammonium tartrate, glutamic acid, glycine or serine substituted for NaNO_3 .

Table 6. Metals analysis of teleomorph and anamorph.

Metal	Metal weight (%) of	
	Teleomorph	Anamorph
Sodium	4.11	7.49
Magnisum	2.69	4.70
Aluminum	8.08	16.81
Silicon	0.0	4.43
Phosphrus	19.88	20.99
Sulfur	7.80	10.70
Chloride	1.54	11.34
Pottassium	24.91	17.63
Calcium	2.44	0.0
Copper	0.0	5.92
Iron	28.53	0.0

0.0, metal not detected.

Table 7. Effect of certain amino acids and metals on growth, teleomorph and anamorph stage formation, at different sucrose concentrations.

Amino acids of Elements	Sucrose concentration % (W/V)								
	2			60			70		
	Cr(cm)	T(%)	A(%)	Cr(cm)	T(%)	A(%)	Cr(cm)	T(%)	A(%)
Control	3.1	92	8	2.5	0	100	1.5	0.0	100
Glycine	3.0	80	20	2.9	40	60	1.9	35	65
Alanine	3.3	95	5	1.9	0.0	100	0.0	0.0	0.0
Aspartic acid	2.9	90	10	2	0.0	100	1.2	0.0	100
Glutamic acid	3.0	91	9	1.8	0.0	100	1.4	0.0	100
Arginine	3.5	83	17	2.3	45	55	0.0	0.0	0.0
Aluminum	2.1	90	10	1.0	0.0	100	0.0	0.0	0.0
Calcium	2.7	88	12	1.5	48	52	1.2	0.0	100

Cr, Colony radius; T, Teleomorph; A, Anamorph

There is a direct relationship between osmotic stress and polyols, phospholipids and lipid composition in filamentous fungi (Hefnawy, 1993). The growth of *Eurotium repens* at low water activity (high osmotic stress) may induce synthesis of compounds which may then regulate their reproduction. This information is consistent with previous studies, where fatty acids or related lipids (Nukina *et al.*, 1981; Goodrich-Ta-nrikulu *et al.*, 1998) and polyols (Feofilova *et al.*, 2000) affected sexual development in filamentous fungi.

The secondary metabolites detected in teleomorph and anamorph stages of *Eurotium repens* were generally different; this may be due to differentiation or may be related to other physiological changes. Many previous studies revealed that the production of fungal secondary metabolites is associated with differentiation (sexual and asexual development) and environmental stress (Cotty *et al.*, 1994; Trail *et al.*, 1995; Adams and Yu, 1998; Pena *et al.*, 1998; Chang *et al.*, 2001; Michael *et al.*, 2001).

From the elemental analysis, calcium was detected only in teleomorph stage, and therefore, when added to the

growth medium it stimulates the sexual reproduction at 60% (w/v) sucrose concentration in *Eurotium repens*. Changes in microcellular Ca^{2+} concentration are known to play an important role in the regulation of all physiological processes occurring in the cell such as growth, division, secretion and development of microbial resting forms (Jackson and Heath, 1993; Berridge *et al.*, 2000). On the other hand, aluminum suppresses the growth and sexual reproduction in the *Eurotium repens*, the reduction of spore germination by aluminum was documented by Dursun *et al.*, 2002.

REFERENCES

- Abellana, M., Magri, X., Sanchis, V. and Ramos, AJ. 1999. Water activity and Temperature effects on Growth of *Eurotium amstelodami*; *E. chevalierie* and *E. herbariorum* on a sponge cake analogue. Inter J. Food Microbiol. 52:97-103.
- Adams, TH., Wieser, JK, and Yu, JH. 1998. Asexual sporulation in *Aspergillus nidulans*. Microbial Mol. Biol. Rev. 62(1):35-54.

- Adams, TH. and Yu, JH. 1998. Coordinate Control of Secondary metabolite Production and Asexual Sporulation in *Aspergillus nidulans*. Curr. Opin. Microbiol. 1(6):674-677.
- Berridge, MJ., Lipp, P. and Bootman, MD. 2000. The Versatility and Universality of Calcium Signaling. Nature Rev. Mol. Cell biol. 1:11-12.
- Bluham HB., Reuhs, BL. and Woloshuk, CP. 2005. Glass – Fiber Disks provide suitable medium to study Polyol Production and Gene Expression in *Eurotium rubrum*. Mycologia 97(4):743-750.
- Bok, JW., Chiang, YM., Szewczyk, E., Reyes-Dominguez, Y., Davidson, AD., Sanchez JF., Lo, HC., Watanabe, K., Strauss, J., Oakley, BR., et al. 2009. Chromatin-level regulation of Biosynthetic Gene Clusters. Nat. Chem Biol. 25(7):462-464.
- Chang, P., Bennett, JW. and Cotty, PJ. 2001. Association of Aflatoxin Biosynthesis and Sclerotial development in *Aspergillus parasiticus* Mycopathologia. 153:41-48.
- Corry, JEL. 1987. Relationship of Water activity to Fungal growth. In: food and Beverage Mycology. Ed. Beuchat, LR. York, Van Nostr and Rienhold. 51-88.
- Cotty, PJ., Bayman, P., Egel, DS. and Elias, DS. 1994. Agriculture, Aflatoxins and *Aspergillus*. In the genus *Aspergillus*. New York: Plenum Press. 1-27.
- Dursun, S., Boddy, L. and Franklaand, J. 2002. Effects of pH and Aluminum ion concentration on Spore germination and Growth of some Soil Fungi. Turk J. Biol. 26:99-107.
- Engelkes, CA., Nucllo, RL. and Fravel, DR. 1997. Effect of Carbon, Nitrogen and C: N ratio on Growth, Conidiation, and Biocontrol Efficacy of *Taloromyces flavus*. Phytopathology. 87:500-505.
- Feofilova, EP., Tereshina, VM., Khokhlova, NS. and Memorskaya, AS. 2000. Different Mechanisms of the Biochemical adaptation of Mycelial Fungi to Temperature Stress: Changes in the cytosol carbohydrate composition. Microbiology. 69(5): 504-508.
- Goodrich-Tanrikulu, M., Howe, K., Stafford, A. and Nelson, M. 1998. Changes in Fatty acid composition of *Nerospora crassa* accompany Sexual Developmentad Ascospore Germination. Microbiology. 114:1713-1720.
- Griffin, DH. 1994. Fungal Physiology (2nd ed.). New York John Wiley and Sons. pp458.
- Hefnawy, MA. 1993. Influence of Certain Stress Condition on a Metabolic Disorders of Some Fungi. Ph.D. Thesis, Faculty of Science, Minoufiya University, Egypt.
- Hocking, AD. 1988. Moulds and Yeasts associated with Foods of reduced water activity: Ecological Interactions. In: Food Preservation by Moisture Control. Ed. Seow, CC. London. Elsevier Applied Science. 57-72.
- Jackson, SL. and Heath, IB. 1993. Roles of Calcium Ions in Hyphal tip Growth. Microbiological Reviews. 57:367-382.
- Jay, JM. 1992. Intrinsic Parameters of Foods that Affect Microbial Growth. In: Modern Food Microbiology. Ed. Jay, JM. Chapman and Hall, New York. 38-62.
- Mc Aplin, CE. and Wicklow, DT. 2005. Culture Media and Sources of Nitrogen Promoting the Formation of Stromata and Ascocarps in *Petromyces alliaceus* (*Aspergillus* section Flavi). Can J. Microbiol. 51:765-771.
- Michael, JC., Sarah, CW. and Graham, WG. 2001. The Fungi. (2nd ed.). London Syney. Tokyo.
- Moore-Landecker, E. 1992. Physiology and Biochemistry of Ascocarp Induction and Development. Mycol . Res. 96:705-716.
- Nesci, A., Rodriguez, M. and Etcheverry, M. 2003. Control of *Aspergillus* Growth and Different Conditions of Water Activity and pH. J. Appl. Microbiol. 95:279-287.
- Nester, EW., Pearsal, NN., Roberts, CE., Nester, MT. and Lidstrom, MF. 1983. Microbiology. (3rd ed.). CBS College Publishing, New York. 10:273.
- Ni, X. and Streett, DA. 2005. Modulation of Water Activity on Fungicide Effect on *Aspergillus niger* Growth in Sabouraud Dextrose Agar Medium. Letters in Applied Microbiology. 41:428-433.
- Nukina, M., Sassa, T., Ikeda, M., Takahasi, K. and Toyota, S. 1981. Linoleic acid Enhances Perithecial Production in *Neurospora crassa*. Agric Biol. Chem. 45:2371-2373.
- Paterson, RR. and Bridge, PD. 1994. Biochemical Techniques for Filamentous Fungi. CAB International, Wallingford, UK.
- Pena, D., Aguirre, J. and Ruiz-Herrera, J. 1998. Correlation between the Regulation of Sterigmatocystin Biosynthesis and Asexual and Sexual Sporulation in *Emericella nidulans*. Antonie van Leeuwen hoek. 73:199-205.
- Pitt, JI. 1975. Xerophilic Fungi and the Spoilage of Foods of Plant Origin. In Water Relations of Foods. Plant Origin. In: water Relations of Foods. Ed. Duckworth, RB. Academic press, London.
- Rapper, K.B. and Fennel, DI. 1965. The Genus *Aspergillus*. The Williams and Wilkins Company, Baltimore, USA.

Rose, AH. 1983. Food Microbiology. Academic Press. London, New York. Toronto, Sydney, San Francisco. 174-198.

Ross, RG. and Bremner, FDJ. 1971. Effect of Ammonium Nitrogen and Amino acids on Perithecial formation of *Venturia inaequalis*. Can. J. Plant. Sci. 51:29-33.

Trail, F., Mahanti, N. and Linz, J. 1995. Molecular Biology of Aflatoxin Biosynthesis. Microbiology. 141:755-765.

Wilkinson, HH., Sim, SC. and Keller, NP. 2004. Increased Conditions Associated with Progression along the Sterigmatocystin Biosynthetic Pathway. Mycologia. 96 (6):1190-1198.

Received: June 21, 2011; Accepted: March 29, 2012

SURVIVAL OF COMPOST MICROBIAL COMMUNITY IN TWO COMPOSTING SYSTEMS

*Felix Kutsanedzie¹, George NK Rockson¹, Elias D Aklaku¹, Charles Quansah² and Ato Bart-Plange¹

¹Department of Agricultural Engineering, KNUST, Kumasi

²Department of Soil and Crop Science, KNUST, Kumasi, Ghana

ABSTRACT

Temperature development during composting was studied in Turned windrow and Dome Aerated Technology composting systems to ascertain their effectiveness in the reduction or elimination of pathogens in the final product. Also, an assessment of potential health hazard was investigated. Temperature, moisture and pH development in the two composting systems were monitored for thirteen weeks to assess their effects on total viable count, total coliform count, total fungi count and helminth eggs count. The Hydrogen ion concentration (pH) and moisture measured in both systems gave a p-values of 0.25 and 0.68 respectively at $\alpha = 5\%$, indicating existence of no significant difference between these parameters in both systems. Generally, the total viable count reduced while total fungi increased at the end of week 12 in all the systems. However, total coliform reduced to 0 during week 4. Microorganisms such as *Listeria spp.*, *Penicillium spp.* and *Mucor spp.* survived the process in the Dome Aerated Technology system.

Keywords: Composting, microorganism, maturity, decomposition, composting systems.

INTRODUCTION

Composting is one of the widely used methods for treating biodegradable waste. It is increasingly gaining attention compared to the other known waste disposal methods such as incineration, landfilling and anaerobic digestion because of its environmental friendliness as well as the commercial benefits derived from its final product as soil conditioner and fertilizer (Eriksson, 2003).

Composting is a self-heating, aerobic microbial decomposition of organic materials. A typical composting process goes through a series of phases, including a rapid temperature increase, sustained high temperatures and a gradual cooling of the composting mass (Ryckeboer *et al.*, 2003). Different microbial communities dominate during these various composting phases, each adapted to a particular environment (Ryckeboer *et al.*, 2003). As a process involving microorganisms; it is affected by all factors that affect the lives of microorganisms such pH, temperature, moisture, air and nutrients (Miller, 1993). Compost microbial community comprises beneficial and harmful microbes that are active in varied conditions and are classified as such: mesophilic and thermophilic; in terms of temperature; aerobic and anaerobic, in terms of utilisation of oxygen (Madigan *et al.*, 2000; Miller, 1993).

Heat energy released by the microbes during composting, as a result of their metabolic activities, increases the

temperature of compost masses and consequently help inactivates pathogens present (Miller, 1993). However, when excessive heat generated is not dissipated quickly, it leads to the drying of compost masses and killing of beneficial microbes, and thus, resulting in complete failure of the process (Miller, 1993). Different systems would allow dissipation of heat generated during the process at different rates depending on their designs; and this, affect the dynamics of compost microbial community. In the selection of composting systems for organic waste treatment, there is a need to consider systems' effectiveness in reducing or eliminating pathogens in the final product via temperature development: in order to prevent the penetration of pathogens into the food chain (Droffner and Brinton, 1995). Many countries have developed regulations to further reduce pathogens prior to land application of compost materials using temperature as the cardinal factor. The US Environmental Protection Agency stipulates that, to further reduce pathogens, a minimum activation of 55°C must be achieved for a minimum of 3 days during in-vessel and aerated static pile composting. The minimum conditions for windrow composting are 55 °C for 15days and five minimum turnings during the composting period. The regulation requires the quantification of the faecal coliforms and *Salmonella spp.* in the finished product. The recommended values for final counts of faecal coliforms and *Salmonella spp.* are < 1000 most probable number (MPN/g[dry]) and < 3

*Corresponding author email: kingkut11@yahoo.co.uk

MPN/4g[total solids] respectively (Cekmecelioglu *et al.*, 2005). The regulations for biowaste composts in Europe shows slight variations: the regulations require >55 °C for at least 3 weeks or 60 for at least 1 week in Switzerland; >55 for at least 2 weeks in Denmark; >60 for 1 week for in-vessel composting and >55 for at least 2 weeks or >65 for at least 1 week in Germany (Cekmecelioglu *et al.*, 2005).

Mesophilic and thermophilic microorganisms are involved in composting and their succession is important in the effective management of composting process (Beffa *et al.*, 1996; Ishii *et al.*, 2000). Since plant and animal waste possibly contains viral, bacterial, and protozoan zoonotic pathogens, the application of untreated livestock wastes to plants could be a hygienic risk for humans (Dai *et al.*, 2005). Several pathogens known to cause diseases and death in humans have been identified in manure and foodwaste. Some of these microorganisms include *Salmonella spp.*, *Listeria spp.*, *Clostridium spp.*, *Staphylococcus spp.*, *Escherichia spp.*, *Aspergillus spp.* and *Penicillium spp.* For instance, *Listeria monocytogenes*, *Salmonella spp.* and *Escherichia coli* O157:H7 infections are important to food safety as these classes of pathogens combine to cause approximately 1.5 million illnesses and 60% of all deaths related to foodborne illnesses (Mead *et al.*, 1999). Solomon *et al.* (2002) reported that failure to inactivate pathogens in the compost microbial community can allow their penetration into the food chain via the use of final compost on farm and consequently, result in serious public health problems. *Escherichia coli* O157:H7 is responsible for 20000 cases of infection and 250 deaths per year in the US as a result of diarrhoea and haemorrhagic colitis while *Salmonella spp.* caused human salmonellosis, which is associated with 2,000,000 infection cases and 50 to 2000 deaths per year (Lung *et al.*, 2001). Since these microorganisms are found during composting, it becomes important to treat animal wastes and plant materials harbouring these pathogens, to limit the risks of pathogenic microorganisms entering the food chain via the use of the compost on the farms.

Literature indicates the regulation of temperatures developed in different composting systems as the most used indicator of compost safety but there is however lack of enough data on the inactivation of pathogenic microorganisms in different systems. This thus has necessitated the study, to ascertain the effects of temperatures developed in two different composting systems: dome aerated technology, passive system; and turned windrow, an active system, on the survival of compost microbial community and safety of their final products vis-à-vis microbial hazards.

The objectives of this study are to quantify and identify the various microorganisms present in both systems from

the start to the end of the composting process. Result obtained would allow one ascertain and compare the systems' effectiveness and efficiency in inactivating pathogens present; and the possible health hazards likely to be presented to the public by the survived pathogens. The findings would also help farmers and compost manufacturers to consider choosing appropriate composting systems to safeguard the safety of finished compost from pathogen penetration into the food chain.

MATERIALS AND METHODS

The study was carried out at Volta River Estate Limited Farms (VREL), one of the leading organic banana and pine apple producing farms in Ghana. Compost materials included: River reed, harvested into canoes and brought to the site; banana stock, obtained from VREL Farms; cocoa seed husk, rice husk, cow and poultry manure, obtained from farms and households nearby. The composition of the feed stocks are given as follows: River Reed (RR)-75%, Clay(C)-10%, Banana Stalk/Stem (BS)-5%, Cow Manure/Dung (CM)-4%, Rice Chaff (RC)-4%, Cocoa Seed Husk (CSH)-1% and Poultry Manure (PM)-1%. A starter containing genetically modified organisms such as *Bacillus spp.* and *Corynebacterium spp.* was mixed in the proportion 500g: 40L (m/v) water and added to the feed stocks to facilitate the decomposition process.

Description of Compost Systems Understudy

Dome Aerated Technology (DAT)

The DAT is a passive aeration system that utilizes thermal convection to drive the aeration process within a windrow of waste. The principle of the DAT method is the creation of large voids in a windrow of waste (Trois and Polstera, 2007), using in this case bamboo structures, called domes and channels. Domes are positioned centrally in the windrow to allow for venting of the hot gases generated by the degradation reactions through the channels and chimneys. The layout of the DAT system is shown in figure1. This pile is composed of 4 bamboo domes and 4 chimneys (4 in. dia., and 2.5m high). Additionally, 10 pieces of perforated uPVC (4 in. dia.) used as channels, were inserted into the compost pile to promote the chimneys effect and the chimney pipes supported by cables. Dimensions for the construction of the pile and triangular bamboo dome were 13.7m (L) ×2.7m (B) ×1.8m (H) and 1.4m(H) x 0.75m equilateral base respectively.

Turned Windrows

As regard the turned windrow system, the feedstock was initially turned four times and used to form long piled compost rows of dimensions 35m (L) ×2m (B) ×0.9m (H).A front-loader (165 HP) was used to reshape the pile after which a Toptex (fleece) sheet was used to cover the windrow. Subsequent turnings were conducted with Sandberger ST 300 pulled by a 90 HP tractor.

Sampling of Compost Mass for Physico-chemical and Microbiological Analysis

Compost masses were sampled at the top, middle and bottom locations in the different systems mounted weekly for laboratory study on moisture, pH and microbial analysis. However, temperature measurements of compost masses were done *in situ* with a long-stem thermometer. The samples taken were bulked to obtain a representative sample, packed with ice cubes in an ice chest and transported weekly to the laboratory. The samples were kept in a refrigerator at a temperature of 4°C for a day before microbial analysis performed.

Physico-chemical parameters Analysis

Temperature Determination

Temperature readings from three different locations; The top, middle and bottom of compost masses from the different systems under study were taken daily using the long stem thermometer (Salmoiragh Co. thermometer model 17506) at the site. The daily ambient temperatures were also determined.

pH Determination

The representative samples from each system were thawed. Three sub samples of 10g were taken from the representative sample of each system and poured into labelled beakers for the pH determination. The triplicated sub samples were suspended in distilled water in the ratio (1:10) and shaken on a rotary shaker for 30mins. The supernatant was then poured into a beaker and pH determined using a pH meter (Scientific Instruments Co., Italy., model 9000/3). The pH of the triplicated samples for each system were averaged to represent pH of compost mass in each system.

Moisture Determination

A well mixed sample of 10g each of from the different systems were weighed in triplicates for moisture content determination using the oven method. Samples were kept in the oven at 105°C for 24hrs and change in weight of samples were averaged and used as the measure of moisture content of compost mass in each system.

Microbiological Analysis

Serial Dilution for Total Viable, Coliform and fungi Count

Representative samples of 1g are taken from each of the systems mounted for study was weighed into 9ml of 0.1% peptone water contained in 4 different McCartney bottles and incubated at 37°C for 15minutes. They were well mixed and 1ml of the supernatant was drawn from each of the bottles and diluted using 10-fold dilution into 4 other McCartney bottles each containing 9ml of sterile 0.1% blank peptone water. Different pipettes were used for each of the dilution. 1ml of the diluents taken from dilution factors: 1:10³, 1:10⁴ and 1:10⁵ were transferred into 2 sets of 3 different McCartney bottles one set

containing 9ml of molten Plate Count Agar(PCA) for viable count and the other set 9ml of Violet Red Bile Agar for coliform count. Both sets were kept in water bath at 45°C to prevent solidification (Collins and Lyne, 1983). They were mixed by swirling and then poured into sterile Petri-dishes aseptically and allowed to set. For fungi enumeration, 1ml of the neat representing compost mass taken from each system was transferred onto the Sabouraud agar in labelled Petri-dishes. The whole set was incubated at 37°C for 24hours and at 30°C for 2-7 days respectively for bacteria and fungi. Cultures showing between 30-300 colonies were counted using the colony counter (AOAC, 1983).

Cultures and subcultures

Cultures were made from the neat dilutions onto Blood agar, MacConkey agar and Sabouraud agar using plate-out technique as described by Heritage *et al.* (1996). The cultures were incubated for 24h at 30°C made on Blood agar and MacConkey plates, and 2-7 days at 30°C for those made on Sabouraud agar. After growth was observed, identified colonies were purified by subculturing on Blood agar, MacConkey agar and Sabouraud agar. Subcultures were made on Brilliant Green agar and Eosin Methylene Blue agar in order to isolate the *Salmonella spp.* and *coli* forms present

Isolation and Identification

The colonial morphology and cultural characteristics were studied for size, shape and colour on the different media used for the subcultures. Bacteria were Gram stained and their reactions examined by using the light microscope at x100 magnification with oil immersion. The colonial morphology and cultural characteristics of bacteria identified were compared with characteristics of bacteria outlined in Cheesbrough (1984) for confirmation. Fungi were stained with lactophenol cotton blue stain and examined at x10 magnification. They were identified using microscopy and colonial morphology as used in Schneierson (1960). This was because the API (Analytical Profile Index) for bacteria and fungi were not available.

Helminths Eggs Analysis

This was done using a modified McMaster technique of that described in Murray *et al.* (1983). 3g of sample obtained from each system was weighed into labelled plastic container. The samples were emulsified with 45ml of distilled water and sieved with a wire mesh of 0.15 apertures into a bowl. The sieved solution was poured into claytone-lane test tube to 15.5ml mark and centrifuged at 1500 rpm for 3 minutes. The supernatant was poured off and the suspended sediment mixed with saturated saline solution. The samples were replicated for each system and resulting solution was loaded into a McMaster egg counting chamber with dropping pipette and examined under the light microscope with x10 eyepiece.

RESULTS AND DISCUSSION

The hydrogen ion (pH) concentration of the compost masses in the two systems were measured for the 13 weeks with their average weekly readings determined and used in plotting the graph in figure 1.

The graph shows that the pH values in both systems ranged from 7-8.5 during the process. The pH values rose from 7.69 and 7.79 in the DAT and T-W systems respectively during week 0 to a peak of 8.18 in DAT during week 2 and 8.16 in T-W during week 3. However falls in pH values were observed in both systems during week 5. During subsequent weeks of composting, the patterns observed were similar with values recorded in DAT systems being higher. There was a gradual fall in the pH values towards neutrality in both systems at the end of the process. ANOVA performed on the pH values of compost masses in both systems yielded a p-value of 0.25 at $\alpha = 0.05$, indicating that no significance difference existed in both systems in terms of the pH values. Eklind *et al.* (1997) revealed that organic acids such as lactic and acetic acid are frequently produced during the initial microbial degradation of food waste which reduces the pH of compost materials to between 4-5. The peculiar trend taken by the pH values recorded in the both systems may be due to the inclusion of 500g/40L of starter containing genetically modified microorganisms such as *Corynebacterium spp.* and *Bacillus spp.* that might have eliminated the organic acids, thus preventing the characteristic initial low pH of 4-5 reported by Eklind *et al.* (1997). This confirms the result from Nakasaki *et al.*

(1996) that the degradation rate at the initial stage of composting can be significantly increased by inoculation of acid-tolerant thermophilic bacteria. Choi and Parks (1998) also reported the use of microorganisms such as thermophilic yeast to eliminate the organic acids produced initially during composting to stimulate the growth of thermophilic bacteria, hence preventing the low pH inhibiting factor associated with the transition from the mesophilic to the thermophilic phase of composting. Sundberg (2005) reported that during successful and fully developed composting, the pH often rises to 8-9. Hydrogen ion concentration (pH) values in both systems ranged from 7-8.5 during the process.

ANOVA performed on the average moisture content of compost masses in both systems gave a p-value of 0.68 at $\alpha = 0.05$, indicating the existence of no significant differences in moisture contents recorded in both systems. The patterns of the moisture values are illustrated in figure 2.

The rise and fall moisture patterns illustrated by the curves in figure 3 was as a result of the variations in the temperature and aeration in the different systems causing different rates of evaporation of moisture from compost mass in each system. The correlation between temperature and moisture in both systems were $r = 0.86$ and $r = 0.29$ in T-W and DAT respectively. The higher positive correlation observed in T-W was due to the lower temperatures recorded in that system as a result of better aeration, hence low water evaporation as compared to the DAT system. However, it must be noted that, the positive

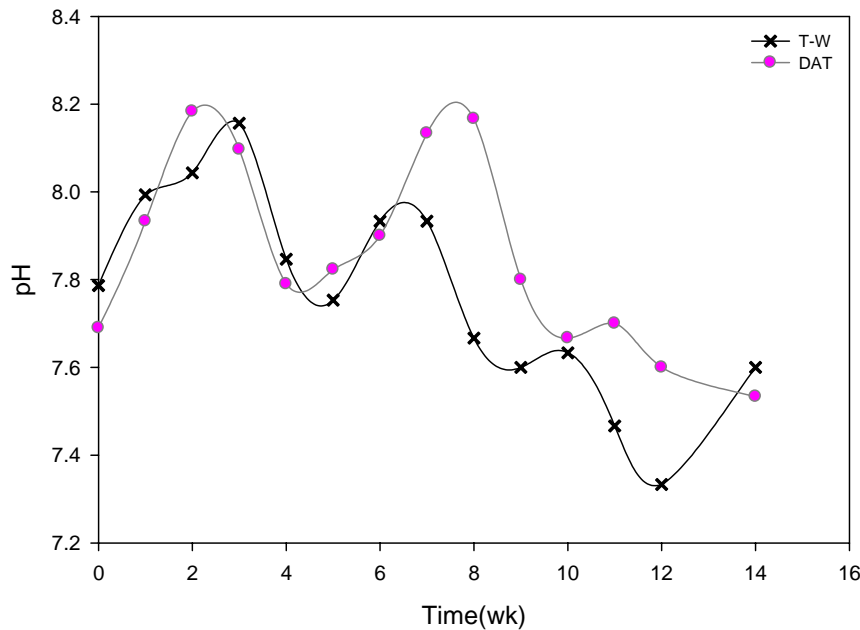


Fig. 1. Average pH readings in the systems understudied.

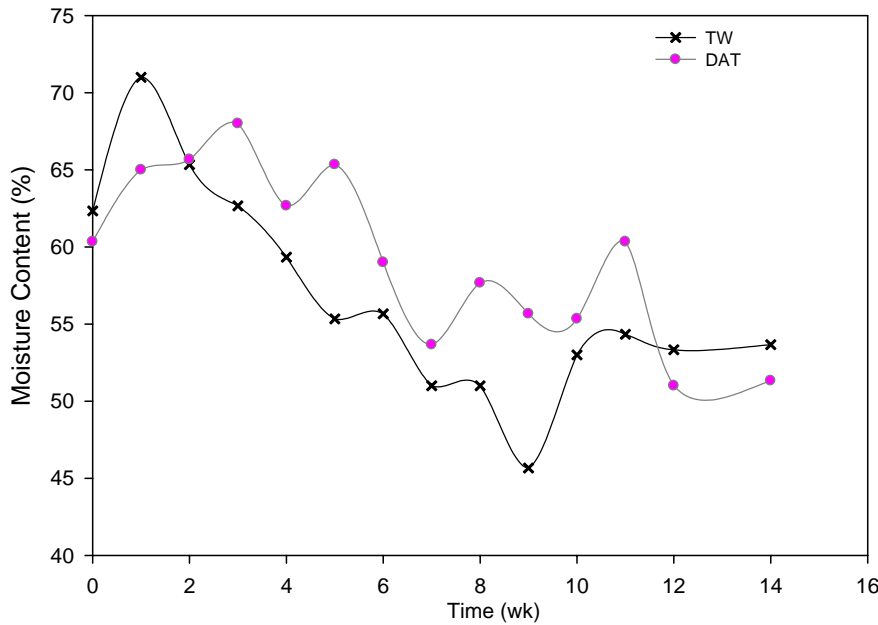


Fig. 2. Average moisture contents in the composting systems understudied.

correlation coefficient values achieved in both systems were as a result of regular rehydration of compost mass to avoid drying up by the heat produced during the process. The moisture contents were high initially in both systems but reduced at the end of the process. The moisture values recorded during the process ranged from 40% - 70% in both systems with values from the last 6 weeks ranging between 46 - 60%.

The average temperature values recorded in both systems were significantly different as ANOVA performed on such values yield a p-value of 0.01 at $\alpha = 0.05$. Temperature distribution patterns as recorded in both systems during the process are shown in figure 3.

The peak temperatures recorded were 63.24 and 62.56°C in DAT and T-W systems respectively. It was observed that temperatures fell gradually in both systems but at different rates and to different extent. Temperature values recorded were higher in the DAT system than the T-W as a result of better aeration in T-W. Temperature values recorded in the DAT system ranged between 63.24°C recorded in week 1 to 48.14°C recorded in week 12 whereas those in T-W ranged between 62.56°C in week 1 to 37.89°C in week 11. Thus, the variations in temperature in both systems implied the succession of different microbial communities in all the systems as reported in Miller (1993) and hence different rate of decomposition rate as indicated by Sundberg, (2005). However, the ambient temperature took nearly a linear pattern ranging from 27 °C in week 0 to 24.33°C in week 12.

The distribution of microorganisms in the systems in relation to temperature variation is shown in figures 5 and 6. While figure 4 shows that every temperature change recorded in the DAT system affected the total viable count. Rise in temperature from 53.20°C to 63.24°C (week 0 to week 1); saw a slight decline in total viable count from $7.31\log\text{CFU/g}$ of compost to $7.21\log\text{CFU/g}$ of compost. Every rise and fall in the temperatures recorded in the DAT during the subsequent weeks resulted in the decrease and increase respectively in the total viable count until week 12 when it reduced to $7.08\log\text{CFU/g}$ of compost. The rises and falls in the total viable count show that temperature inactivated some of the microorganisms while others increased during the process. However, the final total viable count ($7.08\log\text{CFU/g}$ of compost) was lower than the initial total viable count ($7.31\log\text{CFU/g}$ of compost) indicating a decrease in microbial population as the process came to an end.

Bacillus spp., *Staphylococcus spp.*, *Streptococcus spp.*, *Clostridium spp.*, *Campylobacter spp.*, *Listeria spp.*, *Corynebacterium spp.*, *Yersinia spp.* and *Enterobacter spp.* were the bacteria identified during the composting process. At the end of week 12, only *Bacillus spp.* (33.33%), *Listeria spp.* (8.33%) and *Corynebacterium spp.* (58.33%) survived. *Bacillus spp.* and *Corynebacterium spp.* were the genetically modified microorganisms in the starter used to aid the decomposition process. *Listeria spp.* are found in the soil and known to be zoonotic. Banwart (1989) reported that *Listeria spp.* causes listeriosis which has several

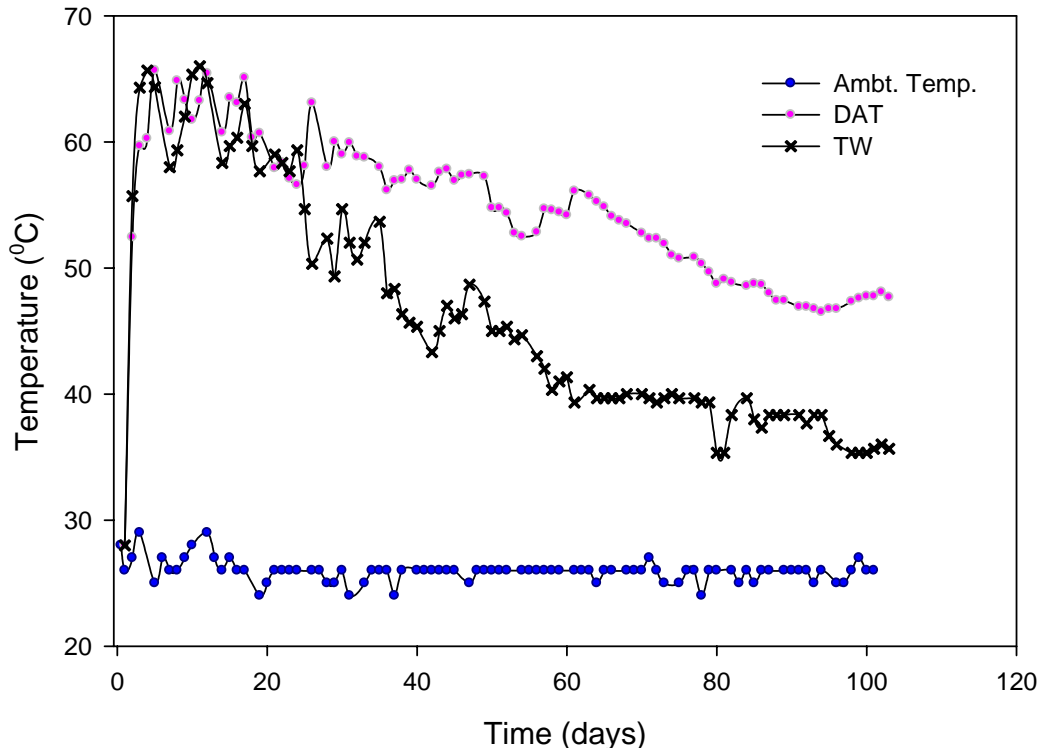


Fig. 3. Average Temperature Readings Recorded in the Systems Understudied.

manifestations including septicaemia (leading to abortion or stillbirth in women), endocarditis, pneumonia, conjunctivitis, pharyngitis, urethritis and meningitis.

Total coliform count in the DAT system decreased from $7.21\log\text{CFU/g}$ of compost to $6.26\log\text{CFU/g}$ with rise in temperature from week 0 to week 1. Fall in temperature during week 2 resulted in increased total viable counts from $6.26\log\text{CFU/g}$ of compost to $6.82\log\text{CFU/g}$ of compost. *Enterobacter spp.* was the only coliform that was identified and did not survive the process. The total coliform count was reduced to 0 in week 4 as seen in fig.5 when temperature was at 59.08°C , indicating the reduction in faecal contamination.

The total fungi count increase from $1.11\log\text{CFU/g}$ of compost in week 0, with slight rises and falls in numbers during the subsequent weeks, until finally reaching $2.13\log\text{CFU/g}$ of compost in week 12. The increase recorded in fungi population towards the end of the process in the DAT system was due to the temperature decrease which presented favourable conditions for them to decompose the cellulose, chitin and lignin known to be prevalent at the latter stages of composting as reported in Compost Microbiology and Soil Food Web (2008). The

fungi identified during the process were *Aspergillus spp.*, *Penicillium spp.*, *Mucor spp.* and *Rhizopus spp.* with *Penicillium spp.* (97.79%) and *Mucor spp.* (2.21%) surviving the process. *Penicillium spp.* is reported to produce mycotoxins such as citrinin, luteoskyrin, ochratoxins and rubratoxin which cause illnesses in humans. Luteoskyrin is associated with high incidence of liver cancer in humans (Banwart, 1989). However, *Mucor spp.* is not known to cause diseases in human (Banwart, 1989).

The total viable count decreased from $7.79\log\text{CFU/g}$ of compost to $7.40\log\text{CFU/g}$ of compost with a rise in temperature from 57.60°C to 62.56°C during week 0 to week 1 in the T-W system. Temperature fell gradually from week 2 to week 7 but was within the thermophilic range. This temperature range caused almost uniform rises and falls in the total viable count during week 2 to week 7. As the temperature fell to 41.17°C (mesophilic condition) during week 8, total viable count decreased to $7.19\log\text{CFU/g}$ of compost. There was a rise in the total viable count from week 10 to 11 and a slight fall in week 12 when temperature fell within the mesophilic range. It was noted also that the percentage frequencies of *Corynebacterium spp.* increased from week 9 to week 12.

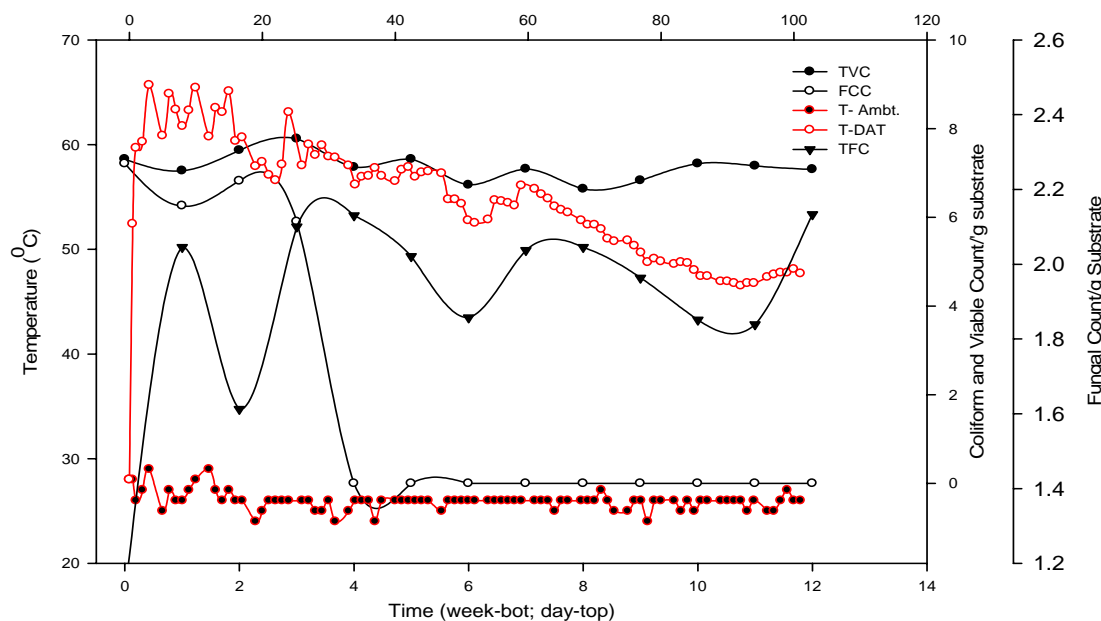


Fig. 4. Temperature and microbial survival in DAT System.

The fall in the total viable count during week 12 might be due to nutrient depletion. The bacteria identified during the process were *Bacillus spp.*, *Staphylococcus spp.*, *Streptococcus spp.*, *Clostridium spp.*, *Campylobacter spp.*, *Listeria spp.*, *Corynebacterium spp.*, *Yersinia spp.* and *Enterobacter spp.* with *Bacillus spp.*(28.57%) and *Corynebacterium spp.*(71.43%) surviving the process. Regular turning of compost masses made in T-W system might have aided the inactivation of the *Listeria spp.* as it helped uniform distribution of heat through the compost mass.

The total coliform count decreased from $6.88\log\text{CFU/g}$ of compost to $6.56\log\text{CFU/g}$ of compost with rise in temperature from 57.60°C at start-up of pile to 62.56°C at week 1 as seen in Figure 5. The total coliform count decreased until the week 4 when the total coliform count yielded $0\log\text{CFU/g}$ of compost at a temperature of 51.83°C . The total coliform count of $0\log\text{CFU/g}$ of compost obtained in week 4 indicates the reduction of faecal contamination. *Enterobacter spp.* was the only coliform identified during the process.

Total fungi count in T-W system decreased from $1.68\log\text{CFU/g}$ of compost to $1.45\log\text{CFU/g}$ of compost with increased in temperature from 57.60°C start-up of pile to 62.56°C at week 1. The total fungi count increased as temperature fell from week 1 to week 4 and subsequently decline in week 5. The total fungi count further rose to values ranging between $1.90\log\text{CFU/g}$ of compost to $2.15\log\text{CFU/g}$ of compost during week 6 to week 11. A fall was recorded in the total fungi count

during week 12. This distribution of fungi during 6 to 11 confirms the fact that they tolerate low temperature and largely present at the latter stages of composting to decompose cellulose, chitin and lignin. The fungi identified during the process were *Penicillium spp.*, *Aspergillus spp.*, *Mucor spp.* and *Rhizopus spp.* The only fungus that survived the process was *Penicillium spp.*

It must be noted that helminths egg was not found in both systems for the duration of the experiment.

CONCLUSION AND RECOMMENDATIONS

Data collected on temperature, moisture content, pH, total viable count, total coliform count, total fungi count and Helminths eggs determined during composting in two different systems at VREL Farms for a period of thirteen weeks were analysed to ascertain the effects of temperature, moisture and pH on the microbial survival.

Moisture content and pH values ranged between 40 - 70% and 7-8.5 respectively during the thirteen weeks monitoring period. There were no significant differences in pH and moisture content values for both systems. Temperature values recorded however were significantly different in both systems and affected the microbial distribution during the process. Temperature values recorded in the DAT system ranged between 48 - 64°C whereas those in T-W ranged between 37 - 63°C .

Enterobacter spp. was the only coliform identified in the systems and was inactivated in week 4. *Bacillus spp.*,

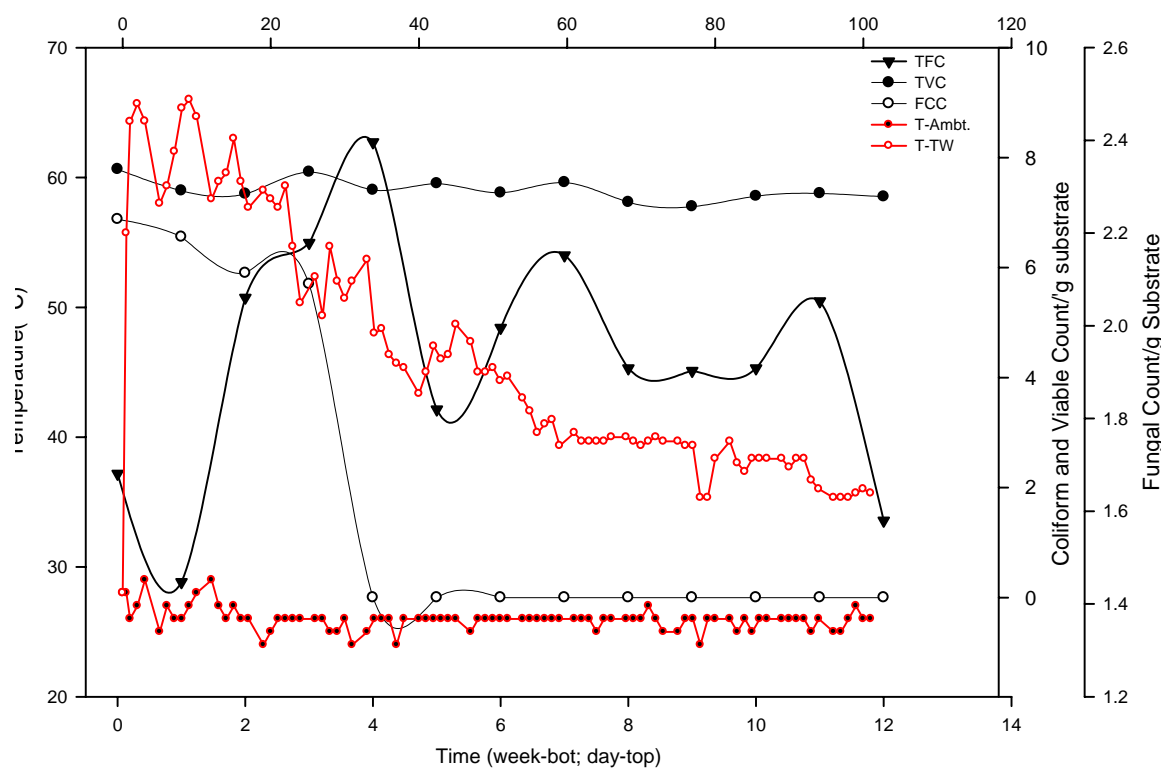


Fig. 5. Temperature and microbial survival in T-W System.

Staphylococcus spp., *Streptococcus spp.*, *Clostridium spp.*, *Campylobacter spp.*, *Listeria spp.*, *Corynebacterium spp.*, *Yersinia spp.* and *Enterobacter spp.* were the bacteria identified during composting process in the systems. *Bacillus spp.* (33.33%), *Listeria spp.* (8.33%) and *Corynebacterium spp.* (58.33%) survived the process in the DAT system while *Bacillus spp.* (28.57%) and *Corynebacterium spp.* (71.43%) survived in T-W system. *Bacillus spp.* and *Corynebacterium spp.* were the genetically modified microorganisms present in the starter used to aid the decomposition process.

Aspergillus spp., *Penicillium spp.*, *Mucor spp.* and *Rhizopus spp.* were the fungi identified during the composting process in the different systems. *Penicillium spp.* (97.79%) and *Mucor spp.* (2.21%) survived the process in DAT system with only *Penicillium spp.* (100%) surviving in T-W system. However, no helminths egg was found during the process.

Some members of the compost microbial community identified in compost masses in the two different systems are responsible for causing diseases in humans. Banwart (1989) reported that *Listeria spp.* causes listeriosis, which has several manifestations including septicaemia (leading

to abortion or stillbirth in women), endocarditis, pneumonia, conjunctivitis, pharyngitis, urethritis and meningitis. *Penicillium spp.* is reported to produce mycotoxins such as citrinin, luteoskyrin, ochratoxins and rubratoxin which cause illnesses in humans. Luteoskyrin is associated with high incidence of liver cancer in humans. Since *Listeria spp.*, known to be zoonotic survived in compost processed in DAT system and *penicillium spp.* in both, protective measures need to be worn by compost manufacturers and farmers to safeguard their health. Also, regular turning of compost masses must be done as it helped in uniform distribution of heat through compost masses; hence, the inactivation of *Listeria spp.* in the T-W system.

ACKNOWLEDGEMENTS

The authors wish to dedicate this paper to the memory of Dr. AD Adjei (was a co-supervisor to this work) and a special thanks to Dr. H Atysina, Mr. C Takyi-Arthur and Mr. S Ogbetey, all of the Microbiology Department of the Animal Research Institute – CSIR, Ghana and Mr H van der Broek of the Volta River Estate Limited for their assistance throughout the research.

REFERENCES

- AOAC. 1983. Enumeration of Coliforms in Selected Foods. Hydrophobic grid membrane filters method, official first action. Journal of Association of Official Analytical Chemists. 66:547-548.
- Banwart, GJ 1989. Basic Food Microbiology. (2nd ed.) Chapman and Hall, London. pp1-5.
- Beffa, T., Blanc, M., Marilley, L., Fischer, JL., Lyon, PF. and Arangno, M. 1996. Taxonomic and Metabolic Microbial Diversity during Composting. In: The Science of Composting. Eds. de Bertoldi, M., Sequi, P., Lemmes, B. and Papi, T. Chapman and Hall, London. pp149-161.
- Cheesbrough, M. 1984. Medical Laboratory Manual for Tropical Countries. Butterworth-Heinemann Ltd. 2:187-193.
- Choi, MH. and Park, YH. 1998. The Influence of yeast on Thermophilic Composting of Food Waste. Letters in Applied Microbiology. 26:175-178.
- CIWMB. 2008. Compost Microbiology and the Soil Food Web. California Integrated Waste Management Board Site. Retrieved on January 5, 2008 from < www.ciwmb.ca.gov/publications/organics/>.
- Collins, CH. and Lyne, PM. 1983. Microbiological Methods. (5th ed.). Butterworth and Co., London. pp5 & 89.
- Dai, H., Kazutaka K., Yasuyuki F. and Kiyonori H. 2005. Effect of Addition of Organic Waste on Reduction of *Escherichia coli* during Cattle Feces Composting under High-moisture Condition. Journal of Bioresource Technology. 30:30-34.
- Droffner, ML. and Brinton, WF. 1995. Survival of *E. coli* and *Salmonella* Population in Aerobic Thermophilic Compost as Measured with DNA Gene Probes. Zentralbl Hygiene. 197: 387-397.
- Eklind, Y., BeckFriis, B., Bengtsson, S., Ejlertsson, J., Kirchmann, H., Mathisen, B., Nordkvist, E., Sonesson, U., Svensson, BH. and Torstensson, L. 1997. Chemical Characterization of Source-separated Organic Household Waste. Swedish Journal of Agricultural Research. 27:167-178.
- Eriksson, O. 2003. Environmental and Economic Assessment of Swedish Municipal Solid Waste Management in a Systems Perspective. Ph.D. thesis. Royal Institute of Technology Stockholm, Sweden. pp54.
- Heritage, J., Evans, ECV. and Killington, RA. 1996. Introductory to Microbiology. Cambridge University Press. 2:129-138.
- Ishii, K., Fukui, M. and Takii, S. 2000. Microbial Succession During a Composting Process as Evaluated by Denaturing Gradient Gel Electrophoresis Analysis. J. Appl. Microbiol. 89:768-777.
- Cekmecelioglu, D., Demirci, A., Graves, RE. and Davitt, NH. 2005. Applicability of Optimised in-vessel Food Waste Composting for Windrow Systems. Biosystems Eng. 91:479-486.
- Lung, AJ., Lin, CM., Kim, JM., Marshall, MR., Hordstedt, R., Thompson, NP. and Wei, CI. 2001. Destruction of *Escherichia coli* O157:H7 and *Salmonella enteritidis* in Cow Manure Composting. Journal of Food Protection. 64(9):1309-1314.
- Madigan, MT., Martinko, JM. and Parker, J. 2000. Brock-Biology of Micro Organisms. (9th ed.). Prentice-Hall. Upper Saddle River, NJ., USA. pp991.
- Mead, PS., Slutsker, L., Dietz, V., McCaig, LF., Bresee, JS., Shapiro, C., Griffin, PM. and Tauxe, RV. 1999. Food-related Illness and Death in the United States. Emerging Infectious Diseases. 5:607-625.
- Miller, FC. 1993. Composting as a Process Based on the Control of Ecologically Selective Factors. In: Soil Microbial Ecology. Ed. Metting, FB. Marcel Dekker, New York, USA. 515-544.
- Murray, M., Trail, JCM., Turner, DA. and Wissocq, Y. 1983. Livestock Productivity and Trypanotolerance. Retrieved on 4th July, 2008 from <<http://www.ilri.org/InfoServ/Webpub/Fulldocs/LivProd/Toc.htm#TopOfPage>>.
- Nakasaki, K., Uehara, N., Kataoka, M. and Kubota, H. 1996. The Use of *Bacillus licheniformis* HAI to Accelerate Composting of Organic Wastes. Compost Science and Utilization. 4(4):47-51.
- Ryckeboer, J., Mergaert, J., Vaes, K., Klammer, S., DeClercq, D., Coosemans, J. and Insam, Schneierson, SS. 2003. Atlas of Diagnostic Microbiology. Abbott Laboratories, North Chicago, Illinois, USA. pp44-45.
- Sundberg, C. 2005. Improving Compost Process Efficiency by Controlling Aeration, Temperature and pH. Ph.D thesis. Swedish University of Agricultural Science (SLU), Uppsala.
- Trois, C. and Polster, A. 2007. Effective Pine Bark Composting with the Dome Aeration Technology. Waste Management. 27:96-105.

THE ESSENTIAL OIL COMPONENTS OF *IRVINGIA GABONENSIS* AND *IRVINGIA WOMBOLU* FROM SOUTHERN NIGERIA

Matilda Iyayi Ikhataua¹ and *Abiodun Falodun²

¹Department of Forestry and Wildlife, Faculty of Agriculture, University of Benin, Benin City

²Department of Pharmaceutical Chemistry, Faculty of Pharmacy, University of Benin, Benin City, Nigeria

ABSTRACT

The chemical composition of volatile compounds from seeds of *Irvingia gabonensis* and *Irvingia wombolu* (Irvingiaceae) grown in Southern Nigeria has been studied. Essential oils from two species of the plant were obtained by solvent extraction in conventional Clavenger- like apparatus. The major compounds in these essential oils were identified using gas chromatography-mass spectrometry GC and GC/MS. Twelve and ten components were identified in *I. gabonensis* and *I. wombolu*, respectively, of which carboxylic acids and esters were the major components in both species. The oils obtained from the two species have been profiled by GC/MS to obtain data and they showed similarities but also differences in their composition. Fatty acids and esters compounds were the most abundant components in the oils. The present study may represent the first of its kind on the characterization of the volatile constituents in *Irvingia* species and useful contribution to the better understanding of interspecies relationships in this genus.

Keywords: Essential oil, *Irvingia gabonensis*, *Irvingia wombolu*, chemical constituent

INTRODUCTION

The tropical rainforest zone is rich in medicinal plants possessing array of potential medicinal properties but the Phyto-pharmaceuticals and ethno-medicinal values have not been fully utilized (Baladrin *et al.*, 1993; Stephen *et al.*, 2009; Oladosu *et al.*, 2011). These potential benefits are due not only to the species richness of the tropical flora, but also to the parasites and pathogens which the plants must provide some level of defensive mechanism. Many of these defense phytochemicals secreted (such as alkaloids, tannins, saponins) can be used as remedies against diseases and infections in humans, and also to eradicate other organisms (Farnsworth, 1988, Falodun *et al.*, 2009; Falodun, 2010; Naresh *et al.*, 2011; Adisa *et al.*, 2011). Essential oils form one of the numerous pharmacologically active metabolites in plants, and they are widely used as medicines in the form of medicaments, pharmaceuticals and food additives (Reische *et al.*, 1998; Cowan, 1999; Onwuliri *et al.*, 2004, Gehan *et al.*, 2008; Quang *et al.*, 2011).

Irvingia gabonensis also known as wild mango is a forest fruit tree widely available in Africa (Eka, 1980). *Irvingia gabonensis* (Aubry-Lecomte ex O'Rorke) Baill. and *I. wombolu* Vermoesen (family Irvingiaceae) are the two species of the genus in Nigeria (Harris, 1996). The pulp surrounding the fibrous-coated, hard-shelled nut of *I. gabonensis* is sweet and edible when ripe while that of *I. wombolu* is bitter and inedible. The nuts of both species, also known as dika nuts, are widely used in Nigeria as a

soup thickener because they gelatinize into a thick, viscous sauce base for vegetable soup when heated (Onyeike *et al.*, 1995). Though these thickening properties are due to the carbohydrate content of the kernel (Ndjouenkeu *et al.*, 1996; Okolo, 2000), fat represents its main component (51–72 %), with a fatty acid profile mainly made up of myristic acid (33–50 %) and lauric acid (38–58%) (Leakey, 1999; Leakey *et al.*, 2005). Some potential industrial applications of the dika nut oil that have been identified include its usefulness in the preparation of margarine, cooking oil, soap, and perfumery, and as a lubricant in tablet formulations (Abaelu and Akinrimisi, 1980; Udeala and Onyeachi, 1980; Osagie and Odutuga, 1986).

Of the Non-timber forest products (NTFPs) *Irvingia* is one of the indigenous fruit trees with multiple uses and generates a high cash income within and outside Nigeria (Okafor, 1985; Okafor, 1991; Ladipo and Boland, 1994; Akubor, 1996; Ladipo, 1999). Its kernels are highly priced as soup condiments (Okafor, 1985; Okeke, 1995). The pulp of *I. gabonensis* is used for the preparation of juice, jelly and jam; while the extracted fat from both varieties is used in soap making, pharmaceutical preparations and domestic use (Okafor, 1985). Ejiofor *et al.* (1987) reported the composition of *I. gabonensis* var *excelsa* (now *I. wombolu*) as 51.3% fat, 26.0% total carbohydrate, 2.5% ash, 7.4% crude protein, 0.9% crude fibre, 9.2mg 100-1 vitamin C and 0.6mg 100-1 vitamin A. Proximate analysis of the nutritive composition of healthy kernels of *I. gabonensis* and *I. wombolu* obtained from

*Corresponding author email: faloabi@uniben.edu

retailers showed significant differences in some nutritive components (Ikhataua *et al.*, 2010). Values obtained were 9.2 and 9.7% crude protein; 2.1 and 2.3 % ash; 97.8 and 97.8% organic matter; 9.8 and 8.6% crude fibre; 39.7 and 38.4% fat, and 39.2 and 41.0% carbohydrate respectively. In contrast to numerous papers reporting about the ethnomedicinal and Pharmaceutical uses of *I. gabonensis* and *I. wombolu* secondary metabolites, particularly fatty acids, as well as their anti-obesity and other possible applications in phyto-therapy, we observed a relative paucity of data on the essential oil composition of the plants. To the best of our knowledge, there are no published reports on the essential oil composition of seeds from *I. gabonensis* and *I. wombolu*.

The aim of this study therefore, was to explore and determine whether there are differences in the essential oil composition of the two species or not, using GC and GC/MS analyses.

MATERIALS AND METHODS

Plant collection and identification

Fruits of *Irvingia gabonensis* and *Irvingia wombolu* were obtained from standing trees in Ujabhole-Irrua in Esan Central Local Government Area of Edo State, Nigeria during the harvest season of 2010. These were processed for their stones (endocarp with the seeds within) dried, and cracked to obtain the kernels (seeds).

Extraction and isolation of essential oil

The powdered *Irvingia gabonensis* and *Irvingia wombolu* were extracted by Clevenger like apparatus for 3hours, to give yellow color oil. The oil was subjected to filtration and drying using an anhydrous sodium sulphate. The sample was stored in a refrigerator at -4°C before running in GC and GC-MS analysis.

Identification of the components

The chemical principles of the essential oil from the GC - MS analysis were identified by simple comparative analysis of their retention indices and mass spectra with those already reported (Adams, 1989, 2001; BP, 1980; Julian and Konig, 1989).

Gas Chromatography

The oil obtained from the extraction was subjected to GC and GC-MS respectively in order to obtained qualitative and quantitative data. A Shimadzu GC-17A system, furnished with an AOC-20i auto sampler and split/splitless injector was used for the analysis. A DB-5 column having 30m, 0.25mm i.d, 0.25 μ m df coated with 5% diphenyl-95% polydimethylsiloxane, conditioned to an oven temperature of 50°C (1minute), 3°C/minute to 250°C (5 minutes), 2°C/minute to 280°C. The carrier gas, nitrogen at 30 cm/s linear velocity and inlet pressure 99.8KPa; temperature of detection 280°C, flow rate 50

ml/minute, while the air flow rate of 400ml/min, make-up (H₂/air), 50ml/min, sampling rate, 40ms were used. Acquisitions of quantitative and qualitative data were obtained by Shimadzu GC solution software.

Gas chromatography-mass spectrometry analysis

The carrier gas (helium) composition was made of agilent 6890N interfaced with a VG 70-250s double focusing mass spectrometer. The operating conditions of the Mass spectrometer include ion source 250°C electron voltage at 70 eV. The GC was had DB-5 column. Similar operating parameters to those of GC (previously described) were used.

RESULTS AND DISCUSSION

The solvent extraction of *I. gabonensis* and *I. wombolu* seed part yielded light yellow oil. The identity of the constituents, their retention indices on a DB-5 column, and their percentage composition are listed in tables 1and 2, where the compounds are arranged in order of their GC elution on the DB-5 capillary column. GC and GC-MS analysis enabled the identification of a total of 12 and 10 constituents, representing 99.0 and 93.0% of the total oils, respectively.

In *I. gabonensis* oil, dodecanoic acid (50.7%), tetradecanoic acid (30.5%) and octadecanoic acid (8.6%) were found to be the major constituents; all the other components were detected at concentrations below 5% of the total oil. Carboxylic acids (94.9%), esters (5.7%) and ketones (0.9%) were the main groups of constituents of the essential oil. The oil of *I. wombolu* had esters consisting mainly of dodecanoate (2.9%), tetradecanoic acid (50.7%), oleic acid (12.5%) and hexadecanoic acid (7.5%) as major chemical principles. Aldehydes and ketones were completely absent. The presence of (Z, Z)-9,12-octadecadienoic acid in *I. wombolu* is noteworthy because this acid, considered an essential fatty acid, is the precursor of prostaglandins PG1 and PG2 (Carmen *et al.*, 2008). Esters were found to be copious in both species of *Irvingia* as shown by the identified components. Esters are known to be formed mainly at the stage of ripening of fruit, and they are also important for the sweet and fruity aroma of most fruits (Dimick and Horkin, 1983). It could be broadly inferred that the characteristic aroma of the *Irvingia* species could be attributed to the heterocyclic compounds and the organic acids.

On comparing our results of *I. gabonensis* oil with *I. wombolu* oil compositions, it was observed that out of 12 and 10 constituents present in the above oils, respectively, seven constituents were common to both oils. It was also observed that the fatty acid composition in *I. gabonensis* and *I.wombolu* were 94.9 and 89.2% respectively which is in agreement with published data of (Ekpo *et al.*, 2007).

Table 1. Volatile oil composition of seeds of *I. gabonensis* from GC-MS analysis.

Peak	Components	RI	Content (%)
1	Methyl tetradecanoate	1002	0.2
2	Dodecanoic acid methyl ester	1056	0.5
3	Dodecanoate propyl ester	1101	0.3
4	Dodecanoic acid	1205	50.7
5	Octanoic acid ester	1209	1.5
6	Undecanone	1283	0.9
7	Decanoic acid	1365	0.4
8	Dodecanoate ethane ester	1390	0.5
9	Hexadecanoic acid	1767	4.7
10	Tetradecanoic acid	1769	30.5
11	Octadecanoic acid	1984	8.6
12	cis-Linoleic acid methyl ester	2091	2.2
		Total	99.0

Table 2. Volatile oil composition of seeds of *I. wombolu* from GC/MS analysis.

Peak	Components	RI	Content (%)
1	Methyl tetradecanoate	1002	0.5
2	Dodecanoic acid methyl ester	1056	2.9
4	Dodecanoic acid	1205	59.0
5	Hexadecanoic acid	1767	7.5
6	Tetradecanoic acid	1769	7.6
7	Octadecanoic acid	1858	2.1
8	Oleic acid	1958	12.5
9	(Z,Z)-9,12-octadecadienoic acid	2225	0.5
10	Dodecanoate propyl ester	-	0.5
		Total	93.0

The identification was performed by calculation of retention index (RI) on a DB-5-; BP.

Future research will focus on the biological and pharmacological investigations of the essential oils of both species.

CONCLUSION

From the above results it is evident that there is slight variation in the percentage composition of the volatile oils of *I. gabonensis* and *I. wombolu* major constituents, which could be indicative of different biosynthetic and biogenetic pathways since both are agro climatically and geographically related.

ACKNOWLEDGEMENT

Special thanks to University of Benin and Usmanu Danfodiyo University (Sokoto) for facilities in analyzing the samples.

REFERENCES

- Abaelu, AM. and Akinrimisi, EO. 1980. Amino acid composition of *Irvingia gabonensis* oil seed proteins. Niger. J. Nutr. Sci. 1(2):133-135.
- Adams, RP. 1989. Identification of Essential oils by Ion Trap Mass Spectroscopy. Academic Press, New York, USA.
- Adams, RP. 2001. Identification of Essential oils by Gas Chromatography Quadrupole Mass Spectrometry. Allured Publishing Corporation, Carol Stream, USA.
- Adisa, RA., Abas, K., Oladosu, IA., Ajaz, A., Choudhary, MI., Olorunsogo, OO. and Rahman, A. 2011. Purification and Characterization of Phenolic compounds from the leaves of *Cnestis feruginea* : investigation of antioxidant activity. Research Journal of Phytochemistry. 5(4):177-189.

- Akubor, PI. 1996. The Suitability of African Bush Mango to Wine Production. *Plant Food and Human Nutrition.* 49:213-219.
- British Pharmacopoeia. HM. 1980. Stationary Office, London, II, P.A. pp109.
- Baladrin, MF., Kinghorn, AD. and Farnsworth, NR. 1993. Plants derived Natural products in drug Discovery and Development. In *Human medicinal Agents from Plants, Symposium Series.* 534.
- Baladrin, MF (ed.). American Chemical Society, Washington DC. pp2-12.
- Carmen, F., Enrico, M., Felice, S., Svetlana, B., Maurizio, B. and Sergio, R. 2008. Volatile Constituents of Aerial Parts of *Centaurea sibthorpii* (Sect. Carduiformes, Asteraceae) from Greece and their Biological Activity. *Natural Product Research.* 2(10):840-845.
- Cowan, MM. 1999. Plant Products as Antimicrobial Agents. *Clin. Microbiol. Rev.* 12:12-582.
- Dimick, PS. and Horkin, JC. 1983. Review of Apple Flavor – state of the art, *Crit. Rev. Food Sci. Nutr.* 18:387-409.
- Ejiofor, MA., Onwubuke, SN. and Okafor, JC. 1998. Developing Improved Methods of Processing and Utilization of Kernels of *Irvingia gabonensis* (var. *gabonensis* and var. *excelsa*). *Int. Tree Crops J.* 4(3):283-290.
- Eka, OU. 1980. Proximate composition of bush mango tree and some properties of dikafat. *Niger. J. Nutr. Sci.* 1(1):33-36.
- Ekpo, IW., Amor, ID. and Morah, FN. 2007. Seed oils and Nutritive Studies on the Seeds of *gabonensis* and *wombolu* Varieties of *Irvingia gabonensis*. *The Nigerian Academic Forum.* 13 1.
- Falodun, A. 2010. Herbal Medicine in Africa, Distribution and standardization. *Research Journal of Phytochemistry.* 4(3):154-161.
- Falodun, A., Qadir, IM., Omogbai, EKI. and Choudhary, MI. 2009. Bioactive Chemical constituents of *Stereospernum kunthianum* (Bignoniaceae). *Research Journal of Phytochemistry* 3(2):35-43.
- Farnsworth, NR. 1988. Screening Plants for New Medicines. In: *Biodiversity.* Eds. Wilson, EO. and Peter, FM. National Academy Press, Washington, DC, USA. 83-96.
- Gehan A, El-Shoubaky., Amal M., Youssef, M. and Essan, AS. 2008. Comparative Phytochemical Investigation of Beneficial Essential fatty acids on a variety of Marine Sea weeds Algae. *Research Journal of Phytochemistry.* 2(1):18-26.
- Harris, DJ. 1996. A Revision of the Irvingiaceae in Africa. *Bulletin Jard. Bot. Belg.* 65:143-196.
- Ikhataua, MI., Egharevba, RKA. and Asa'a, LN. 2010. Microbial spoilage of *Irvingia* Kernels in Benin City. Nigeria. *Achieves of Applied Science Research.* 2(5):168-176.
- Julain, D. and Konig, WA. 1989. *The Atlas of Spectral data of Sesquiterpene Hydrocarbons.* Verlag, Harburg.
- Ladipo, DO. and Boland, DJ. 1994. Trade in *Irvingia* Kernels. In: *Proceedings of the International Workshop on Irvingia in West Africa.* Eds. Ladipo, DO. and Boland, DJ. International Centre for Research in Agro-Forestry (ICRAF), Nairobi, Kenya. 98-112.
- Ladipo, DO. 1999. The Development of Quality Control Standards for Ogbono (*Irvingia gabonensis* and *Irvingia wombolu*) Kernel. In: *Effects Towards Encouraging Organised and Further International trade in N.W.F.P. of West and Central Africa.* Eds. Ladipo, DO. and Boland, DJ. Paper presented at NRI-IPGRI International workshop on African Indigenous Nuts, Limbe Cameroon. 22-28.
- Leakey, RRB. 1999. Potential for Novel Food Products from Agroforestry: A Review. *Food Chem.* 66:1-14.
- Leakey, RRB., Greenwell, P., Hall, MN., Atangana, AR., Usoro, C., Anegbeh, PO., Fondoun, JM. and Tchoundjeu, Z. 2005. Domestication of *Irvingia gabonensis*: 4. Tree-to-tree variation in food-thickening properties and in fat and protein contents of dika nut. *Food Chem.* 90:365-378.
- Naresh, SG., Rashmi, A and Shiv, RK. 2011. Evaluation of Antioxidant, Anti inflammatory and Analgesic Potential of *Luffa acutangula* Roxb. Var. amara. *Research Journal of Phytochemistry.* 5(4):201-208.
- Ndjouenkeu, R., Goycoolea, FM., Morris, ER. and Akingbala, JO. 1996. Rheology of Okra (*Hibiscus esculentus* L.) and dika nut (*Irvingia gabonensis*) polysaccharides. *Carbohydr Polym.* 29:263-269.
- Okafor, JC. 1985. Commercial Production of 'Ogbono' and 'ugiri'. In: *Information series on Agriculture in Anambra State. How to grow selected fruit trees.* Booklet No. 4. 25-30.
- Okafor, JC. 1991. Importance of Indigenous Fruit trees in Nigerian Economy. Invited paper presented at the symposium marking the 11th Food day celebration in Nigeria. Sheraton Hotel, Abuja. pp21.
- Okeke, A. 1995. Nursery Observations on the Growth of *Irvingia gabonensis* var *excelsa* (Ogbono) for small scale farmers. In: *Forestry and the Small Scale Farmers.* Ed. Oduwaiye, EA. Proc. of the 24th Annual Conference of the Forestry Association of Nigeria (FAN), Kaduna. 247-253.

- Okolo, HC. 2000. Industrial Potential of various *Irvingia gabonensis* Products, such as oil, ogbono and juice. In: *Irvingia*: Uses, Potential and Domestication. Eds. D. Boland, D. and Lapido, DO. ICRAF, Nairobi, Kenya.
- Oladosu, IA., Ogundayo, AL., Aiyelaagbe, OO. and Emenyonu, N. 2011. Phytochemical and Antituberculosis Activity of *Coffea brivipes*, hiern extracts. Research Journal of Phytochemistry. 5:130-135.
- Onwuliri, VA., Attah, I. and Nwankwo, JO. 2004. Anti-Nutritional Factors, Essential and Non Essential Fatty acids Composition of Ugba (*Pentaclethra macrophylla*) Seeds at Different Stages of Processing and Fermentation. Journal of Biological Sciences. 4:671-675.
- Onyeike, EN., Olungwe, T. and Uwakwe, AA. 1995. Effect of Heat-treatment and Defatting on Proximate Composition of some Nigerian local Soup thickener. Food Chem. 53:173-175.
- Osagie, AU. and Odutuga, AA. 1986. Chemical Characterization and Edibility of the Oils Extracted from four Nigerian oil seeds. Niger. J. Pure Appl. Sci. 1:15-25.
- Quang, DN., Nga, TT. and Tham, LX. 2011. Chemical composition of Vietnamese Black Lingzi *Amauroderma subresinosum* Murr. Research Journal of Phytochemistry. 5(4):216-221.
- Reische, DW., Lillard, DA. and Eitenmiller, RR .1998. Antioxidants in food lipids. In: Chemistry, nutrition and Biotechnology. Eds. Ahoh, CC. and Min, DB. Marcel Dekker, New York, USA. 432-448.
- Stephen, UA., Abiodun, F., Osahon, O. and Ewaen, E. 2009. Phytochemical Analysis and Antibacterial Activity of *Khaya grandifoliola* stem bark. Journal of Biological Sciences. 9(1)63: 67.
- Udeala, OK, Onyechi, JO. and Agu, SI. 1980. Preliminary Evaluation of Dika fat, New tablet lubricant. J. Pharm. Pharmacol. 32:6-9.

Received: Feb 3, 2012; Revised: Feb 19, 2012;

Accepted: March 28, 2012

GLIRICIDIA SEPIUM (JACQ.) WALP.: HARDWOOD WITH POTENTIAL FOR PULP AND PAPER-MAKING

*W M Kpikpi and I Sackey

Department of Applied Biology, Faculty of Applied Sciences
University for Development Studies, PO Box 24, Navrongo, Ghana

ABSTRACT

The anatomy of the wood of *Gliricidia sepium* has been studied for suitability as pulpwood. Dimensions of the wood fibre were measured microscopically to determine Runkel ratio and the Flexibility coefficient. The fibre morphology ratios inform preliminary decisions on the suitability of the species as pulpwood. Slides of microtome sections were made of the wood for microscopic study of the cell and tissue types and their relative proportions that constitute the wood. Low Runkel and high Flexibility ratios and a preponderance of fibres relative to other cells are desirable and would normally encourage the pulping and paper-making trials. The wood was pulped and hand-made paper sheets were tested for physical strength properties. The studies were duplicated for *Gmelina arborea*, which is already in use as pulp and paper-making hardwood, for comparison. *Gliricidia sepium* has Runkel ratio of 1.22 and coefficient of flexibility of 0.45 compared with *Gmelina*'s 0.19 and 0.88 respectively. The relative fibre volume for *Gliricidia* is 58.9% and about 41% other cells combined, while *Gmelina* has 72% fibres and 28% all other cells together. Pulp yields in *Gliricidia* and *Gmelina* are 46.5% and 49.2% respectively, while both species showed some good physical properties in the paper sheets: *Gliricidia* produced Burst property of 3.75 kg cm^{-2} and Tear of 155g at pulp freeness of 51^0 SR , while *Gmelina* recorded 3.98 kg cm^{-2} and Tear of 165g at freeness 36^0 SR . These values of physical strength properties combined with the reported features of the wood anatomy and the vegetative growth characteristics reported from the literature support the conclusion that *Gliricidia sepium* has great potential as a good pulpwood.

Keywords: *Gliricidia sepium*, *Gmelina arborea*, pulp, paper.

INTRODUCTION

Increased consumption of paper and paper products by society encourages the paper industry to increase production. This increased production requires a search for new suitable vegetable material, like tree species, that can be used for pulp and paper. Determining suitability of new hardwood species involves studies in the anatomical features of the wood and the natural availability of the species and its growth characteristics. For example, rapid growth rate and high pulp yield together with good fibre morphology are some of the properties a good pulpwood must have. Such studies are usually conducted in comparison with the characteristics of hardwoods already established and are in use as pulp woods. *Gliricidia sepium* is a fast growing species. Simons and Dunsdon (1992) observed that *Gliricidia* grows very quickly after germinating to about 3 m at the age of 6 – 8 months before flowering, and this rapid growth makes it an early colonizer of re-growth forest lands left to fallow. Because *Gliricidia* is such a fast growing tree species and also amenable to plantation development, the species was selected for investigation of its wood structural characteristics as to suitability for pulp and paper production.

Pulp is defined as the crude fibre produced from cellulosic raw material that can be converted, after suitable treatment, to paper and paper products. Paper, on the other hand, is defined as the matted or felted sheets of fibre formed on a wire screen from a water suspension of pulp (Kpikpi, 2005). The investigation of a hardwood species for its suitability as pulpwood is usually done in two phases: the microscopic characteristics of the wood followed by pulping trial and testing of hand-made paper sheets.

In this work, therefore, microscopic wood structure of *Gliricidia sepium* is examined and pulping characteristics are investigated using a laboratory digester and hand-made paper sheets tested for some physical properties. The investigations are conducted alongside *Gmelina arborea*, which is a hardwood already established as pulpwood (Kpikpi, 1992).

Biology of *Gliricidia sepium*

Gliricidia sepium (Jacq.) Walp. is a native of Central America, Mexico, from where it was introduced into West Africa, India and other tropical, sub-tropical regions of the world. It is a small to medium-sized leguminous tree, nitrogen-fixing, belonging to the family Fabaceae-Papilionoideae. The stem is smooth-barked, without

*Corresponding author email: franciskpikpi@yahoo.com

thorns, whitish to grey in color and dotted all over with lenticels. The leaves are pinnately compound, about 25 to 30 cm long bearing about 6 – 20 ovate to elliptic leaflets on a central rachis. The flower is a pinkish to white, clustered inflorescence of characteristic papilionaceous flowers of a roundish standard and keel for petals. The unripe fruit is greenish turning yellowish-brown on ripening. Though deciduous, the tree is hardly leafless in the dry season. It is propagated by seed and stem cuttings. In Nigeria and Ghana and other areas of the West African sub-region, it is propagated by stakes, which is considered as a major advantage in its survival, since seed production in this plant depends on a marked dry season, and stakes up to 1m long have been found to give better establishment and subsequent growth (Adejuwon, 1991). *Gliricidia sepium* is a multi-purpose tree, useful as fuel wood, animal fodder, tree for honey production by bees, green manure and therefore really always has a reason to go under plantation development.

MATERIALS AND METHODS

Wood Anatomy

The structure of the wood of *Gliricidia sepium* and *Gmelina arborea* was studied from slide preparations made from two each of the species. *Gliricidia* trees were felled from a re-growth forest and *Gmelina* from an old abandoned homestead in Ado Ekiti, Nigeria. Wood discs were cut from the butt, the breast height (1.3 m up the bole) and just below the point where the stem branches up to form the crown of the tree. Four quadrants were sketched on the wood discs and from each quadrant wood blocks were scooped and macerated in Schultze's solution (Bradbury, 1976). Temporary mounts of the materials were made in glycerin on glass slides and examined under the microscope for the cell morphology. Measurements were made, from the microscope with micrometers, of the fibre dimensions for the derived ratios of Runkel ratio and Flexibility coefficient. Wood blocks were also scooped and microtome sections were cut, stained differentially in Saffranin and Fast green and permanently mounted in Canada balsam for microscopic examination and description of the wood structure with respect to proportions of tissues making up the wood.

Wood Density

The wood density of *Gliricidia* and *Gmelina* was determined by measurements based on Archimedes principle described by Browning (1967)

Ash content

The ash content of the wood of *Gliricidia* and *Gmelina* was determined by incinerating the wood shavings in an oven at 550°C. The ash, being the inorganic deposit left after the organic matter has volatilized, was weighed and reported.

Pulping/Refining/Hand paper sheets formation

Wood chips of *Gliricidia* and *Gmelina* were cooked separately in laboratory digester in the Paper Laboratory of the Nigerian Paper Mill, Jebba, Kwara State. Cooking of the two test species was done under identical cooking conditions (Table 1) adopted from Lopez *et al.* (2000). Cooked chips were defibred manually to pulp which was refined in a laboratory refiner, Valley beater. The pulp freeness, by Schopper Riegler scale (SR°) was measured after every 10 minutes of beating and paper sheets were formed at the changing freenesses for comparison of the physical properties at the varying pulp freenesses.

Table 1. Cooking conditions for wood chips.

Parameter	Parameter value
Liquor-to-wood ratio	4:1
Total active alkali: NaOH/Na ₂ S (g/l)	73.53/7.35
Sulphidity (%)	18
Maximum temperature (°C)	160
Maximum pressure (Kpa)	7 x 10 ⁵
Time at maximum T°	2 hrs

RESULTS

Wood Structure

Average fibre lengths for *Gliricidia* are 1.001 mm, ranging between 0.4 mm and 2.0 mm (Figs.1a, 1b and Table 2). The fibre diameter is narrow, ranging between 15.7 and 20.01 µm with mean of 19.14 µm, all mostly libriform fibres (Fig. 1c). The cell wall is thick, with a wall thickness average of 5.3 µm, ranging between 4.5 and 6.0 µm, and an average lumen/cavity of 8.7 µm (Figs. 1d, 1e). This gives a Runkel ratio of 1.22 to the *Gliricidia* fibre and coefficient of flexibility of 0.45 (Table 2). *Gmelina* has average fibre length of 1.05 mm, ranging between 0.4 and 1.8 mm, average fibre diameter of 34 µm and a very thin fibre wall, average thickness, 2.67 µm with a range of 2-3.2 µm and a lumen cavity of 28.77 µm conferring a Runkel ratio of 0.19 and flexibility coefficient of 0.88 (Figs. 1c, 1d, 1e and Table 2) as above for *Gliricidia*.

The structure of *Gliricidia* wood, compared with that of *Gmelina*, as shown by the results, is a good source of cellulose. The relative volume of fibre is about 59%, vessel, about 9.8%, ray and axial parenchyma are respectively 11.8% and 18.9%, with fibre to vessel (F/V) and fibre to non-fibrous tissue (F/NF) ratios respectively 6 and 1.2 (Fig. 1f and Table 1). For *Gmelina*, the relative volumes (as indicated in the same Table and Figure) are 72.2% fibres, 7.5% vessels, 4.9% parenchyma and 15.4 % rays. The fibre to vessel (F/V) and fibre to non-fibrous tissue (F/NF) ratios, respectively, are 9.6 and 2.6.

Pulping/Refining /Hand-made Paper Sheets

Pulp refining proceeded in a total beating time of 70 minutes, with the highest recorded freeness for *Gliricidia*

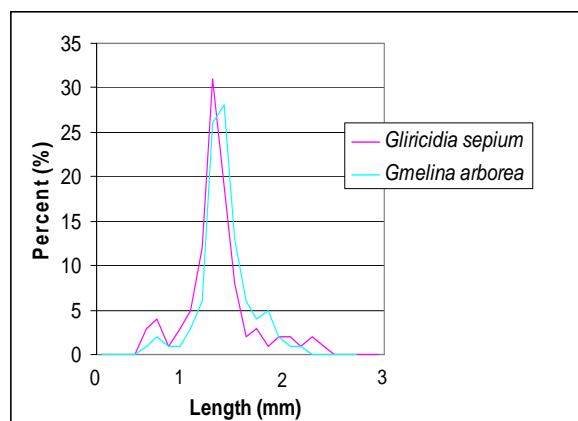


Fig. 1a. Fibre length distribution in wood of *Gliricidia sepium* and *Gmelina arborea*.

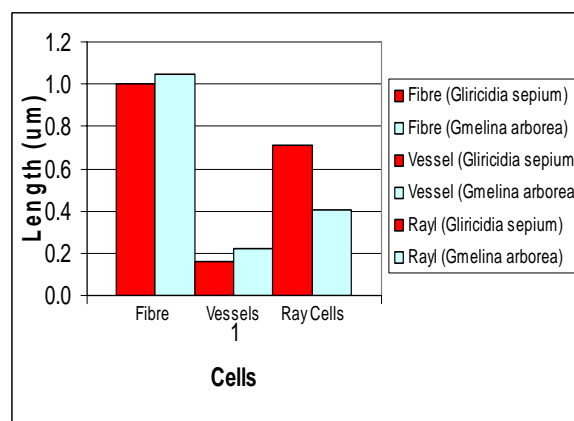


Fig. 1b. Average fibre length of *Gliricidia sepium* and *Gmelina arborea*.

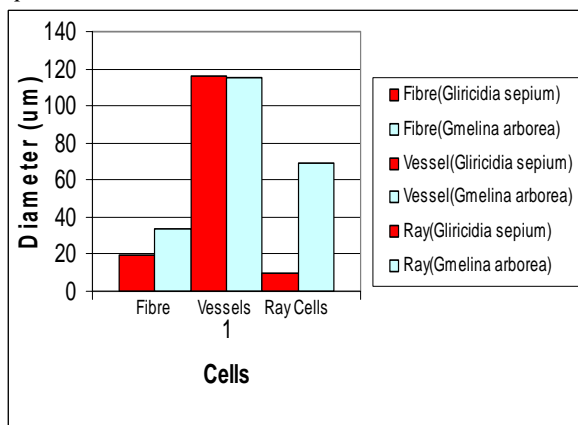


Fig. 1c. Average cell diameter of *Gliricidia sepium* and *Gmelina arborea*.

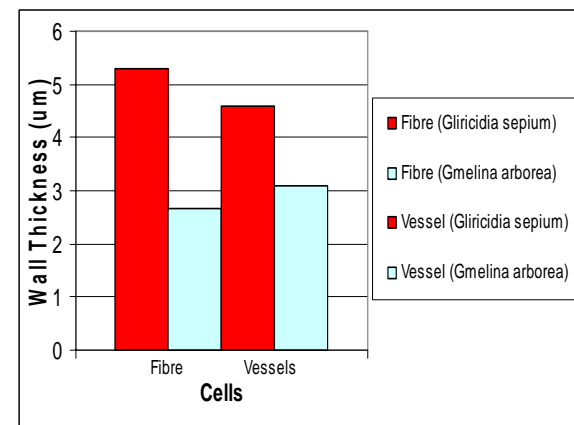


Fig. 1d. Average cell wall thickness of *Gliricidia sepium* and *Gmelina arborea*.

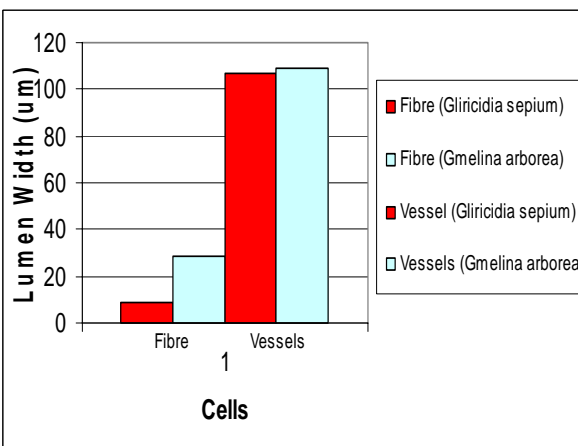


Fig. 1e. Average cell lumen of *Gliricidia sepium* and *Gmelina arborea*.

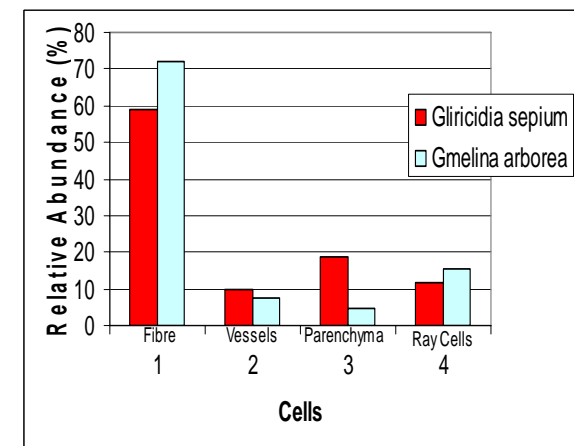


Fig. 1f. Relative abundance of tissues of *Gliricidia sepium* and *Gmelina arborea*.

pulp in 70 minutes being 51° SR, while *Gmelina* pulp in the same time recorded 65° SR (Fig. 2 and Table 2). Tested Paper sheets made out manually at chosen freenesses showed enhanced physical properties with increasing refinement of pulp for both *Gliricidia* and *Gmelina* pulps, as presented in (Figs. 3a, 3b, 3c, 3d and

Table 2). *Gliricidia* wood chips cooked under the adopted cooking conditions of Lopez *et al.* (2000) gave a pulp yield of 46.5% with 1.01% rejects, while *Gmelina* chips cooked under identical conditions yielded 49.2% with no rejects (Fig. 4a and Table 2).

Table 1. Summary of Characteristics of *Gliricidia sepium* and *Gmelina arborea*.

Characteristics	<i>Gliricidia sepium</i>	<i>Gmelina arborea</i>
Wood anatomy		
Mean fibre length (mm)	1.001 Range(0.4-2.0)	1.047. Range (0.4-1.8)
Runkel ratio	1.22	0.19
Flexibility coefficient	0.45	0.88
Fibre volume (%)	58.9	72.2
Vessel member (%)	9.8	7.5
Parenchyma (%)	18.9	4.9
Ray (%)	11.8	15.4
Wood density (kg m^{-3})	710	460
Pulp yield (%)	46.5	49.2
Ash content (%)	2.7	1.3
Pulp refinement time		
30 min freeness (SR°)	23	29
40 min freeness (SR°)	28	36
60 min freeness (SR°)	48	59
Paper physical properties		
Burst strength (kg cm^{-2})	1.93-3.78	2.78-3.98
Tear strength (g)	126-155	145-165
Breaking weight (kg)	3.86-5.24	4.81-7.56
Breaking length (m)	1988-3820	2880-5120

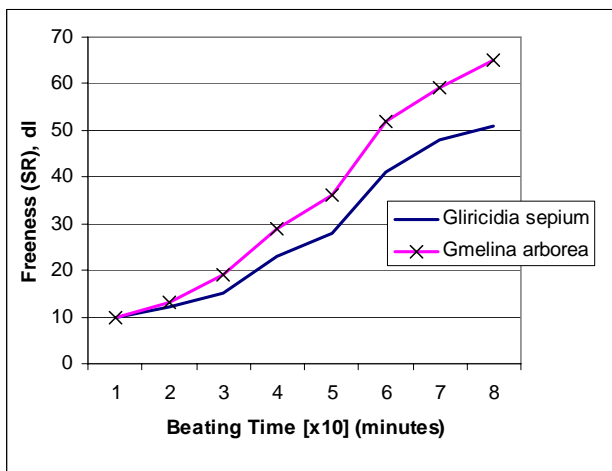


Fig. 2. Pulp Freeness as a function of Beating/Refining Time Freeness on Schopper Riegler, SR, Scale.

Wood Density/Ash Content

The wood density of *Gliricidia sepium* is reported as 710 kg m^{-3} compared with 460 kg m^{-3} for *Gmelina*. The corresponding wood ash contents were 2.7% and 1.3%, respectively (Figs. 4b, 4c and Table 2).

DISCUSSION

The average fibre lengths of both *Gliricidia* and *Gmelina* are short, about 1.0 mm, within a range of 0.4 mm and 2.0 mm. Short fibre lengths are characteristic of hardwoods, and Britt's observation (1970) that long fibres are essential for making paper of high tear and tensile strengths, properly applies to softwoods and not to

hardwoods like the ones under investigation. The capacity of hardwood fibres to make strong papers depends more on the entire fibre morphology, of the relationship of the thickness of the fibre wall to its entire diameter. A fibre of a given diameter, (D), having a wide internal cavity, (I), naturally will have a thin cell wall (C), from the relationship (D-I), which collapses more easily under pressure that is generated during the pulp dehydration and paper mat formation. Fibres with collapsed cell walls have better exposed cellulose bonding surfaces in a web which bond together to form the paper sheets.

The ratio of the fibre wall thickness to its internal diameter ($2C/I$), known as Runkel ratio, thus controls the paper physical property in hardwoods than the fibre lengths alone. A low Runkel ratio means thin fibre walls and therefore better cell wall collapsibility; stronger inter-fibre bonding and therefore stronger paper sheets formation. Papers of various kinds like cardboards for paper boxes, newsprints or tissue papers requiring different strength properties can however be made from fibres of differing morphological characteristics. Comparing the fibre morphology of *Gliricidia* to *Gmelina*, the respective Runkel ratios of 1.22 and 0.19, shows *Gmelina* to be superior to *Gliricidia*, although both can be used to make some kind of paper.

The Runkel ratio gives almost the same information as does the Coefficient of flexibility which relates the internal cavity, (I), to the external diameter of the fibre, (I/D). The coefficient of flexibility in the *Gliricidia* fibre (0.45), gives *Gliricidia* a preponderant wall material, relative to the entire volume of the fibre which naturally

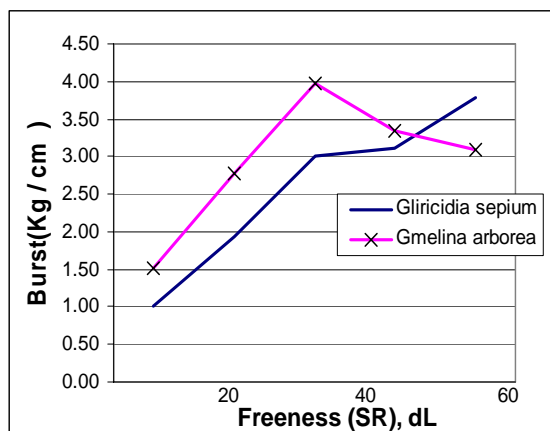


Fig. 3a. Physical property (Burst) of paper handsheet as a function of Pulp Freeness.

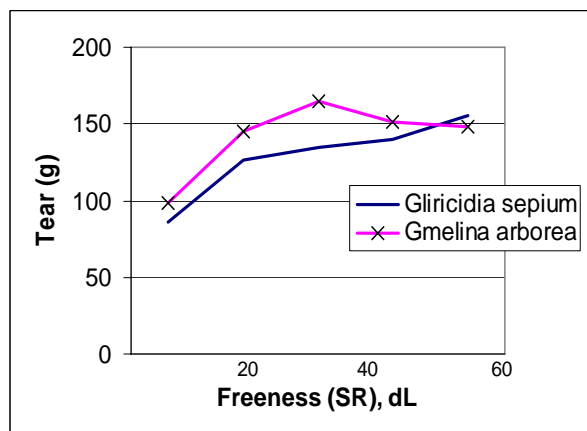


Fig. 3b. Physical property (Tear) of paper handsheet as a function of Pulp Freeness.

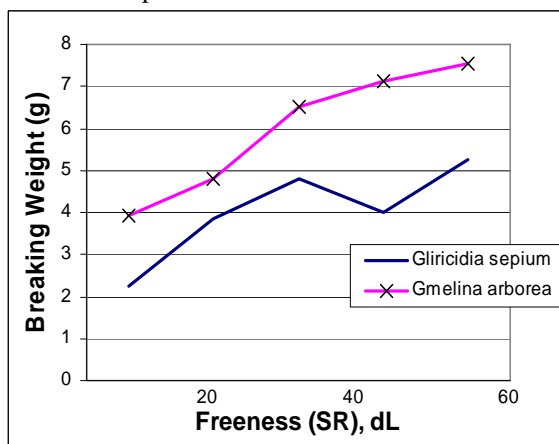


Fig. 3c. Physical property (Breaking Weight) of paper handsheet as a function of Pulp Freeness.

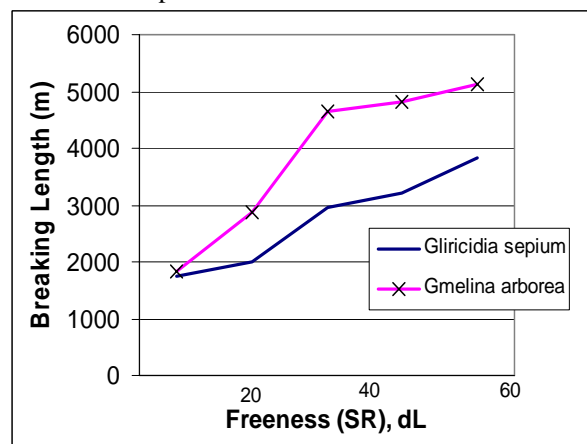


Fig. 3d. Physical property (Breaking Length) of paper handsheet as a function of Pulp Freeness.

leaves only a small internal cavity that can be filled with air compared with 0.88 of *Gmelina*'s thin walls and large cavity. The wood of *Gliricidia* is thus much higher in density (710 kg m^{-3}) than *Gmelina* (460 kg m^{-3}). The Ash content of *Gliricidia* (2.7%) is about twice as much as the ash content of the *Gmelina* wood (1.3%). The ash content of wood in pulp can lead to pitch problems in paper as the ash increases the black liquor mineral load and that of the bleach wash water, hence, its monitoring in pulpwood. Though the mineral deposit in *Gliricidia* is higher than that of *Gmelina*, the levels in both species are not excessive.

Pulp/Paper Characteristics

The yield of pulp, 46.5% for *Gliricidia* and 49.2% in *Gmelina* is quite good for both species. The pulp refined well in the laboratory refiner, Valley beater. The results of refining and the tests of the physical properties of the hand-made paper sheets formed show the two hardwood pulps are quite good for making paper. For example, paper sheet of *Gliricidia*, GSM 104 at SR 51° elicited Burst property of 3.78 kg m^{-2} and Tear strength of 155 g

while *Gmelina* paper sheet of GSM 102 at SR 52° produced a Burst property of 3.34 kg cm^{-2} and Tear of 151 g. The best physical property of Burst 3.98 kg m^{-2} however, was obtained from *Gmelina* pulp at 36° SR° of freeness after 40 minutes of pulp beating/refinement and the best Tear Property of 165 g at the same time of beating and the same freeness. At 40 minutes of pulp refinement, *Gliricidia* showed a pulp freeness of only 28° SR and the Burst Property at this freeness was 1.98 kg cm^{-2} and a Tear of 126 g. These two results show that the differences in the quality of fibre morphology translates into differences in costs of fibre preparation (refinement) for paper-making, and sometimes, these differences can be very important in deciding which pulps to use for which kind of paper.

CONCLUSION

The fibre morphology and the wood structure of *Gliricidia sepium* show that the wood of *Gliricidia* compares quite favourably with that of *Gmelina arborea*. Although there is such great difference between the two

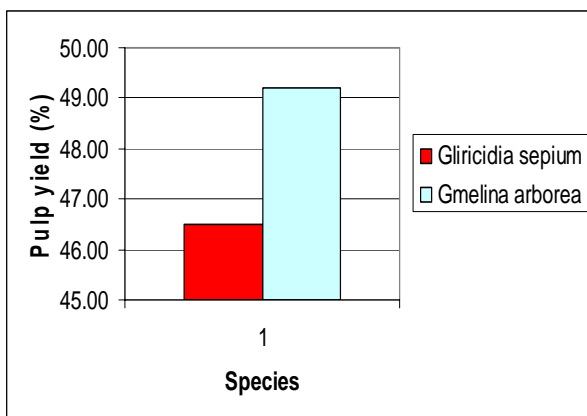


Fig. 4a. Pulp yields of *Gliricidia sepium* and *Gmelina arborea* from the laboratory digester.

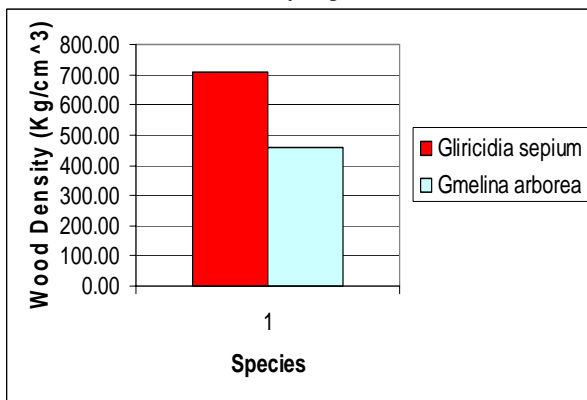


Fig. 4b. Wood density of *Gliricidia sepium* and *Gmelina arborea*.

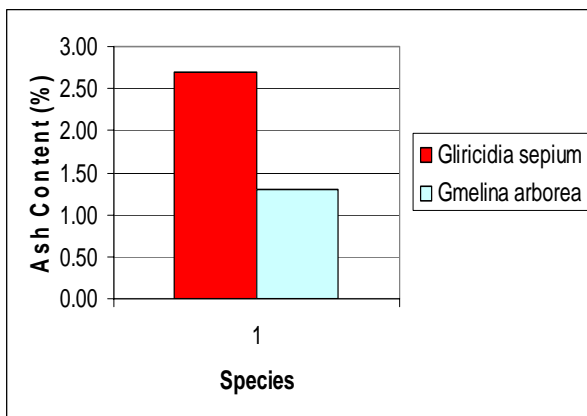


Fig. 4c. Ash content of *Gliricidia sepium* and *Gmelina arborea*.

Runkel ratios of *Gmelina* and *Gliricidia*, 0.19 and 1.22, the paper qualities produced, were comparably good. The vegetative growth habit of *Gliricidia*, illucidated from the literature, makes it such a good plantation species and this should compensate for some anatomical deficiencies. *Gliricidia sepium*, from all the test results, should be considered as a suitable hardwood species having good potentials for making pulp and paper.

ACKNOWLEDGEMENT

We acknowledge, with thanks, the kind courtesies of the Management of the Jebba paper Mills, Nigeria, in allowing the use of their Paper Laboratories.

REFERENCES

- Adejuwon, JO. 1991. The Effect of length and girth of Vegetative planting material upon forage yields and quality of *Gliricidia sepium*. Tropical Agriculture. 68:63-65.
- Bradbury, S. 1973. Peacock's Elementary Microtechnique. (4th ed.). Edward Arnold. pp246.
- Britt, KW. 1970. Handbook of pulp and paper technology. (2nd ed.). Britt KW Van Nostrand Reinhold Co., New York, USA.
- Browning, BL. 1967. Methods in Wood Chemistry. (vol. 1). Wiley, Interscience, New York, USA.
- Kpikpi, WM. 1992. Rating *Musanga cecropioides* and *Delonix regia* as Paper-making Hardwoods. Tappi Journal. 75(12):73-75.
- Kpikpi, WM. 2005. The Potentials of *Manihot glaziovii* Muell. Arg. For Pulp and Paper Production. Journal of Tropical Forest Resources. 21(1):166-175.
- Lopez, F., Ariza, J., Perez, I. and Jimenez, L. 2000. Influence of the Operating conditions on Properties of paper sheets obtained by kraft pulping of Olive tree wood. Bioresource Technology. 72(2):147-151.
- Simons, AJ. and Dunsdon, AJ. 1992. Evaluation of the genetic improvement of *Gliricidia sepium*. (unpublished report submitted to ODA on the Forestry Research Project, R.4525). Oxford Forestry Institute. pp176.

Received: Sept 22, 2011; Accepted: March 15, 2012

TOXIC AND FEEDING DETERRENT EFFECTS OF *HYPTIS SUAVEOLENS* AND *HYPTIS SPICIGERA* EXTRACTS ON COWPEA WEAVIDS (*CALLOSOPRUCUS MACULATUS*)

*Mbatchou V Chi and Sachyere P Apiah

Department of Applied Chemistry and Biochemistry, University for Development Studies
PO Box 24, Navrongo, Ghana

ABSTRACT

In the present work, two plants *Hyptis suaveolens* and *Hyptis spicigera* were studied to identify their toxic and anti-feeding effects on cowpea weevils (*Callosobruchus maculatus* F.). Active ingredients of both plant samples were separately extracted and partitioned using ethanol, chloroform and distilled water solvents. Extracts and fractions obtained were tested on cowpea weevils for toxic and anti-feeding effects using cowpea seeds by two-choices bioassay technique. Results indicated that extracts and fractions from the plant samples were effective in restricting cowpea weevils from feeding on cowpea seeds. Also, extracts and fractions from the plant samples demonstrated cowpea weevil mortalities. These were indications that the plant samples contained toxicants and anti-feedants which prevented the weevils from feeding on the cowpea seeds. Thus, ingredients from *Hyptis suaveolens* and *Hyptis spicigera* should be used to protect cowpea seeds and other grains from infestations by *Callosobruchus maculatus* and other grain infesting insects. Chloroform soluble fraction of the two plants recorded the least percentage consumption index of cowpea seeds and the highest percentage mortality of cowpea weevils which confirmed that it contained the most active ingredients. Hence, chloroform solvent should be used to isolate anti-feedants and pesticide compounds from *Hyptis suaveolens* and *Hyptis spicigera* by column chromatographic method.

Keywords: Extracts, fractions, toxicants, anti-feedants, % mortality and consumption index.

INTRODUCTION

In 1939, Paul Muller discovered that diphenyl dichloro trichloroethane (DDT) and other synthetic compounds were very effective pesticides. His discovery prompted many manufacturers in the 1940's to produce synthetic pesticides in large amounts because they were widely used (Daly *et al.*, 1998).

The use of DDT and other synthetic chemicals as pesticides began to pose serious threats to human health and the environment. In the 1960's, it was discovered that DDT was preventing many birds from reproducing, which was a serious threat to biodiversity (Lobe, 2006).

The agricultural use of DDT, lindane, and karate, is now banned under the Stockholm Convention on Persistent Organic Pollutants, but these pesticides are still used in some developing countries to store grains and prevent tropical diseases by spraying on interior walls and fields to kill or repel insects (Lobe, 2006).

Surveys conducted in vegetable growing areas in Ghana identified lindane, karate, unden and dithane as the most used pesticides by farmers. However, the agricultural use

of these compounds has been banned and the pharmaceutical use of lindane is prohibited in some countries because it causes damage to the central nervous system and weakens the immune system (Glover-Amengor and Tetteh, 2007).

There are concerns that some pesticides used on food crops to control pests are harmful to people who consume foods from such crops because the pesticides contain small amounts of toxins which remain in the foods even when they are washed with water or peeled. Sometimes, these toxins are left in the soil as residues for long periods after the application and could be carried by rain into water bodies or absorbed by plants. These cause serious health effect and environmental problems.

The cumulative effects resulting from the use of synthetic chemical compounds had diverted the attention of most chemists and environmentalists to the search of compounds from natural sources which are directly or indirectly non-toxic to humans, wildlife and the ecosystem. In the 17th century, nicotine sulphate was extracted from tobacco leaves for use as an insecticide. The 19th century saw the introduction of two more natural pesticides, pyrethrum which is derived from

*Corresponding author email: mcvalentinechi@gmail.com

chrysanthemums and rotenone which is derived from the roots of tropical vegetables (Miller, 2002).

The objective of this study is to identify solvents that can extract active ingredients from *Hyptis suaveolens* and *Hyptis spicigera*, which can be used to isolate pesticides by column chromatographic technique. It is the aim of the work to prove that *Hyptis suaveolens* and *Hyptis spicigera* have feeding deterrent and pesticide potentials. This can be proven by applying extracts of these two plants on cowpea seeds and subjecting these seeds to cowpea weevils (*Callosobruchus maculatus F.*).

MATERIALS AND METHODS

Materials

The materials used in this work included digital chemical balance, separatory funnels, beakers (600 and 300ml), retort stand, funnels, Whatman no. 1 filter paper, vials, micro liter syringes, cowpea seeds, cowpea weevils (*Callosobruchus maculatus F.*), screen cages demarcated into compartments, Winchester bottles, Aluminium foil, 95% ethanol, methanol, chloroform, petroleum ether and distilled water. Reagents used were analytical grades bought from Timster Laboratory Suppliers Limited, Accra, Ghana.

Plant collection and treatment

Hyptis suaveolens Lam and *Hyptis spicigera Lam* were used for the experiment due to their local use in some African countries and Northern Ghana in particular to

protect grains from insect infestations. Both plants were randomly harvested behind the Microbiology Laboratory of University for Development Studies, Navrongo Campus, Ghana in November, 2008. The entire plants were separately air dried for twenty one days and later pulverized with the aid of a clean mortar and pestle.

Inhalation of the powdered samples during pulverizing caused dizziness and severe sneezing. The pulverized samples were stored in cleaned air-tight containers and kept in a cool dry place.

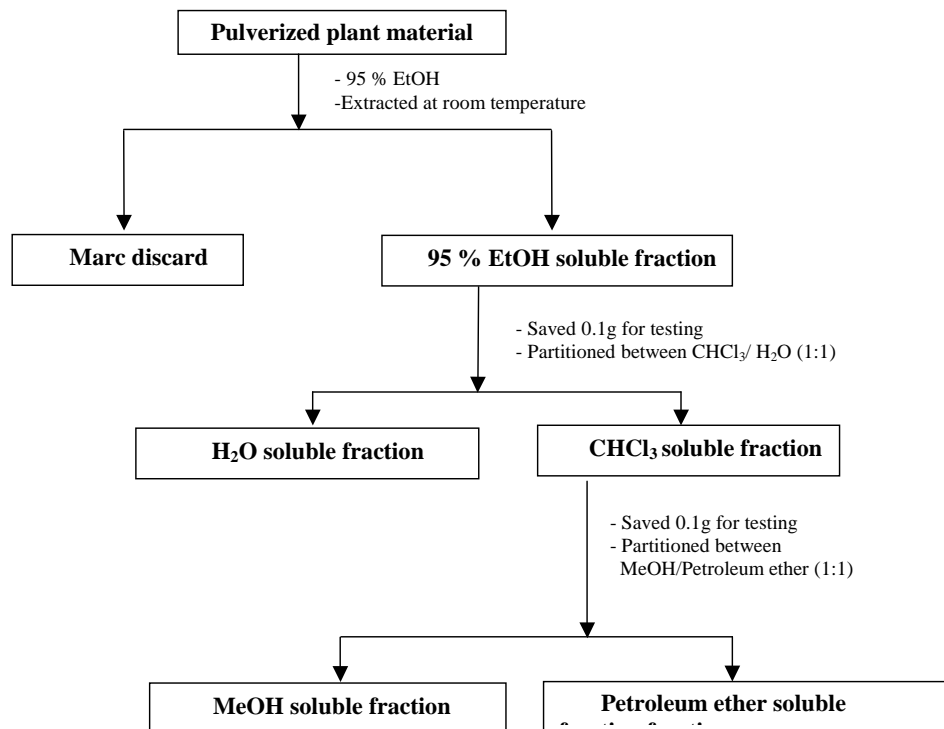
Extraction

The *Hyptis suaveolens* and *Hyptis spicigera* pulverized samples (400 and 500g) were separately soaked in 2200 millilitres of 95% ethanol with intermittent shaking for two weeks. Percolates were evaporated to dryness at room temperature to give crude extracts of the two plants which were each subjected to partition process.

Partition process

Crude extracts obtained as described above were partitioned between chloroform and distilled water (1:1, 100ml) using separating funnels. The chloroform and distilled water soluble fractions of each plant sample were separately evaporated to dryness at room temperature.

The chloroform soluble fraction of each plant was later partitioned between methanol and petroleum ether (1:1, 100ml). The methanol and petroleum ether soluble fractions were then separated and concentrated. The



fractions derived in the whole process were transferred into vials and used in a two- choices cowpea weevil bioassay (Abdullahi *et al.*, 1995). The flow chart for the extraction and partition processes is as shown:

The two-choices cowpea weevil bioassay

The extracts and fractions employed in this research were in each instance weighed (10mg) and dissolved in 1ml of methanol solvent. 250 μ l of the solution formed was poured into a vial and kept overnight to evaporate to dryness. To the residue obtained, 5 ml of methanol solvent was added to re-dissolve it to form a concentration of 500 μ g/ml, and 40 cowpea seeds were then immersed in the solution. The vial and its contents were shaken for a few seconds and allowed to dry at room temperature. Also, concentrations of 250 μ g/ml and 125 μ g/ml were prepared in the same manner as the 500 μ g/ml concentration by transferring 125 μ l and 62.5 μ l of the solution in to two distinctive vials and topping each of them with 5ml of methanol solvent. Control cowpea seeds were introduced into 5 ml of methanol in a similar manner as the treated seeds and the treated seeds were prepared in duplicates. Both the treated and control cowpea seeds were separately placed in compartments

demarcated by cardboards at the bottom of a screen cage and the seeds were infested with weevils. At the end of two weeks interval, the perforated and unperforated cowpea seeds, and dead weevils were counted.

The percentage consumption index (% C.I) and mortality were calculated using the following formulae:

$$\% \text{ C.I} = \frac{\% \text{ treated cowpea seeds perforated}}{(\% \text{ treated cowpea seeds perforated} + \% \text{ control cowpea seeds perforated}) \times 100}$$

$$\begin{aligned} \% \text{ mortality} &= \frac{(\% \text{ test mortality} - \% \text{ control mortality})}{(100 - \% \text{ control mortality})} \times 100 \end{aligned}$$

RESULTS AND DISCUSSION

From table 1, there were zero % consumption indices for both the 250 and 500 μ g/ml concentrations of the chloroform soluble fraction of *Hyptis suaveolens*. This implied that the solvent soluble fraction protected the cowpeas from being infested by the weevils. The 125 μ g/ml concentration of the chloroform soluble fraction recorded the least consumption index of 21.42% when

Table 1. Feeding deterrent activity of *Hyptis suaveolens* extracts on cowpea weevils.

SOLUBLE SOLVENT EXTRACT/ FRACTION	CONCENTRATION (μ g/ml)	NUMBER OF PERFORATED SEEDS		% TREATED SEEDS PERFORATED	% CONTROL SEEDS PERFORATED	% CONSUMPTION INDEX (% C.I)	MEAN % CONSUMPTION INDEX
		TREATED	CONTROL				
ETHANOL	500	2	9	10	45	18.18	26.29
	250	3	9	15	45	25.00	
	125	5	9	25	45	35.71	
CHLOROFORM	500	0	11	0	55	0.00	7.14
	250	0	11	0	55	0.00	
	125	3	11	15	55	21.42	
DISTILLED WATER	500	1	10	5	50	9.09	21.83
	250	3	10	15	50	23.08	
	125	5	10	25	50	33.33	
PETROLEUM ETHER	500	1	9	5	45	10.00	21.92
	250	3	9	15	45	25.00	
	125	4	9	20	45	30.76	
METHANOL	500	1	8	5	40	11.11	21.48
	250	2	8	10	40	20.00	
	125	4	8	20	40	33.33	

Table 2. Feeding deterrent activity of *Hyptis spicigera* extracts on cowpea weevils.

SOLUBLE SOLVENT EXTRACT/ FRACTION	CONCENTRATION ($\mu\text{g/ml}$)	NUMBER OF PERFORATED SEEDS		% TREATED SEEDS PERFORATED	% CONTROL SEEDS PERFORATED	% CONSUMPTION INDEX (% C.I)	MEAN % CONSUMPTION INDEX
		TREATED	CONTROL				
ETHANOL	500	0	8	0	40	0.00	
	250	3	8	15	40	27.27	20.20
	125	4	8	20	40	33.33	
CHLOROFORM	500	0	9	0	45	0.00	
	250	1	9	5	45	10.00	11.67
	125	3	9	15	45	25.00	
DISTILLED WATER	500	1	11	5	55	8.33	
	250	2	11	10	55	15.34	19.65
	125	6	11	30	55	35.29	
PETROLEUM ETHER	500	1	8	5	40	11.11	
	250	3	8	15	40	27.27	23.90
	125	4	8	20	40	33.33	
METHANOL	500	1	10	5	50	9.09	
	250	3	10	15	50	23.07	20.24
	125	4	10	20	50	28.57	

Table 3. Effects of *Hyptis suaveolens* extracts on the mortality rates of cowpea weevils.

SOLUBLE SOLVENT EXTRACT/ FRACTION	CONCENTRATION ($\mu\text{g/ml}$)	TEST MORTALITY	CONTROL MORTALITY	% TEST MORTALITY	% CONTROL MORTALITY	% MORTALITY	MEAN %MORTALITY
ETHANOL	500	6	2	60	20	50.00	
	250	4	2	40	20	25.00	29.16
	125	3	2	30	20	12.50	
CHLOROFORM	500	6	1	60	10	55.56	
	250	6	1	60	10	55.56	40.74
	125	2	1	20	10	11.11	
DISTILLED WATER	500	6	1	60	10	55.56	
	250	3	1	30	10	22.22	29.63
	125	2	1	20	10	11.11	
PETROLEUM ETHER	500	6	1	60	10	55.56	
	250	3	1	30	10	22.22	29.63
	125	2	1	20	10	11.11	
METHANOL	500	5	2	50	20	37.50	
	250	4	2	40	20	25.00	25.00
	125	3	2	30	20	12.50	

Table 4. Effects of *Hyptis spicigera* extracts on the mortality rates of cowpea weevils.

SOLUBLE SOLVENT EXTRACT/ FRACTION	CONCENTRATION (μg/ml)	TEST MORTALITY	CONTROL MORTALITY	% TEST MORTALITY	% CONTROL MORTALITY	% MORTALITY	MEAN % MORTALITY
ETHANOL	500	5	1	50	10	44.44	29.627
	250	4	1	40	10	33.33	
	125	2	1	20	10	11.11	
CHLOROFORM	500	6	1	60	10	55.56	33.333
	250	4	1	40	10	33.33	
	125	2	1	20	10	11.11	
DISTILLED WATER	500	5	1	50	10	44.44	33.330
	250	4	1	40	10	33.33	
	125	3	1	30	10	22.22	
PETROLEUM ETHER	500	6	3	60	30	42.85	28.567
	250	5	3	50	30	28.57	
	125	4	3	40	30	14.28	
METHANOL	500	5	2	50	20	37.50	25.000
	250	4	2	40	20	25.00	
	125	3	2	30	20	12.50	

compared to all the other tested extracts of the same concentration. This clearly gave a clue that the chloroform soluble fraction of *Hyptis suaveolens* contained the most active components which prevented the weevils from feeding on the cowpea seeds.

From the same table, the ethanol soluble extract at 125 and 500 μg/ml concentrations recorded the highest consumption indices of 35.71 and 18.18% respectively when compared to all the other tested soluble fractions at these concentrations. This indicated that the ethanol soluble extract was the least active in terms of deterring the weevils from feeding on the cowpea seeds. A contributing factor to the least activity of the ethanol soluble extract was the presence of components or impurities in its content which masked its active ingredients, thus preventing it from exhibiting its complete feeding deterrent property.

Table 2 results showed that the chloroform soluble fraction of *Hyptis spicigera* had the least consumption indices at the tested concentrations when compared to all the other soluble extracts or fractions. Hence, it was a clear indication that the chloroform soluble fraction contained the most active component(s) of the plant, and was capable of deterring the weevils from feeding on the cowpea seeds. On the contrary, the petroleum ether soluble fraction of *Hyptis spicigera* gave the highest average consumption index of 23.90% when compared to those of all the other tested extracts or fractions. Therefore, this fraction contained the least active component(s) of the plant which deterred the weevils from feeding on the cowpea seeds.

Table 3 results showed the chloroform soluble fraction of *Hyptis suaveolens* with the highest average mortality of 40.74% and the ethanol soluble extract with the least average mortality of 29.16%. These values revealed that the chloroform soluble fraction contained the most active component(s), while the ethanol soluble extract contained the least active component(s) of the plant which caused dead of the weevils.

From table 4 results, the chloroform soluble fraction of *Hyptis spicigera* recorded the highest average mortality of 33.33% and was closely followed by the distilled water soluble fraction with an average mortality of 33.330%. The petroleum ether soluble fraction of the plant presented the least average mortality of 28.56%. These stated values explained that the chloroform soluble fraction contained the most active component(s) of the plant, while the petroleum ether soluble fraction contained the least.

Thus, the chloroform soluble fraction was the most active ingredient for both plants, while the ethanol soluble extract and the petroleum ether soluble fraction were the least active for *Hyptis suaveolens* and *Hyptis spicigera* respectively.

CONCLUSION

Results for the anti-feeding and mortality tests revealed that extracts/fractions of the two plants were toxic to cowpea weevils by killing and preventing them from feeding on the cowpea seeds. In all, the chloroform soluble fraction was identified to contain the most active ingredient responsible for protecting the cowpea seeds from being infested, and for causing dead of the cowpea

weevils because of the least percentage consumption indices and the highest percentage mortalities it recorded. There is a correlation between the feeding deterrent activity and toxicity of this fraction to cowpea weevils. Hence, chloroform solvent should be used to isolate anti-feedants and pesticides from *Hyptis suaveolens* and *Hyptis spicigera* by column chromatographic method.

RECOMMENDATION

It is recommended that extracts/fractions of these plants should be used to protect cowpea seeds and other grains from damage by cowpea weevils and other grain infesting insects. Also, further research should be conducted on both *Hyptis suaveolens* and *Hyptis spicigera* by the use of chloroform solvent to help isolate active compounds which could serve as pesticides for keeping the desirable qualities of cowpea seeds. This will go a long way to avoid the use of synthetic pesticides that leave residues on plants and in the soil that may be harmful to both humans and the environment at large.

REFERENCES

- Abdullahi, MN., Fatima, MM. and Majekodunmi OF. 1995. Pesticidal Effects of Extracts from *Balanites aegyptiaca* (L). Spectrum. 1:83.
- Daly, H., Doyen, JT. and Purcell, AH. 1998. Introduction to Insect Biology and Biodiversity, Oxford University Press, New York, USA. 273-300.
- Glover-Amengor, M. and Tetteh, FM. 2007. Effects of Pesticide Application on Yield of Vegetables and Soil Microbial Communities. Applied Ecology. 12:41-47.
- Lobe, J. 2006. 'WHO urges DDT for malaria control strategies'. In: Commondreams.org. Proceedings of the WHO Conference, Inter Press Service, Geneva. 4-7.
- Miller, GT. 2002. Living In the Environment. Thompson Learning Inc., California, USA. 211-216.

Received: Sept 21, 2011; Revised: March 22, 2012;

Accepted: March 24, 2012

PLANTS EXTRACTS CORROSION INHIBITION OF ALUMINIUM ALLOY IN H₂SO₄

*C A Loto^{1,2} and A P I Popoola²

¹Department of Mechanical Engineering, Covenant University, Ota, Nigeria

²Department of Chemical & Metallurgical Engineering, Tshwane University of Technology, Pretoria 0001, South Africa

ABSTRACT

Effects of tobacco (*Nicotiana*) and Kola tree (*Cola acuminata*) extracts on the corrosion inhibition of an aluminium alloy 2S (1200) grade specimens immersed in 0.5M sulphuric acid was investigated at ambient temperature by gravimetric and metallographic methods. Extracts of kola plant and tobacco in different concentrations were used as 'green' inhibitors. This paper reports the results obtained from the weight loss method, calculated corrosion rates, inhibitor efficiencies and the optical microscopy metallographic observations. Addition of different concentrations of the plants extracts gave clear reduction in weight loss and in the corrosion rate of the test samples. This apparent corrosion inhibition was associated with the protective film provided on the aluminium alloy's surface by the complex chemical constituents of the plants extracts.

Keywords: Inhibition, corrosion, aluminium alloy, kola tree, tobacco, sulphuric acid.

INTRODUCTION

Corrosion phenomena, control and prevention are unavoidable major scientific issues that must be addressed daily as far as there are increasing needs of metallic materials in all facets of technological development. Chemical inhibitors have been very effective in addressing this among other corrosion protection methods. In very recent time, however, there has been the need to look at some other environment friendly substances, especially from natural sources that could be used to inhibit/reduce incessant corrosion problems apart from the synthesized inorganic and other organic chemicals, some which are toxic to the environment. Many scientific researchers have responded to this need and it has generated increased research studies into the use of plant extracts (Loto, 2005; Okafor, 2007; Davis and Fraunhofer, 2003; Fraunhofer, 1995; Davis *et al.*, 2001; Fraunhofer, 2000 and Loto, 2003). Very encouraging results have been obtained in this regard. Attempt at making a contribution to this growing research area has necessitated the present investigation. Parts of the plants that have been used include leaves, bark, fruit and the roots. In very many cases, the corrosion inhibitive effect of some of the plants' extracts has been attributed to the presence of tannin in their chemical constituents (Loto, 2003). Also associated with the presence of tannin in the extracts is the bitter taste in the bark and /or leaves of the plants. The present investigation is focused on the use of kola tree (nut, leaves) and tobacco. Extracts of tobacco (genus – *Nicotiana*: family- *Solanaceae*), as an environmental benign corrosion inhibitor had been

shown(3 - 6, 8) to be effective in preventing the corrosion of steel and aluminium in saline environments; and in fact, exhibiting a greater corrosion inhibition effect than chromates (4 – 6). Tobacco plants produce ~ 4,000 chemical compounds – including terpenes, alcohols, polyphenols, carboxylic acids, nitrogen – containing compounds (nicotine), and alkaloids (WHO-IARC, 1985). These constituents may be effective in showing corrosion inhibition performance, particularly as in the present investigation likewise, kola nut tree's chemical composition consists of caffeine (2.0 - 3.5%), theobromine (1.0 – 2.5%), theophylline, phenolics – such as phobaphens, epicachins, D- catechin, tannic acid (tannin), sugar – cellulose, and water (Wikipedia, 2011). As reported in some previous studies (Okafor, 2007; Loto, 2003), tannin is known to possess corrosion inhibitive properties on metals – particularly, mild steel. The other chemical composition in kola tree extracts may have the capacity also to exhibit electrochemical activity such as corrosion inhibition for aluminum alloy in H₂SO₄. In this work, a positive result is anticipated that could be beneficial technologically and economically.

MATERIALS AND METHODS

Preparation of specimen

The aluminum alloy test specimen used was of the 2S (1200) grade and had a nominal percent composition of: 0.60%Fe, 0.30% Si, 0.05% Mn the rest being Al. The cylindrical steel bar was cut into various pieces of different lengths and the specimens were de-scaled by wire brushing. They were then ground with silicon

*Corresponding author email: akinloto@gmail.com

carbide abrasive paper of 240, 320, 400, and 600 and polished with 1.0μ diamond paste. They were thoroughly cleaned, rinsed in ultrasonic cleaner, dried, and kept in desiccators for further weight loss tests.

Test media

The experiments were performed in 0.5M H_2SO_4 of AnalaR grade. The extracted juices used as the corrosion inhibitor were separately extracted from the leaves of kola tree and tobacco and were prepared in different concentrations.

Extraction of plants extracts

The nuts and leaves of the Kola tree (*Cola acuminata*) and Tobacco (*Nicotiana*) were cut separately into pieces which were then oven dried at $105^\circ C$ for two hours, cooled, and trimmed to be uniformly 0.70kg each. They were separately ground into powder, and soaked in different containers containing ethanol for five days in order to extract the juice by leaching. Each of the different juice extracts in each container was filtered at the end of the soaking period. The solutions were distilled at $79^\circ C$ to remove the ethanol from the juice extracts and concentrate the inhibiting chemical(s). Each of the juice extracts (the respective distillates) was stored in a clean bottle and covered properly.

Preparation of the test media and juice extracts

100ml of 0.5M H_2SO_4 was measured into different beakers. In addition to the original extract which was taken as 100% concentration, other different percent concentrations of 80 (tobacco extract alone), 60 and 30 by dilution from the original extracts were made of which 10ml of each of the extracts - the tobacco, kola leaf, and kola nut extracts, was separately added to the acid in each of the beakers. This was repeated for every concentration of the extracts made. One beaker was left plain, that is, contained only the test medium, the H_2SO_4 ; this served as the control experiment.

Weight loss experiment

Weighed test specimens were totally immersed in each of the test media contained in a 250ml beaker for 24 days. Experiments were performed with acid chloride test medium in which some had the solution extract added. Test specimens were taken out of the test media every 3 days, washed with distilled water, rinsed with methanol, air-dried, and re-weighed. Plots of weight loss versus the exposure time and of calculated corrosion rate versus time of exposure (Figs. 1 to 6) were made. Corrosion rates were calculated from the recorded weight loss values from this formula:

$$mm/yr = 87.6W/DAT \dots \dots \dots (1)$$

where W is the weight loss in milligrams, D is the density in g/cm^3 , A is the area in cm^2 , and T is the time of exposure in hours.

The percentage inhibitor efficiency, P, was calculated from relationship:

$$P = 100 (1-W_2)/(W_1) \dots \dots \dots (2), \text{ where:}$$

W_1 and W_2 are the corrosion rates in the absence and presence, respectively, of a predetermined concentration of inhibitor. The per cent inhibitor efficiency was calculated for all the inhibitors for every 3 days of the experiment, and the results are presented in Table 1. All the experiments were performed at ambient temperature(s).

Micrographs

Some optical micrographs of the test specimen before and after immersion in sulphuric acid were made in the experiments. The representative micrographs are presented in figure 7 (a-d).

RESULTS AND DISCUSSION

Weight loss method

The results obtained for the variation of weight loss and corrosion rate with exposure time respectively for the aluminum alloy test specimens immersed in 0.5 M sulphuric acid with varied concentrations of added kola tree (leaves and nuts) and tobacco extracts are presented in figures 1 to 6.

The Kola tree leaves extract

As presented in figure 1, the test medium with 100 % concentration of kola leaves extract addition on the last day of the experiment, recorded the highest values of weight loss throughout the experimental period. Weight loss values that ranged from 157.80mg on the 3rd day to 452.60 mg on the 24th day of the experiment were recorded. This concentration of the leaves extract appeared to accelerate corrosion as it showed no corrosion inhibition performance. In fact, better corrosion weight loss values were obtained with the test environment without extract addition except on the 18th day when both achieved the same weight loss value of 335.80mg. However, the extracts with 30% concentration of the added kola leaves extract, recorded the lowest weight loss values of 70.70; 156.50 and 321mg on the 12th, 15th and 24th day of the experiment. The 60% extract concentration, similarly recorded low weight loss values that ranged from 70.70 on the 12th day, 221.80 on the 15th to 321 mg on the 24th day of the experiment. The strong acidic test medium contributed to the high weight loss values achieved. Clearly, the order of increasing percent corrosion inhibition performance was: 30 > 60 > 100. Only the 30 and 60% extract concentrations addition performed well when compared with the test medium which contained no extract addition.

The results obtained for the corresponding corrosion rate versus the exposure time, figure 2, followed the same

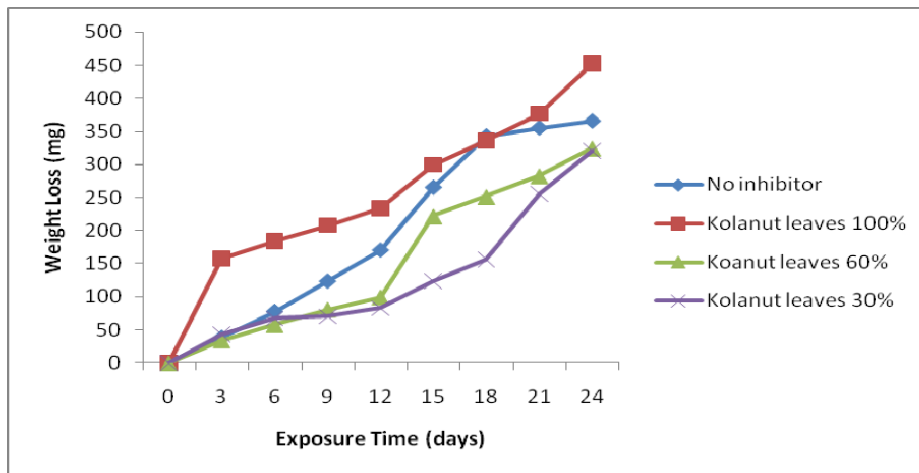


Fig. 1. Variation of weight loss with exposure time for the aluminium alloy specimen immersed in 0.5 M H_2SO_4 with varied concentrations of added kola tree leaves extract.

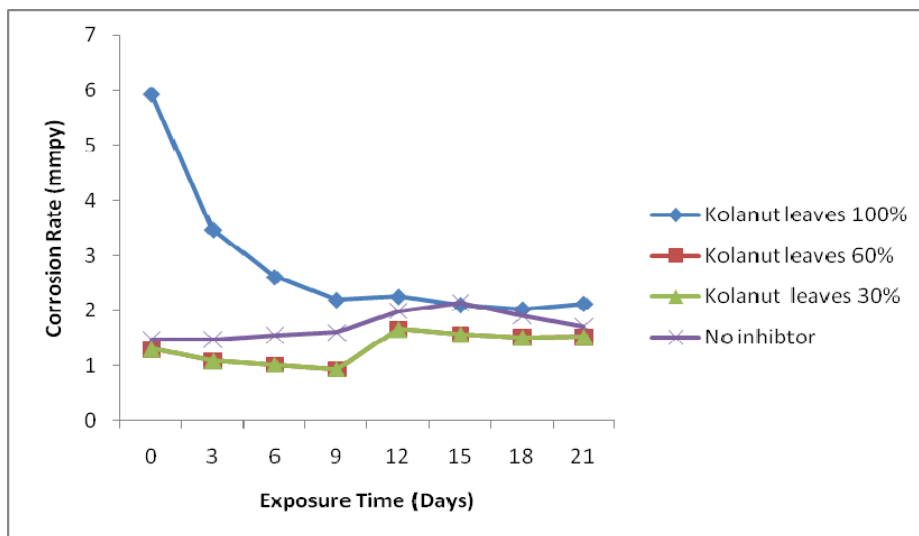


Fig. 2. Variation of corrosion rate with exposure time for the aluminium alloy specimen immersed in 0.5 M H_2SO_4 with varied concentrations of added kola tree leaves extract.

trend of corrosion inhibition performance. The lowest corrosion rate values were obtained for the kola leaves extract at the concentrations of 30 and 60%. The recorded corrosion rate values throughout the experimental period remained the same; and these ranged from 1.303 at the beginning to 1.523 mm/yr on the 21st day of the experiment. The test medium with 100% concentration of added leaves extract, recorded the highest corrosion rate values that ranged between 5.96 at the beginning to 2.12 mm/yr at the end of the experiment. The 30 and 60% extract concentrations addition had lower corrosion rate values than the test without extracts addition; but it was not so the 100% concentration addition. Characteristically, all inhibitors have different optimum concentrations of effective performance in different environments and for different metallic alloys.

No doubt, the constituents of kola leaf extract exhibited a reasonable degree of electrochemical corrosion inhibition activity that was concentration dependent and /or sensitive – this is usually very characteristic of inhibitors in general. The observed corrosion inhibition performance here could be attributed to the presence of tannin and the synergistic effect of combination of other constituents that were mentioned above in the introduction.

The Kola nut extracts

The curves for the variation of weight loss and corrosion rate with exposure time for the aluminum alloy test specimen immersed in 0.5M H_2SO_4 with varied concentrations of added kola nut (fruit) extract are presented in figures 3 and 4 respectively. In figure 3, the trend of weight loss values obtained with respect to

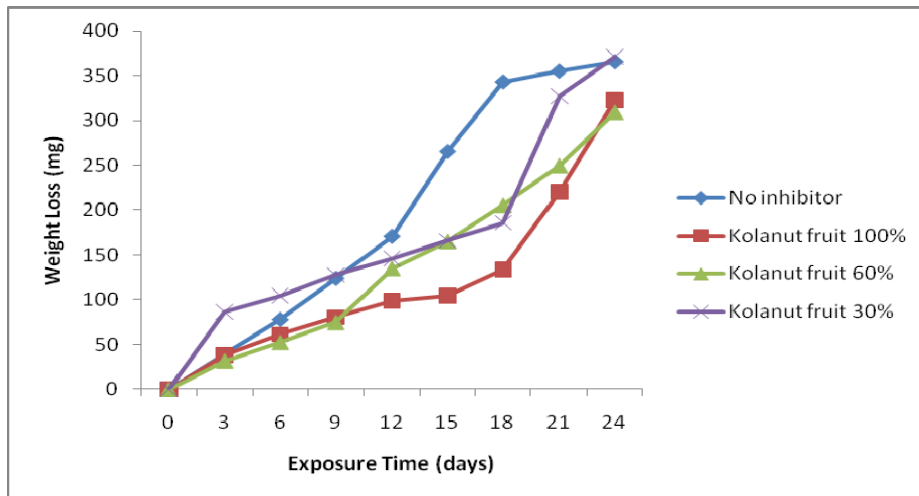


Fig. 3. Variation of weight loss with exposure time for the test specimens immersed in 0.5M H_2SO_4 with varied concentrations of added kola tree nuts extract.

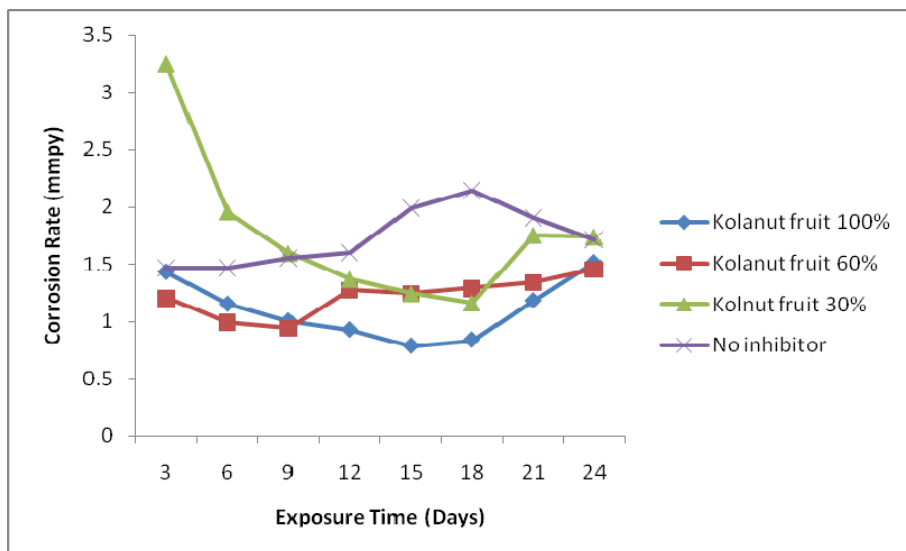


Fig. 4. Variation of corrosion rate with exposure time for the test specimens immersed in 0.5M H_2SO_4 with varied concentrations of added kola nuts extract.

percent concentrations of added extract was different from the one obtained in figure 1 for the leaf extract values. Lowest weight loss values of 32, 104.60, 220 and 322.30 mg were recorded for the 100% extract concentration of kola nuts on the 3rd, 15th, 21st and 24th day of the experiment respectively. The 60% extract concentration addition recorded almost the same weight loss values as the 100%'s up to the 9th day of the experiment. Weight loss values of 165.70 and 205.60mg were subsequently obtained and recorded on the 15th and 18th day respectively. The corrosion inhibition performance with the use of this 60% concentration as indicated by the weight loss values was less than that of the 100% concentration of the nuts extract. The lowest corrosion inhibition performance was recorded when the 30% concentration of the extract was used; with weight

loss values of 86.50, 185.70 and 370.60 mg recorded on the 3rd, 18th and 24th day of the experiment respectively. All the per cent extract concentrations used had lower weight loss values than the test performed without added extracts. Apparently some degree of corrosion inhibition was exhibited by the extracts addition. However, why the trend of this nuts extract differed in corrosion inhibition characteristic/ performance is difficult to explain, except again for differences in chemical constituents and the inhibitors characteristic behavior.

The corresponding corrosion rate values obtained are presented in figure 4. The lowest corrosion rate values were obtained for the 100% extract concentration addition. Values of 0.927, 0.785, 0.837 and 1.453 mm/yr were recorded on the 12th, 18th, 21st and 24th day of the

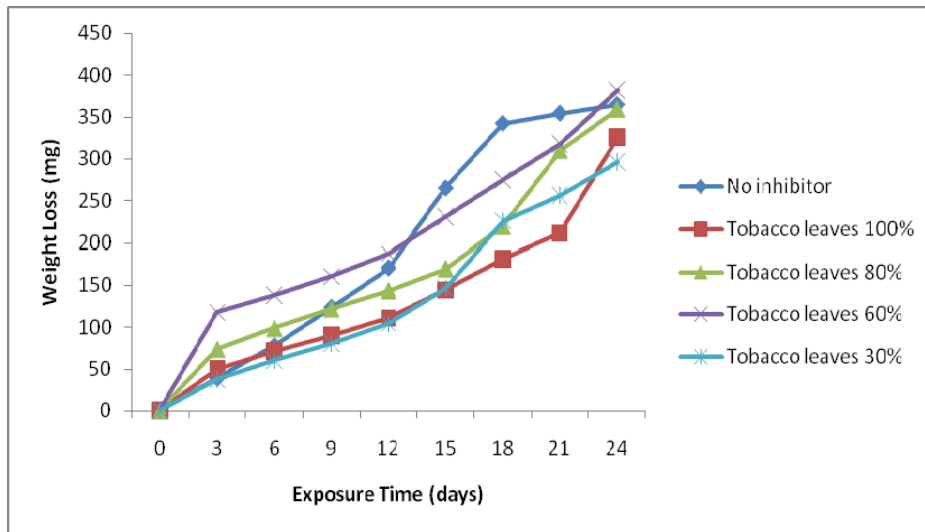


Fig. 5. Variation of weight loss with exposure time for the test specimen immersed in 0.5M H_2SO_4 with varied concentrations of added tobacco leaves extracts.

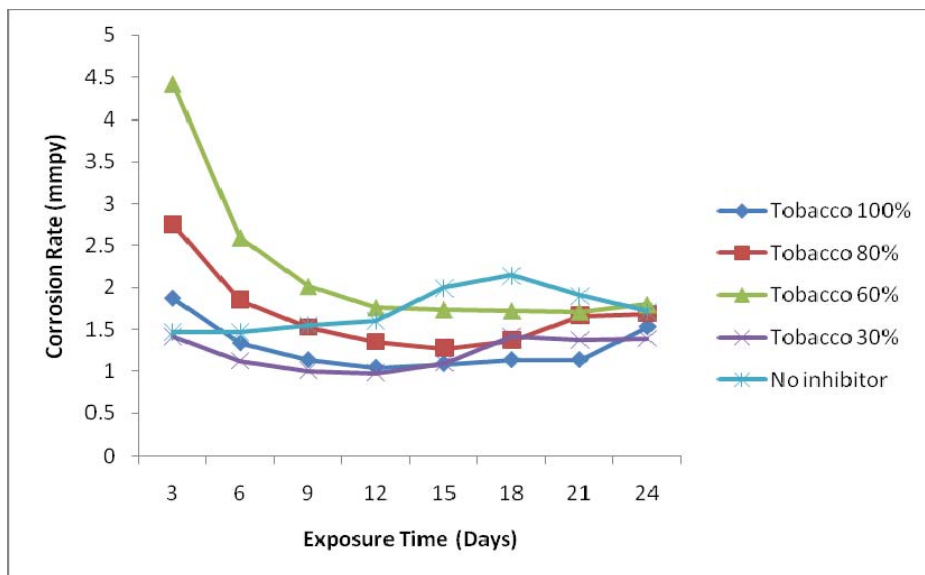


Fig. 6. Variation of corrosion rate with exposure time for the aluminium alloy specimen immersed in 0.5M H_2SO_4 with varied concentrations of added tobacco leaves extracts.

experiment respectively. For the 60% extract concentration addition, the corrosion rate values were slightly higher than the former. The values obtained ranged from 1.202, 0.989, 0.939 to 1.753 and 1.713 from the 3rd to 21st and 24th day of the experiment respectively. With 30% concentration addition, the corrosion rate values were higher than the 60%'s except from the 12th to the 18th day of the experiment when they achieved the same corrosion rate values. Results obtained for the test without extract addition showed it to have the highest corrosion rate with values that ranged from 1.466 (3rd day) to 1.991 (15th day), 2.144 and 1.71 mm/yr on the

18th and 24th day respectively. The corrosion rate values had good correlation with the weight loss values in figure 3.

Tobacco leaves extracts

The results for the variation of weight loss with exposure time for the aluminum specimen immersed in 0.5M H_2SO_4 with varied concentrations of added tobacco extract are presented in figure 5. The corresponding corrosion rate results are similarly presented in figure 6. Here, there were four different percent concentrations used (30, 60, 80, and 100%).

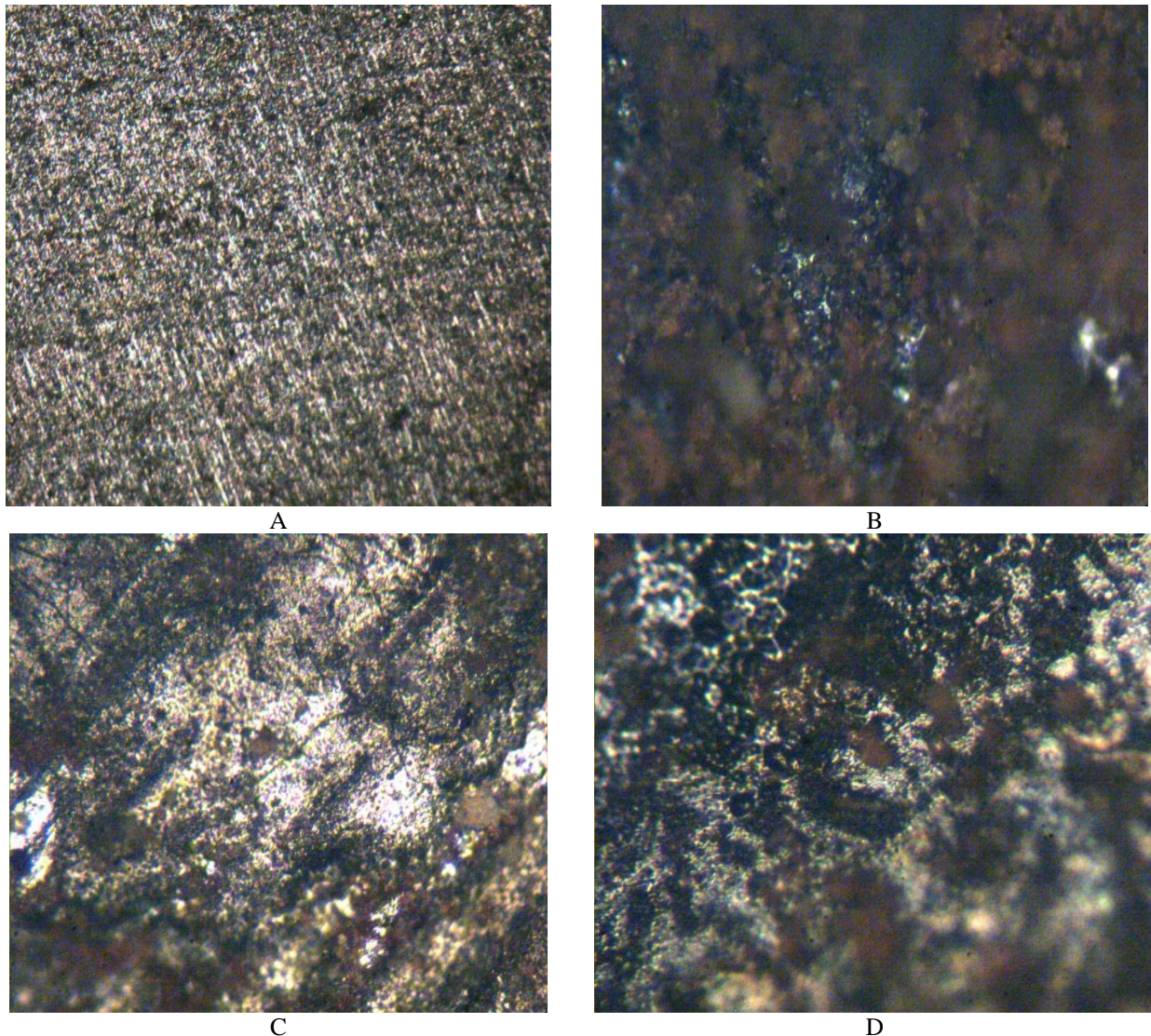


Fig. 7. Micrograph of aluminum test specimens before and after immersion in the test media; A - Before immersion; B - After 24 days of immersion in H_2SO_4 ; C - After 24 days of immersion in H_2SO_4 + extract of Kola tree nuts; and D - After 24 days of immersion in H_2SO_4 + extract of Kola tree leaves

Just like the previous extracts of kola tree parts, the 100% here represents the original extract without dilution. All the different extract concentrations addition recorded weight loss values that increased with time- an indication of active corrosion reactions throughout the experimental period. All the results were very close in weight loss values particularly those with the 100, 30, and 80% extract concentrations addition. The addition of 100% concentration seemed to give averagely, the lowest weight loss value and this was closely followed by the 30% extract concentration addition with weight loss values of 37.5 and 295.9 mg at the beginning and end of the experiment respectively. The 80 and 60% extract concentrations also followed in that order. It did not

follow any particular trend. All the per cent extract concentration additions gave better weight loss values than the blank test, that is, the one without inhibitor addition. The corresponding corrosion rate values also follow the same trend as just described. Corrosion rates values that ranged between 1.87 at the beginning and 1.68 mm/yr at the end of the experiment were recorded for the 100% extract concentration addition. Similarly values of 1.47 and 1.39 mm/yr were recorded at the 3rd day and at the end of the experiment respectively.

Inhibitor efficiency

The results of the inhibitor efficiency obtained by calculations are presented in table 1.

Table 1. Inhibitor Efficiency for Aluminium alloy in H₂SO₄.

ENVIRONMENT	CONCENTRATION	INHIBITOR	INHIBITOR CONCENTRATION	INHIBITOR EFFICIENCY (%)								
				EXPOSURE TIME (DAYS)	3	6	9	12	15	18	21	24
SULPHURIC ACID	0.5M	NONE			NIL							
SULPHURIC ACID	0.5M	KOLANUT LEAVES EXTRACT	30%		-12.2762	13.18822	42.93785	51.25952	53.30064	54.30657	28.00338	12.05479
			60%		11.2532	25.60819	34.54399	41.65202	16.33346	26.62774	20.27637	11.09589
			AS OBTAINED		-303.581	-136.236	-68.2002	-36.8483	-13.1271	1.956204	-6.37338	-24
SULPHURIC ACID	0.5M	KOLANUT FRUIT EXTRACT	30%		-121.228	-33.4187	-2.90557	14.58699	37.49528	45.78102	7.83982	-1.53425
			60%		18.15857	32.52241	39.46731	20.73814	37.57073	39.9708	29.55443	15.17808
			AS OBTAINED		2.557545	21.51088	35.18967	42.17926	60.54319	60.93431	37.95826	11.69863
SULPHURIC ACID	1M	TOBACCO EXTRACT	30%		4.092072	23.68758	35.35109	39.19156	45.03961	34.16058	27.94698	18.93151
			60%		-201.023	-76.6965	-29.6207	-9.66608	12.86307	19.73723	10.37789	-4.73973
			80%		-87.7238	-26.1204	1.856336	15.99297	36.13731	36.05839	12.63395	1.671233
			AS OBTAINED		-27.6215	8.834827	27.03793	35.03222	45.45455	47.15328	40.35533	10.63014

The best result obtained for aluminium alloy was provided by kola tree nuts extract at 100% concentration with an efficiency of 60.54 and 60.91% respectively on the 12th and 15th day of the experiment. Kola leaf extract at 30% concentration addition also gave a fairly good corrosion inhibition performance with an inhibitor efficiency of 51.26, 53.80 and 54.31% on the 12th, 15th and 18th day of the experiment respectively.

For the tobacco leaves extract, the best inhibitor efficiency was obtained with the 100% extract concentration (as received) which recorded 45.45 and 47.15% on the 15th and 18th day respectively. Inhibitor efficiency values were generally low on the 24th day of the experiment.

In general, the effective corrosion inhibition performance of kola tree and tobacco extracts could be associated with their complex chemical compounds which include tannin as earlier mentioned. Also, constituents such as epicatechin, D-catechins, theophylline and theobromine contained in the constituents of kola leaf and nut extracts could act as inhibiting passive film formers on the aluminium substrate surface. The film that was formed could act as a barrier between the alloy and corrosive environment interface and thus preventing and/or stifling corrosion reactions of anodic oxidation – (dissolution) and the cathodic reduction processes. Similarly, the very complex structural compounds and the multifarious constituent composition of tobacco would have provided a more stable adherent film on the surface of the aluminium specimen to hinder active corrosion reactions. Thus the penetration of the SO₄²⁻ reacting species through the surface film barrier would be hindered. The

synergistic action/reaction of these compounds on the surface of the test specimens could also hinder the sulphate ion reacting species, promote more stable passive film formation on the surface of the aluminium alloy and hence inhibit and stifle corrosion reactions at the metal / environment interface as mentioned above.

Photomicrographs

Some of the micrographs made before and after immersion of the test specimens in sulphuric acid, with and without the use of the kola tree extracts are presented in figures 7(a-d). There was significant corrosion with corrosion products of the aluminium alloy specimens in the test medium without the added extracts as observed in figure 7(b). Figure 7(c) shows a surface feature with very moderate or minimal corrosive action for the test with the addition of kola nut extract. A similar surface feature though with some pits observed, was obtained as presented in figure 7(d) for the test with added kola tree leaf extract. These micrographs observations bear very close correlation with the results obtained from the weight loss experiments and the calculated corrosion rates.

CONCLUSION

The best corrosion inhibition performance for the aluminium alloy was achieved with the use of kola tree nuts extract at 100% concentration in 0.5M H₂SO₄ with an inhibitor efficiency of 60.91% on the 15th day of the experiment. Kola leaf extract at 30% concentration addition also gave a fairly good corrosion inhibition performance with an inhibitor efficiency of 54.31% on the 18th day of the experiment. The best inhibitor efficiency for the tobacco leaves extract was obtained with the 100%

extract concentration (as received) with an inhibitor of 47.15% on the 18th day. Inhibitor efficiency values were generally low on the 24th day of the experiment. The extracts of kola leaf, kola nut and tobacco at the concentrations used, and under the other working conditions could be said to be effective as environment friendly extracted inhibitors for the aluminum alloy in sulphuric acid which is a very strong acid.

ACKNOWLEDGEMENT

The authors acknowledge the laboratory investigation contribution of Mr. E.I. Agobe, and also, the Department of Mechanical Engineering, Covenant University, Ota for the provision of research facilities for this work.

REFERENCES

- Davis, GD and Fraunhofer, JA. 2003. Tobacco Plant Extracts as Environmentally Benign Corrosion Inhibitors. Materials Performance. 2:56-60.
- Davis, GD., Fraunhofer, JA., Krebs, LA. and Dacres, CM. 2001. The Use of Tobacco Extracts as Corrosion Inhibitors, CORROSION (Houston).
- Fraunhofer, JA. 2000. Inhibiting Corrosion with Tobacco, Advanced Materials and Processes, 158:33.
- Fraunhofer, JA. 1995. Tobacco Extract Composition and Methods, US. Patent 43, 941.
- Loto, CA. 2003. The Effect of Bitter leaf extract on the Inhibition of Mild steel in HCl and H₂SO₄. Corr. Prev. and Control. 50:43-49.
- Loto, CA. 2005. Corr. Prev. and Control. 52:13-21.
- Okafor, PC. 2007. Eco-friendly Corrosion Inhibitors: Inhibitive action of Ethanol extracts of Garcinia Kola for the Corrosion of Mild steel in H₂SO₄ solutions Pigment and Resin Technology. 36:5.
- WHO, IARC. 1985. Monographs on the Evaluation of the carcinogenic Risk of Chemicals to Humans. 37:9.
- WWW: Wikipedia.org. 2011. Answers.com: Kola nut Internet, Accessed 10th March.

Received: Jan 27, 2012; Accepted: March 7, 2012

SPECTRAL DECOMPOSITION IN ILLUMINATING THIN SAND CHANNEL RESERVOIR, ALBERTA, CANADA

*Mohammed Farfour, Wang Jung Yoon and Youngeun Jo
Geophysical Prospecting Lab

Department of Energy and Resources Engineering, Chonnam National University
300 Yongbong-Dong, Buk-gu, Gwangju 500-757, Korea

ABSTRACT

In this study, we analyzed 3-D seismic and well-log data from the Blackfoot Field, Strathmore, Alberta, Canada, using seismic inversion and spectral decomposition to resolve the channel-fill Glauconitic sand. The Glauconitic sand is of Early Cretaceous age and forms the oil-bearing reservoir in this field. The sandy channel fill basically is characterized by low acoustic impedance whereas shale plugged channels are characterized by high acoustic impedance. However, the presence of non producing shale zones with low impedance similar to that of the oil sand made the acoustic impedance not an unambiguous diagnostic of hydrocarbon bearing sand. Additionally, regional geology wells producing from shallower zone show also a similar response to that of the sandy channel, thus, the need for another indicator to remove this ambiguity became a necessity. Spectral decomposition has been selected to play this role. To achieve this objective we relied on the fact that this attribute has proven to have the potential to selectively illuminate formations at their tuning frequency which can be different for hydrocarbon and non hydrocarbon saturated rocks. Interestingly, Short Window Fourier Transform workflow could successfully image the channel's stratigraphic features and differentiate shale from sand. Furthermore, the attribute could discriminate the regional geology from oil sand-fill channel in dry wells located in relatively low impedance area where the differentiation using P-impedance was ambiguous.

Keywords: Glauconitic channel, spectral decomposition, short time widow Fourier transform.

INTRODUCTION

Unlike faults, depositional channels and other stratigraphic features usually are confined to a given stratigraphic horizon. Ideally, one would pick that horizon and slice through the appropriate attribute volume to display the channel as it might have looked at a given point in geologic time. Within this horizon the seismic polarity of the channel reflection depends not only on the impedance of the channel fill which changes within the channel system but also on the impedance of the lithologies that underlie and overlie the channel fill (Chopra and Marfurt, 2007). Taking all these characters into account and aiming to better image these geologic interesting events and overcome difficulties regarding mapping their extensions, different approaches and techniques have been developed over the years. Inverting seismic data for different impedances and spectrally decomposing data into sub frequencies are good examples in this regard.

In this study, after using seismic inversion results to define the channel location, we used Fourier spectral analysis to study the spectral-decomposition response to stratigraphic features of Glauconitic oil sand reservoir of Early Cretaceous age from Alberta, Canada.

Acoustic impedance and spectral decomposition in reservoir studies

The original use of seismic data, and still the main use today, has been to identify the geometry of reflections and ascertain their depths. This is possible because seismic waves reflect at interfaces between materials of different acoustic properties. However seismic data contain information beyond reflector location. That is every reflection changes the amplitude of the returned wave. The controlling property in this change at the interface is the contrast in impedance which is the main objective of variety of seismic inversion techniques.

Seismic inversion is simply the transformation of seismic data into pseudo acoustic impedance logs at every trace. This fact provides an acoustic impedance model contains more information than seismic data. Indeed, it contains all the information in the seismic data without the complicating factors caused by wavelets and adds essential information from the log data (Latimer *et al.*, 2000).

It is noted that over the last decades inverting seismic data into acoustic impedance has become a rapidly growing field due to many advantages that acoustic impedance has over seismic. As a result, many types of seismic

*Corresponding author email: m84.farfour@gmail.com

inversions are now available and have been widely used in reservoir studies; each has its own advantages and limitations (Lancaster and Whitcombe, 2000; Hampson and Russell, 1991; Hampson *et al.*, 2005; Russell and Hampson, 2006; Francis, 1997, 2005; Cooke and Cant, 2010).

Spectral decomposition is an innovative seismic attribute more recent than seismic inversion. It is used for reservoir imaging and interpretation technology, originally developed and commercialized by BP, Apache Corp. and Landmark (Partyka *et al.*, 1999). The technology utilizes a sequence of seismic frequency slices through an area of interest to create a suite of amplitude maps which can be selectively combined to yield much higher resolution images of reservoir boundaries, lithologic heterogeneities and interval thicknesses than the traditional full band seismic displays (Burns and Street, 2005). Note that over the last decade extensive studies have been performed on the effect of thickness and fluid of reservoir on the tuning frequency, and these studies have been published by Marfurt and Kirlin (2001), Laughlin *et al.* (2002), Chopra and Marfurt (2007) and Chen *et al.* (2008). Other studies have discussed how this new attribute can be used to differentiate both lateral and vertical lithologic and pore-fluid changes (Burnett *et al.*, 2003; Sinha *et al.*, 2003;

Goloshubin *et al.*, 2006; Suarez *et al.*, 2008). It can also delineate stratigraphic traps and identify subtle frequency variations caused by hydrocarbons (Burnet *et al.*, 2003; Castagna *et al.*, 2003; Goloshubin *et al.*, 2006; Miao *et al.*, 2007). All these studies among others proved that spectral decomposition can be applied in different areas around the globe, and in a variety of environments.

Note that although we have used acoustic impedance as indicator, our focus is mainly on the spectral decomposition response to reservoir fluids from glauconitic channel.

In order to decompose the seismic band into its individual frequencies, we used a fixed length analysis window for all frequencies. This allows us to determine which frequency component is dominant within our area of interest and use these frequency components to map our channel stratigraphic features. The decomposition reveals that the amplitude contrast between the oil sand and shale is much higher at individual frequencies than it was in seismic full band imaging.

Geologic setting

The Blackfoot field is located in the south-east of Strathmore, Alberta, Canada (Fig. 1). The 3C-3D seismic

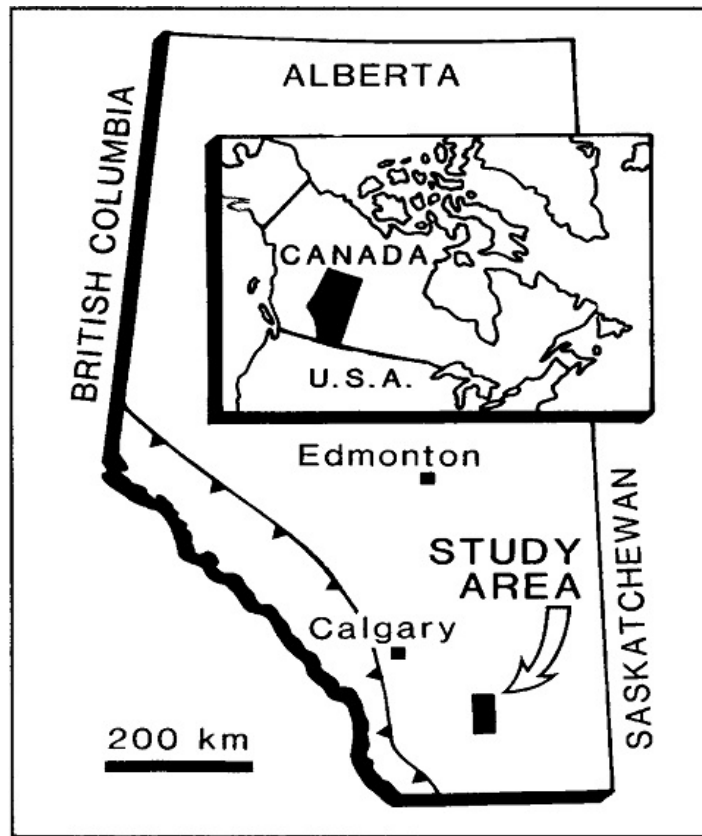


Fig. 1. Index map showing location of study area in the plain of southern Alberta, Canada (Source: Wood and Hopkins, 1992).

survey was acquired over a Lower Cretaceous incised channel filled with sand and plugged shale. The producing formation is cemented channel sand deposited as incised valley fills sediments in clastic sequences which uncomfortably overlie carbonates of Mississippian age. The Glauconitic sandstone is up to 35-m thick and is approximately 1550 m below surface in the Blackfoot area.

The average porosity is near 18% in the producing sandstone and cumulative production throughout southern Alberta exceeds 200 million barrel of oil and 400 billion ft³ of gas (Margrave *et al.*, 1998).

Data set used in the study

The Blackfoot 3C-3D seismic survey was acquired near Strathmore, Alberta, Canada in 1995. The resulting 3-C data were processed for both *P-P* and *P-S* primary reflections to produce two independent 3-D migrated volumes. Final signal bandwidths were 10-80 Hz for *P-P* and 10-40 Hz for *P-S*. The subset we use in this study is consisting of 119 lines and 81 cosselines. The bin size is 30x30 m and offsets ranged from 300 to 1700 m with 11 wells in the covered area. Note, several published work have discussed thoroughly the Blackfoot dataset's processing, interpretation (Dufour *et al.*, 1998, 2002, Margrave *et al.*, 1998; Swisi and Morozov, 2009). The studies represent very rich and helpful references for further studies addressing this field.

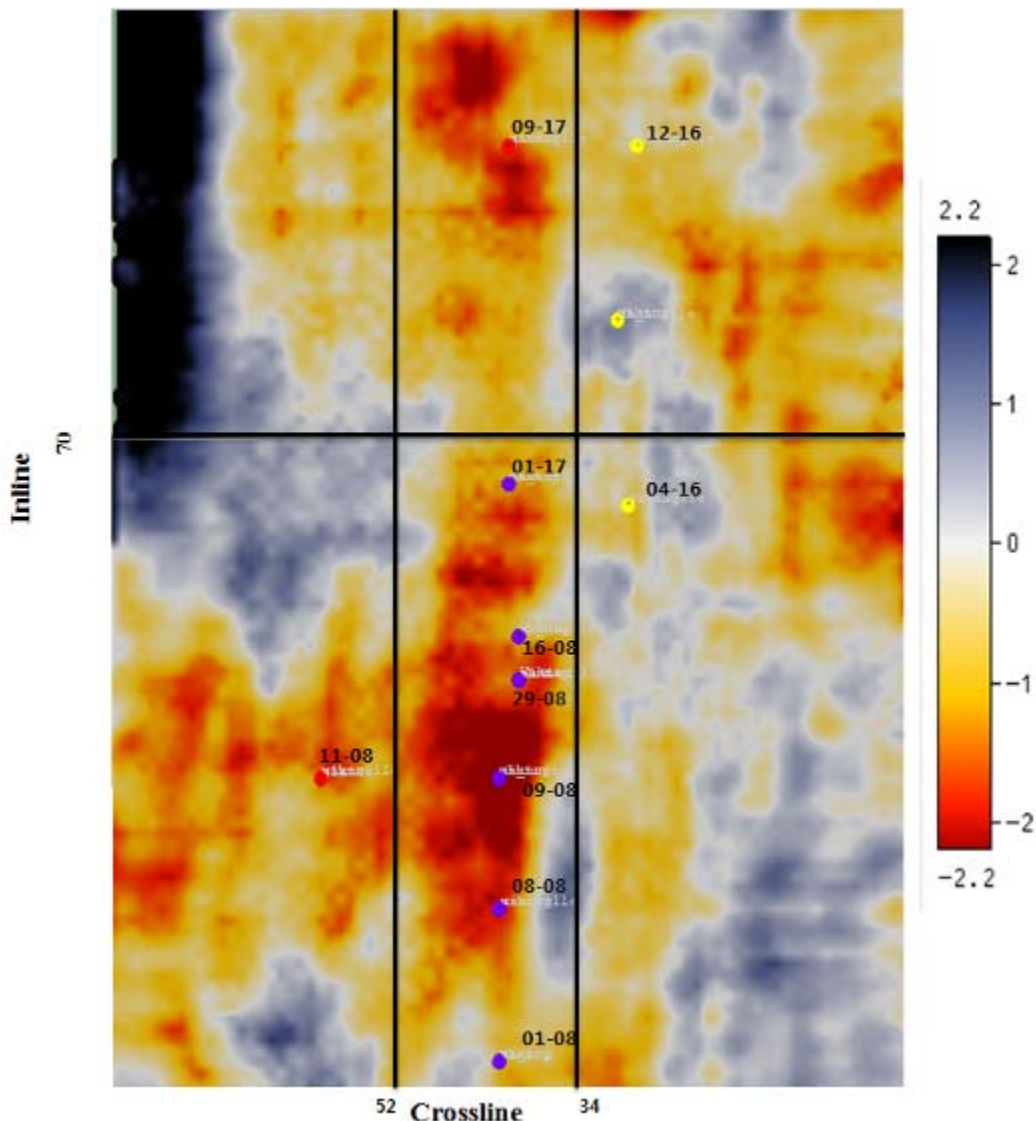


Fig. 2. Seismic broad band amplitude slice through the channel. Although some lateral changes are apparent, the channel remains invisible and difficult to map.

MATERIALS AND METHODS

Methodology

The emphasis in this study is to delineate the channel boundaries and to distinguish sand-fill from shale-fill and regional geology within the channel system. First, seismic inversion was implemented to identify the glauconitic sand channel. Seismic inversion allows us to remove the wavelet effects, thus avoiding its relevant problems such as wavelet side lobes interference and false stratigraphic like effects. In addition, the acoustic impedance data support fast inspection and accurate volume-based interpretation techniques and analyses. According to well data analysis performed at control wells from previous

work published by Swisi and Morozov (2009) the channel is thin and exhibit low acoustic impedance compared to its surrounding. We, therefore, expected that decomposing the seismic broadband into its individual components may help image the channel and deliver more information.

On the other hand, minimizing uncertainty and errors that might be generated from tracking which certainly will affect all further processes pose a new challenge for us. For this purpose, we first, selected a geophysically recognizable horizon based on well ties and calibration to well data. Then, for such careful tracking we have invoked Horizoncube. Horizoncube is new commercial

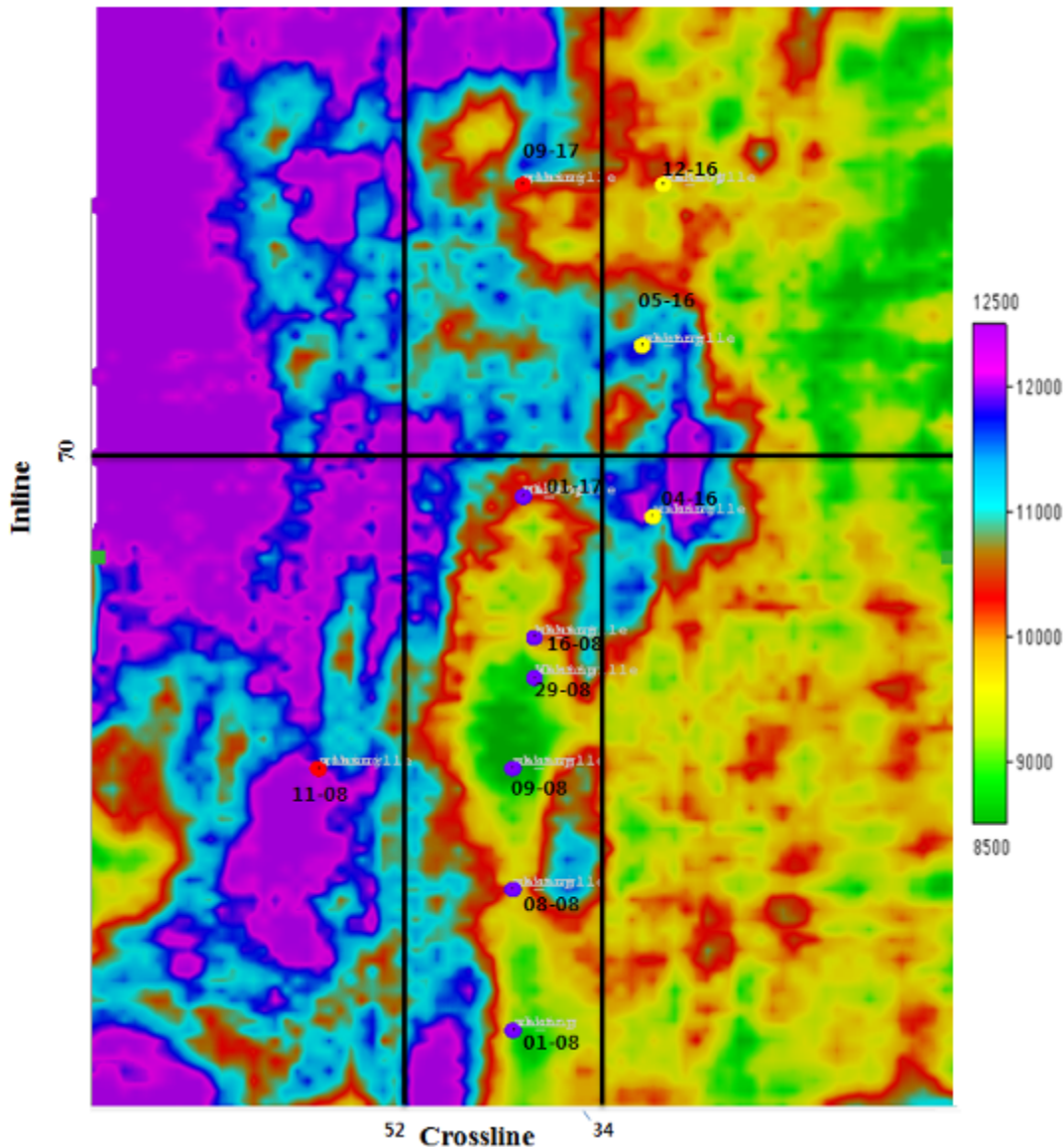


Fig. 3. Acoustic impedance slice through the channel interval shows low impedance along the oil sand channel.

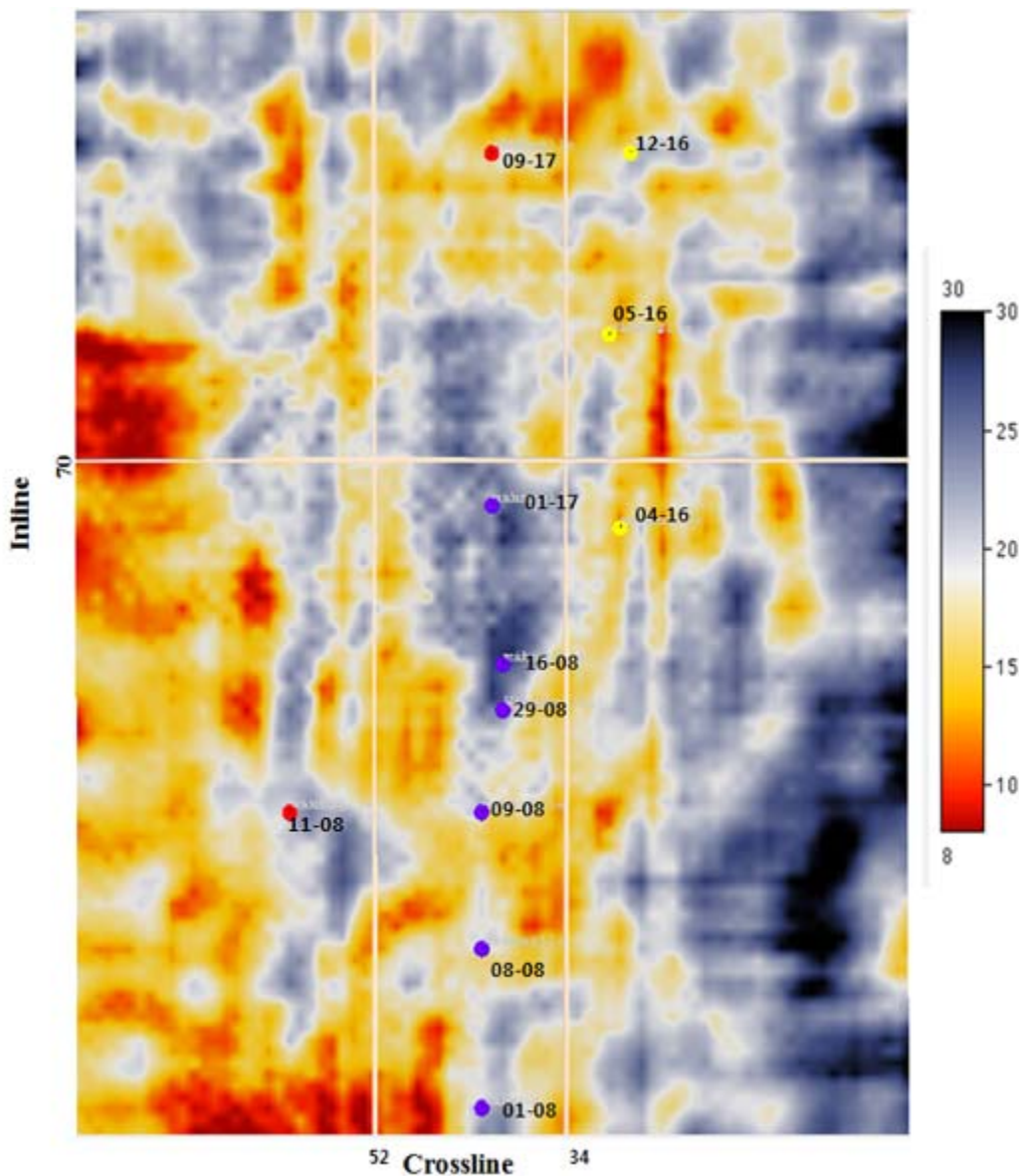


Fig. 4. Spectral amplitude at 15 Hz showing some details of the channel.

plugin in opendtect software (De Grout *et al.*, 2010). The approach currently being adopted for generating the horizon cube involves two main steps. First, a dip “steering cube” is generated which calculates local dip azimuth values of coherent features within the seismic. The steering cube is subsequently used to generate the horizon cube. A special autotracker tracks the dip/azimuth field to generate horizons that are typically separated by one sample at the starting position. This densely tracked horizons mapping enables us to extract more information with very complex structures. We then calculated our attributes and performed our analysis at the time that a reservoir interval occurred. After that we studied carefully the spectral-decomposition response to the different channel fills for different frequencies. Each frequency

component was expected to help understand and interpret subtle details of the stratigraphic framework of the oil reservoir.

RESULTS AND DISCUSSION

Starting by seismic broadband amplitude analysis, seismic time slice was taken across the channel. The slice shows that some lateral changes are present in the channel location; however channel’s seismic expressions are still difficult to discern (Fig. 2). Results obtained from seismic inversion indicate that the channel like structure is clearly pronounced between crosslines 34 and 52, with low acoustic impedance relative to the surrounding formations (Fig. 3). As shown in figure 3, a total of 11 wells were

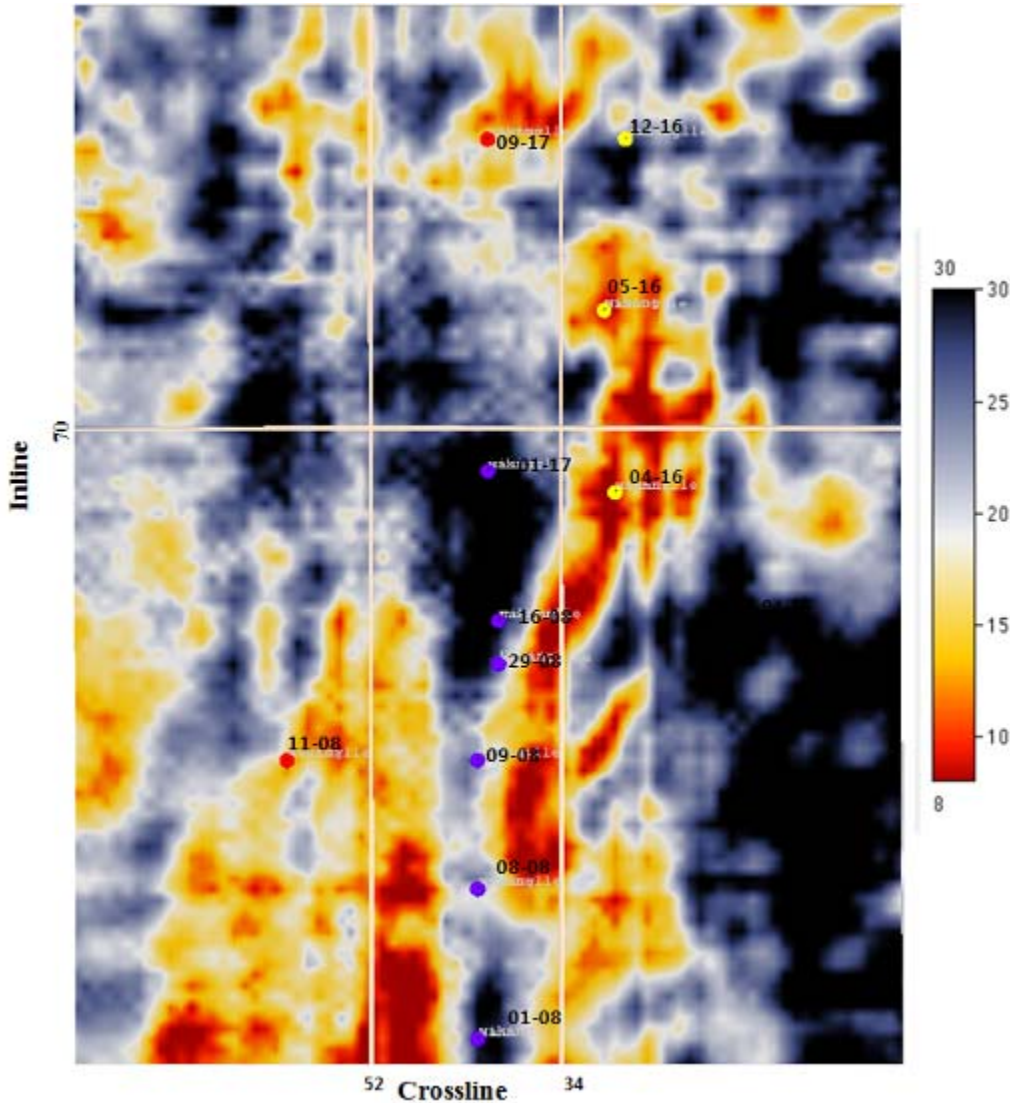


Fig. 5. Spectral amplitude at 30 Hz showing the channel's like structure. Note that oil wells (purple) are along the channel area with high amplitude, while dry wells (yellow) are beyond the channel with low amplitude.

used in the study are displayed. Wells at 01-08, 08-08, 09-08, 16-08 and 29-08 (purple) all encountered sandstone at the upper valley level, whereas 04-16, 05-16, and 12-16 (yellow) have only the upper valley shale fill; wells at 09-17 and 11-08 (red) are regional wells with gas production from shallower zones (Dufour *et al.*, 2002; Todorov, 2000). Note that all the producing oil wells at 01-08, 08-08, 09-08, 16-08 and 29-08 (purple), positioned within the sand-fill channel, correlate with a low-impedance anomaly; while, the dry wells 04-16, 05-16, (yellow) in the shale-plugged channel fall into high-impedance zone. Consequently, the inversion result can be used to discriminate the sand-fill from the shale-fill channel. However, one dry well (12-16) and the regional geology well 09-17 were found being located in relatively low-

impedance area making the differentiation between the sand-fill channel and the regional geology ambiguous (Todorov, 2000). Nevertheless, the acoustic impedance pointed out also high impedance zones separating these wells from the producing wells. The zones are most likely to be associated to lithology change occurred between producing and non-producing wells. Thus, the need for another indicator to confirm this assumption and distinguish oil sand fill over shale fill and regional geology and remove the ambiguity is unavoidable. Spectral decomposition was the key seismic attribute to achieve this goal. Several frequencies were computed for a single horizon. The seismic horizon and its corresponding frequency components at 15 and 30 Hz are displayed in figure 4 and 5. At 15 Hz the channel is

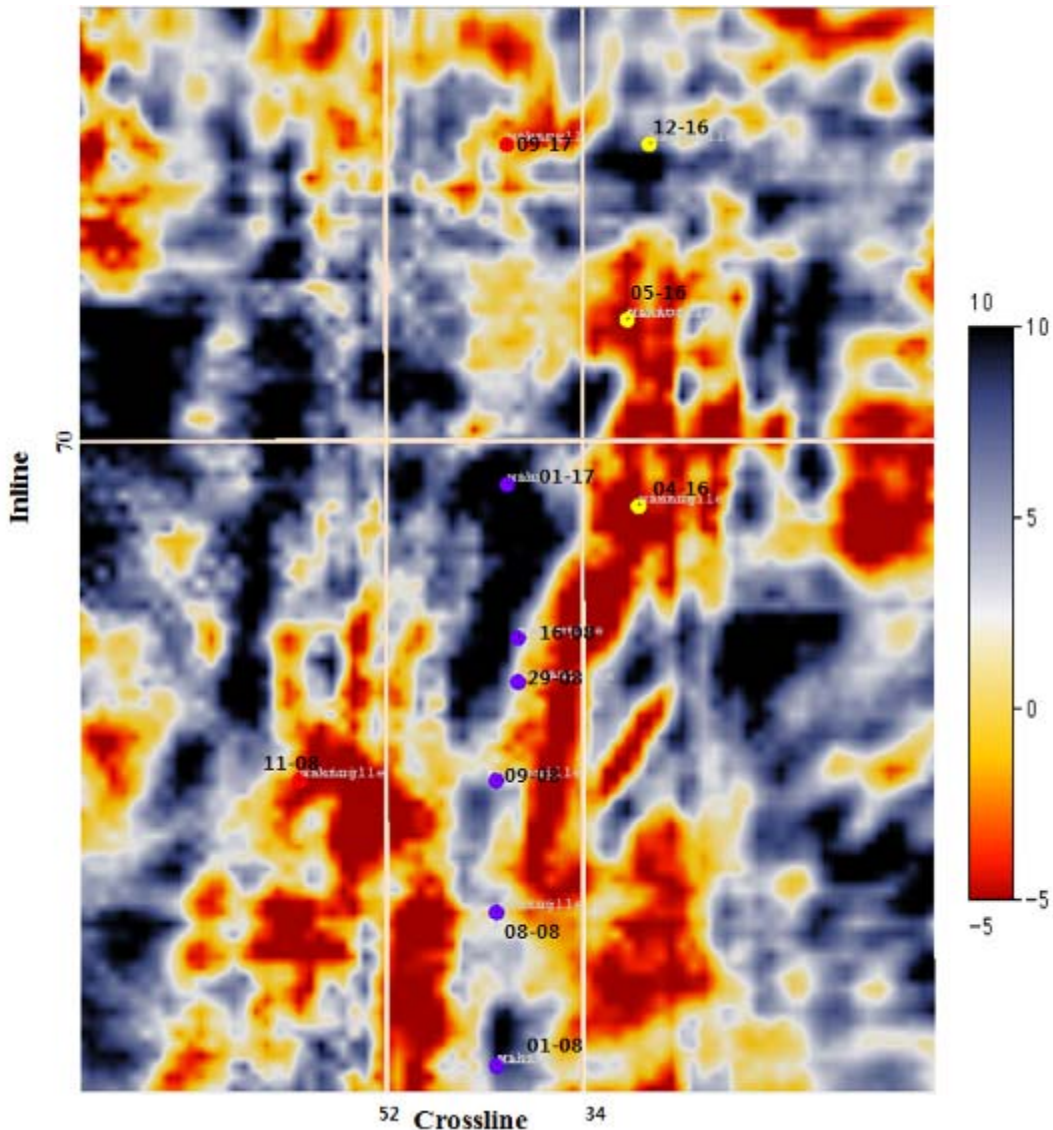


Fig. 6. The difference between 30 Hz and 15 Hz. The channel is clearly visible showing higher frequency amplitude contrast relative to the surrounding rocks along the channel.

poorly imaged but is clearly visible on 30-Hz spectral component, ensuring that 30 Hz is closer to the tuning frequency than 15 Hz is. Thus, the anomalous amplitude present along the channel between crossline coordinates 34 and 52 and ends around 70 inline in figure 5 can be attributed to the result of both thin bed tuning and hydrocarbon charge which is observed only in oil producing wells zone. In fact, the oil presence makes the reservoir reflectivity coefficients larger than those in the adjacent non hydrocarbon filled areas. The thin bed tuning effect of those large reflection coefficients preferentially reflects higher frequencies, then, making the sand channel brighter and clearer at 30 Hz than at other frequencies. In addition, the frequency maps show different distributions of frequency amplitude within the

reservoir. A possible reason for this might be due to change in thickness of the reservoir.

As shown in figure 5 and 6, all the oil producing wells (in blue) found to be inside the mapped channel, while dry wells lie outside the channel with low amplitude, except one well (12-16) exhibiting high anomaly quite similar to the oil wells. The frequency map does indicate also a possible reason for this dry well anomaly which is most likely to be associated with tuning effect. A low amplitude barrier separating this well from the oil channel appear clearly in figure 5 can be interpreted as indicator of depositional variation explaining why the well does not encounter oil bearing sandstone. However, it is important to say that high spectrum amplitude alone is not

diagnostic of hydrocarbon charged sand. Indeed, it is with the help of the other data (well logs, production history) that the anomalously high amplitude along the channel thought to be related to hydrocarbon presence. The difference between the two frequencies components was also calculated (Fig. 6). The frequency difference horizon slice shows that the significant frequency contrast is mainly distributed along the channel, ensuring the effect of the hydrocarbon presence on the frequency behaviour of the channel. It also outlines the channel and indicates much better the presence of the amplitude barrier between the dry wells and the oil sand. It is important to notice that all these interpretations, derived from spectral decomposition, are consistent with inversion results and well information.

We saw that oil sand frequency behaviour was noticeably different than the non producing shale; thus, the wells 09-17 and 12-16 that could not be differentiated from producing wells in the inversion images could be easily distinguished in spectral decomposition maps. Interestingly, the study correlate also with several AVO analyses and inversion studies published by Margave *et al.* (1998), Dufour *et al.* (1999, 2002) and Swissi and Morozov (2009); thus representing an additional source in the direction of characterizing the glauconitic sand in Alberta, South Canada.

Note that the inversion results are the result of incorporating sonic and density well logs from different wells with seismic to predict pseudo well logs in every single trace location. In other words, the acoustic impedance volume is dictated basically by well logs from control wells and constrained by the seismic. On the other hand, spectral decomposition images are fully extracted from decomposing the broad band of the seismic into its individual frequency components without any assistance from well logs. However, the latter could successfully confirm information that the seismic inversion has revealed. Indeed, this study demonstrates that spectral decomposition can work well in somewhat seismically difficult environment where targets are not easy to resolve and exhibiting acoustic impedance that is not enough to discriminate sand from non producing shale.

Throughout this work it might have been noticed that the technique has several advantages over the seismic inversion process in that it is simple to use and to interpret. Furthermore, the fact that it has no relationship with seismic wavelet extraction and well ties and correlations, that seismic inversion depends heavily on, makes this attribute free of several sources of risk and errors. This makes its released information considered as an independent source of data that confirm and increase accuracy and confidence in other sources or even supply new information about the targets. However, it is worth emphasizing that without the assistance of prior

reconnaissance and information (geology, reservoir engineering, inversion, etc), that provide some prior knowledge about the target the technique might have a limited success in addressing some seismic targets. This is due to the fact that strata of different lithology and thickness display different spectrum features in the frequency domain, in addition to various factors that may affect the frequency spectrum recorded. Thus, this can generate some difficulties in tuning the optimum frequencies that have the potential to image the desired target through only the repeated experiments and experience rule. However, there are other techniques, more complex, developed mainly to overcome these limitations and to deal with more complex situations and to target reservoirs when there is few or no prior information available (Maoshan *et al.*, 2010; Zhang *et al.*, 2009).

CONCLUSION

Spectral decomposition did reveal successfully stratigraphic information that could not be derived from broadband seismic. In addition to its routine use in delineating reservoirs extension and highlighting hydrocarbon attenuation effect, spectral decomposition could discriminate sand filled channel from shale filled channel and regional geology where differentiation based on P impedance was ambiguous.

Note that although spectral decomposition is a frequency dependent attribute that doesn't have any relationship with well logs information, it could confirm results that were obtained from seismic inversion where acoustic impedance is amplitude related attribute that relies significantly on well correlations and wavelets.

This study presents an example among many other successful applications of spectral decomposition for delineating channels older and less porous than rocks in tertiary basins such as the Gulf of Mexico and West Africa over which spectral decomposition was first successfully applied.

ACKNOWLEDGMENT

We would like to thank dGB Earth Sciences Company and the people from opendtect.org for providing the software (Opendtect), and Hampson-Russell for providing the software (Strata). Our thanks also go to Korean Gas Corporation (KOGAS) for their support.

REFERENCES

- Burnett, MD., Castagna, JP., Méndez-Hernández, E., Rodríguez, GZ., García, LF., Martínez-Vázquez, JT., Avilés, MT. and Raúl Vila-Villaseñor, R. 2003. Application of Spectral Decomposition to Gas Basins in

- Mexico. *The Leading Edge*. 22:1130-1141.
- Burns, S. and Street, K. 2005. Hart's E&P, March, Spectral decomposition highlights faults. <http://www.epmag.com/archives/digitalOilField/2135.htm>.
- Castagna, JP., Sun, S. and Siegfried, RW. 2003. Instantaneous Spectral Analysis: Detection of low-frequency shadows associated with hydrocarbons. *The Leading Edge*. 22:120-127.
- Chen, G., Matteucci, G., Fahmi, B. and Finn, CH. 2008. Spectral-decomposition Response to Reservoir fluids from a deepwater West Africa Reservoir. *Geophysics*. 73:C23-C30.
- Chopra, S. and Marfurt, KJ. 2007. Seismic attributes for Prospect Identification and Reservoir Characterization. Society of Exploration Geophysicists. Tulsa, OK. pp456.
- Cooke, D. and Cant, J. 2010. Model-based Seismic Inversion: Comparing Deterministic and Probabilistic approaches. *CSEG RECORDER*. 22-39.
- De Grout, P., Huck, A., de Bruin, G., Hemstra, N. and Bedford, J. 2010. The Horizon Cube: A Step change in Seismic Interpretation. *The Leading Edge*. 29:1048-1055.
- Dufour J., Goodway, B., Shook, I. and Andy Edmunds, A. 1998. AVO Analysis to Extract Rock Parameters on the Blackfoot 3C-3D Seismic data. *SEG Expanded Abstracts*. 174-177.
- Dufour, J., Squires, J., Goodway, WN., Edmunds, A. and Shook, I. 2002. Integrated Geological and Geophysical Interpretation Case Study, and Lamé Rock Parameter Extractions using AVO Analysis on the Blackfoot 3C-3D Seismic Data, Southern Alberta, Canada. *Geophysics*. 67:27-37.
- Francis, A. 1997. Acoustic Impedance Inversion Pitfalls and some Fuzzy Analysis. *The Leading Edge*. 16:275-280.
- Francis, A. 2005. Limitations of Deterministic and Advantages of Stochastic Seismic Inversion. *CSEG RECORDER*. 2:5-11.
- Goloshubin, G., Vanschuyver, C., Korneev, V., Silin, D. and Vingalov, V. 2006. Reservoir Imaging Using Low Frequencies of Seismic Reflections. *The Leading Edge*. 25:527-531.
- Hampson, DP. and Russell, B., H. and Bankhead, B. 2005. Simultaneous Inversion of Pre-stack Seismic Data. 75th Annual International Meeting of Society of Exploration and Geophysics (Expanded Abstract). Houston. 1633-1637.
- Hampson, DP. and Russell, BH. 1991. AVO Inversion, Theory and Practice. *The Leading Edge*. 10:39-42.
- Lancaster, S. and Whitcombe, D. 2000. Fast-track 'coloured' inversion. 70th Annual International Meeting of Society of Exploration and Geophysics (Expanded Abstract), Calgary. 1572-1575.
- Latimer, R., B., Davidson, R. and van Riel P. 2000. An Interpreter's Guide to Understanding and Working with Seismic-derived Acoustic Impedance Data. *The Leading Edge*. 19:242-256.
- Laughlin, K., Gassino, P. and Partyka, G. 2002. Spectral Decomp Applied to 3-D. *AAPG Explorer*, May, http://www.aapg.org/explorer/geophysical_corner/2002/05gpc.cfm.
- Marfurt, KJ. and Kirlin, RL. 2001. Narrow-band Spectral Analysis and Thin-bed Tuning. *Geophysics*. 66:1274-1283.
- Miao, X., Todorovio-Marinic, D. and Klatt T. 2007. Enhancing Seismic Insight by Spectral Decomposition, 77th Annual International Meeting of Society of Exploration and Geophysics (Expanded Abstract). San Antonio.1437-1441.
- Maoshan, C., Zhonghong, W., Hongying, Z. and Haizhen, Z. 2010. Spectral Decomposition and Derived Techniques for Clastic Reservoir Identification and its Application. 80th Annual International Meeting of Society of Exploration and Geophysics (Expanded Abstract), Denver.1571-1575.
- Margrave, G., Lawton, D. and Stewart, R. 1998. Interpreting Channel Sands with 3C-3D Seismic Data. *The Leading Edge*. 17:509-513.
- Partyka, G., Gridley, J. and Lopez, JA. 1999. Interpretational Applications of Spectral Decomposition in Reservoir Characterization. *The Leading Edge*. 18:353-360.
- Russell, B. and Hampson, D. 1991. Comparison of Poststack Seismic Inversions Methods. 61st Annual International Meeting of Society of Exploration and Geophysics (Expanded Abstract), Houston. 876-878.
- Russell, B. and Hampson, D. 2006. The Old and New in Seismic Inversion. *CSEG Recorder*. 12:5-11.
- Sinha, SP., Routh, P., Anno. and Castagna, JP. 2003. Time-frequency Attribute of Seismic Data using Continuous Wavelet Transform. 73rd Annual International Meeting of Society of Exploration and Geophysics (Expanded Abstract), Dallas. 1481-1484.
- Suarez, Y., Marfurt, JK. and Falk, M. 2008. Seismic Attribute-assisted Interpretation of Channel Geometries and Infill Lithology: A Case Study of Anadarko Basin Red Fork Channels. 78th Annual International Meeting of Society of Exploration and Geophysics (Expanded Abstract), Las Vegas. 963-967.
- Swiss, A. and Morozov, IB. 2009. Impedance Inversion of Blackfoot 3D Seismic Dataset, CSPG CSEG CWLS

Convention. 404-407.

Todorov, TL. 2000. Integration of 3C-3D Seismic Data and Well Logs for Rock Property Estimation. MS. Thesis. University of Calgary, Canada. pp86.

Wood, JM. and Hopkins, JC. 1992. Traps Associated with Paleo-valleys and Interfluvies in Unconformity Bounded Sequence: Lower Cretaceous Glauconitic Member, Southern Alberta, Canada. AAPG Bulletin. 76(6):904-926.

Zhang, K., Marfurt, KJ., Slatt, RM. and Guo, Y. 2009. Spectral Decomposition Illumination of Reservoir Facies. 79th Annual International Meeting of Society of Exploration and Geophysics (Expanded Abstract), Houston. 3515-3519.

Received: March 13, 2012; Revised: April 25, 2012;

Accepted: April 26, 2012

WILL RISING WATER DROPLETS CHANGE SCIENCE?

C K G Piyadasa

Department of Physics, University of Colombo, Colombo 03, Sri Lanka

*Department of Electrical and Computer Engineering

Engineering Information and Technology Complex

University of Manitoba, Winnipeg, 75 Chancellor's Circle MB R3T 5V6 Canada

ABSTRACT

The movement of liquid water droplets against the gravitational field has been shown. This was observed when projecting condensed steam droplets downwards. The observations show that the droplets decelerated and turned around at a point with their velocity becoming zero and begin moving upwards against the earth's gravitational attraction. Further to the above observation, condensed steam droplets kept in an inverted container were examined. Some of these droplets showed upward drift while others drifted downward. The higher density of water droplets relative to surrounding air doesn't satisfy the condition for the buoyancy to be responsible for the upward movement. The conditions required to create convection current were also not present at the region where droplets begin their upward movement. Therefore, no adequate explanation of this droplet movement against gravity can be given with conventional laws and hence a novel way of thinking is needed to explicate the behavior.

PACS: 04.80.Cc

Keywords: Gravity, density, buoyancy, convection, latent heat.

INTRODUCTION

Archimedes (287 BC – 212 BC) discovered a method of finding a forged gold crown. He discovered a technique in determining a property which is unique to each and every substance when he stepped into a bathtub and watched it overflow. He uncovered that the weight of the displaced fluid is equal to the apparent loss of weight of an object which is partially or totally immersed in the fluid. He realized that this unique property of a metal, density can be found from its weight and its weight loss in water. Subsequently the observation of Archimedes came to be established as the principle of Archimedes which is conveniently used in explaining some of the observations of nature. Although the concept of buoyancy originated with two different forms of matter (water and gold), it was then extended to any form of matter with different states of packing - tight or loose.

One of the most seen phenomena in nature is cloud formation. Condensation of water vapor in any air mass that becomes saturated above the Earth's surface creates clouds. Air containing water vapor is forced to rise because of the physical presence of elevated land or if sufficient surface heating occurs at the ground. The main constituents of atmospheric air; nitrogen (78%, molecular mass ~ 28.02amu), oxygen (21%, molecular mass ~ 32.00amu) and a trace of argon (0.93%, atomic mass ~ 39.94amu), which exists in mono atomic form and other gases such as carbon dioxide and water vapor. The

average molecular mass of air is 28.97 g/mol. Assuming Avogadro's Law and the ideal gas law, water vapor and air will have a molar volume of 22.414 liter/mol at STP. A molar mass of air and water vapor occupy the same volume of 22.414 liters (<http://www.tiptheplanet.com/wiki/Water>, 2011). The molecular mass of water is 18.02 g/mol. The density (mass/volume) of water vapor is 0.804 g/liter, which is significantly less than that of dry air at 1.292 g/liter at STP. This means that at the same temperature, a column of dry air will be denser or heavier than a column of air containing any water vapor. Thus, any volume of moist air will rise/float if placed in a larger volume of dry air. This is the standard explanation of transport of water vapor leading to cloud formation. Hence, It appears that vertical drift generally observe in water vapor (due to surface heating) could be explained using Archimedes law of buoyancy.

Apart from the cloud formation there is one other interesting phenomena in nature called fog or mist which is mainly categorized by the number density and the size of the water droplets in air. If we can see more than 1 km through the cloud of water droplets, it is known as mist. If the visibility falls less than that, it is called fog. Mist and fog usually form on a calm night when the air is too cold to hold all its moisture. Volume mean diameter (VMD) of fog droplets are observed up to about 65 μ m (Kumar, 1973; Lenham and Clay, 1982) and in mist the VMD tends to be little higher than fog. In another word, mist is heavier and lies close to the ground. The separation

among these droplets is relatively large compared to their size. The number density of these droplets is around 25 droplets per cm^3 (Kumar, 1973).

One curious observation is that these water droplets (fog or mist) float in an undisturbed atmosphere. This can be explained by the standard explanation of buoyancy because as stated above the density of water vapor is less than dry air. These droplets contain an enormous water quantity as single masses relative to the water vapor in the surrounding air. Each droplet is separated with a large distance relative to their size and no known forces exist among them other than the gravitational (Newton, 1687; Hawking and Israel, 1996; Flandern, 1996) and electromagnetic (Maxwell, 1865) forces which are experienced by all other objects in the universe.

One could ask a plausible question whether the concept of density could be correctly applied to the collection of widely separated water droplets where the inter-particle interactions are only of electromagnetic or gravitational nature. Hence, according to the traditional explanation we are considering the “dispersed water droplet state” as a bulk material or single object, such as a solid or a liquid when measuring the density. Therefore certain ambiguities arise when we apply Archimedean concept to this situation.

Figure 1 shows an example of water droplets, due to condensation of steam, coming out from a tube directed downward and changing direction and traveling upwards. The steam is in the gaseous phase which has been converted from its liquid form by acquiring Latent heat. According to the steam-tables the density of steam at 1 atm and 100 °C is 0.6 kg/liter. The picture (Fig. 1) shows the condensed-steam as a white cloud which indicates that the droplets/particles in the condensed-steam are large enough to reflect/scatter visible light. However, within the region where the condensed-steam is seen as a white mist, the particle dimension exceeds the order of the wavelength of the visual spectrum. Several studies (Fan *et al.*, 2009; Tatsuno and Nagao, 2000; Cinar and Yilbas, 1998; Petr and Kolovratník, 2000) show that the size of these droplets/particles ranging up to several tens of microns, peaking around $0.1 - 0.5 \mu\text{m}$. Even a condensed-steam droplet (CSD) with $0.1 \mu\text{m}$ diameter contains a rather large number of molecules making the CSD denser than its surrounding air. With this in mind how do water droplets in mist or fog float in air without falling down to the earth surface in the absence of air turbulent or convection currents? Also why do these water droplets in figure 1 with heavier density relative to the surrounding air go up? There are two possibilities. One is buoyancy (possibility 1) due to density of the displaced air volume by the CSD; this is similar to Archimedes’ explanation. The other possibility is that the resultant upward

movement exerted by the rising hot air molecules (possibility 2) creating a convection current.



Fig. 1. Photograph of the path of condensed-steam or water droplets projecting downward direction. Photograph shows a stream droplets coming out from a tube downward direction and turning around and move upward. The droplets are visible as a white mist.

In this study, I examined the conditions required for possibilities 1 and 2 to drive water droplets in an upwards direction, which is against earth’s gravitational pull. For the 1st possibility the density of the CSD which is in liquid form has a higher density than that of surrounding hot air. The next question is that whether any temperature gradient is present which is required to create convection current that causes the rising of air molecules as seen in figure 1. For this I have shown that the condition required to create convection current is also not present at turning-around point (TAP). These 2 conditions were not met. This will lead to a clear doubt for the cause of the rise of CSD.

MATERIALS AND METHODS

Experimental

Ex.1

Steam produced by an electrically boiling water pot was sent in a downward direction through a tube as shown in figure 1. Rate of production of steam can be changed by the electric power supplied to the water pot and hence the velocity of the CSD coming out from the downward oriented tube. The temperature distribution and droplet movement of the emitting CSD were observed by imaging with Cryogenically cooled third generation forward looking infra red(FLIR)thermal camera 3-5 μm and 7.5-13 μm (Flir, model B-CAM) infrared (IR) wavelengths.

Ex. 2

Condensed-steam was over-filled in a vertical inverted container (bottom opened and top closed) as in figure 2. The temperature distribution, droplet size and their movement of the CSDs were measured as in Ex. 1. CSDs were illuminated by highly intense halogen light beam and a digital SLR camera was used to image droplet size at its optimum setting. A fine wire with a diameter 40 μm was placed with condensed-steam in order to get approximate droplet size.

OBSERVATIONS

As seen in the figure 1, in Ex.1, downward projected CSDs come out from the tube and traveled some distance downward decelerating their speed and became zero at a point where the droplets turned around and started moving upwards. Temperature measured at the TAP by

IR imaging is between 60°-55°C.

The upward movement of CSD is clearer in the Ex.2 due to slow movement of droplets at the bottom of the container. An interesting observation was that in Ex. 2, some of the CSDs drift upward from the edge of the container as shown in figure 2, while others drifted downward as leaving the container from the open bottom. Also there were some droplets which do not travel up or down but rather just randomly float below the open bottom.

The observed water droplets in Ex.2 are also well recognized by the naked eye and movements are slow enough to be captured by a digital SLR (Fig. 3). The measured average diameter of water droplets is nearly 20 μm , and the approximate separation among droplets were 0.32mm to several mm.

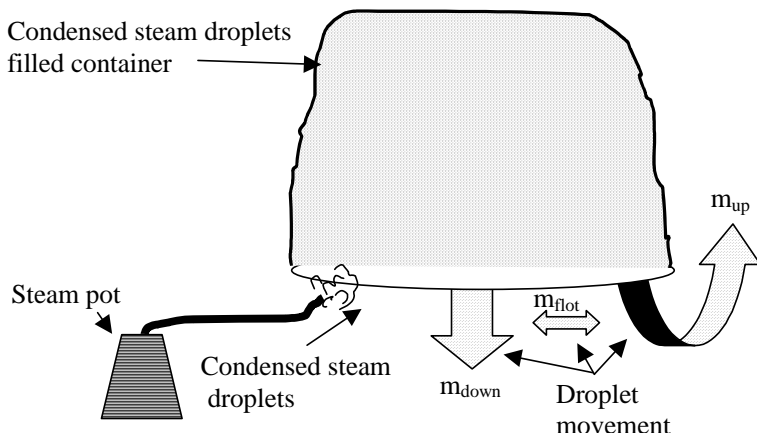


Fig. 2. Movement of the condensed-steam droplets in bottom opened container. Steam generated in a steam pot was fed into the container. The condensed-steam droplets inside the container made three kinds of movements, upward, downward and float at the same time. Infrared imaging clearly shows these three different droplet movements at the bottom of the container.

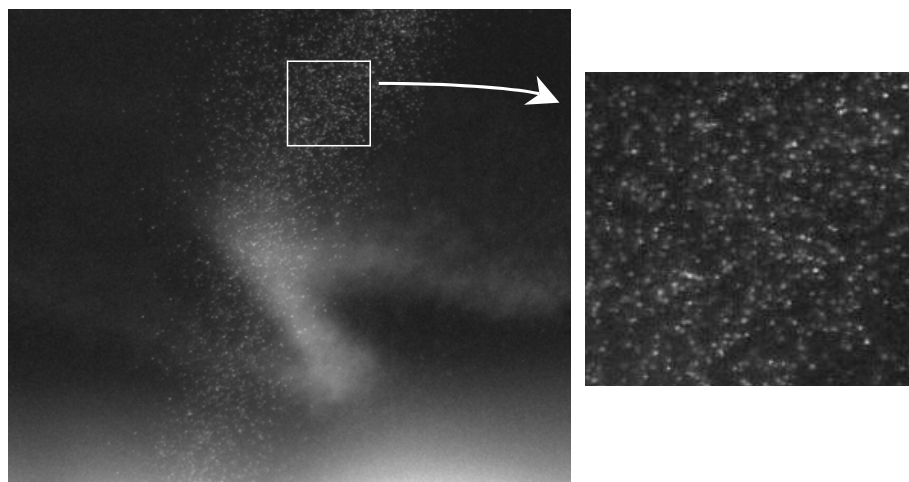


Fig. 3. Photograph of condensed-steam droplets. Water droplets are clearly seen. They are well apart and diameter is around 20 μm and below.

DISCUSSION

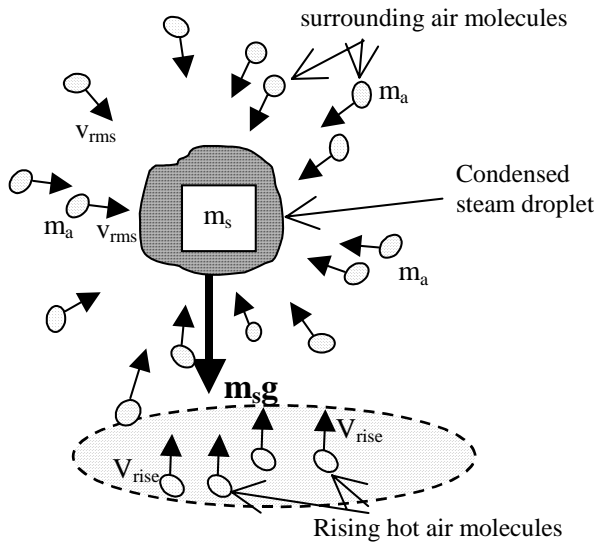
Perfect gas law says that, density of dry air,

$$\rho_{dry} = \frac{p}{RT} \quad (1)$$

where p is the pressure in dry air, R is the specific gas constant and T is the absolute temperature. The density of air at STP is 1.264 Kg/m^3 . CSD which are in the liquid phase at 90°C has a density of $\sim 965 \text{ kg/m}^3$ which is far greater than that of the density of air. The observation (Ex. 1) shows that almost all the visible water droplets emerging from the tube rise up. Hence Archimedes law of buoyancy is not a valid reason for the upward movement of the water droplet. So obviously the *possibility 1* itself is not the reason for the upward movement of CSDs.

According to the ideal gas law, the droplet will be uniformly bombarded by surrounding air molecules from all directions (Fig. 4 a). The total number of collisions, N_{coli} per unit time per unit area is given by

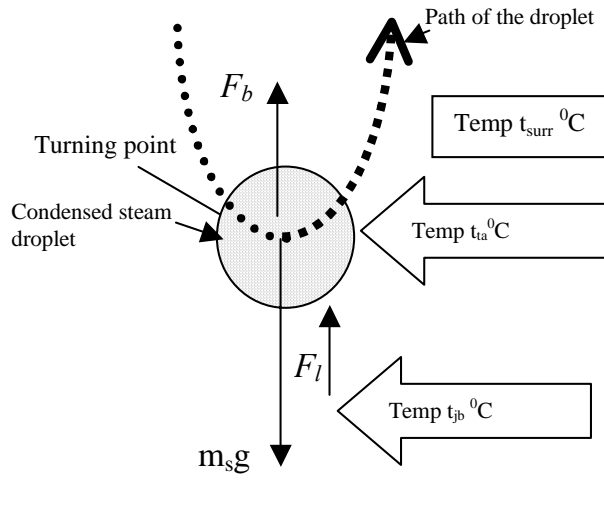
$$N_{coli} = \rho / 4\sqrt{8kT / \pi m_a} \quad (2)$$



(a)

where ρ is the particle density in unit volume, k is the Boltzmann constant, m_a is the mass of the air molecule. The velocity of the CSD coming down from the tube (Fig. 1) becomes zero at a certain depth and rises upwards. Figure 4(b) shows the forces acting on the droplet with mass m_s at the (TAP), assuming that the steam droplets have a spherical shape. F_b is the buoyancy force acting on steam droplet, F_l is the force exerted by rising air molecules (lift force). m_sg is the force due the gravitational field exerted by the earth. m_sg is approximately 825 times higher than F_b (when density of water @ 60°C is 983 kg/m^3 , density of air @ 24°C 1.19 kg/m^3). i.e. *Possibility 1* not met. Our next attempt is to check whether convection current exists in the turning around area and if so, is the magnitude strong enough to lift the droplet?

There is no primary thermal source below the TAP and only the radiation from the hot water droplet and water vapor emanating from the tube can cause temporary heating to activate convection. In other words, the temperatures measured at turn around point (t_{ta}) and just below (t_{jb}) should cause convection of surrounding air/vapor that leads to the upward lift of the CSD. Thermal image reveals that there is no significant increase



(b)

Fig. 4. Condensed-steam droplet in air. (a) CSD with mass m_s is subjected to the two kinds of influence by surrounding and rising air molecules. CSD is uniformly bombarded by surrounding air molecules from all directions while experiencing a force exerted by rising air. m_sg is the force exerted by the earth's gravitational field. (b) Figure shows the path and forces acting on the droplet at the turning-around point, assuming that the droplets have spherical shape. F_b is the buoyancy force acting on steam droplet, F_l is the force exerted by rising air. m_sg is the gravitational force and the temperature measured at turning-around point is $55^\circ - 60^\circ\text{C}$. Below the TAP the temperature was approximately $\sim 24^\circ\text{C}$ (RT).

in temperature measured below the turning point (Fig. 5) by the radiation of heated water droplets moving above. Instead a decreasing temperature gradient (Fig. 5c) is found. This does not support the upward movement of liquid or gas by the current knowledge of convection. Fig. 5a shows the thermal image of the TAP of CSD. The temperature intensities are converted in to a color gradient and presented in figure 5b for better visualization of the temperature distribution at the TAP. The lower part, from

UV to XY shows (Fig. 5c) decreasing temperature from 60°C to 24°C (RT) which definitely inhibits any possible upward convection movement.

In Ex. 2, upward movement of CSD is prominent when the container is filled. With time, downward movement of CSDs arises. It is also observed that with time when downward movement of CSD is significant, there is also upward movement of CSDs present at the same time. See

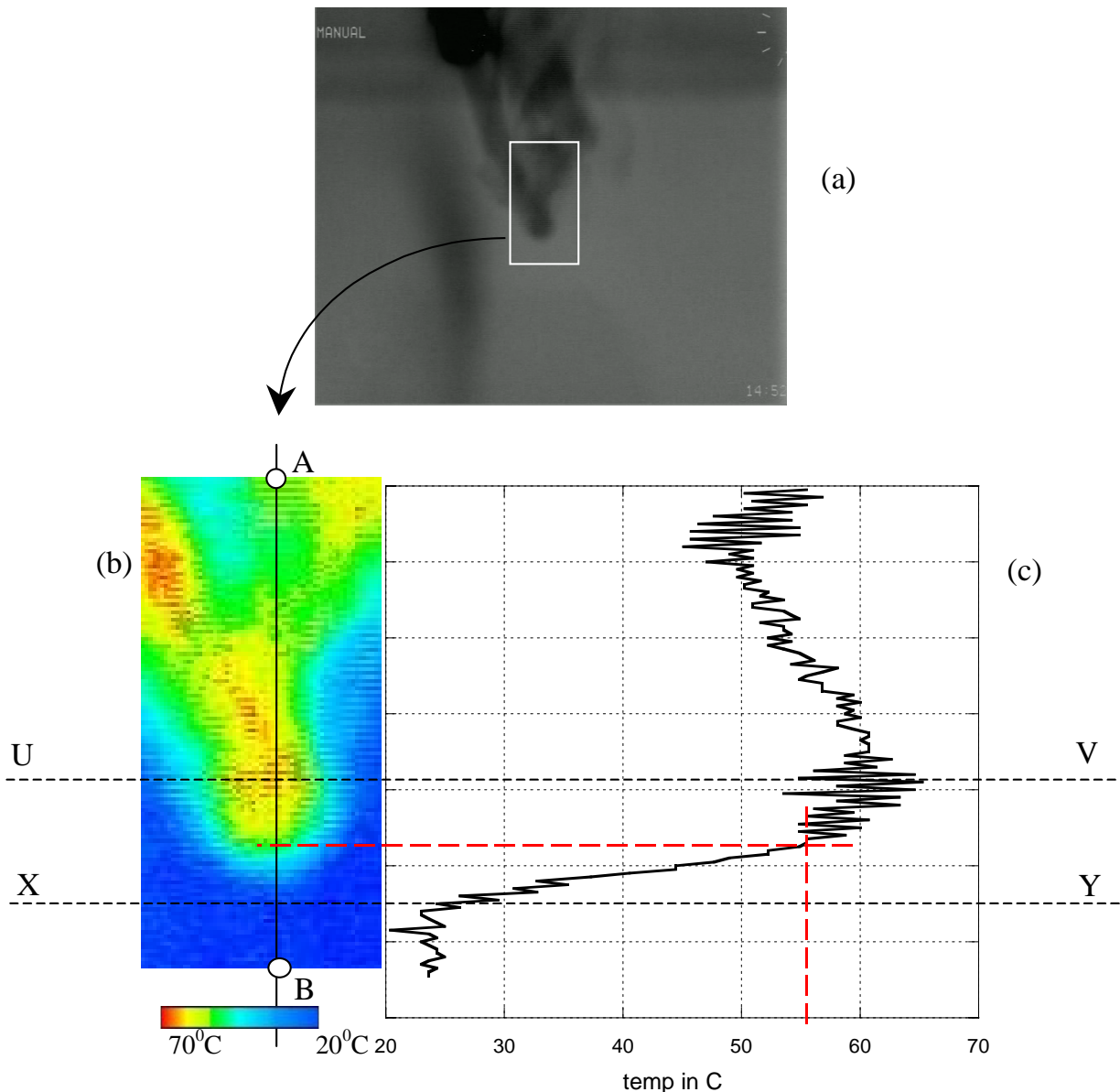


Fig. 5. Thermal image of TAP of the stream of CSD and the vertical temperature distribution of the middle of TAP area. (a) Thermal image of downward projected CSD taken from the Cryogenically cooled third generation forward looking infrared (FLIR) thermal camera ($3\text{-}5\mu\text{m}$). (b) Temperature distribution at the droplet turning around area. Color gradient is proportional to the temperature as shown in the plate below (c) Temperature distribution along the line AB in (b).

Fig. 6. In the meantime floating droplets around the mouth of the container were observed. The thermal images reveal that the temperature distribution in the bottom of the container lies between 50°-60°C. It is noted that the temperature at the lowermost point of the TAP is between 55-60°C in Ex. 1.

The forces acting on the water droplet at the TAP where its velocity become zero in a undisturbed surrounding can be written as

$$F_u = F_b + F_l \geq F_d = m_s g \quad (3)$$

where F_u is the total upward force, F_d is the total downward force, m_s is the mass of the condensed-steam droplet and g is the gravitational acceleration. It is shown that the ratio of densities of water to air at TAP in Ex.1 is approximately 825. i.e. $m_s g$ is approximately 825 times higher than F_b . However, there is no apparent rise of temperature (hence, the convection current) just below the turning point of condensed-steam droplets. In the absence of the known forces, that cause the rising of CSD, arises possibility of whether there is unknown force acting on the droplet.

Downward heat evaporated iodine in a vacuum chamber has also shown similar upward movement against the direction of gravitational attraction (Piyadasa, 2011) in the absence of buoyancy and convection lift. In that experiment, it is observed that iodine was in

independent/isolated cluster state (liquid and/or gaseous state) with a certain amount of latent heat. A similar situation is seen with the condensed-steam droplets which contains molecular cluster (as droplet) with certain amount of latent energy (as hidden internal energy). Within the temperature range of 50° – 60°C at mouth of inverted container in Ex.2, some upward and some downward moving CSDs having diameter under 20μm were observed. Above approximately 55°C at TAP almost all the droplets moved upward as in Ex. 1. As seen in figure 6 droplet may experience net upward force F_u and net downward force F_d depending on its temperature and its weight. With the increase of time, CSD cools by radiation and also increased by weight by condensation of surrounding water vapor.

To the present knowledge, the upward force F_u is only due to buoyancy and lift caused by the convection of surrounding air. Both these mechanisms do not explain the situation where upward movement of CSD as shown elsewhere Piyadasa (2011). Downward force F_d is due to the weight of the droplet and could be due to increase of condensation with time and thereby increase of the weight of the droplets. Simultaneously radiation/convection loss of heat reduces its internal energy which is mainly stored as latent heat. In all three experiments, evaporated Iodine and condensed steam droplets, the common feature was the latent heat. Therefore a plausible explanation could lie in the temperature differences of the CSDs.

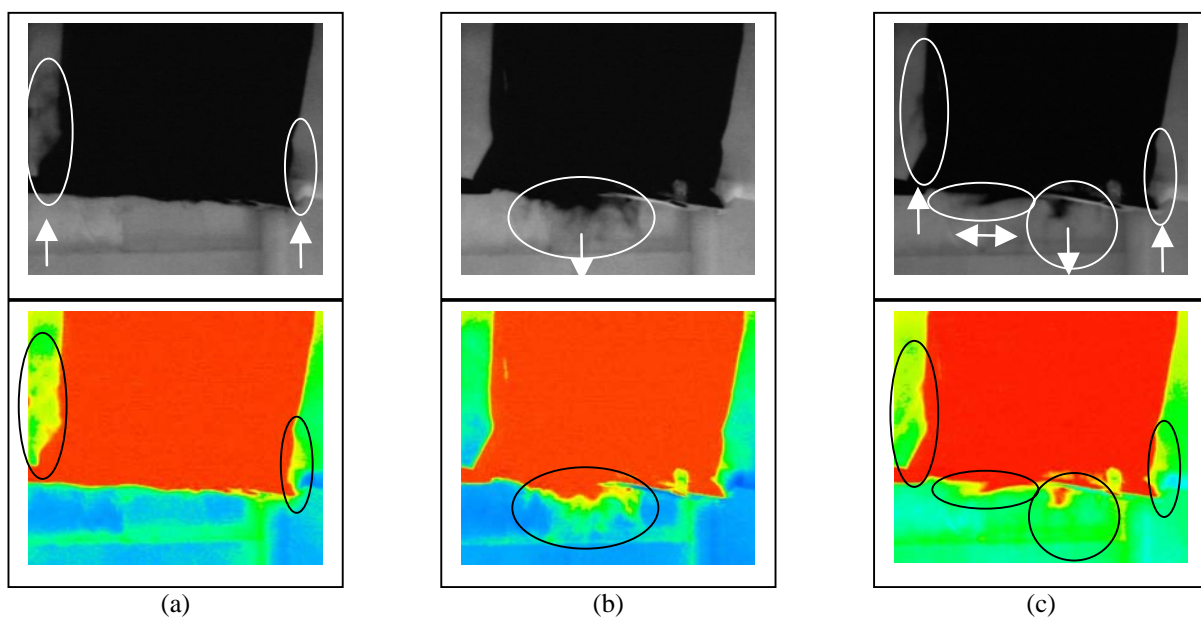


Fig. 6. Thermal images of condensed-steam filled vertically inverted container. Upper - B/W. and Lower - Color gradient is proportional to the temperature as shown in the plate in Fig. 5 (a) water droplets move upwards (b) water droplets move downwards (c) some of the water droplets move upwards while others move downward. Some droplets randomly float below the open bottom of the inverted container.

CONCLUSIONS

Now that the buoyancy force and convection force are untenable due to the density and temperature profile in the media respectively, thus we have to speculate the driving force behind the upward movement of condensed-steam droplets against gravity in the atmosphere. It seems that the latent heat/internal energy of the CSD may be related to the upward force. With buoyancy and convection ruled out as the cause of the upward mobility in the particles observed, strongly suggests an unknown force, it could be Antigravity: perhaps, an avenue for further research.

ACKNOWLEDGMENTS

The Author gratefully acknowledges financial support by the National Science Foundation in Sri Lanka (Grant No. NSF/Scientist/2007/01 and Department of Physics, University of Colombo for providing me equipment and laboratory facilities to conduct this research work. Special thanks go to H. Piyadasa and GS Palathiratne for their critical reading of the manuscript.

REFERENCES

- Cinar, G. and Yilbas, BS. 1998. Experimental Study into Droplet Formation in Steam Flows. *Applied Scientific Research*. 59:1-9.
- Fan, X., Jia, Z., Zhang, J. and Cai, X. 2009. A Video Probe Measurement System for Coarse Water Droplets in LP Steam Turbine. The 6th International Symposium on Measurement Techniques for Multiphase Flows. *Journal of Physics. Conference Series*. 147 – 012065.
- Flandern, TV. 1996. Possible new properties of gravity, *Astrophys. & Space Sci.* 244:249-261 (1996)
- Hawking, SW. and Israel, W. 1996. Three Hundred Years of Gravitation. Eds. Penrose, R. *et al.*, Cambridge Univ. Press. 34-127.
- Kumar, M. 1973. Arctic Fog Droplet Size Distribution and Its Effect on Light Attenuation. *Journal of Atmospheric Sciences*. 30(4):635-643.
- Lenham, AP. and Clay, MR. 1982. Drop-size distribution of fog droplets determined from transmission measurements in the 0.53-10.1- μ m wavelength range. *Drop-size distribution of fog droplets determined from transmission measurements in the 0.53-10.1- μ m wavelength range. Applied Optics*. 21(23):4191.
- Maxwell, JC. 1865. A Dynamical Theory of the Electromagnetic Field. Royal Society Transactions. Vol. CLV:459.
- Newton, I. 1687. Mathematical Principles of Natural Philosophy (part II, revised by Davis, W. 1803). Knight & Compton. London. pp177.
- Petr, V. and Kolovratník, M. 2000. Modelling of the droplet size distribution in a low-pressure steam turbine. *Proc Instn Mech Engrs.* 214 Part A.
- Piyadasa, CKG. 2011. Antigravity - Is it already under our nose? *Canadian Journal of Pure and Applied Sciences*. 5(2):1585-1588.
- Tatsuno, K. and Nagao, S. 2000. Water Droplet Size Measurements in an Experimental Steam Turbine Using an Optical Fiber DropletSizer. *J. Heat Transfer*. 108(4):939.
- www.tiptheplanet.com/wiki/Water, 2011

Received: Nov 25, 2011; Accepted: Feb 21, 2012

ANALYSIS OF THE EFFECTS OF THE SAMPLE INCLINATION ON RESULTS OF VICKERS HARDNESS TESTING

*Gouda Mohamed¹, Magdi Ibrahim¹, Ali Abu Ezz¹, Mahmoud Adly² and Ali Khatab²

¹National Institute for Standards (NIS) of Egypt, El Haram, PO Box 136 Giza

²Cairo University, Faculty of Engineering, Design and Production Department, Giza, Egypt

ABSTRACT

The objective of this paper is to analyse the influence of the specimen inclination on Vickers hardness measurements. A primary Vickers hardness testing machine (PVHM), and hardness reference test blocks with different hardness levels are used. A different values of inclination angles for the tested specimens are obtained through a calibrated test rig. Theoretical and experimental analyses were conducted to evaluate the hardness tested samples tilting effects. The tests results were validated by analysis of variance (ANOVA). The results show that there is significant effect due to specimen inclination where the surface area of contact was found to be higher for tilted indentation and hence underestimates of hardness. Inclination is partially depending on the hardness level where the effects of inclination angle are reduced at higher levels of hardness values. Empirical formula was obtained to correlate between inclination angle and Vickers hardness error.

Keywords: Vickers hardness, tilting effects, indenter inclination.

INTRODUCTION

The Vickers test is the standard method for measuring the hardness of metals, particularly those with extremely hard surfaces: the surface is subjected to a standard pressure for a standard length of time by means of a pyramid-shaped diamond with a vertex angle of 136°.

The diagonal of the resulting indentation is measured under a microscope. The full load is normally applied for 10 to 15 seconds (ISO, 2005). The Vickers hardness is the quotient obtained by dividing the kgf load by the square mm area of indentation. Only a few micron differences in diagonal length could cause significant error in HV scale. There are several factors that may affect the Vickers results. In order to improve the accuracy of material characterization, it is required to consider all the affecting parameters in calculations. Some of the various factors that should be taken into account in Vickers are purely geometrical, such as surface roughness, indenter geometry, and tip rounding. The influence of surface roughness has been reported in several papers (EA, 2005). The geometry of indenter and the tip rounding have also been found to be important in Vickers tests.

There is another geometrical source of error that seems to have been neglected. The assumption that the axis of the indenter is perpendicular to the surface being indented is important when either the sample surface is tilted or the indenter axis is tilted with respect to the indentation.

The aim of the submitted work was to study the effect of sample surface tilting on the results of sample testing with diamond Vickers indenter is addressed from a geometrical point of view. Sample inclination is one of the parameter which effects on the error percentage of HV values, and it doesn't subject to sufficient study to detect how it can affect the measured hardness values. The results of the experiments were analyzed and evaluated by one factor analysis of variance (ANOVA).

MATERIALS AND METHODS

Equipment and CRMs

A primary Vickers hardness standard machine (PVHM) was used to perform the experiments. PVHM was provided by a calibrated test rig which was utilized as a sample base for the variation of inclination angles under investigation. Olympus stereo microscope was used to measure the indentation diagonals (Fig.1).

Certified reference materials (CRM) in the form of hardness test blocks were used as a standard for investigation.

Geometrical analysis for the contact between a pyramidal indenter and tilted sample surface.

The ideal four-sided pyramid diamond Vickers indenter is a perfect square base pyramid with an angle θ (Satoshi *et al.*, 2006) (typically 68.00°) between the central axis and each face. This model also assumes that all four faces

*Corresponding author email: goudamohamed15@yahoo.com



Fig.1. Stere microscope and PVHM.

meet at a singular point (that is, the line of conjunction length is zero).

Area function for pyramidal indentation into untitled samples

Ideally, in Vickers the real contact depth is h_c , the real contact projection area is as follows (Fig. 2).

$$HV = \frac{F}{A_s} = \frac{2F \cdot \sin\left(\frac{\alpha}{2}\right)}{d^2} \quad (1)$$

Where A_s is the contact area when the displacement equals h_c (Fig 1)

$$A_s = 24.5h_c^2 \quad (2)$$

$$d = 2\sqrt{2} \cdot a \cdot \sin\left(\frac{\alpha}{2}\right) \quad (3)$$

$$d = 2\sqrt{2} \cdot \frac{h}{\cos(\theta)} \cdot \sin\left(\frac{\alpha}{2}\right) = 2\sqrt{2} \cdot h_c \cdot \tan\left(\frac{\alpha}{2}\right) \quad (5)$$

$$\begin{aligned} A_{real} &= \frac{1}{2} \left(2\sqrt{2} \times h \times \tan\left(\frac{\alpha}{2}\right) \right)^2 \\ &= 4 \cdot h_c^2 \times \tan^2\left(\frac{\alpha}{2}\right) = 4 \times \left(\frac{d}{7}\right)^2 \times \tan^2\left(\frac{\alpha}{2}\right) \quad (6) \end{aligned}$$

Area function for pyramidal indentation into titled samples

When the axis of the indenter is loading on the surface of the sample un-vertically, the real contact projection area can't be calculated by Eq. (6). Since the axis may be inclined in the different orientations, it'll induce the calculation of the area to be very complicated. Therefore, the calculation method of the real contact projection area A_s is introduced only for the angle ζ between the actual axis in the axial middle section of the opposite sides at the bottom of the Vickers indenter and the ideal axis of the indenter assuming The rotation angle specifies the direction of the tilt with respect to one of the edges of the pyramid is zero, as shown in figure 3.

When the indented depth is h_c , the real contact projection area can be calculated as follow.

$$\begin{aligned} A_1 &= \frac{(a_1 + b_1) + (a_2 + b_2)}{2} \\ a_1 &= \frac{h_c \tan\left(\frac{\alpha}{2}\right)}{\left[\left(1 - \tan(\theta) \times \tan\left(\frac{\alpha}{2}\right) \right) \cos\left(\frac{\alpha}{2}\right) \right]} \\ b_1 &= \frac{h_c \tan\left(\frac{\alpha}{2}\right)}{\left[\left(1 + \tan(\theta) \times \tan\left(\frac{\alpha}{2}\right) \right) \cos\left(\frac{\alpha}{2}\right) \right]} \end{aligned}$$

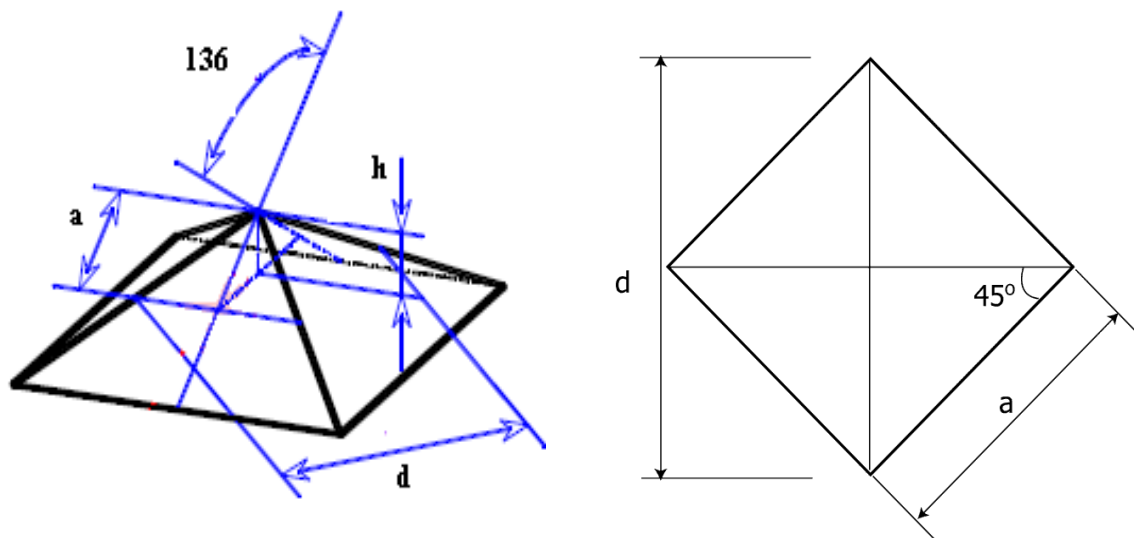


Fig. 2. Geometrical parameters of Vickers indenter and untitled contact area.

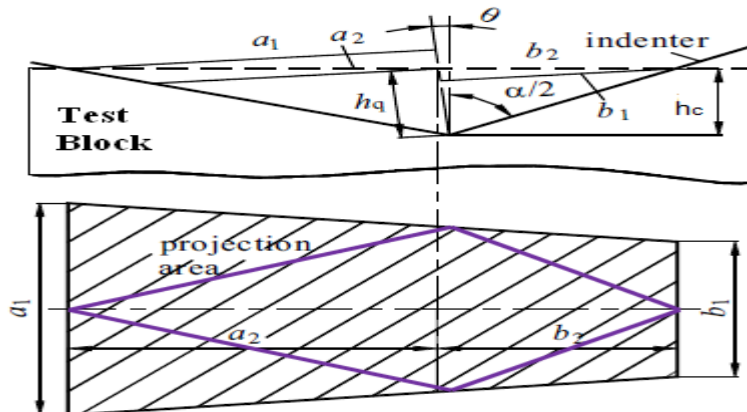


Fig. 3. Schematic of contact between indenter and tilted sample.

$$a_2 = \frac{h_c \tan\left(\frac{\alpha}{2}\right)}{\left[\left(1 - \tan(\theta) \times \tan\left(\frac{\alpha}{2}\right) \right) \times \cos^2\left(\frac{\alpha}{2}\right) \right]} \quad (10)$$

$$b_2 = \frac{h_c \tan\left(\frac{\alpha}{2}\right)}{\left[\left(1 + \tan(\theta) \times \tan\frac{\alpha}{2} \right) \times \cos^2\left(\frac{\alpha}{2}\right) \right]} \quad (11)$$

$$A_\theta = \frac{24.5 \times h_c^2}{1 - 3 \tan^2(\theta) \tan^2\left(\frac{\alpha}{2}\right) - 2 \tan^3(\theta) \tan^3\left(\frac{\alpha}{2}\right)} \quad (12)$$

$$A_\theta = \frac{0.5 \times d^2}{1 - 3 \tan^2(\theta) \tan^2\left(\frac{\alpha}{2}\right) - 2 \tan^3(\theta) \tan^3\left(\frac{\alpha}{2}\right)} \quad (13)$$

Theoretical calculation for contact area and hardness for tilted and untitled

For ideal case of indentation without samples tilt, the surface area of the pyramidal indenter would be a four sided figure with equal sides.

Ideal surface area can be calculated by eq. No 1 or 2 at angle of inclination 0° and the inclined surface area can be calculated by eq. No 13 after measurement of the indentation diagonals produced from testing assuming the angle of inclination from 0.2° up to 1.5° .

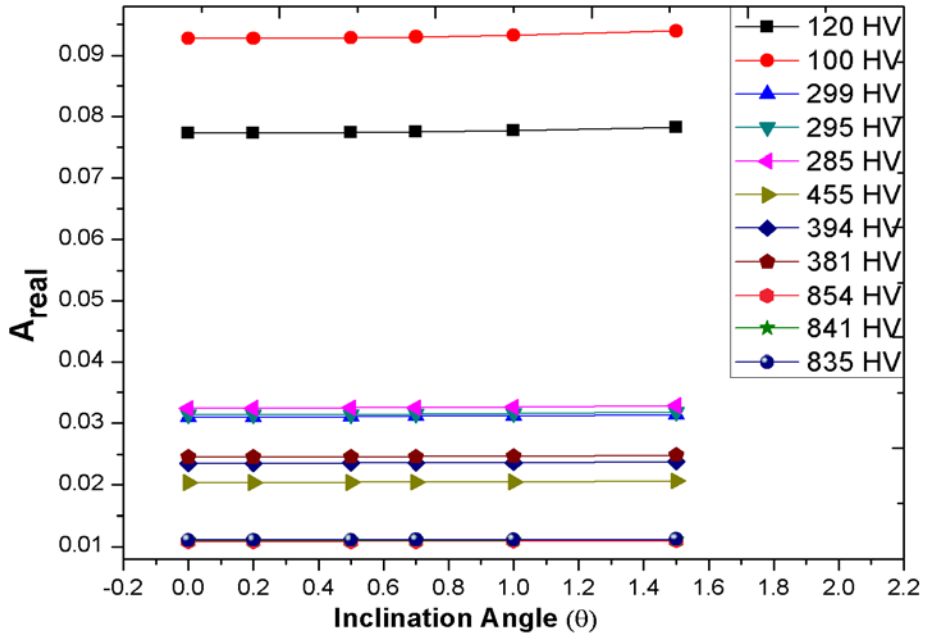


Fig. 4. Theoretical calculated mean area of contact at various hardness levels.

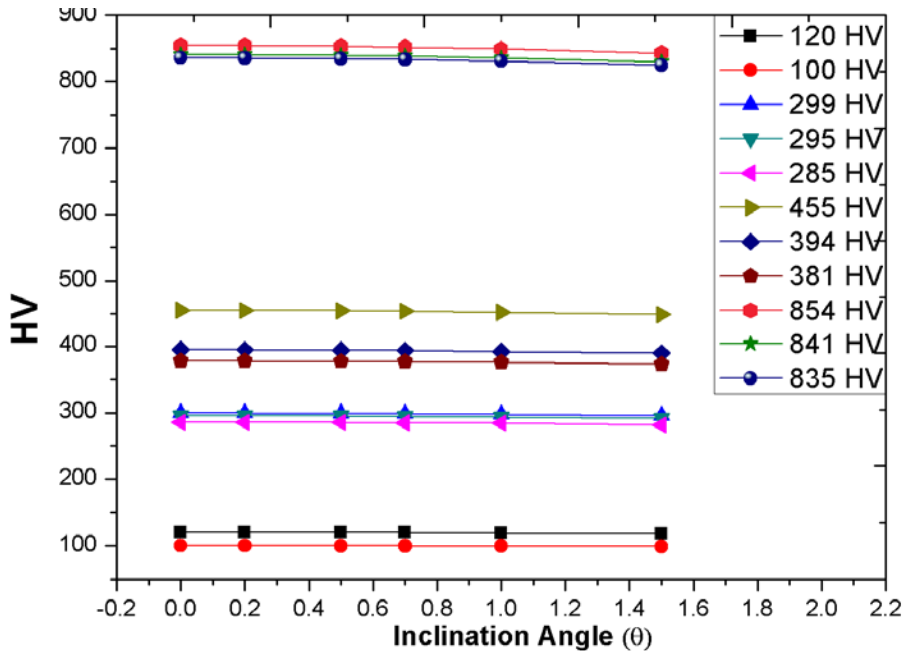


Fig. 5. Theoretical calculated hardness at various hardness levels.

It was noted that the contact area is significantly affected by the inclination angle where increasing the inclination of the surface under test tends to overestimates of contact area and hence under estimates of hardness as shown from the following figures. Figures 4 and 5 shows the theoretical inclination effects on the contact area and hardness.

Experimental procedure

PVHM which has been evaluated through comparison with Physikalisch-Technische Bundesanstalt (PTB) primary Vickers hardness testing machine (Menalo *et al.*, 2010; Mohammed *et al.*, 2010). A calibrated inclination test rig is used to imply the various angles. Variation of the angle will be done by micromere which is inserted in

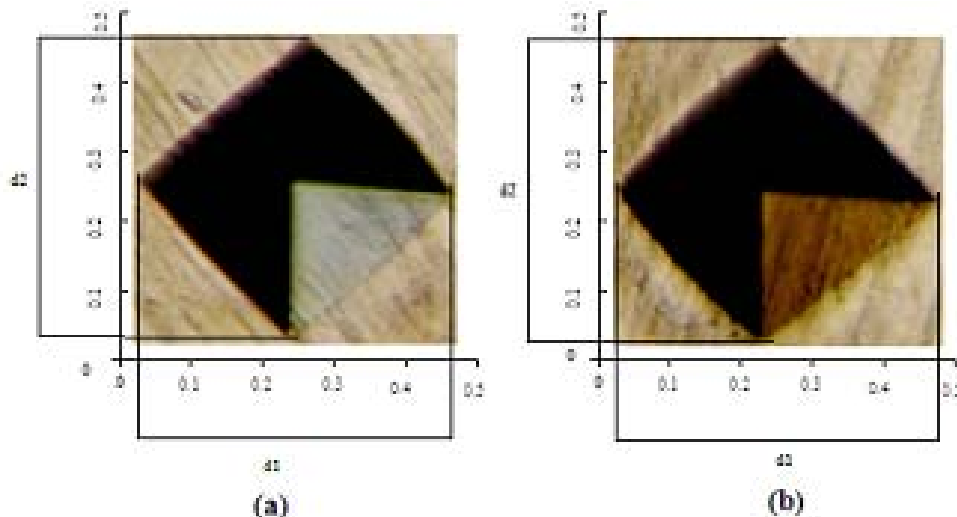


Fig. 6. Scanned impression of indentations for (a) the untitled sample and (b) the one degree tilted.

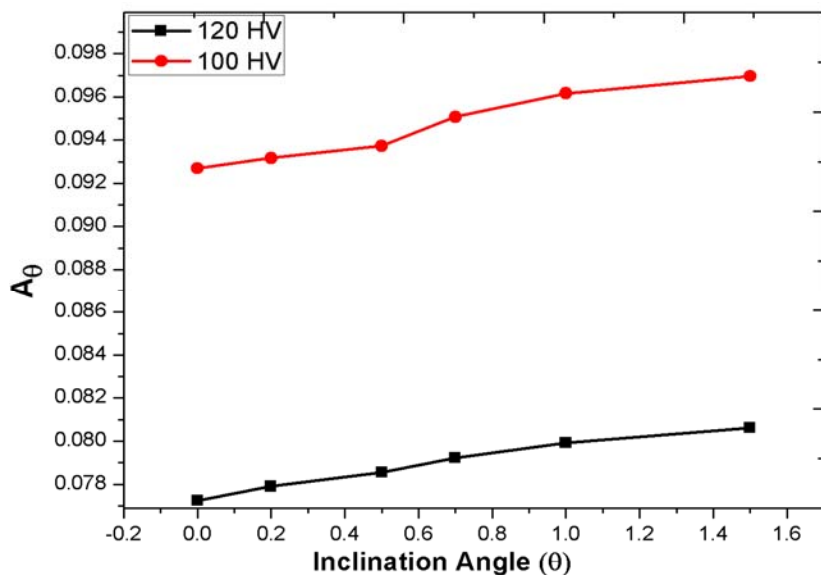


Fig. 7. Experimental surface area at hardness level (120,100) HV.

the test rig. The selected angles which were been investigated are 0.2° , 0.7° , 0.5° , 1° and 1.5° . The experiments started by measuring the hardness of standard blocks at 0° of inclination, the hardness results at this state will be used as reference to calculate the error for other measurements at varying inclination angle using test rig.

After area function calibration, the same test specimen was mounted on different degree angle values (0.2 , 0.5 , 0.7 , 1 , and 1.5) and five indentations were made. The scanned impressions of indentations with nominal diagonals are shown in Fig 6 for both untitled and on

degree tilted samples. It can be seen that the indentations on tilted sample are not a right square anymore, and which have slightly higher projected area.

RESULTS AND DISCUSSION

From the experiments the surface area of contact was found to be higher for tilted indentation (see Figs. 7 to 10) and hence underestimates of hardness (see Figs. 11 to 14). The test results analysis shows that the effects of inclination is partially depending on the hardness level and the effects of inclination angle is reduced at higher level of hardness values.

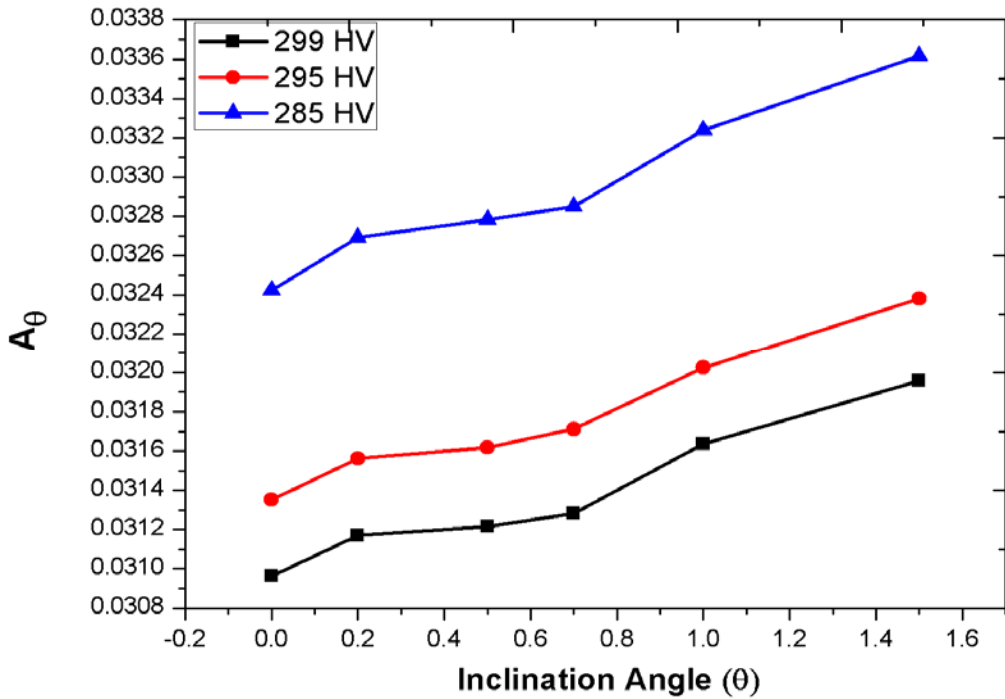


Fig. 8. Experimental surface area at hardness level (299, 295, 285) HV.

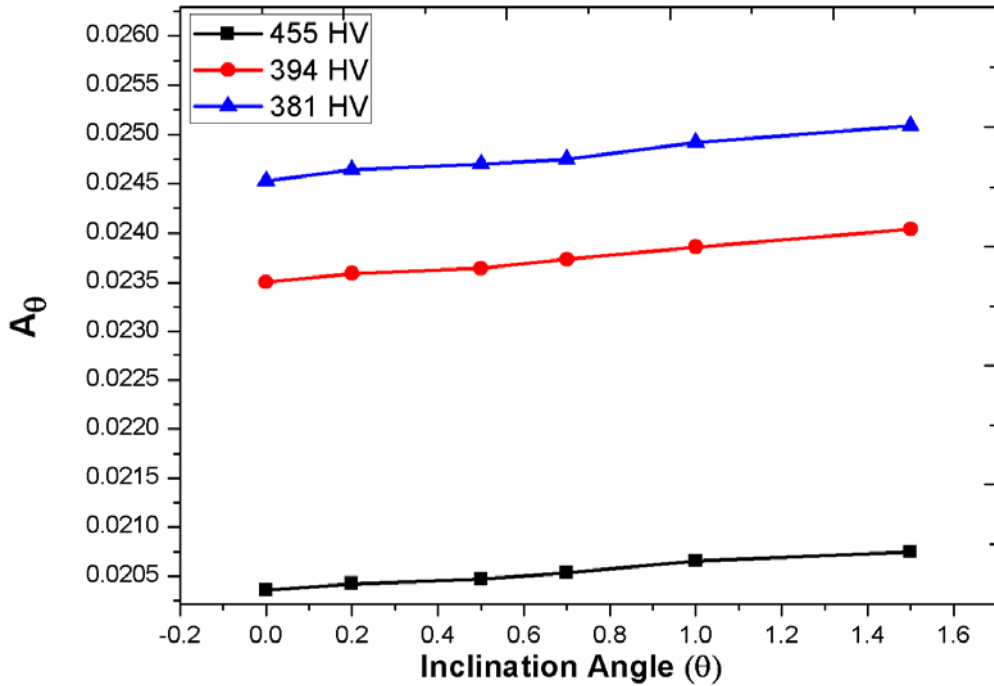


Fig. 9. Experimental surface area at hardness level (455, 394, 381).

The figures shows that the effects of inclination can be significantly increased at low hardness levels, for tilting angle 1° at hardness level 100HV, 120HV the hardness results will be reduced by more than 3.5%, for hardness level 285HV, 295HV and 299HV the hardness results will

be reduced by more than 2%, for hardness level 835HV, 841,854HV the effects of inclination can be significantly reduced where the error doesn't exceed 1%. For tilting angle 1.5° at hardness level 100HV, 120HV the hardness results will be reduced by more than 4%, for hardness

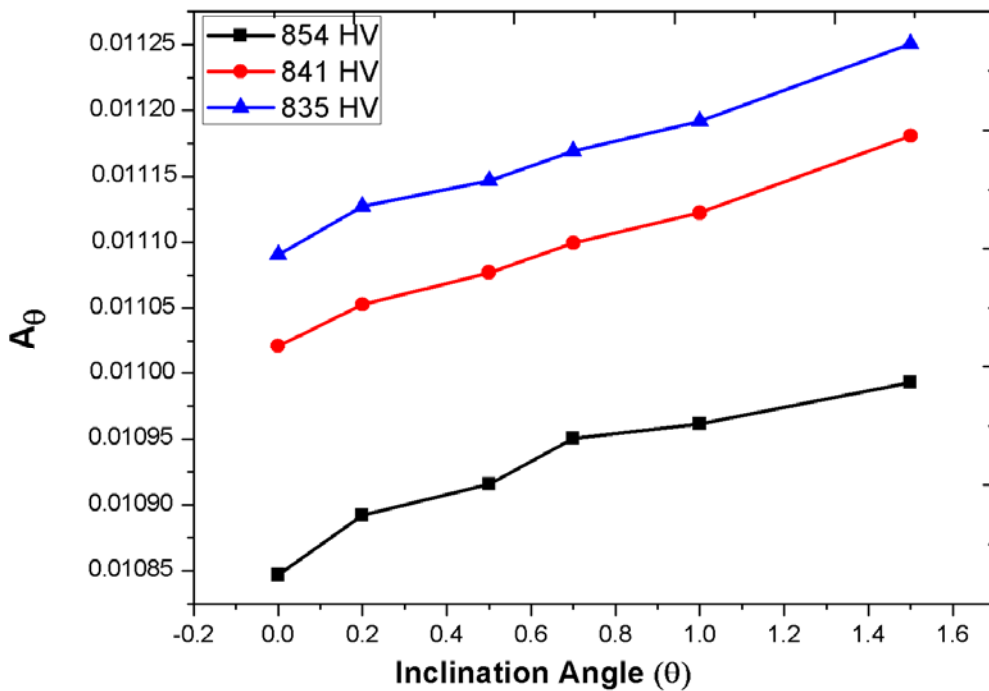


Fig. 10. Experimental surface area at hardness level (854, 841, 835) HV.

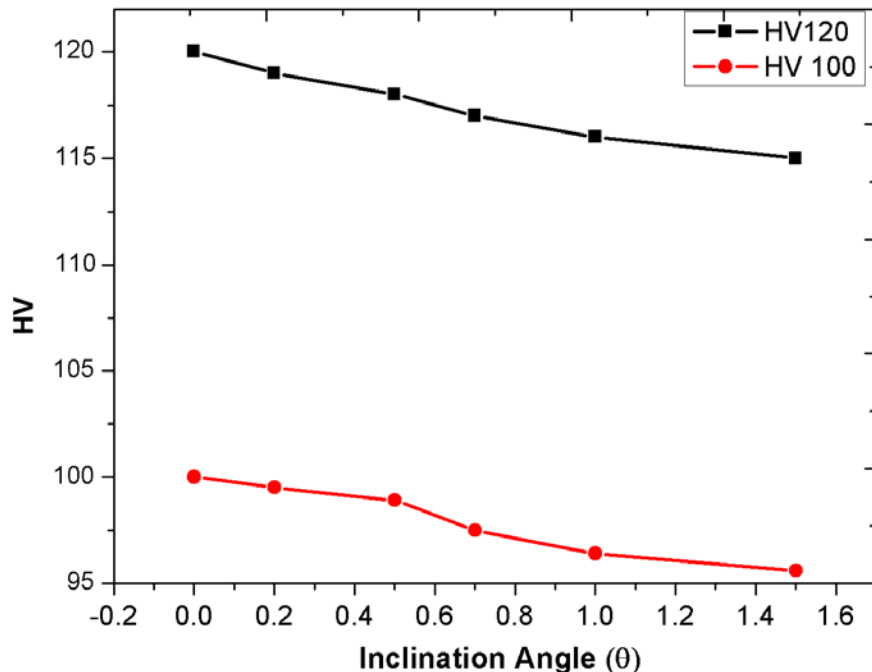


Fig. 11. Experimental hardness at hardness level (120, 100) HV.

level 285HV, 295HV and 299HV the hardness results will be reduced by 3%, for hardness level 835HV, 841, 854HV the effects of inclination can be significantly reduced where the error doesn't exceed 1.2% (see Figs. 7 to 14).

STATISTICAL ANALYSIS

In this work all empirical model was developed using the values obtained from experimental investigation for hardness testing of metallic materials. The empirical

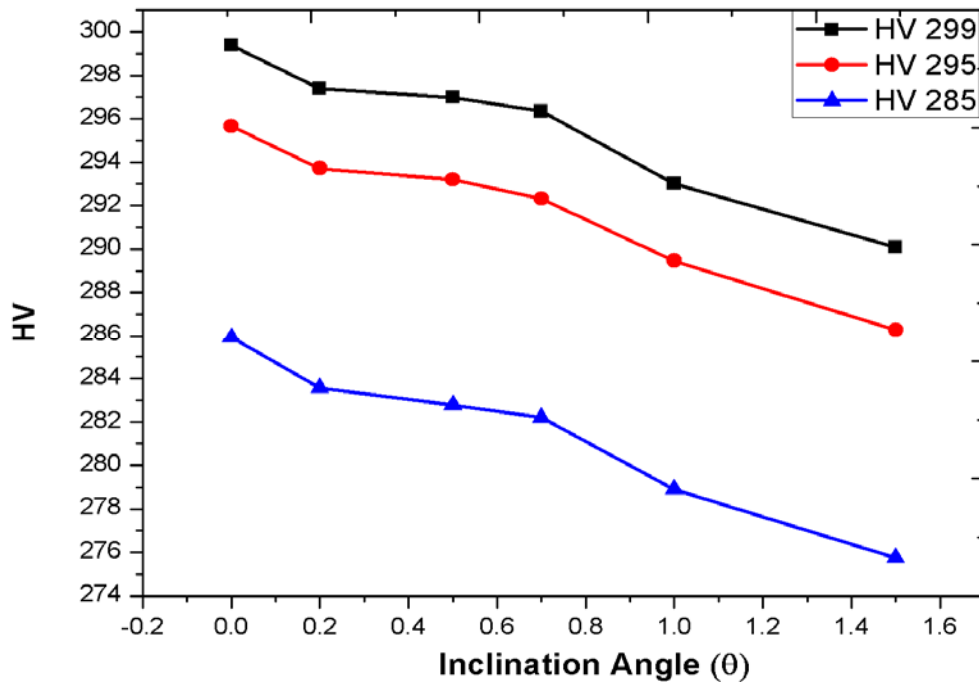


Fig. 12. Experimental hardness at hardness level (299, 295, 285) HV.

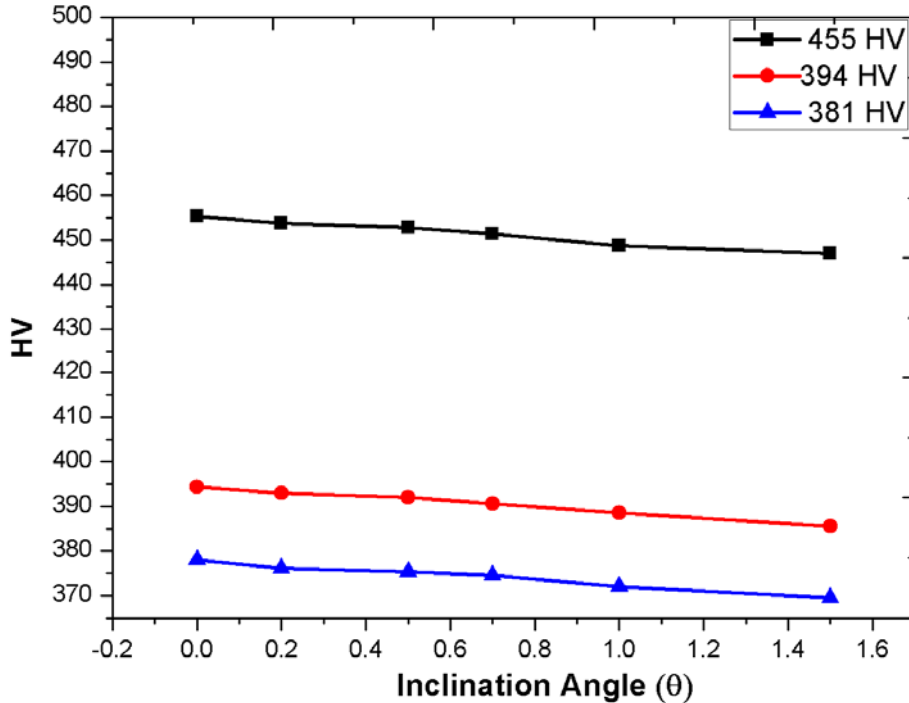


Fig. 13. Experimental hardness at hardness level (455, 394, 381) HV.

model was used to predict the effects of sample tilting on the hardness testing results. OriginPro8 statistical analysis software was used in the present case to establish an empirical correlation between sample under test titling and the produced error of measurements expressing the

outputs in the linear form as shown in Equation 15. Curve fitting and ANOVA statistical methods is utilized for the purpose of results analysis. From experiments it was noted that there are significant dependence of hardness level on the produced tilting error.

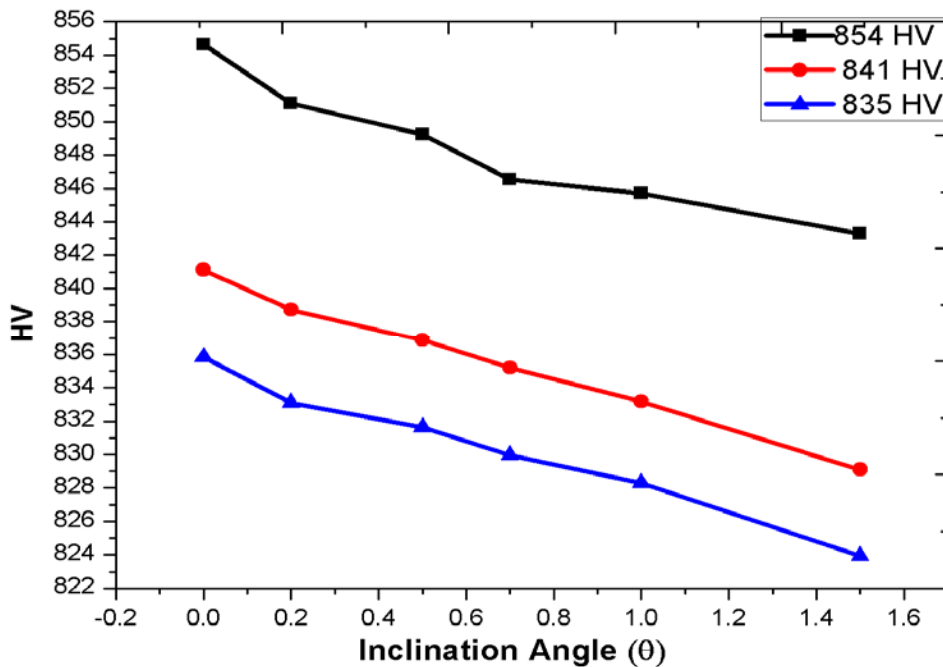


Fig. 14. Experimental hardness at hardness level (854, 841, 835) HV.

Empirical model can be formulated as follow,

$$HV_{\text{error}\%} = F(HV, \theta) \quad (14)$$

From statistics the empirical equation was as follow,

$$HV_{\text{error}\%} = -2.89169 \times \text{Angle} + 0.00259 \times HV \times \text{Angle} \quad (15)$$

Accuracy and validity of model

The model was validated by comparing the predicted values with experimental values. The predicted values were found to compare favorably with experimental values the mean percentage error Determined using Equation 15 were found to be ranging from (0.01 to 0.4) % in hardness .The empirical model developed is reasonably accurate to predict the influence on sample tilting on the measured hardness value.

Theoretical and experimental investigation for the amount of error due to surface tilt for the Vickers hardness indenter can be observed that Vickers hardness testing indenter is sensitive to this source of error. There are slightly differences between the test results produced from theoretical and experimental investigations this difference due to the partial effects of material hardness levels. The effects of inclination can be significantly increased at low hardness levels where it can reduced the hardness test result up to 3.5 %, but at the very high hardness levels the reduction in hardness values doesn't exceed 1%, this effect due to the great effect of sliding resistance for the inclined indenter at higher levels of hardness.

CONCLUSION

Theoretical and experimental study for the effect of surface tilt on results of Vickers hardness tests is conducted. The true projected and surface area for indenter and indented zone based on the exact three dimensional geometry of the contact zone between the indenter and test sample is calculated. Geometrically there is significantly affect due to surface inclination of the sample under test a correction factor can be included. It is found from the experiments the surface area of contact was found to be higher for tilted indentation and hence underestimates of hardness. The test results analysis show that the effects of inclination is partially depending on the hardness level and the effects of inclination angle is reduced at higher level of hardness values. The empirical model developed is reasonably accurate to estimate the mean effect of sample inclination of the results of hardness testing. The model performance was found to be satisfactory and show good predictability. It is hoped that this produced empirical model for computing predicted inclination effect will be useful and serve as guide for correcting the unvertical Vickers hardness testing results.

ACKNOWLEDGEMENTS

This work was supported by National Institute for Standard of Egypt (NIS) the authors would like to express special thanks to Dr Konrad Herrmann and Mr Febo Menelao from Physikalisch-Technische Bundesanstalt

(PTB) for their availability to evaluate NIS Primary Vickers hardness testing machine.

REFERENCES

- ISO 6507-1. 2005. Metallic Materials-Vickers Hardness Test-Part 1: Test method.
- EA-10/16. 2005. Guidelines on the Estimation of Uncertainty in Hardness Measurements, European Cooperation.
- Satoshi, T., Kazuyuki, K., Takashi, U., Haruo, K. and Kazutomi, H. 2006. Wide-range Verification of the Geometry of Vickers Diamond Indenters. XVIII IMEKO World Congress Metrology for a Sustainable Development September. Rio de Janeiro, Brazil.
- Menalo, F., Mohamed, G., Mohamed, MI., Abuelezz, AA., Adly, M. and Khatab, AA. 2010. Development of Primary Vickers Hardness Testing Machine. IMEKO 2010 TC3, TC5 and TC22 Conferences Metrology in Modern Context, Pattaya, Chonburi, Thailand.
- Mohamed, G., Ibrahim, M., Abuelezz, AE and M. Adly, A. Khatab. 2010. Metrological Characterization of a Primary Vickers Hardness Standard Machine - NIS Egypt. MAPAN- Journal of Metrology Society of India. 25(2):89-95.

Received: March 14, 2012; Accepted: April 23, 2012

BREAKTHROUGH CURVE STUDIES FOR THE REMOVAL OF HEAVY METALS IN A FIXED BED COLUMN

*J T Nwabanne and P K Igbokwe

Department of Chemical Engineering, Nnamdi Azikiwe University, PMB 5025, Awka, Nigeria

ABSTRACT

Breakthrough curve studies for the removal of heavy metals using activated carbon derived from palmyra palm nut (PPN) was carried out in a fixed bed column. The effects of important parameters such as inlet ion concentration, flow rate and bed height on the breakthrough curve were studied. Breakthrough time increased with increase in bed height, inlet ion concentration and flow rates. Increasing the flow rate gave rise to a shorter time for saturation. Breakthrough was achieved in lesser time for Cu^{2+} adsorption than Pb^{2+} adsorption. As flow rate increased from 5 to 10ml/min breakthrough was achieved between 1200 to 1500 min for Pb^{2+} adsorption while breakthrough was reached between 220 and 350 min for adsorption of Cu^{2+} . The experimental breakthrough data correlated well with the breakthrough profile calculated by Yoon and Nelson method for activated carbon. Palmyra palm nut was found to be an efficient adsorbent for the removal of lead (11) and Copper (11) in a continuous mode using fixed bed column.

Keywords: Fixed bed column, palmyra palm nut, breakthrough curve, heavy metals, activated carbon.

INTRODUCTION

Many industries in Nigeria discharge their wastewater into surface waters (Oceans, seas, rivers and stream) without any form of remediation or treatment. Equally, the wastewaters are not properly treated before they are disposed off. An estimated 90 percent of all wastewater in developing countries is discharged untreated directly into rivers, lakes or the oceans (UNEP, 2010). These heavy metals are not biodegradable and their presence in water leads to bioaccumulation in living organisms causing health problems in animals, plants, and human beings (Ong *et al.*, 2007). Lead is a pollutant that is present in drinking water and in air. Lead is known to cause mental retardations, reduces haemoglobin production necessary for oxygen transport and it interferes with normal cellular metabolism (Qaiser *et al.*, 2007). Lead has damaging effects on body nervous system. It reduces IQ Level in children. Copper is metal that has a wide range of applications due to its good properties. It is used in electronics, for production of wires, sheets, tubes, and also to form alloys (Antonijevic and Petrovic, 2008). Since copper is a widely used material, there are many actual or potential sources of copper pollution. Copper is essential to life and health but, like all heavy metals, is potentially toxic as well. For example, continued inhalation of copper-containing spray is linked with an increase in lung cancer among exposed workers.

Industrial effluents contain enormous quantities of inorganic and organic chemical wastes, which are steadily becoming more complex and difficult to treat by

conventional technologies. Adsorption onto activated carbon has been found to be superior to other techniques of wastewater treatment because of its capability for adsorbing a broad range of different types of adsorbates efficiently, and its simplicity of design (Ahmad *et al.*, 2006). The major characteristic of the dynamic behaviour of fixed-bed adsorption is the history of effluent concentration (Tien, 1994). These concentration-time curves are commonly referred to as the breakthrough curves, and the time at which the effluent concentration reaches the threshold value is called the breakthrough time. The design of adsorption systems is normally based on accurate predictions of breakthrough curves for specific conditions.

Many theoretical or empirical equations have been proposed for modeling the breakthrough curves in a fixed bed adsorption. Yoon and Nelson model was used to analyze the column performance for the removal of lead (11) and copper (11) using PPN. This model is based on the assumption that the rate of decrease in the probability of adsorption for each adsorbate molecule is proportional to the probability of adsorbate adsorption and the probability of adsorbate breakthrough on the adsorbent (Kavak and Öztürk, 2004). Yoon and Nelson model is less complicated than other models and it requires no detailed data concerning the characteristics of the physical properties of the adsorption bed.

The Yoon and Nelson equation regarding to a single component system is expressed as (Kavak and Öztürk, 2004).

*Corresponding author email: joe_nwabanne@yahoo.com

$$\frac{C_e}{C_o} = \frac{1}{1 + \exp[K(\tau - t)]} \quad (1)$$

Where k is the rate constant (l/min), τ the time required for 50% adsorbate breakthrough (min) and t is the breakthrough (sampling) time (min). The linearized form of the Yoon and Nelson model is as follows:

$$\ln \frac{C_e}{C_o - C_e} = k t - \tau k \quad (2)$$

This is aimed at applying a simple model proposed by Yoon and Nelson for modeling the breakthrough curves of lead (11) and Copper (11) in a fixed bed packed with activated carbon. The effects of parameters such as initial ion concentration, flow rate and bed height on the breakthrough curves were investigated.

MATERIALS AND METHODS

Preparation of activated carbon

Palmyra palm nuts were obtained from the premises of Nnamdi Azikiwe University, Awka, Nigeria. The palm nuts were thoroughly washed with deionized water, dried in the sun, ground into fine particles and sieved to a particle size of 300µm. 200g of sample was impregnated with concentrated orthophosphoric acid at the acid/precursor ratio of 2:2 (on weight basis). The impregnated sample was dried in an oven at 120°C for 24hrs. The dried sample was carbonized in a Muffle furnace for 2hours at 500°C. After cooling to the ambient temperature, the sample was washed with de-ionized water several times until pH 6-7, filtered with Whatman No.1 filter paper and then dried in the oven at 110°C for 8hours. The sample was crushed and passed through different sieve sizes and then stored in a tight bottle ready for use.

Characterization of activated carbon

The pH of the carbon was determined using standard test of ASTM D 3838-80 (ASTM, 1996). Moisture content of activated carbon and raw materials was determined using ASTM D 2867-91 (1991).The bulk density of the activated carbon was determined according to the tamping procedure by Ahmedna *et al.* (1997). The volatile content was determined by weighing 1.0g of sample and placing it in a partially closed crucible of known weight. It was then heated in a muffle furnace at 900°C for 10mins.The percentage fixed carbon was determined as 100 – (Moisture content + ash content + volatile matter). The iodine number was determined based on ASTM D 4607-86 (1986) by using the sodium thiosulphate volumetric method The specific surface area of the activated carbon was estimated using Sear's method (Al-Qadah and Shawabkah, 2009; Alzaydien, 2009) by agitating 1.5g of the activated carbon samples in 100ml of diluted hydrochloric acid at a pH = 3. Then a 30g of sodium chloride was added while stirring the suspension and then the volume was made up to 150ml with deionized water. The solution was titrated with 0.1N NaOH to raise the pH from 4 to 9 and the volume, V recorded. The surface area according to this method was calculated as $S = 32V - 25$. Where, S = surface area of the activated carbon, V = volume of sodium hydroxide required to raise the pH of the sample from 4 to 9.

Breakthrough studies

Experimental procedure

Breakthrough studies were carried out using a glass column of 30mm internal diameter and 300mm length. The activated carbon having 0.425mm to 0.600mm particle size range was used. The activated carbon was packed in the column with a layer of glass wool at the bottom as shown in figure 1. Three different bed heights

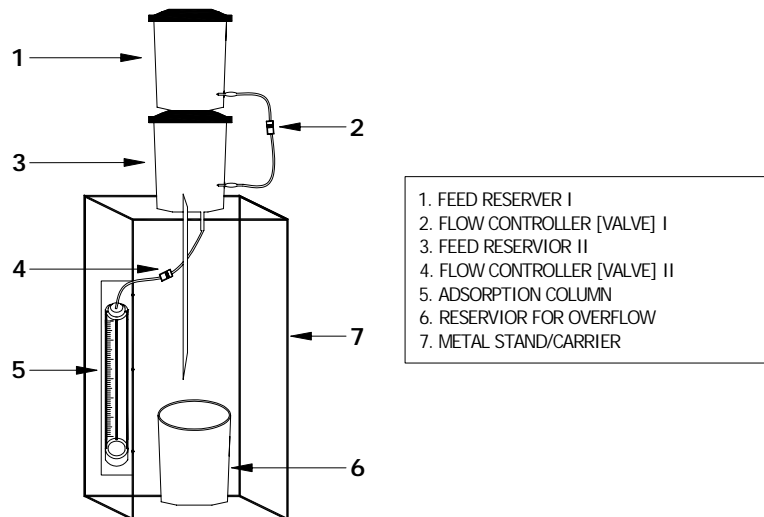


Fig.1. Schematic diagram of the mini adsorption column.

(50mm, 100mm and 150mm) were used. The tank containing the heavy metal solution was placed at a higher elevation so that the metal solution could be introduced into the column by gravitational flow. The first tank delivers the solution to the second tank at a constant flow rate. The second tank is equipped with a pipe to help maintain a constant solution level in the tank in order to avoid fluctuation of the flow rate of the solution being delivered to the column. The second flow controller helps to regulate the flow rate. Three flow rates (5, 7.5 and 10ml/min) and three inlet ion concentrations of 50, 100 and 150mg/l were used. The effluent samples were collected at specified intervals and analyzed for the residual Pb²⁺ and Cu²⁺ concentrations using atomic adsorption spectrophotometer at 217nm and 324.8nm respectively. Column studies were terminated when the column reached exhaustion.

RESULTS AND DISCUSSION

Characteristics of activated carbon derived from nipa palm nut

Table 1. Physico-chemical characteristics of activated carbon derived from palmyra palm nut.

Properties	Values
pH	6.8
Bulk density, g/cm ³	0.61
Iodine number, mg/g	785.78
Moisture content, %	4.10
Volatile matter, %	18.14
Ash content, %	3.40
Fixed carbon, %	78.56
Surface Area, m ² /g	820.37

Breakthrough Studies

Calculation of breakthrough curve is helpful in the design of packed bed (Reinik *et al.*, 2001; Kavak and Öztürk, 2004).

Effect of flow rate on breakthrough curves

The effect of flow rate for the adsorption of Pb²⁺ and Cu²⁺ onto activated carbon derived from palmyra palm nut was studied at flow rates of 5, 7.5 and 10ml/min, inlet ion concentration of 100mg/l and bed height of 100mm as shown in Figures 2 and 3. From figures 2 and 3, it is seen that rapid uptake of metal ion is noticed in the initial stages and rate decreased thereafter and finally reached saturation. This is in agreement with the result obtained by Sivakumar and Palamisamy (2009). When the volumetric flow rate decreased from 10 to 5ml/min more favourable ion exchange conditions were achieved (Kananpanah *et al.*, 2009). As flow rate increased, the breakthrough curves become steeper and reached the breakthrough quickly. This is because of the residence

time of the adsorbate in the column, which is long enough for adsorption equilibrium to be reached at high flow rate. This means that the contact time between the adsorbate and the adsorbent is minimized, leading to early breakthrough (Sivakumar and Palanissamy, 2009). Increasing the flow rate gave rise to a shorter time for saturation. Breakthrough was achieved between 1200 to 1500 min for Pb²⁺ adsorption while breakthrough was reached between 220 and 350 min for adsorption of Cu²⁺. This implies that PPN is a better adsorbent for the adsorption of Pb²⁺.

Effect of bed height on breakthrough curves

Breakthrough curves for the adsorption of Pb²⁺ and Cu²⁺ onto PPN at various bed heights, at the inlet concentration of 100mg/l and flow rate of 5ml/min are shown in figures 4 and 5. The results indicate that the throughput volume of the aqueous solution increased with increase in bed height, due to the availability of more number of sorption sites (Sivakumar and Palanisamy, 2009). The equilibrium sorption capacity decreased with increase in bed height. This shows that at smaller bed height the effluent adsorbate concentration ratio increased more rapidly than for a higher bed height. Furthermore, the bed is saturated in less time for smaller bed heights. Small bed height corresponds to less amount of adsorbent.

3.2.2. Effect of initial ion concentration on breakthrough curves

The effect of inlet ion concentration on the breakthrough curves at bed height of 100mm and flow rate of 5ml/min is shown in Figure 6 and 7. It is observed that as the initial ion concentration increased from 50 to 150mg/l, the break point time decreased. On increasing the initial ion concentration, the breakthrough curves became steeper and breakthrough volume decreased because of the lower mass-transfer flux from the bulk solution to the particle surface due to the weaker driving force (Sivakumar and Palanisamy, 2009; Baek *et al.*, 2007). At higher concentration the availability of the metal molecules for the adsorption sites is more, which leads to higher uptake of Pb²⁺ at higher concentration even though the breakthrough time is shorter than the breakthrough time of lower concentrations.

Modelling the behaviour of Pb²⁺ and Cu²⁺ in a fixed bed adsorption column

Evaluation of the adsorption performance of an adsorbent requires the mathematical model for the simulation of adsorption processes in order to predict the adsorption behaviour (Xiang *et al.*, 2008). Yoon and Nelson model was chosen to fit the experimental data. The experimental breakthrough curves obtained at flow rate of 5ml/min, inlet ion concentration of 100mg/l and bed height of 100mm are presented in figures 8 and 9. The theoretical curves calculated from the proposed model are also shown in figures 8 and 9. It can be seen that the

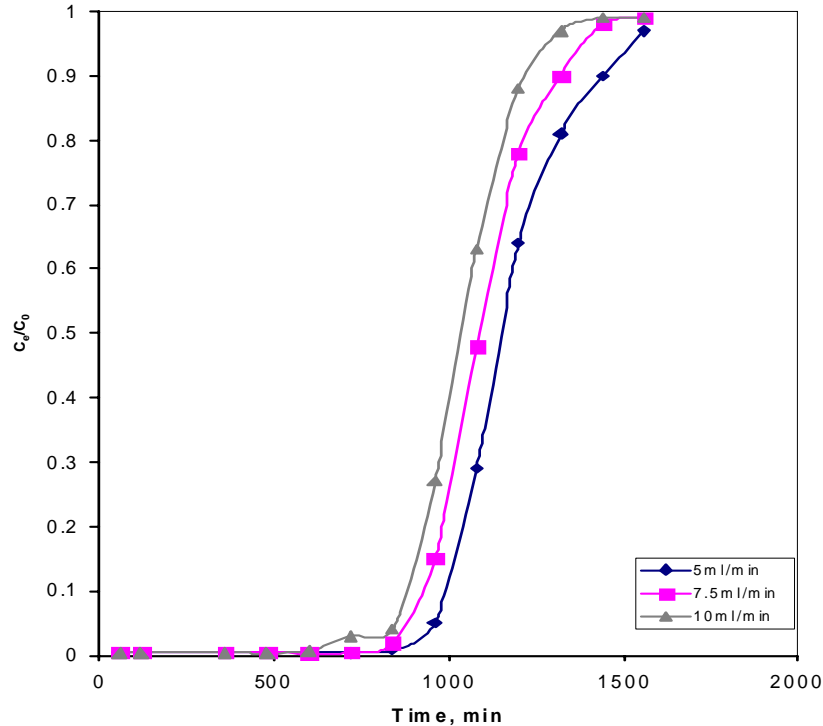


Fig. 2. Effect of flow rate on breakthrough curve for Pb^{2+} adsorption on PPN.

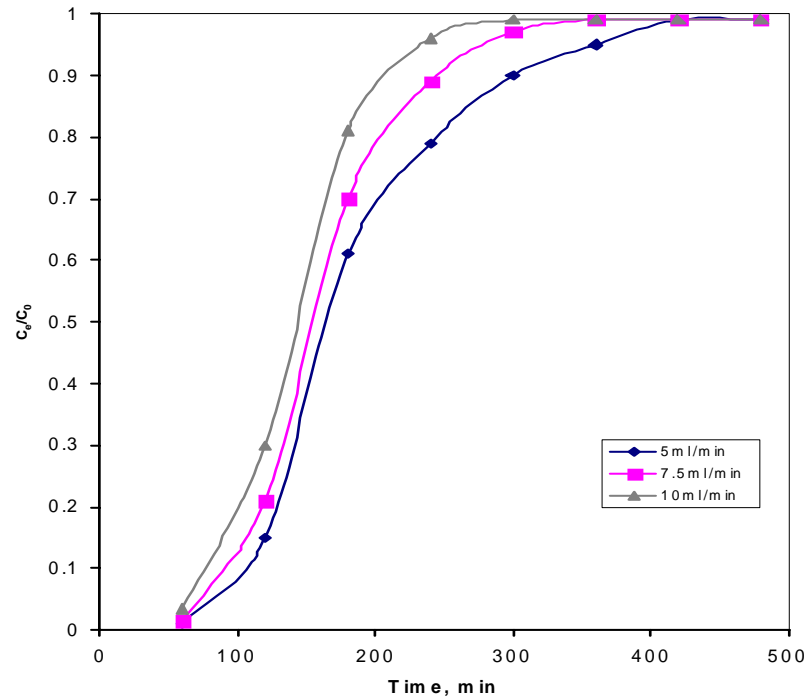


Fig. 3. Effect of flow rate on breakthrough curve for Cu^{2+} adsorption on PPN.

theoretical curves are in good agreement with those of the experimental ones. This means that the slopes of the breakthrough curves that were produced approximate

closely to the experimental breakthrough curves. This is in agreement with the results obtained by Kavak and Öztürk (2004) and Sivakumar and Palanisamy (2009).

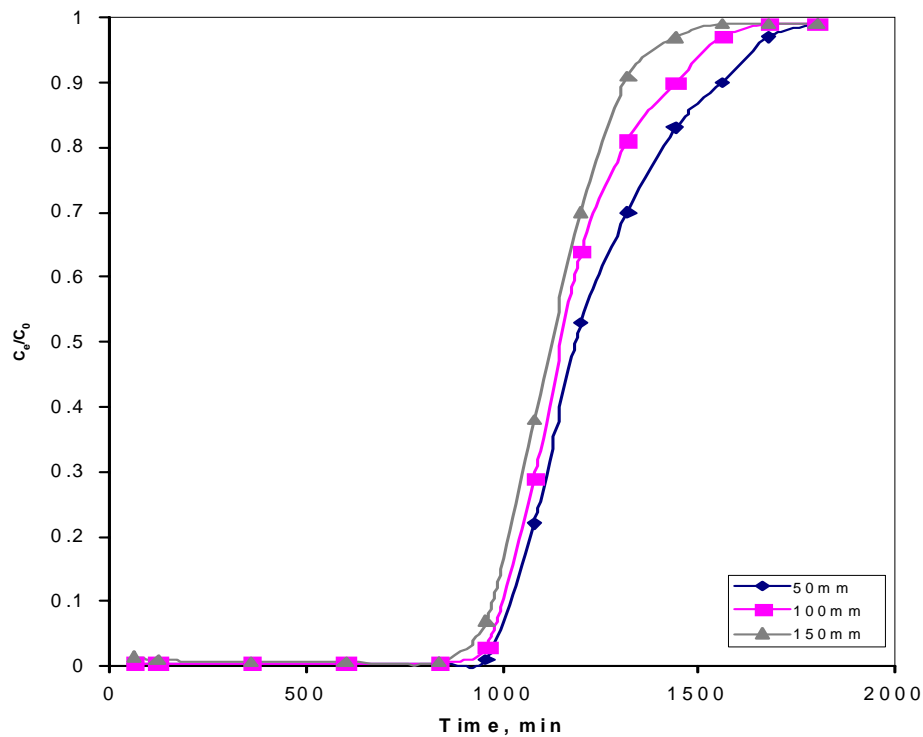


Fig. 4. Effect of bed height on breakthrough curve for Pb^{2+} adsorption on PPN.

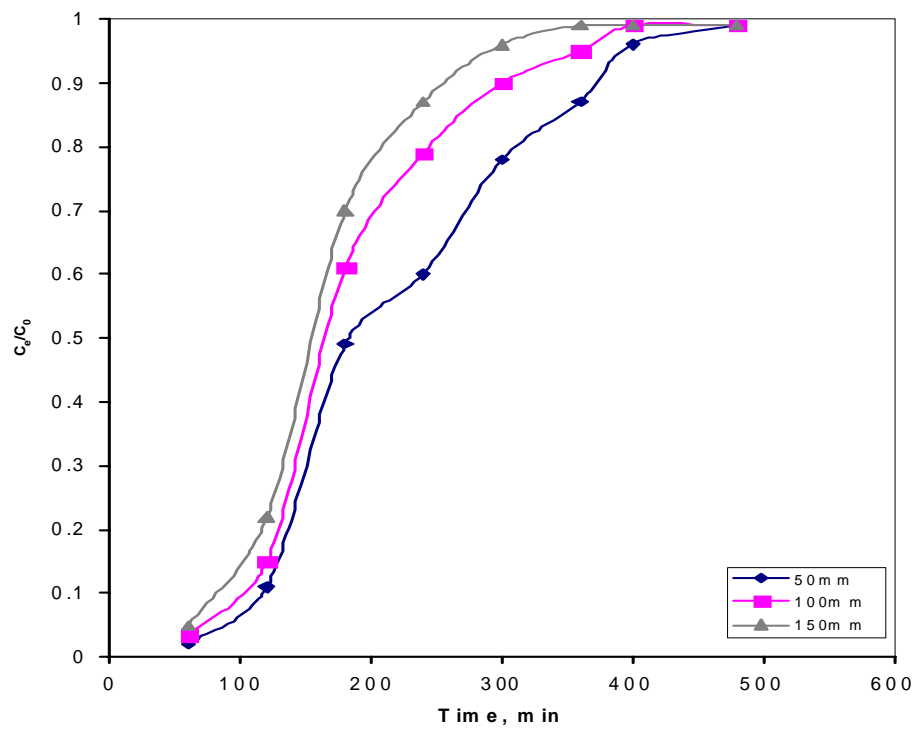


Fig. 5. Effect of bed height on breakthrough curve for Cu^{2+} adsorption on PPN.

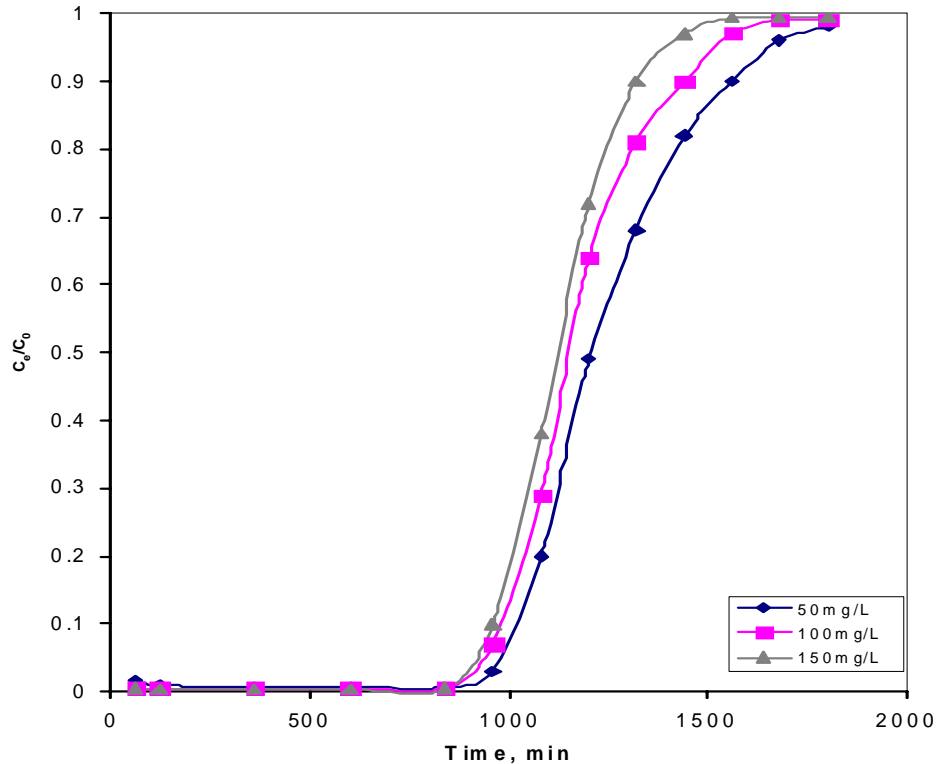


Fig. 6. Effect of initial ion concentration on breakthrough curve for Pb^{2+} adsorption on PPN.

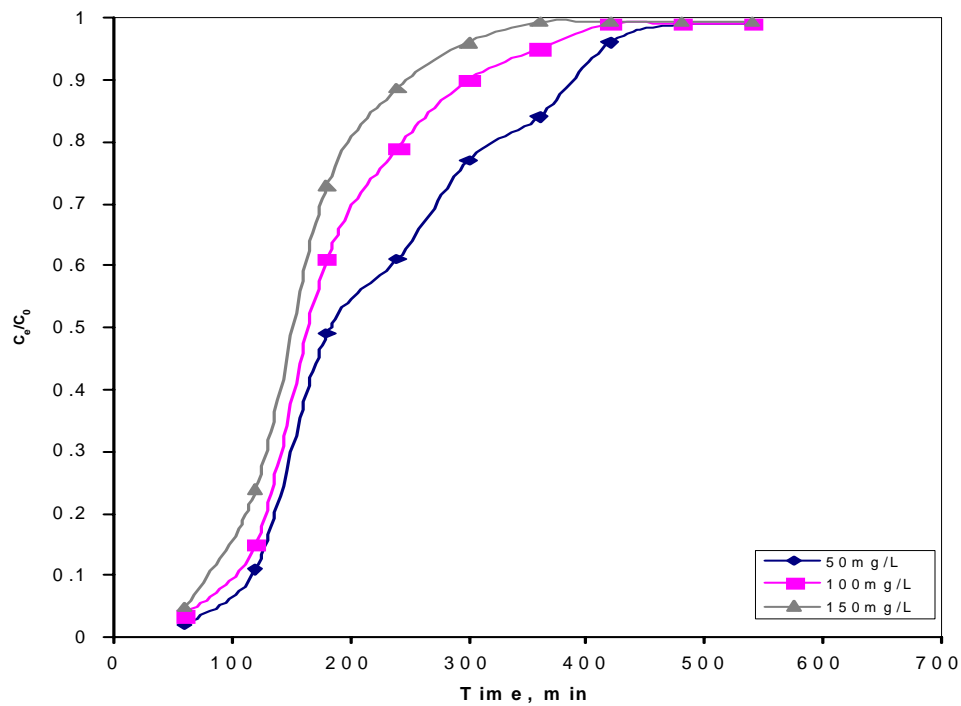


Fig. 7. Effect of initial ion concentration on breakthrough curve for Cu^{2+} adsorption on PPN.

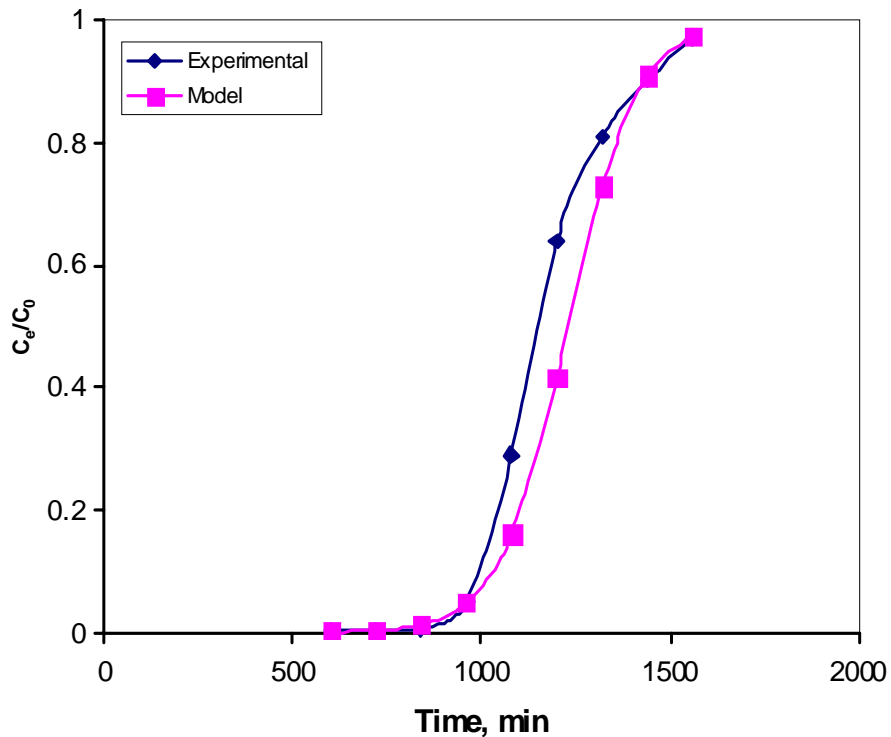


Fig. 8. Comparison of experimental and predicted curves for the adsorption of Pb^{2+} on PPN.

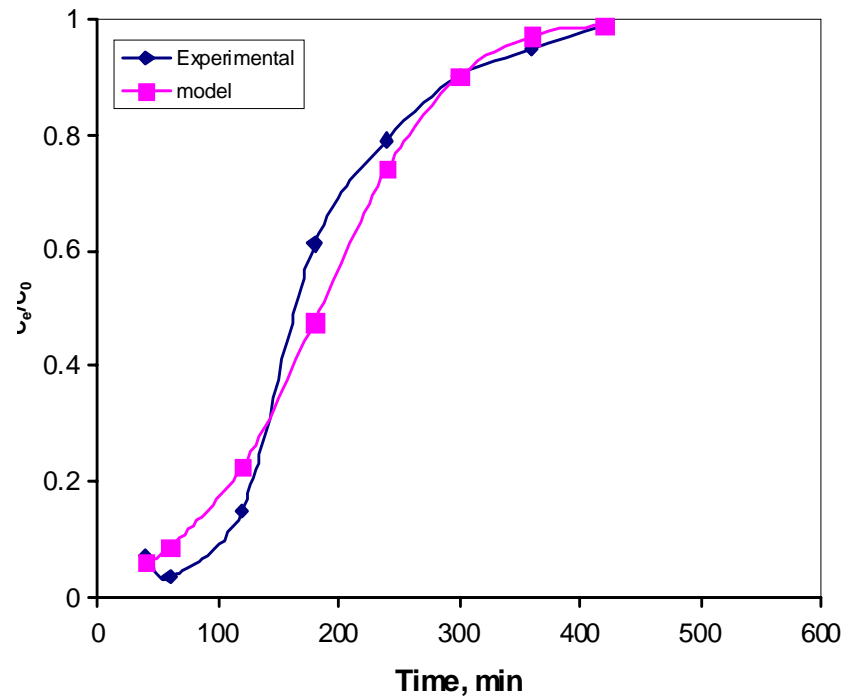


Fig. 9. Comparison of experimental and predicted curves for the adsorption of Cu^{2+} on PPN.

CONCLUSION

Breakthrough studies for the adsorption of Pb^{2+} and Cu^{2+} onto the activated carbon derived from palmyra palm nut at different flow rates of 5, 7.5 and 10 ml/min, an inlet ion concentration of 100 mg/l and bed height of 100 mm in a fixed bed column has been carried out. The effects of inlet ion concentration, flow rate and bed height on the breakthrough curves showed that breakthrough time increased with increase in the inlet ion concentration and bed height and decreased with increasing flow rate. The calculated theoretical breakthrough curves from Yoon and Nelson model was in agreement with the experimental breakthrough profiles.

REFERENCES

- Ahmad, AA., Hameed, BH. and Aziz, N. 2006. Adsorption of Direct dye on palm ash: Kinetic and Equilibrium Modeling. *Journal of Hazardous Materials*. 094:1-10.
- Ahmedna, M., Johns, MM., Clarke, SJ., Marshall, WE. and Rao, RM. 1997. Potential of Agricultural by-product-Based Activated Carbons for use in Raw sugar Decolourisation. *Journal of the Science of Food and Agriculture*. 75:117-124.
- Aksu, Z. and Tezer, S. 2000. Equilibrium and Kinetic Modelling of Bisorption of Remazol black B by Rhizopus arrhizus in a batch system: Effect of temperature. *Process Biochemistry*. 36:431-439.
- Al-Qodah, Z. and Shawabkah, R. 2009. Production and Characterization of Granular activated carbon from activated Sludge. *Braz. J. Chem. Eng.* 26(1):6.
- Alzaydian, AS. 2009. Adsorption of Methylene blue from Aqueous solution onto a low – cost Natural Jordanian Tripoli. *Am. J. Applied Sci.* 6(6):1047-1058.
- American Society for Testing and Materials. 1996. Annual Book of ASTM Standard, Volume 15.01, Refractories, Carbon and Graphic Products; activated Carbon, ASTM, Philadelphia, PA, USA.
- American Society for Testing and Materials. 1986. Standard Test Method for Determination of Iodine number of Activated Carbon. ASTM Committee on Standards. Philadelphia, PA, USA.
- American Society of Testing and Materials. 1991. Standard Test Methods for Moisture in Activated Carbon. ASTM Committee on Standards. Philadelphia, PA, USA.
- Antonijevic, MM. and Petrovic, MB. 2008. Copper Corrosion Inhibitors: A Review. *Int. J. of Electrochemical Science*. 3:1-28.
- Baek, K., Song, S., Kang, S., Rhee, Y., Lee, C., Lee, B., Hudson, S. and Hwang, T. 2007. Adsorption Kinetics of Boron by Anion Exchange Resin in Packed column bed. *J. Ind. Eng. Chem.* 13(3):452-456.
- Kananpanah, S., Ayazi, M. and Abolghasemi, H. 2009. Breakthrough Curve Studies of Purolite A-400 in an Adsorption Column. *Petroleum and Coal*. 51(3):189-192.
- Kavak, D. and Öztürk, N. 2004. Adsorption of Boron from Aqueous Solution by Sepiolite: II. Column studies. *II. Illuslararasi. Bor. Sempozumu*. 23-25:495-500.
- Ong, S., Seng, C. and Lim, P. 2007. Kinetics of Adsorption of Cu (II) and Cd (II) from Aqueous Solution on Husk and Modified Rice Husk. *EJEAFche*. 6 (2):1764-1774.
- Qaiser, S., Saleem, AR. and Ahmed, MM. 2007. Heavy Metal uptake by Agro based Waste Materials. *Environmental Biotechnol*. 10(3):1-8.
- Reinik, J., Viiroja, A. and Kallas, J. 2001. Xyldine – Polluted Groundwater Purification: Adsorption Experiments and Breakthrough Calculations. *Proc. Estonian Acad. Sci. Chem.* 50(4):205-216.
- Sivakumar, P. and Palanisamy, PN. 2009. Adsorption Studies of Basic Red 29 by a Non-Conventional Activated Carbon Prepared from Euphorbia antiquorum L. *International Journal of Chem. Tec. Research*. 1 (3):502-510.
- Tien, C. 1994. Adsorption Calculations and Modelling. (1st ed.), Butterworth-Heinemann Publishers, USA. pp1-8.
- UNEP 2010. Sick Water? The Central Role of Wastewater Management in Sustainable Development, Inhabitant. pp1-75.
- Xiang, LI., Zhong, LI. and Ling'ai, L. 2008. Adsorption Kinetics of Dibenzofuran in Activated Carbon packed bed. *Chin. J. Chem. Eng.* 16(2):203-208.

Received: Feb 10, 2012; Accepted: April 17, 2012

RADIATION ABSORBED DOSE RATES IN THE DEAD SEA REGION, JORDAN

*Sherin A Saraireh¹, Abdul-Wali Ajlouni², Mashhoor Al-Wardat^{1,3} and Hatim Al-Amairyen¹

¹Department of Physics, Al-Hussein Bin Talal University, PO Box. 20, Ma'an, 71111 Jordan

²Ministry of Energy and Mineral Resources, Amman, Jordan

³Physics Department, Yarmouk University, PO Box. 566 Irbid, 21163 Jordan

ABSTRACT

The present study introduces measurements of natural radiation doses due to gamma radio-nuclides in the Dead Sea, Jordan. This exploration implemented in the famous natural curative resource in Jordan, the Dead Sea. Our measurements show that this region has a proper level of external radiation due to gamma radionuclides, it lies within the normal levels of worldwide. The average registered gamma absorbed dose rates along the Dead Sea region is 75 nSvh⁻¹. The range is between 16 to 260 nSvh⁻¹.

Keyword: Dead Sea, radiation, radiation hormoses, gamma radionuclides, black mud, radon.

INTRODUCTION

Assessment of natural doses from natural sources is generally the largest contribution to the collective dose equivalent in the population. The principle sources of natural radiation are cosmic rays, terrestrial, internal radiation and radon gas (UNSCEAR, 2006). Cosmic rays are source of radiation that originates from outer space; the sun and stars. The primary cosmic rays that are incident on the earth's atmosphere are mainly protons, alpha particles, gamma rays, X-rays, electrons and a small number of heavier nuclei. Carbon-14, Tritium-3 and Beryllium-7 are examples of cosmogenic radionuclides which are produced by bombardment of stable nuclides by cosmic rays (NCRP, 1987; UNCECAR, 1993; Bennett, 1997).

Terrestrial radiation is coming from a number of radioactive materials occur naturally in the earth (UNCECAR, 1993; UNSCEAR, 2000). Important examples of radioactive atoms that are still present in the earth are those who have a very long half lives. Those are such as Uranium-235, Uranium-238, Thorium-232, and Potassium-40. These isotopes emit alpha and beta particles and gamma rays. They exist in soil, water and vegetation and in the bodies of the human and animals.

A significant part of the total dose contribution in the forms of natural sources comes from terrestrial gamma radionuclides (UNSCEAR, 2000). The main natural contributions to external exposure from gamma rays are Uranium-238, Thorium-232 and Potassium-40 (UNSCEAR, 2000; UNSCEAR, 2006). The radon gas is also an important source of natural radiation. It has two isotopes radon-220 (Rn^{220} , Thoron) and radon-222 (Rn^{222} , Radon). Both of them are radioactive and result either

from decay of uranium-238 or thorium-232 (Kaplan, 1984; Walker *et al.*, 1984).

Recently, Radiation Hormesis becomes one of the hottest areas in the radioactivity studies. It suggests that a low-level radiation doses motivates protective biological actions at the cellular, molecular, and organism levels, decreasing cancer and other deleterious health effects incidence rates below spontaneous levels (Henschler, 2006; Calabrese and Baldwin, 2001; Calabrese and Baldwin, 2006). Its effects include preventing and modulating aging and its related impairments, enhancement of antioxidant defenses, enzymatic repair of DNA, removal of DNA lesions, apoptosis, and immunologic stimulation.

The radioadaptive response to low-dose radiations is associated with increased lifespan as well as decreased mutations, chromosome aberrations, neoplastic transformation, congenital malformation, and cancer (Luckey, 1982; Luckey, 1999; Feinendegen, 2005).

Hormesis has demonstrated for many diseases, including cardiovascular disease, diabetes, and cancer. Low dose of ionizing radiation improve the health of the people with less diseases (Kant *et al.*, 2003; Jaworski, 1995). Although radiation hormesis data are still incomplete, extensive epidemiological studies have indicated that radiation hormesis is really exist. Many examples of this irrefutable evidence is given in different cases such as (Mifune *et al.*, 1992; Mine *et al.*, 1990; Nambi and Soman, 1987; Frigerion and Stowe, 1976; Kumatori *et al.*, 1980; Cohen, 1998). So it is important to initiate studies to investigate areas with low level of radiation, which are good for health and reduce the possibility of having diseases.

*Corresponding author email: sh2002jo@yahoo.com

Radiometric data have been collected in many countries around the world, using gamma ray spectroscopy methods. This study focuses on the Dead Sea region, which is located in the Jordan valley. It is one of the most well known health seaside resort places around the world. Our aim is to measure the doses of external exposures all around the region, in order to clarify its therapeutic importance and level of ionized radiation.

Regional Geomorphology

Dead Sea, the Salty Sea is a hypersaline lake with its surface and shore are 423 meters below sea level. The Dead Sea is 377m deep, the deepest hypersaline lake in the world. The Dead Sea is 67km long and 18km wide at its widest point. The exact composition of the Dead Sea water varies mainly with season, depth and temperature. The sea is rich in minerals, the concentration of ionic species (in g/kg) of Dead Sea surface water is Cl^- (181.4), Br^- (4.2), SO_4^{2-} (0.4), HCO_3^- (0.2), Ca^{+2} (14.1), Na^+ (32.5), K^+ (6.2) and Mg^{+2} (35.2).

It was one of the world's first health resorts and it has been the supplier of a wide variety of products, which used for fertilizers or cosmetics. The Dead Sea area has become a major center for health research and treatment for several reasons; these such as the mineral content of the water, the very low content of pollens and other allergens in the atmosphere. The Dead Sea becomes the good-place for different types of therapies, which are good for relieving different diseases. Some of those diseases are cystic fibrosis, skin disorder psoriasis, acne, atopic dermatitis, vitiligo (Halevy *et al.*, 1997).

A gray-black mineral-rich mud is deposits on dead seaside due to the Runoff streams. It can help in keeping the human skin feeling healthy and young, and used for treatment of different diseases such as acne, psoriasis, rheumatism, psoriasis, eczema and joint diseases. The major minerals present in this mud are Silicon dioxide (20%), Calcium Oxide (15.5%), Aluminum Oxide (4.8%), Magnesium Oxide (4.5%) Iron(III) Oxide (2.8%), Sodium Oxide (1.7%), Potassium oxide (1.3%), Titanium(IV) Oxide (0.5%), Sulfur trioxide (0.4%), Phosphorus pentoxide (0.3%), Chloride (6.7%), Bromide (0.2%).

MATERIALS AND METHODS

Methods and Measurements

External gamma dose rate levels were measured in two ways. The first way is by using a portable radiation monitor (RADIAGEM 2000), a survey meter that includes an energy-compensated G-M tube. The second way is implemented by an external probe connected to RADIAGEM 2000; the new Canberra Smart Probes SG-1R is designed for gamma radiation measurements. SG-1R, which is a gamma probe with an NaI(Tl) 1"x1"

detector, is not energy dependent, but it measures the dose rate equivalent. It is used for medium sensitivity with a dose-rate range from 10 nGy h⁻¹ to 200 mGy h⁻¹.

Continuous measurements were done using the two detectors in the whole area, with a continuous recording of measurements. We started our data acquisition from the far southern point of the Dead Sea to the far northern point, passing through agricultural, industrial and tourist regions.

RESULTS AND DISCUSSION

All living organisms live and grow in environments packed of ionizing radiation, external as well as internal. For most of the scientists and public it is no doubt that low doses of ionizing radiation produce negative effects comparative to the effects produced by high-level radiation. Though it was reported that low-dose ionizing radiation is not only a harmless agent but often has a positive effect. That is, low doses of ionizing radiation are an essential dynamism factor for life, analogous to many vital trace elements. This idea leads to propose that part of cancer fatalities is avoidable by exposing to a low dose radiation.

A major part of the total dose contribution comes from gamma radiation from naturally-occurring radionuclides in the U-238, Th-232 series and Potassium-40 (K-40). Wherever there is potassium, where the Dead Sea is very rich with, there is potassium-40. If there is enough potassium, the K-40 can be detectable with a simple survey instrument. Thus direct radiation dose measurements can be used to measure the gamma dose rate; this can be done using the survey meters described in the Experimental section. The gamma dose rate measurements are done 1 m above the ground on the sampling points. The sampling points were selected randomly while driving along the road starting from southern end, Fifa, up to the northern end of the Jordanian side of the Dead Sea. Sampling points are shown in figure 1.

Table 1 gives the registered gamma absorbed dose rates in the randomly selected points. The first point is noticed to have a large dose rate; which is due to the present of the agricultural fertilizers, which contains some radioactive compounds such as phosphorus (P) and potassium (K). Sample point 3 is located near the Arab Potash Company (APC) in the Jordanian side of the Dead Sea and has a 100 nSv/h which is little higher than that of the world range of 18-93nGyh⁻¹ (UNSCEAR, 2000). These measurements are sketched in figure 2. Part of the results is in the same level as the results obtained in hot springs in Jordan, except Afra hot spring doses; while many of the results are lower than these (Ajlouni *et al.*, 2009; Ajlouni *et al.*, 2010; AL-Amairyen, 2010; Al-Okour, 2011).

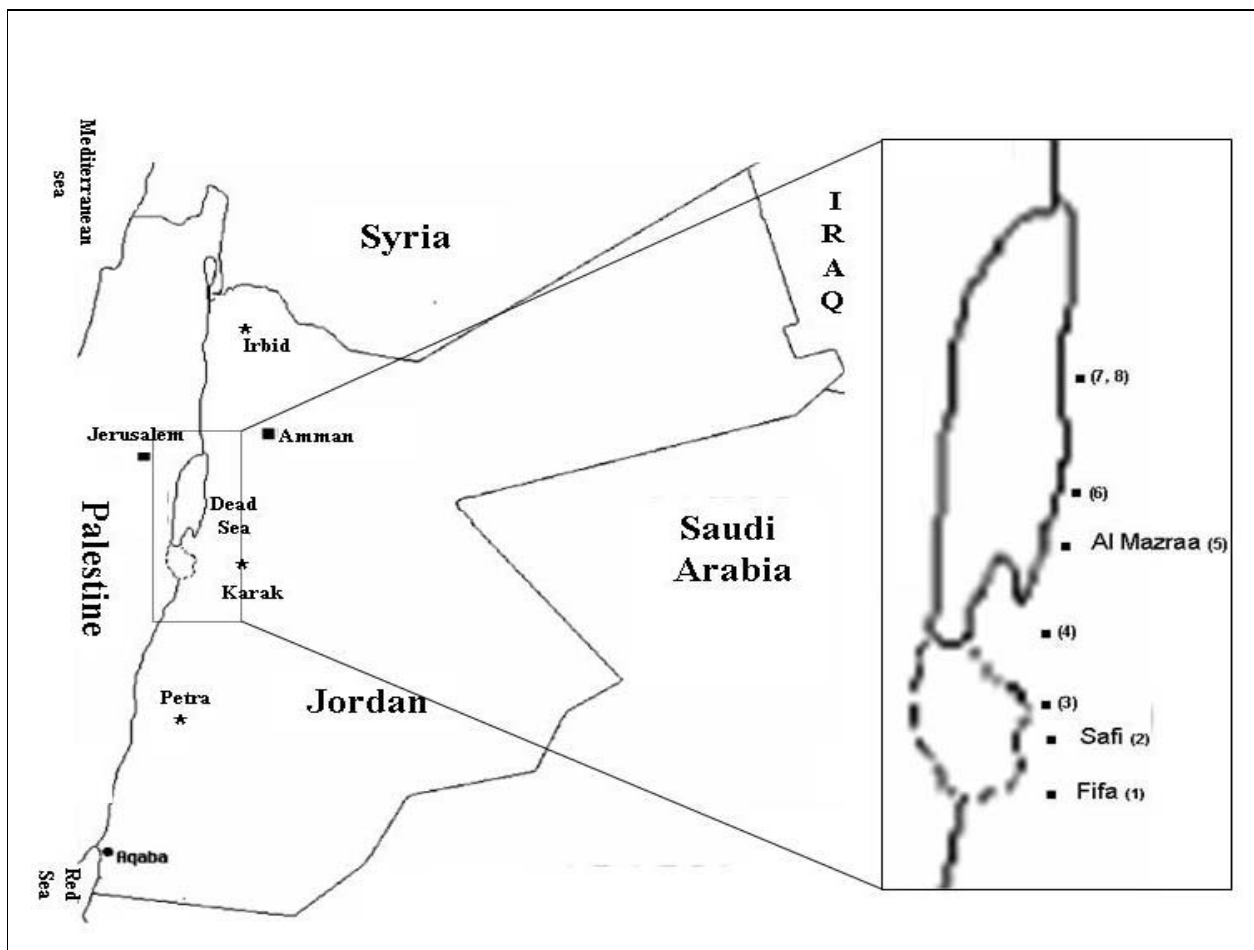


Fig. 1. The Sampling points along the Dead Sea.

Table 1. Registered gamma absorbed dose rates in different points along the Dead Sea region (from south to north).

Location	Characteristic of location	nSv/h
1	Fifa	260
2	Safi	105
3	Near Arab Potash Company (APC)	100
4	Esal	60
5	Al-Mazra'a	60
6	5 km from Al-Mazra'a to the north	130
7	Dead Sea Health Centre number one (DSHC.1)	45-85
8	Dead Sea Health Centre number two (DSHC.2)	30-50

Table 2 gives the dose rate in air in different locations at the Dead Sea Health Center number one (DSHC.1), which is located 50 km from Amman, the capital of Jordan. These locations vary in their distances from 500 meter away from the seaside up to the water body of the sea. The dose rates are increased as we approach the black-mud region, which resides on the seaside as shown in figure 3. Spot (7) which measured on the top of the Black-Mud register the highest dose in the DSHC.1 (80-85 nSv/h). Spot 8 shows the smallest dose on the whole study region, this value is because of the existing of the salt which is covered the mud and limited the radioactivity rate. The dose rate from results the water body ranges from 50 to 60 nSv/h.

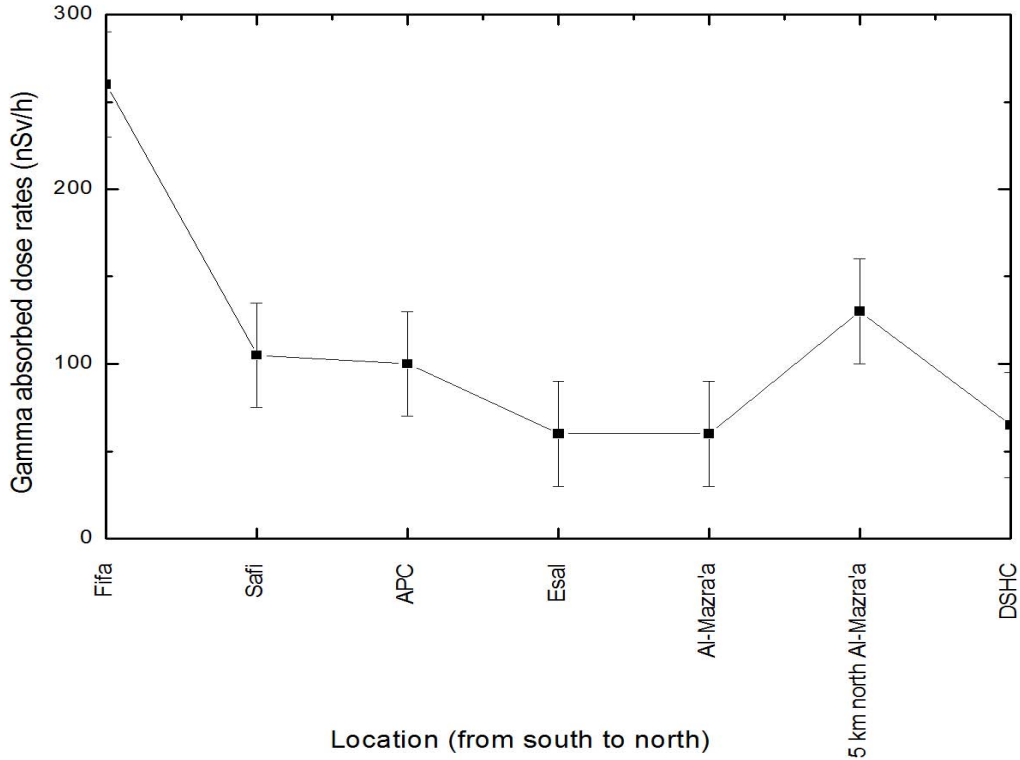


Fig. 2. The Measured Gamma absorbed doses at different locations along the Dead See from south to north.

Table 3 shows the dose rates in air at different locations in the Dead Sea Health Center number two (DSHC.2). These locations vary in its distance from the seaside (from 700m up to 1m and on the top of the sea side). The dose rates in all locations are between 30-50 nSv/h. Location Number 3 has residences of black-mud and show a dose rate of 50 nSv/h.

Table 2. Registered gamma absorbed dose rates at different locations inside the DSHC.1.

Location No.	Distance from the seaside (m)	Characteristic of location	nSv/h
1	500	Center Hall	50
2	400	Near first swimming pool	55
3	300	Near second swimming pool	45
4	200	On the coast	60
5	100	On the coast	70
6	1	Near the water	70-77
7	1	Top of the Black-Mud	80-85
8	1	Top of the salt	15
9	0	Water-body	50-60

Table 3. Registered gamma absorbed dose rates at different locations inside the (DSHC.2).

Location No.	Distance from the seaside (m)	Characteristic of location	nSv/h
1	700	Hotel Hall	40-50
2	100	On the coast	30-40
3	1	On the coast	50
4	0	Water-body	50

Natural radiation doses, someone gets in staying in this region, go together with other features like hot and mineral springs, mud baths and wraps, herbal baths, exposing to sun and dry climate and salt lakes will demonstrate its good effect on stimulating the psychological state of the patient and accelerating his recovery, and improve the health of non-patients.

CONCLUSION

The Dead Sea is one of the important health resorts on the world because of its location, environment and the compound that is used from it. Our data shows that this region has a proper level of external radiation. The gamma dose rates were between 15 nSv h^{-1} and 260 nSv h^{-1} . The average dose on all the sampling points is 75 nSv h^{-1} .

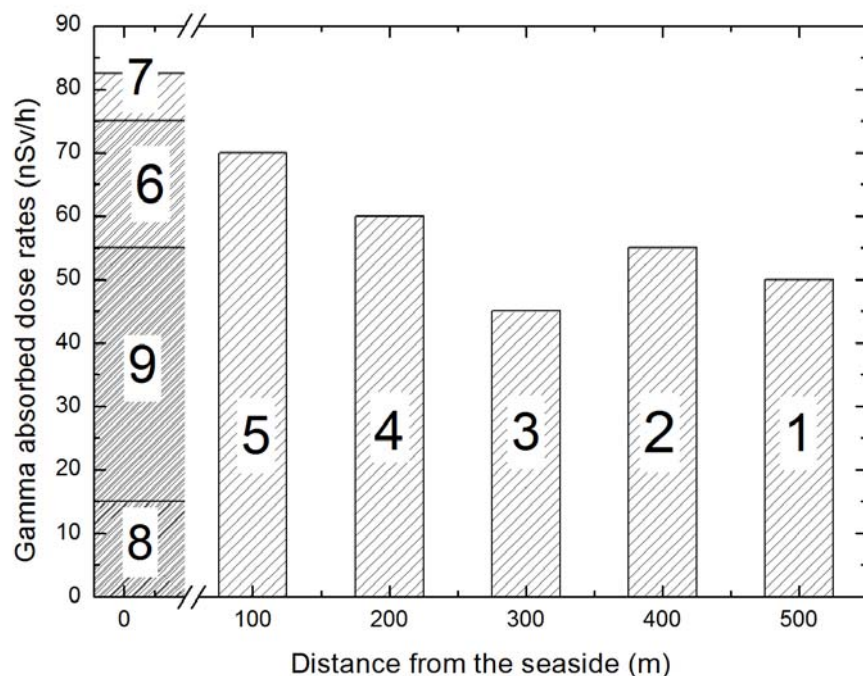


Fig. 3. Dose rates as measured at different locations inside the (DSHC.1) starting from 500m away from seaside till the water body.

which is in not far a lot from the average worldwide external exposure rates from terrestrial gamma radiation of 57 nGy^{-1} . The average rate of the gamma dose is in the world range of $18\text{-}93 \text{ nGy}^{-1}$.

REFERENCES

- Ajlouni, AW., Abdelsalam, M., Abu-Haija, O. and Joudeh, B. 2009. New Findings: A very high natural radiation area in Afra hot springs, Jordan. *Radiation Protection Dosimetry*. 133:115-118.
- Ajlouni, AW., Abdelsalam, M., Abu-Haija, O. and Almasa'efah, YS, 2010. Radiation doses due to Natural Radioactivity in Afra Hot Spring. *Int. J. Low Radia.* 7:48-52.
- AL-Amairyen, H. 2010. Radiation doses due to natural Radioactivity in Wadi Bin Hammad, Al-Karak, Jordan. *International Journal of the Physical Sciences* 5:1486-1488.
- Al-Ookour, A. 2011. Radiation Doses Due to Natural Radioactivity in North-Shuneh Hot Springs, Jordan. *European Journal of Scientific Research* 51:582-586.
- Bennett, BG., 1997. Exposure to natural Radiation Worldwide. In: Proceedings of the Fourth International Conference on High Levels of Natural Radiation: Radiation Doses and Health Effects, 1996, Beijing, China. Elsevier, Tokyo. 15-23.
- Calabrese, EJ. and Baldwin, LA. 2001. Hormesis: A Generalizable and Unifying Hypothesis. *Crit. Rev. Toxicol.* 31:353-424.
- Calabrese, EJ., Baldwin, LA. 2001. Scientific Foundations of Hormesis. *Crit. Rev. Toxicol.* 31:351-624.
- Calabrese, EJ. and Baldwin, LA. 2006. The Frequency of U-shaped Dose Responses in the Toxicological Literature. *Toxicol. Sci.* 62:330–333.
- Cohen, BL. 1998. Test of the Linear no-threshold Theory of Radiation Induced Cancer. The Annual Congress of the South African Radiation Protection Association, Kruger National Park, South Africa.
- Feinendegen, LE. 2005. Evidence for Beneficial Low level Radiation Effects and Radiation Hormesis. *The British Journal of Radiology.* 78:3-7.
- Frigerio, NA. and Stowe, RS. 1976. Carcinogenic and Genetic Hazard from Background Radiation. *Biological and Environmental Effects of low-level Radiation*, IAEA, II:285-293.
- Henschler, D. 2006. The Origin of Hormesis: Historical Background and Driving Forces. *HumExp Toxicol.* 25:347-35149.
- Halevy, S., Giryes, H., Friger, M. and Sukenik, S. 1997. Dead Sea Bath Salt for the Treatment of Psoriasis Vulgaris: A Double-blind Controlled Study. *Journal of*

- the European Academy of Dermatology and Venereology. 9(1):237-242.
- Jaworowski, Z. 1995. Stimulating Effects of Ionizing Radiation: New Issues for Regulatory Policy. *Regulatory Toxicology and Pharmacology* 22:172-179.
- Kant, K. *et al.* 2003. Hormesis in Humans Exposed to low-level ionizing Radiation. *Intern. J. Low Radiat.* 1:76-87.
- Kaplan, I. 1984. Nuclear Physics. Addison-Wesley, Reading Ma., USA.
- Kumatori, T., Ishihara, T., Hirshima, K., Sugiyama, H., Ishii, S. and Miyoshi, K. 1980. Follow up Studies over a 25 Year Period on the Japanese Fishermen Exposed to Radioactive Fallout in 1954. In: *The Medical Basis for Radiation Preparedness*. Eds. Hubner, KF. and Fry, AA. Elsevier, New York, USA. 35-54.
- Luckey, TD. 1982. Radiation Hormesis. CRC Press, Boca Raton, FL, USA.
- Luckey, TD. 1982. Physiological Benefits From Low-level Ionizing Radiation. *Health Phys.* 43:771-789.
- Luckey, TD. 1999. Nurture with Ionizing Radiation: A Provocative Hypothesis. *Nutrition and Cancer*. 34:1-11.
- Mifune, M., Sobue, T., Arimoto, H., Komoto, Y., Kondo S. and Tanooka, H. 1992. Cancer Mortality Survey in a Spa area (Misasa, Japan) with a High Radon Background. *Japanese Journal of Cancer Research*. 83(1):1-5.
- Mine, M., Okumura, Y., Ichimaru, M., Nakamura, T. and Kondo, S. 1990. Apparently Beneficial Effect of Low to Intermediate Doses of A-bomb Radiation on Human Life Span. *International Journal of Radiation Biology*. 58:1035-1043.
- NCRP. 1987. Exposure of the Population of the United States and Canada from Natural Background Radiation. Report No. 94, National Council on Radiation Protection and Measurements, Bethesda, Maryland, USA.
- Nambi, KSV. and Soman, SD. 1987. Environmental Radiation and Cancer in India. *Health Physics*. 52:653-657.
- UNSCEAR. 1993. Sources and Effect of Ionizing Radiations. United Nations Scientific Committee on the Effect of Atomic Radiation, United Nations, New York, USA.
- UNSCEAR. 2000. Sources and Effects of Ionizing Radiations. United Nations Scientific Committee on the Effect of Atomic Radiation, United Nations, New York, USA.
- UNSCEAR 2006. Effect and Risks of Ionizing Radiations. United Nations Scientific Committee on the Effect of Atomic Radiation, United Nations, New York, USA.
- Effect of Atomic Radiation, United Nations, New York, USA.
- Walker, FW., Miller, DG. and Feiner, F. 1984. Chart of Nuclides. General Electric Company, San Jose, CA, USA.

Received: April 3, 2011; Accepted: May 7, 2011

COMPARATIVE STUDIES OF EXTRACTED RESIN FROM PLANTAIN PEELS AS A POTENTIAL BINDER AND CO-BINDER WITH CEMENT IN PARTICLEBOARD PRODUCTION

*AJ Anifowose¹, L Lajide², SH Awojide¹ and KA Fayemiwo¹

¹Department of Chemical Sciences, Osun State University, Osogbo, Nigeria

²Department of Chemistry, Federal University of Technology, Akure, Nigeria

ABSTRACT

In this study, natural resin from dry, ground peels of unripe plantain were extracted with benzene/ethanol (2:1). This was employed as binder as well as co-binder with cement in the production of particleboards. Boards C (ratio 3:2:0 of sawdust:resin:cement by weight), A (ratio 3:1:1 of sawdust:resin: cement by weight) and B (ratio 3:0:2 of sawdust:resin:cement by weight) were all produced, while B serve as control. Board C exhibited least density (0.38 gcm^{-3}), while B had highest (1.05 gcm^{-3}). There appeared better physical properties for board A (water absorption - WA, thickness swelling - TS, linear expansion - LE and abrasion – ABS - values of 15.51%, 3.82%, 4.42% and 0.79% respectively) than B and C. However, the mechanical properties of board B appeared better than that of A as its modulus of rupture (MOR) and modulus of elasticity (MOE) were higher, though board A still had significant MOR and MOE values of 2.02 Nmm^{-2} and 2131.40 Nmm^{-2} respectively. The MOR and MOE tests on board C failed due to its lack of load-bearing capacity, though with least value of LE. The reduced density and improved physical qualities of board A exposed the extracted resin as a good potential binder if more research is geared towards developing its binding capacity. Infrared spectroscopy showed O-H and C=O bonds on the resin, while its chemical interaction with the cement reduced the functional group to C=O bond.

Keywords: Plantain, peels, particleboard, resin, cement.

INTRODUCTION

Over the years, plantain has been more importantly utilized as foods. The fruits are either eaten raw or processed as foods and raw material for industrial purposes. The peels are well known animal feeds due to their high moisture content, sources of fibres for the manufacture for paper, textile material and leather production (Morton, 1987). In some African countries like Kenya and Uganda, they serve as raw materials and source of binder for briquettes (a fuel resource made from any agro-industrial wastes that can be recycled for cooking or heating) as reported by Megan (2007) little is known about the exploitation and application of their natural resins present in peels. Resins from plants are known for their binding characteristics (Mantell, 1942; Harborne, 1984). Promising cement-bonded wood composites for structural purposes have evolved over many years. Its production is aimed at utilizing large quantity of sawdust at sawmills. Petroleum-based synthetic resins (e.g., phenolic and urea-formaldehyde), employed as binders have been well known to be efficient and as such became costly items in the processing of wood panel products (Frybort *et al.*, 2008). These costly products led to high cost of production of particleboards. Their ready availability is also a concern and crucial factor, especially in Nigeria where most of these products

are imported; hence, the need for cheap and readily available binders that would be of equal or better qualities to these synthetic products has become imperative. Due to the high cost of thermosetting resin in board production in Nigeria, a great deal of interest is being developed on the use of cement as a binding agent, fortified with other mineralizing agents (Ajayi, 2000). Different mineral binders, including Portland cement, magnesia and gypsum, are used to fabricate boards with different properties (Simatupang and Geimer, 1990). However, the most expedient binder, concerning strength, durability and acoustic insulation properties is Portland cement (Frybort *et al.*, 2008) but their density has become a major concern as increased strength was always facilitated by more cement.

In the present study, natural resin, extracted from the peels of unripe plantain was employed as binder as well as in combination with cement for the production of particleboards, using cold-press method. The properties of the boards and the effects of mixing the extracted resin with cement on the properties of the board produced were investigated and compared with cement-bonded particleboards which have been well reported for their quality strength and other properties (Badejo, 1986; Fuwape, 1992; Frybort *et al.*, 2008).

*Corresponding author email: chemistbanjo@yahoo.com

MATERIALS AND METHODS

Sample Collection and Preparation

The plantains (unripe) used for the study were bought along Okitipupa road, Ondo State, Nigeria. They were washed thoroughly with water, peeled, chopped into pieces with knife and sun-dried. The dried sample was pounded with mortar and pestle, blended and sieved to 300 µm with laboratory sieve at the department of Geology, Federal University of Technology, Akure, Nigeria.

Extraction of Resin from the Sample

The prepared sample was first defatted with N-hexane to remove all fat, after which resin was exhaustively extracted with benzene/ethanol (2:1) in a soxhlet extractor (TAPPI, 1998). Solvent was recovered from the extract by distillation. The resin was purified by evaporating off all the remaining solvent till there was no perceivable odour of the solvent in a fume cupboard.

The yield was calculated thus:

$$\% \text{yield} = \frac{\text{weight of dry resin}}{\text{weight of sample}} \times 100$$

Infra-Red Spectroscopy of the Resin

The infrared spectroscopic analyses contained in this work were carried out using model 500 Infra-red Spectrophotometer, Buck Scientific Inc., Norwalk, CT, USA using KBr.

Particleboard Production

Production of the particleboards was carried out at the Department of Forest Products Development and Utilization (FPDU), Forestry Research Institute of Nigeria (FRIN), Jericho, Ibadan, Nigeria. The sawdusts used were mixture of hardwood species. They were pre-treated with hot water in an aluminum pot at 80°C for about one hour to remove the water-soluble, all extractives like resin acids, terpenes, inorganic salts, fats, certain carbohydrates, tannins which might be present in the wood and capable of inhibiting the setting of the binders (Eero, 1981). They were later washed in cold water for 10 minutes; the leachate was separately removed and exposed to atmospheric air to dry and then transferred to controlled laboratory environment at moisture content of approximately 12%.

Calculation of the Weight of Materials Required

The quantities of materials required for the production of 350mm x 350mm x 6mm were calculated and measured out according to the level of combination in the experiment. Such variables were hardwood specie sawdust, the natural resin, cement and additive. Hardwood specie sawdust and binder (resin) were calculated based on the mixing ratio of the two

components comprising the mass of the board. Benzene/ethanol solvent system was used as the liquid medium for the resin, while water was used for that of cement-bonded particleboards. The experimental combinations were as follows:

Board A - 3:1:1 (sawdust:resin:cement by weight ratio)

Board B - 3:0:2 (sawdust:resin:cement by weight ratio)

Boards C - 3:2:0 (sawdust:resin:cement by weight ratio)

Blending of Production Variable

The additive (CaCl_2) for the production of cement bonded board was first dissolved completely in water and added to the sawdust before mixing with the cement. The required quantity of water derived based on the relationship developed by Simatupang (1979) and also adopted by Erakhrumen *et al.* (2008) was added and thoroughly mixed afterwards in an aluminum bowl until a homogenous mixture was formed and the cement paste completely hydrated.

$$\text{Required water (litres)} = 0.35C + (0.30 - M)W$$

Where C = Cement weight (kg), M = Moisture content of the sawdust (oven-dry basis) and W = oven-dry weight of the sawdust.

All materials (the natural resin and sawdust) for the resin bonded particleboard produced were measured in kilogram based on the working ratio into an aluminum bowls and hand-mixed thoroughly until well blended, lump-free finishes were obtained.

Mat Formation and Processing

The furnish was hand formed into a uniform mat inside a wooden box of 350 mm x 350 mm that was placed on a caulk plate made of iron. The mat formed was pre-pressed using wooden caulk plate. Prepress was done in order to reduce the thickness of the mat formed, for free loading unto the cold press. The steel caulk plate was covered with polythene sheet before board formation to prevent the sticking of the board to the plate. After board formation, the wooden plate was removed; another polythene sheet was placed on the mat before placing the metal caulk plate. The board was loaded into the hydraulic press and pressure was applied at 1.23 Nmm^{-2} for 24 hours, before de-moulding.

Curing

After pressing, the mat still under compression was cured in the oven at 105 °C for about 4 hours. The boards were removed, allowed to cool, wrapped with polythene sheet and kept in the laboratory environment for 28 days to enhance further curing of the resin, while those experimental boards with only cement binders were air-dried after release from the hydraulic press, wrapped with polythene sheet and kept in the laboratory environment for 28 days to enhance further curing of the cement. Possible loss of water from the boards was prevented

through proper wrapping of the sheet so as to maintain constant ambient condition. Boards were trimmed to avoid edge effect on test specimens, thereafter the board was stack for 21 days inside a controlled laboratory environment at relative humidity of $65\pm2\%$ and temperature of 20°C . All the other boards were produced through the production process as stated above.

Laboratory Tests on the Particleboards

Both the physical and mechanical properties of all the boards were determined in accordance with BS 373 (1979). Board specimen dimension of 152mm x 152mm x 6mm was used to investigate the physical properties such as thickness swelling, water absorption and linear expansion, while 194mm x 50mm x 6mm was used to investigate the mechanical properties such as modulus of rupture and modulus of elasticity on tensiometre at Department of Forest Products Development and Utilization (FPDU), Forestry Research Institute of Nigeria (FRIN), Jericho, Ibadan, Nigeria.

Physical Properties

Water Absorption

This is a measure meant to test the dimensional stability of board, to have this test done; each test specimens was soak in water (at room temperature) for moisture uptake for 24 hours. The new weight was measured using highly sensitive weighing balance before and after soaked. Water absorption was expressed as the percentage increase in weight of the board over the original or initial weight.

$$\text{WA} = \frac{W_2 - W_1}{W_1} \times 100$$

Where: WA = water absorption (%), W_1 = initial weight, W_2 = final weight.

Thickness Swelling

The same procedure was used to determine the thickness swelling, using the same specimens at the same period of time for soaking. The thickness of the boards was measured using electronic veneer caliper before and after soaking for 24 hours at room temperature. The thickness swelling was expressed as the percentage of increase in thickness of the board over the original thickness. Thickness swelling was expressed as

$$\text{TS} = \left(\frac{T_2 - T_1}{T_1} \right) \times 100$$

Where: TS = thickness swelling (%); T_2 = final thickness; T_1 = initial thickness

Linear Expansion

This was also carried out by taking measurement of the initial length (L_1) with the aid of a veneer caliper at two different points along the length of the test specimen. The sample was soaked in water for 24 hours at room temperature and the measurement of the final length (L_2)

was carried out at the designated two different points. The linear expansion (%) was estimated using:

$$\text{LE} (\%) = \left(\frac{L_2 - L_1}{L_1} \right) \times 100$$

Where: LE = Linear Expansion (%); L_2 = Final length (mm); L_1 = Initial length (mm)

Abrasion Test

The surface of the board was brushed 20 times with iron brush and the weight was determined before and after brushing the surface with the tool. Abrasion (%) was estimated using the formula below:

$$\text{ABS} (\%) = \left(\frac{A_2 - A_1}{A_1} \right) \times 100$$

Where: ABS = Abrasion (%); A_2 = Final weight (g); A_1 = Initial weight (g)

Mechanical Properties

Bending Strength

The test specimens of 194mm \times 50mm \times 0.6mm were cut from the boards and subjected to a force or load on the tensiometer with the support span. The specimens were supported by two rollers at each ends and loaded at their centres. The forward movement of the machine leads to gradual increase of load at the middle span until failures of the test specimens occurred. At the point of failure, the force exerted on the specimen that caused the failure was recorded; the Modulus of Rupture (MOR) of the test specimens was calculated using the formula;

$$\text{MOR} = \frac{3\rho L}{2bd^2}$$

Where;

MOR= Modulus of Rupture; ρ = Failing load; L= Span between centers of support (mm);
 b = Width of test specimen (mm); d = mean thickness of the specimen (mm).

The panel's stiffness, Modulus of Elasticity (MOE), was determined from the bending test performed on each specimen and MOE was calculated using the formula;

$$\text{MOE (N/mm}^2\text{)} = \frac{\rho L^3}{4bd^3 H}$$

Where;

MOE= Modulus of elasticity of panel stiffness; L= Span between centres of support (mm)
 b = Mean thickness of the specimen (mm); H= Increment in deflection (mm).

RESULTS AND DISCUSSION

Extraction of the Resin

The yield was found to be 9.13%.

As shown in table 1, the density of the boards ranged between 0.38 g/cm^3 and 1.05 g/cm^3 . The density of the cement bonded particleboard was reduced by about 57% when half of equal weight of the cement was substituted with the resin (i.e., 1:1) with no significant variation in other physical properties. The higher the proportion of cement in the boards, the higher the density (boards A and B). This is in conformity with publication by Erakhrumen *et al.* (2008). This is an important development as high density boards are difficult to handle, cut, nail and transport (Zhou and Kamdem, 2002) coupled with the cost of implication associated with higher content of cement in production. Board C which had the extracted resin as the sole binder possessed the least density value but its exhibition of high values of other physical properties except for linear expansion called for more research on improving the glueing strength of the resin.

The mean values of WA ranged from 15.51 to 87.90%. The values obtained are similar to those reported by Erakhrumen *et al.* (2008). Experimental board C had the highest values, while board A had the least value; hence, the combination of the extracted resin and cement in ratio 1:1 produced board with more water resistance quality. This could be due to the encapsulation of the fibre of the board by the resin.

TS is an important attribute concerning dimensional

stability of wood panel products. The compiled mean TS values for the experimental boards ranged from 3.82 to 22.67% (Table 1). These range values compared favourably to figures reported by Erakhrumen *et al.* (2008). The combination of both resin and cement again produced experimental board (A) of mono-dimensional stability when compared with the other boards.

The mean values for LE ranged from 2.42 to 4.80%. Experimental boards B had the highest value (4.80%), while the lowest was interestingly found in the board C. Boards A and B had values that competed favourably with each other. The trend of all the results showed that application of the extracted resin as sole binder lowers the linear expansion – a factor in measurement of dimensional stability of panel products. This could be attributed to non-hydrophilic nature of the resin. There was significant difference in the LE value obtained for board C and that of other boards at 5% level of probability (Table 1).

The mean values of ABS ranged from 0.79 to 55.44%. The lowest value was recorded for board A (Table 1). Board C had exceptionally high value (55.44%). The results were clear indication that there was an improved surface quality of the board produced with mixture of resin and cement (1:1). However, using the natural resin alone as binder resulted in poor abrasion. This could be

Physical Properties of the Boards Produced

Table 1. Mean Physical Properties of the Particleboards produced.

Board	Density (g/cm^3)	WA (%)	TS (%)	LE (%)	ABS (%)
A	0.45 ^a	15.51±1.01 ^a	3.82±2.78 ^a	4.42±0.29 ^b	0.79±0.68 ^a
B	1.05 ^b	16.97±2.96 ^a	4.47±1.84 ^a	4.80±0.32 ^b	1.17±0.43 ^a
C	0.38 ^a	87.90±24.20 ^b	22.66±4.64 ^b	2.42±0.57 ^a	55.44±19.68 ^b

All data represent the mean of three replicates. Values followed by the same superscripts in each column are not significantly different at ($p < 0.05$)

Table 2. Mean Mechanical Properties of the Particleboards produced.

Board	MOR (N/mm^2)	MOE (N/mm^2)
A	2.02 ^a ±0.16	2,131 ^a .40±548.98
B	6.13 ^c ±0.24	8,903 ^c .48±3,079.92
C	0.00	0.00

All data represent the mean of three replicates. Values followed by the same superscripts in each column are not significantly different at ($p < 0.05$)

MOR – modulus of rupture; MOE – modulus of elasticity

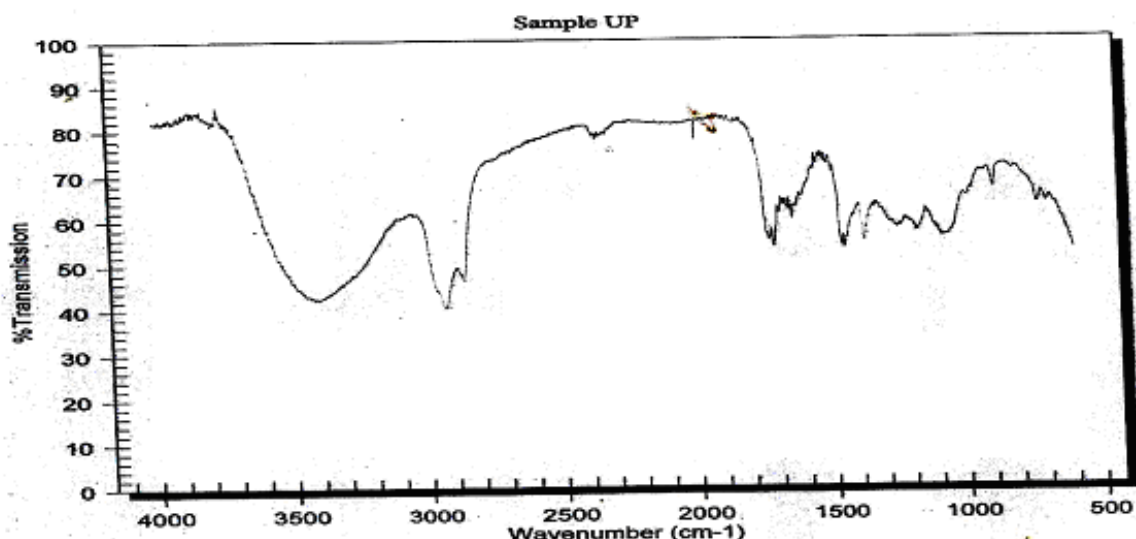


Fig. 1. Infrared Spectroscopy of the Extracted Resin from Plantain Peels.

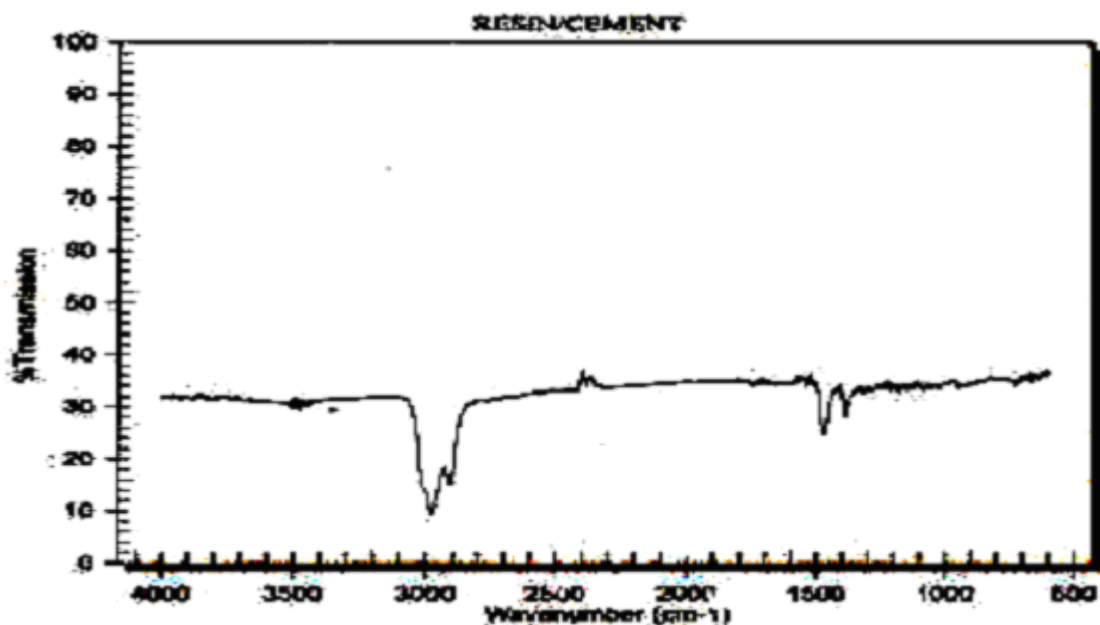


Fig. 2. Infrared Spectroscopy of the Mixture of the Extracted Resin with Cement (1:1).

due to lack of strong chemical bond between the resin and the lignocellulosic part of the board fibres.

The MOE reveals the ability of the boards to withstand stress, while the MOR reveals the bending strength of the boards. The mean values of Modulus of Rupture (MOR) and Modulus of Elasticity (MOE) of the three experimental boards are summarized in table 2. Board B had the highest MOR and MOE values – 6.13 N/mm^2 and $8,903.48\text{ N/mm}^2$ respectively, significant of best load strength. Nevertheless, the MOR and MOE values of 2.02 N/mm^2 and $2,131.40\text{ N/mm}^2$ respectively, obtained for board A, still compete favourably with publications by

Kwon and Geimer (1998), Ajayi (2002) and Zheng *et al.* (2007). However, the bending and tensile strength of board C could not be determined due to lack of mechanical strength to withstand the testing load; hence, the MOR and MOE tests failed (i.e., no MOR and MOE values) despite the fact that the board appeared to be physically strong and stable. The trend of influence of the resin proportion on MOR and MOE of the panels at each of the boards showed better strength with cement.

Infrared spectroscopic absorptions at 3500 cm^{-1} , 2850 cm^{-1} and 1750 cm^{-1} show presence of the O-H, methylene and C=O groups respectively in the extracted resin (Fig.

1). In figure 2, the absence of absorption at 3500 cm^{-1} showed that there was a chemical interaction between the extracted resin and the added cement. This could be explained by the probable ionic bond formed between the calcium atom of the cement and hydroxyl group on the resin

CONCLUSION

The extracted resin from plantain peels (unripe) had some binding characteristics that could serve some industrial purposes as applied in the production of the particleboards. Combination of the extracted resin and cement (1:1 by weight) as a binder for production of particleboard resulted in board with better physical properties and acceptable mechanical properties.

ACKNOWLEDGEMENT

The authors want to thank the management and staff of the Forestry Research Institute of Nigeria (FRIN), Ibadan, Nigeria and the entire staff of the Departments of Chemistry and Geology, Federal University, Akure, Nigeria, where the analyses and production contained in this work were carried out.

REFERENCES

- Ajayi, B. 2000. Strength and Dimensional Stability of Cement-Bonded Flake Board Produced from *Gmelina arborea* and *Leucaena leucocephala*. Ph.D Thesis, Department of Forestry and Wood Technology, Federal University of Technology, Akure, Nigeria. pp176.
- Ajayi, B. 2002. Preliminary Investigation of Cement-Bonded Particleboard from Maize Stalk Residues. Nig. J. For. 32(1):33-37.
- AOAC 1990. Official Methods of Analysis. (15th ed.) Association of Official Analytical Chemists, Inc., Virginia, USA.
- Badejo, SOO. 1986. Dimensional Stability of Cement-Bonded Particleboard from Eight Tropical Hardwoods Grown in Nigeria. Nigeria Journal of Forestry. 16(1&2):11-19.
- British Standard Institution: B.S. 5669. 1979. Specification for wood chipboard and methods of test for particleboard BSI, London.
- Eero, S. 1981. Wood Chemistry – Fundamentals and Applications. Academic Press, Inc., Florida, USA. 81-89.
- Erakhrumen, AA., Areghan, SE., Ogunleye, MB., Larinde, SL. and Odeyale, OO. 2008. Selected Physico-Mechanical Properties of Cement-Bonded Particleboard made from Pine (*Pinus caribaea* M.) Sawdust-Coir (*Cocos nucifera* L.) Mixture. Scientific Research and Essay. 3(5):197-203.
- Frybort, S., Mauritz, R., Teischinger, A. and Müller, U. 2008. Cement Bonded Composites – A Review. Bioresources. 3(2):602-626.
- Fuwape, JA. 1992. Sorption Property of Wood-Cement Particleboard as Influenced by Cement/Wood Ratio. J. Ind. Acad. Wood Sci. 23(1):1-9.
- Harborne, JB. 1984. Phytochemical Methods. (2nd ed.), London. Chapman and Hall Ltd. 49-188.
- Kwon, HE. and Geimer, RL. 1998. Impact of Steam Pressing Variables on the Dimensional Stabilisation of Flakeboards. For. Prod. J. 48(4):55-61.
- Mantel, CL. 1942. The Technology of Natural Resins. John Wiley and Sons, New York, USA. pp506.
- Megan, H. 2007. EcoVentures International. Kenya Study Tour: Biomass Briquetting.
- Morton, J. 1987. Fruits of Warm Climates. Miami, USA. pp29-46.
- Simatupang, MH. 1979. The Water Requirement of Manufactured Cement-Bonded Particleboard. Holz als Roh-und Werkstoff. 37:379-382.
- Simatupang, MH. and Geimer, R. 1990. Inorganic Binder for Wood Composites – Feasibility and Limitations. Wood Adhesives. Madison, Wisconsin USA. 169-176.
- TAPPI. 1998. Acid-Insoluble Lignin in Wood and Pulp, TAPPI Standards T222 OM-98.
- Zheng, Y., Zhongli, LP., Zhang, RH., Jenkins, BM. and Blunk, S. 2007. Particleboard Quality Characteristics of Saline Jose Tall Wheatgrass and Chemical Treatment Effect. Bioresource Tech. 98(6):1304-1310.
- Zhou, Y. and Kamdem DP. 2002. Effect of Cement/Wood Ratio on the Properties of Cement- Bonded Particleboard using CCA-Treated Wood Removed from Service. For. Prod. J. 52(2):73-81.

Received: Sept 16, 2011; Revised and Accepted: April 9, 2012

Short Communication

A NOTE ON LINEAR FUNCTIONAL IN A^p SPACE

Maher MH Marzuq

School of Natural Resources Engineering and Management

Department of Water Engineering and Management

German Jordanian University, PO Box 35247, Amman 111 8, Jordan

ABSTRACT

In this paper we will generalize theorem 9 of Hahn and Mitchell (1969) in bounded symmetric domain on Hardy Space to Bergman Space.

1. Definition and Preliminary Results.

Let D be a bounded symmetric domain in the complex vector space C^N ($N > 1$) in the canonical Harisch Chandra realization. It is known that D is circular and star-shaped with respect to $0 \in D$ and has a Bergman-Silov boundary b, which is circular and measurable. Let Γ be the group of holomorphic automorphisms of D and Γ_0 its isotropy subgroup with respect to 0. The group Γ is transitive on D and the holomorphic automorphisms extend continuous to the topological boundary of D.

The group Γ_0 is transitive on b and b has a unique normalization Γ_0 invariant measure μ which is given by $d\mu_t = V^{-1}ds_t$, V the Euclidean volume of b and ds_t the Euclidean volume element at t (Koranyi and Wolf, 1965).

Let $H(D)$ denotes the class of holomorphic functions on as A^p ($0 < p < \infty$) D, we define the Bergman space follows:

$$A^p = A^p(D) = \left\{ f : f \in H(D) \text{ and } \|f\|_{A^p} = \left(\frac{1}{V} \int |f(z)|^p dv_z \right)^{\frac{1}{p}} < \infty \right\},$$

or equivalently (Marzuq, 1984a) as,

$$A'^p = A'^p(D) = \left\{ f : f \in H(D) \text{ and } \|f\|_{A'^p} = \sup_{0 < r < 1} \left(\frac{1}{V} \int |f(rz)|^p dv_z \right)^{\frac{1}{p}} \right\}.$$

In the rest of the paper C is a positive constant not depending on the function, and not necessarily the same at each occurrence.

2. Let T be a linear functional on A^p .

Then, $T \in (A^p)^*$ if and only if it is bounded on the sphere in A^p

Topologies $(A^p)^*$ by setting,

Corresponding author email: maher_marzuq@yahoo.com

$\|T\| = \sup_{\|f\|_{A^p}=1} |T(f)|$, $(A^p)^*$ is Banach Space (Rudin, 1974).

$$\text{For, } z \in D \text{ set } \gamma_z(f) = f(z) \quad (2.1)$$

Marzuq (1984b) studied linear functional in A^p space.

3. Weak convergence.

Let $\{f_n\}$ be a sequence $A^p(D)$. Then (f_n) is said to converge weakly to $f \in A^p(D)$, written $f_n \rightarrow^w f$, if and only if $\gamma(f_n) \rightarrow \gamma(f)$ as $n \rightarrow \infty$, for every $\gamma \in (A^p)^*$. We call f is the weak limit of $\{f_n\}$.

The weak limit of a weakly convergent sequence is unique, for if $\gamma(f_n) \rightarrow \gamma(f)$ and $\gamma(f_n) \rightarrow \gamma(g)$ for all $\gamma \in (A^p)^*$ then,

$$\gamma(f - g) = \gamma(f - f_n) + \gamma(f_n - g) = 0 \text{ as } n \rightarrow \infty.$$

Thus $\gamma(f - g) = 0$ for all $\gamma \in (A^p)^*$, and hence $f = g$, since if $f \neq g$, by Corollary (Marzuq, 1984b), there exist $\gamma \in (A^p)^*$, such that $\gamma(f - g) \neq 0$ which contradicts the conclusion $\gamma(f - g) = 0$ for all $\gamma \in (A^p)^*$.

We have the following theorem which generalizes theorem 9 (Han and Mitchell, 1969).

Theorem1. Let $f_n \rightarrow^w f$, where $f_n \in A^p$ then, $\lim_{n \rightarrow \infty} f_n(z) = f(z)$ uniformly or compact bounded symmetric D, where D is an irreducible bounded symmetric domain.

We require the following lemma to prove theorem 1.

Lemma 1: let D be as in theorem1 and X =

$\{f \in A^p : \gamma(f) \text{ is bounded on } X \text{ for fixed } \gamma \in (A^p)^*\}$. Then there exists $B > 0$, independent of f , such that,

$$(i) |\gamma(f)| \leq B\|\gamma\|,$$

$$(ii) |f(z)| \leq \frac{BC(n_o, p, D)}{(l-r)^{2N_{n_0}/p}}, z \in \overline{D_r}, \text{ for } f \in X.$$

Proof. The proof of (i) is the same as the proof of theorem 7 (Walters, 1950) (ii) follows from (2.1), and lemma 4 (Marzuq, 1984b).

Proof of theorem 1.

Since $\gamma(f_n) \rightarrow \gamma(f)$ for all $\gamma \in (A^p)^*$, then $\gamma(f_n)$ is bounded independently of n . By lemma 1 we get,

$$(ii) |f_n(z)| \leq \frac{BC(n_o, p, D)}{(l-r)^{2N_{n_0}/p}} \text{ for } z \in \overline{D_r}, \text{ and the bound is independent of } n \text{ and } z.$$

Since $\gamma_z(f_n) = f_n(z)$ by (2.1), $f_n(z) \rightarrow f(z)$ for $z \in \overline{D_r}$.

Hence by Vitali's convergence theorem for C^N [(Valdimirov, 1966), lemma 4] $f_n(z) \rightarrow f(z)$ uniformly on compact subset of D .

4. A necessary and sufficient condition for a holomorphic function to belong to the space $A^p (p > 0)$.

We have the following theorem.

Theorem2. Let D be bounded symmetric domain, $z_o \in D_r, o < r < 1$, and f is holomorphic on D . Then $f \in A^p$ if and only if there exists a constant $C(z_0)$, independent of r , such that,

$$\int_D T(z_o, \bar{\xi}) |f_r(\xi)|^p dv_\xi \leq C(z_o), \quad (4.1)$$

where,

$$T(z, \bar{\xi}) = \frac{|k(z, \bar{\xi})|^2}{k(z, \bar{z})},$$

and $k(z, \bar{\xi})$ is the Bergman Kernel of D .

We need the following lemma for the proof of theorem 2.

Lemma2. The expression $T(z, \bar{\xi})dv_\xi$ is invariant under Γ , (the group of holomorphic automorphisms of D).

Proof. Let $\gamma \in \Gamma$ such that $\gamma(z) = 0$ and $\gamma(\xi) = \xi'$. Then,

$$\begin{aligned} T(z, \bar{\xi})dv_\xi &= \frac{|k(o, \xi')|^2 \left| \frac{\delta z'}{\delta z} \right|_{z'=o}^2 \left| \frac{\delta \xi'}{\delta \xi} \right|^2 \left| \frac{\delta \xi}{\delta \xi'} \right|^2 dv_{\xi'}}{|k(o, o)| \left| \frac{\delta z'}{\delta z} \right|_{z'=o}^2} \\ &= \frac{1}{V} dv_{\xi'}, \end{aligned} \quad (4.2)$$

(Bergman, 1950).

Proof of theorem2. Assume $f \in A^p$ for fixed $z \in D$, $\frac{k(z, \bar{\xi})}{k(z, z)}$ is continuous with respect to ξ on \overline{D} (Stoll, 1977).

Therefore,

$$\begin{aligned} \int_D T(z_o, \bar{\xi}) |f_r(\xi)|^p dv_\xi &\leq \max_{\xi \in \overline{D}} T(z_o, \bar{\xi}) VM_p^{1/p}(r, f) \\ &\leq C(z_o) \|f\|_{A^p} = C(z_o). \end{aligned}$$

This proves the necessity of (4.1).

Conversely, assume (4.1) is satisfied.

Then,

$$\frac{1}{V} \int_D |f(r\xi')|^p dv_{\xi'} = \int_D T(o, \bar{\xi}') |f(r\xi')|^p dv_{\xi'}.$$

For, $\xi \in D$, there exists a holomorphic automorphisms say Y_ξ such that $Y_\xi(z_0) = 0$ which maps ξ into ξ' then by (4.2) we get,

$$\frac{1}{V} \int_D |f(r\xi')|^p dv_{\xi'} = \int_D T(z_0, \bar{\xi}) |f(r\xi)|^p dv_\xi \leq C(z_0).$$

Hence,

$$\sup_{0 \leq r < 1} \left| \frac{1}{V} \int_D |f(r\xi')|^p dv_{\xi'} \right| \leq C(z_0) < \infty,$$

and $f \in A^p$.

REFERENCES

Bergman, S. 1950. The Kernal Function and Conformal Mapping, Math Surveys 5. American Math. Soc., New York, USA.

Marzuq, MMH. 1984^a. Remarks on Bergman space over bounded star-shaped circular domain in $C^N(N > 1)$. Journal of Univ. Kuwait, (Sci). 207-209.

Marzuq, MMH. 1984^b. General form of linear functional in A^p space over irreducible bounded symmetric domain in ($N > 1$). Chinese Journal of Mathematics. 12(2):97-102.

Hahn, KT. and Mitchell, J. 1969. H^p Space on bounded symmetric domains. Trans. Amer. Math. Soc. 146:521-531.

Koranyi, A. and Wolf, JA. 1965. Realization of Hermitian symmetric spaces on generalized half-planes. Ann. of Math. 81:265-288.

Rudin, W. 1974. Real and Complex Analysis (2nd edi.), McGraw-Hill, New York, USA.

Stoll, M. 1977. Mean value theorems for harmonic and holomorphic functions on bounded symmetric domains. J. Reine Ansew. Math. 290:191-198.

Vladimirov, VS. 1966. Method of the Theory of Functions of Several Complex Variables. MIT Press, Cambridge, Mass.

Walters, SS. 1984. The Space H^p with $0 < p < 1$, Proc. Amer. Math Soc. 6:800-805.

Received: Dec 11, 2011; Accepted: March 24, 2012

Short Communication

A NEW APPROACH TO STATISTICAL INFERENCE FOR EXPONENTIAL DISTRIBUTION BASED ON RECORD VALUES

Parviz Nasiri, *Saman Hosseini and Masoud Yarmohammadi
 Department of Statistics, University of Payame Noor, 19395-4697 Tehran, Iran

ABSTRACT

In this paper, we use the upper record range statistic to draw inferences from the scale parameter of the exponential distribution. These inferences are point estimation and interval estimation. We obtained MRE estimations under three different loss functions: Quadratic, Squared error and Absolute error loss function. Moreover, we derive the shortest interval and interval estimation with equal tails. Finally, we present some practical examples and simulations by using the method of inverse distribution transformation.

Keywords: Exponential distribution, scale parameter, record values, upper record range, estimation based on upper record range.

1-INTRODUCTION

Let X_1, X_2, X_3, \dots be a sequence of independent and identically distributed (iid) random variable with cumulative distribution function (cdf) $F(x)$ and probability density function (pdf) $f(x)$. For $n \geq 1$ define

$$T(1) = 1, T(n+1) = \min\{j; X_j > X_{T(n)}\}.$$

The sequence $\{X_{T(n)}\}_{n=1}^{\infty}$ is known as upper record values and the sequence $\{T(n)\}_{n=1}^{\infty}$ is known as record times sequence (Arnold *et al.*, 1998). At first Chandler (1952) introduced the concepts of record values, times and related statistics theoretically. Interested reader may refer to Arnold *et al.*, 1998; Nagaraja, 1988; Nevezorov 1946 for basic concepts of this subject. Some inferential studies based on record values and record times have been done by Ahsanullah (1990), Balakrishnan *et al.* (1995), Feuerverger and Hall (1998). Consider the one-parameter Exponential distribution with scale parameter δ and pdf

$$f(x; \delta) = \frac{1}{\delta} e^{-\frac{x}{\delta}}, x \geq 0, \delta > 0. \quad (1)$$

and cdf

$$F(x; \delta) = 1 - e^{-\frac{x}{\delta}}, x \geq 0, \delta > 0. \quad (2)$$

The exponential distribution occurs naturally when describing the lengths of the inter-arrival times in a homogeneous Poisson process. Exponential variables can also be used to model situations where certain events occur with a constant probability per unit length, such as the distance between mutations on a DNA strand, or between road kills on a given road. In queuing theory, the service times of agents in a system (e.g. how long it takes for a bank teller etc to serve a customer) are often

modeled as exponentially distributed variables. Reliability theory and reliability engineering also make extensive use of the exponential distribution. In physics, if you observe a gas at a fixed temperature and pressure in a uniform gravitational field, the heights of the various molecules also follow an approximate exponential distribution. In hydrology, the exponential distribution is used to analyze extreme values of such variables as monthly and annual maximum values of daily rainfall and river discharge volumes. Balakrishnan *et al.* (1995) have established some recurrence relations for single and product moments of record values from exponential distribution based on record values. Ahmadi *et al.* (2005) have obtained estimation and prediction based on k-record values for two-parameter exponential distribution. Ahsanullah and Kirmani (1991) have obtained some characterizations of the exponential distribution based on lower record values. Finding different methods for statistical inference based on records is the purpose of this article. In the situation that we have only the smallest and the largest data, the statistics based on $X_{T(1)}$ and $X_{T(n)}$ will play an important role in the statistical inferences. This occurs in many real situations such as stock exchange. Consider a statistician who wants to make the statistical inferences about the prices of stocks and shares in a stock market. Usually the middle prices are not recorded and we have only the largest and the base prices. Pharmacy is another instance. For confirming the effectiveness of drugs and poisons the upper and lower levels of effectiveness is used. Because the decisions are made based on the largest and the smallest values, they are of importance. When we want to make inference based on the largest record and the smallest record values, one of the best choices is $R_{U,R}$

*Corresponding author email: s.hosseini.stat@gmail.com

which is defined by $R_{U,R} = X_{T(n)} - X_{T(1)}$. In this article we try to make inference based on this statistic therefore in section 2, we estimate the scale parameter δ using the classical methods consisting MLE and MME, MRE estimation. In section 3, we determine shortest interval and interval with equal tail probabilities based on $R_{U,R}$ also in section 4; we present some practical examples and simulations.

2-UPPER RECORD RANGE AND POINT ESTIMATIONS

Suppose that in a random sample from a population with probability density function $f(x)$, the record values are $X_{T(1)}, X_{T(2)}, \dots, X_{T(n)}$. The joint pdf $f(x_{T(1)}, x_{T(2)}, \dots, x_{T(n)})$ is (see [1])

$$f(x_{T(1)}, x_{T(2)}, \dots, x_{T(n)}, \delta) = f(x_{T(n)}, \delta) \prod_{i=1}^{n-1} h(x_{T(i)}, \delta), \quad (3)$$

where $h(x_{T(i)}, \delta) = \frac{f(x_{T(i)}, \delta)}{1 - F(x_{T(i)}, \delta)}$.

Therefor from (1) and (2), (3) we have

$$f(x_{T(1)}, x_{T(2)}, \dots, x_{T(n)}, \delta) = \frac{1}{\delta^n} \exp\left(-\frac{x_{T(n)}}{\delta}\right),$$

where $x_{T(1)} < x_{T(2)} < \dots < x_{T(n)}$.

Integrating out $X_{T(2)}, \dots, X_{T(n-1)}$, we get the join pdf

$f(x_{T(1)}, x_{T(n)})$ as

$$f(x_{T(1)}, x_{T(n)}) = \frac{1}{(n-2)\delta^n} (x_{T(n)} - x_{T(1)})^{n-2} \exp\left(-\frac{x_{T(n)}}{\delta}\right),$$

where

$0 < x_{T(1)} < x_{T(n)} < \infty$.

Using the transformations $R_{U,R} = X_{T(n)} - X_{T(1)}$,

$U = X_{T(n)}$ and integrating out U, we obtain pdf $f_{R_{U,R}}(r)$ of $R_{U,R}$ as

$$f_{R_{U,R}}(r) = \frac{r^{n-2} \exp\left(-\frac{r}{\delta}\right)}{(n-2)\delta^{n-1}}, r > 0. \quad (4)$$

This means that $R_{U,R} = X_{T(n)} - X_{T(1)}$ is distributed as $\text{gamma}(n-1, \delta)$.

A. The Method of Maximum Likelihood Estimation (MLE) Based on Upper Record Range Statistic

From (4) log likelihood function is,

$$\begin{aligned} L(\delta | r) &= \log \left[f_{R_{U,R}}(r | \delta) \right] = (n-2) \log(r) - \\ &\log(n-2)! - (n-1) \log(\delta) - \frac{r}{\delta} \end{aligned} \quad (5)$$

The MLE of δ can be obtained by solving the following likelihood equation

$$\frac{\partial L}{\partial \delta} = 0. \quad (6)$$

By solving equation (6) the MLE estimation based on upper record range for the parameter δ can be obtained as

$$\hat{\delta}_{MBURR} = \frac{x_{T(n)} - x_{T(1)}}{n-1}, \quad (7)$$

Note that

$$E[\hat{\delta}_{MBURR}] = \delta, \text{Var}(\hat{\delta}_{MBURR}) = \frac{\delta^2}{n-1}.$$

By considering the Factorization theorem and rewriting (4) as below we find that $R_{U,R}$ is the sufficient and complete statistic for the parameter δ .

$$f_{R_{U,R}}(r | \delta) = \frac{r^{n-2} \exp\left(-\frac{r}{\delta}\right)}{(n-2)\delta^{n-1}} = h(r)g(r, \delta). \quad (8)$$

Therefore from (7) and (8), $\hat{\delta}_{MBURR}$, is equal to $\hat{\delta}_{MBURR}$.

B. THE METHOD OF MOMENT ESTIMATION

Let $R_{U,R,i}$ be the iid sample from Upper Record Range statistic. This occurs in the situation that we have m random samples by size n from the pdf $f(x)$. In fact this occurs because we have an upper record range per sample. In this situation the MM estimation is obtained by solving the moment equations

$$E[R_{U,R}^k] = \frac{1}{m} \sum_{i=1}^m R_{U,R,i}^k. \quad (9)$$

From (4) and putting k=1 in (9), the moment equation can be derived as

$$(n-1)\delta = \frac{1}{m} \sum_{i=1}^m r_i.$$

Consequently the MM estimation is given by

$$\hat{\delta}_{MMBURR} = \frac{1}{m(n-1)} \sum_{i=1}^m R_{U,R,i}$$

Note that

$$E[\hat{\delta}_{MMBURR}] = \delta, \text{Var}(\hat{\delta}_{MMBURR}) = \frac{\delta^2}{m(n-1)}.$$

C. MINIMUM RISK EQUIVARIANT (MRE) ESTIMATIONS

In this section we consider three kinds of loss functions to obtain the MRE estimation based on $R_{U,R}$ for the scale parameter δ . The loss functions are i-Quadratic loss ii-Squared error loss iii-Absolute error loss function. Let G be a group of transformations in the form

$$G = \{g_a: g_a(x) = ax, a > 0\}.$$

Then the exponential distribution (1) and the loss functions (i) and (ii), (iii) are invariant under G . By this introduction we try to obtain the MRE estimations based on upper record range in three subsections.

I. MINIMUM RISK EQUIVARIANT (MRE) ESTIMATION BASED ON UPPER RECORD RANGE UNDER THE QUADRATIC LOSS FUNCTION

By considering quadratic loss function (i) the minimum risk equivariant estimation (MRE) of δ is given by Lehmann and Casella (1998)

$$\delta^*(X) = \frac{\delta_0(X)}{\omega^*(X)}, \quad (10)$$

where δ_0 is any scale equivariant estimator of δ and $\omega(\mathbf{Z}) = \omega^*(\mathbf{Z})$ minimizes

$$\mathbb{E}_{\delta=1} \left[\gamma \left(\frac{\delta_0(\mathbf{X})}{\omega(\mathbf{X})} \right) \middle| \mathbf{Z} \right], \quad (11)$$

where $\mathbf{Z} = \frac{\mathbf{R}_{U,R}}{|\mathbf{R}_{U,R}|}$ and γ is an invariant loss function. By considering quadratic loss function (i) we have

$$\omega^*(\mathbf{Z}) = \frac{\mathbb{E}_{\delta=1}[\delta_0(\mathbf{X})|\mathbf{Z}]}{\mathbb{E}_{\delta=1}[\delta_0(\mathbf{X})|^2]}.$$

Because of equivariance of the MLE based on $\mathbf{R}_{U,R}$ (δ_{MBURR}), we assume $\delta_0 = \delta_{MBURR}$. Since \mathbf{Z} is ancillary, by Basu's theorem, δ_0 is independent of \mathbf{Z} , and hence

$$\omega^*(\mathbf{Z}) = \frac{\mathbb{E}_{\delta=1}[\delta_0(\mathbf{X})]}{\mathbb{E}_{\delta=1}[\delta_0(\mathbf{X})]^2} = \frac{n}{n-1}. \quad (12)$$

From (10), (12) and by considering $\delta_0 = \delta_{MBURR}$ the MRE estimation based on $\mathbf{R}_{U,R}$ is

$$\delta_{MRE,1}^* = \frac{\frac{x_{T(n)} - x_{T(1)}}{n-1}}{\frac{n-1}{n}} = \frac{x_{T(n)} - x_{T(1)}}{n}.$$

Note that

$$\mathbb{E}[\delta_{MRE,1}^*] = \frac{n-1}{n} \delta, \quad \text{Var}(\delta_{MRE,1}^*) = \frac{n-1}{n^2} \delta^2.$$

Therefore the MRE estimation based on $\mathbf{R}_{U,R}$ under quadratic loss function is asymptotically unbiased. It also converges in probability to the parameter δ .

III. MINIMUM RISK EQUIVARIANT (MRE) ESTIMATION BASED ON UPPER RECORD RANGE UNDER THE SQUARED ERROR LOSS FUNCTION

Following the last subsection, and considering (10), (11) with Squared error loss function we can obtain the $\omega^*(\mathbf{X})$ as

$$\omega^*(\mathbf{Z}) = \mathbb{E}_{\delta=1}[\delta_0|\mathbf{Z}].$$

Because \mathbf{Z} is an ancillary statistic it satisfies the conditions of Basu's theorem, so δ_0 is independent from \mathbf{Z} and we have

$$\omega^*(\mathbf{Z}) = \mathbb{E}_{\delta=1}[\delta_0] = \frac{n-1}{n-1} = 1. \quad (13)$$

Consequently from (10) and (13) we can easily obtain the MRE estimation based on $\mathbf{R}_{U,R}$ under squared error loss function as

$$\delta_{MRE,2}^* = \frac{\frac{x_{T(n)} - x_{T(1)}}{n-1}}{1} = \frac{x_{T(n)} - x_{T(1)}}{n-1},$$

As it is seen the obtained MRE in this subsection ($\delta_{MRE,2}^*$) is equal to MLE estimation. Therefor

$$\mathbb{E}[\delta_{MRE,2}^*] = \delta, \quad \text{Var}(\delta_{MRE,2}^*) = \frac{\delta^2}{n-1}.$$

As we can see, $\delta_{MRE,2}^*$ converges in probability to δ and also has asymptotically unbiased property.

III. MINIMUM RISK EQUIVARIANT (MRE) ESTIMATION BASED ON UPPER RECORD RANGE UNDER THE SQUARED ERROR LOSS FUNCTION

Considering the absolute error loss function (iii) and $\delta_0 = \delta_{MBURR}$, because δ_0 is independent from \mathbf{Z} (Basu's theorem), ω^* is

$$\omega^*(\mathbf{Z}) = \text{Median}_{\delta=1}(\delta_0|\mathbf{Z}) = \text{Median}_{\delta=1}(\delta_0).$$

After some algebraic manipulation $\omega^*(\mathbf{Z})$ is given by

$$\omega^*(\mathbf{Z}) = \text{Median}_{\delta=1}(\delta_{MBURR}) = \frac{x_{2n-2,0.5}^2}{2n-2},$$

and consequently by (10), (11), the MRE estimation based on $\mathbf{R}_{U,R}$ under absolute error loss function ($\delta_{MRE,3}^*$) can be obtained as

$$\delta_{MRE,3}^* = \frac{\delta_0}{\omega^*(\mathbf{Z})} = \frac{2\mathbf{R}_{U,R}}{x_{2n-2,0.5}^2}.$$

3-INTERVAL ESTIMATION BASED ON UPPER RECORD RANGE STATISTIC

A. CONFIDENCE INTERVAL WITH EQUAL TAILS

In this section we obtain two-sided confidence interval with equal tail probabilities based on $\mathbf{R}_{U,R}$. Adopting the usual approach we consider the pivot quantity (Q) as a function of minimal sufficient statistic (based on $\mathbf{R}_{U,R}$). Therefore from (8)

$$Q = \frac{2\mathbf{R}_{U,R}}{\delta}.$$

By considering the pdf of $\mathbf{R}_{U,R}$ (4) and obtaining the distribution of Q , it is clear that Q is distributed as chi-squared with $2n-2$ degrees of freedom. For obtaining confidence interval with equal tails, a , b must be determined from these equations

$$P(a < Q < b) = \int_a^b f_Q(t) dt = 1 - \alpha, \quad (14)$$

and

$$P(Q < a) = \frac{\alpha}{2}, \quad P(Q > b) = \frac{\alpha}{2}.$$

Some algebraic manipulation gives us a , b as

$$a = x_{2n-2,1-\frac{\alpha}{2}}^2, \quad b = x_{2n-2,1-\frac{\alpha}{2}}^2$$

Therefore the confidence interval with equal tail probabilities based on $\mathbf{R}_{U,R}$ is given by

$$\frac{2\mathbf{R}_{U,R}}{x_{2n-2,1-\frac{\alpha}{2}}^2} < \delta < \frac{2\mathbf{R}_{U,R}}{x_{2n-2,\frac{\alpha}{2}}^2}$$

Consequently the length is

$$L = \frac{2\mathbf{R}_{U,R}}{x_{2n-2,\frac{\alpha}{2}}^2} - \frac{2\mathbf{R}_{U,R}}{x_{2n-2,1-\frac{\alpha}{2}}^2}.$$

B. THE SHORTEST INTERVAL BASED ON UPPER RECORD RANGE STATISTIC

In this section we want to obtain the shortest confidence interval based on upper record range. Using the obtained pivot quantity in last section we have the general intervals as $\frac{R_{UR}}{b} < \delta < \frac{2R_{UR}}{a}$.

Consequently the length of these general interval is $L = 2R_{UR}(\frac{1}{a} - \frac{1}{b})$.

For obtaining the shortest interval we should choose a, b such that minimize the length (15) and satisfy equation (14). Using Lagrange multipliers method

$$\psi(a, b, \lambda) = 2R_{UR}\left(\frac{1}{a} - \frac{1}{b}\right) + \lambda\left(\int_a^b f_q(t)dt - (1 - \alpha)\right)$$

After derivation by λ, a, b we have

$$\begin{cases} \int_a^b f_q(t)dt = 1 - \alpha \\ \frac{-2R_{UR}}{a^2} - \lambda f'(a) = 0 \\ \frac{2R_{UR}}{b^2} + \lambda f'(b) = 0 \end{cases} \Rightarrow \begin{cases} \int_a^b f_q(t)dt = 1 - \alpha \\ a^2 f_q(a) = b^2 f_q(b) \end{cases} \quad (16)$$

The equations (16) have solved by Tate and Klett in 1959 numerically .

4-SIMULATION AND ILLUSTRATIVE EXAMPLE

To illustrate the estimation techniques developed in this section, we consider simulated data bellow from Exponential distribution with $\delta = 1$ using the transformation: $x_i = \delta \ln(1 - u_i)$ where u_i is the uniformly distributed random variable. Suppose that we observed the following simulated data from $\text{Exp}(1)$:

1.179469281, 0.613291030, 0.976919804, 0.940902389, 3.151606189, 0.454850203, 0.333882858, 0.090855689, 0.745590594, 0.817341702, 0.087011920, 0.160546310, 0.415345196, 0.175461572, 3.440819603, 0.208336688, 1.833271636, 2.183783235, 0.446134909, 2.475039374, 1.566538736, 0.886839452, 0.192790814, 2.910071106,

Table 1. MSE's of the estimators $\hat{\delta}_{MBURR}, \hat{\delta}_{MRE,1}, \hat{\delta}_{MRE,2}$

Number of Record	Estimator	Estimated Value	Bias	MSE
n=2	$\hat{\delta}_{MBURR}$	1.9721369	0	3.8893240
		1.1306752	0	0.6392132
		0.8871568	0	0.2623491
		0.6957966	0	0.1210332
n=3	$\hat{\delta}_{MRE,1}$	0.9860685	-0.4930342	0.48616550
		0.7537834	-0.2512611	0.18939649
		0.6653676	-0.1663419	0.11067851
		0.5566373	-0.1113275	0.06196902
n=4	$\hat{\delta}_{MRE,2}$	2.8451921	1.25955245	18.4354005
		1.3473676	0.25822124	1.3556359
		0.9952918	0.12131555	0.4303215
		0.7579359	0.06768867	0.1749957

1.163082090, 0.700168337, 0.628095536, 1.683433609, 0.326647849, 1.505027254, 0.709244532, 0.090130483, 1.733876883, 1.791106060, 1.483518345, 0.806656142, 0.002559691, 0.250612339, 0.665047009, 0.192063370, 0.462457812, 1.534055037, 0.181744265, 0.987930554, 0.942945984, 0.943769307, 0.319857968, 0.391021464, 1.697728186, 0.373492095, 1.798812738, 0.496551487, 0.480822546, 0.733421176, 0.737249271, 0.013362448, 1.343100225, 0.180633059, 0.893504639, 1.635429019, 3.840939633, 1.064201159, 1.292336585, 2.076699583, 0.112648713, 3.287097308, 1.984361935, 0.769430699, 1.943481857, 0.553695515, 0.900427014, 0.618240746, 1.583467962, 1.617647828, 2.022053674, 1.482866347, 0.324673680, 3.962655875, 1.152818131, 0.568594399, 0.990417301, 2.133633081, 1.435067333, 1.404984828, 0.438741200, 2.144196713, 0.585965825, 0.239035694, 0.178914244, 2.684646233, 0.514393762, 1.038429367, 0.533911966, 2.749416188, 0.872397132, 0.505439471, 1.475022686, 0.862180884, 0.660766382, 1.385093522

Therefore, we observe the record values from the simulated data as follows: 1.179469, 3.151606, 3.440820, 3.840940, 3.962656.

Here then, for the simulated records, with $n = 2, 3, 4, 5$ MSE's of the point estimations and Length of the Shortest interval estimation and interval with equal tails are obtained and presented in tables 1, 2 and 3, respectively.

CONCLUSION

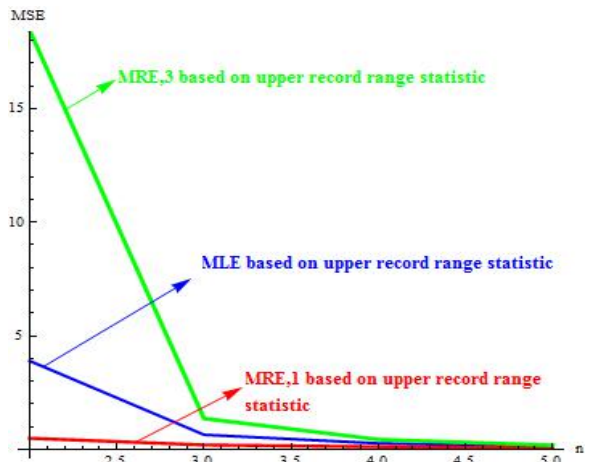
In this paper, the MLE, MME and MRE estimations based on upper record range statistic were obtained. Later MRE estimations were obtained for three types of loss functions. On the other hand, the shortest interval confidence based on R_{UR} was obtained. To get this interval confidence, the researcher encountered equations (16) which Tate and Klett (1959) they have solved numerically. Using these results, the shortest confidence interval was obtained and shown in table 2. Also, the

Table 2. Shortest interval estimation and Lengths based on upper record range statistic.

Number of Record	Confidence level	Lower limit	Upper limit	Length
n=2	90%	0.2190326	18.431186	18.212153
		0.2497874	4.282455	4.032668
		0.2678357	2.447329	2.179493
		0.2525520	1.624649	1.372097
n=2	95%	0.1836152	38.480720	38.297105
		0.2147205	6.386191	6.171471
		0.2340680	3.279086	3.045018
		0.2234172	2.059560	1.836143
n=2	99%	0.1353737	196.232528	196.097155
		0.1646996	15.233077	15.068378
		0.1842307	6.118323	5.934092
		0.1792672	3.394751	3.215484

Table 3. Interval with equal tail probabilities and Lengths based on upper record range statistic.

Number of Record	Confidence level	Lower limit	Upper limit	Length
n=2	90%	0.6583155	38.448240	37.789925
		0.4766895	6.363521	5.886831
		0.4227379	3.254859	2.832121
		0.3589515	2.036997	1.678046
n=2	95%	0.5346168	77.895247	77.360630
		0.4058677	9.336349	8.930481
		0.3683855	4.301908	3.933522
		0.3174518	2.553698	2.236246
n=2	99%	0.3722195	393.440489	393.068270
		0.3043487	21.849947	21.545598
		0.2869884	7.877356	7.590368
		0.2535361	4.140374	3.886838

Fig. 1. MSE's of the estimators $\hat{\theta}_{MBUR}$, $\hat{\theta}_{MRE,1}$, $\hat{\theta}_{MRE,3}$ based on upper record range statistic.

theoretical results of the study are shown and explained numerically by simulation in the following ways. Table 1 shows that MRE estimation based on $R_{U,R}$ under quadratic loss function has the lowest MSE in comparison with MLE estimation based on $R_{U,R}$ with MRE estimation

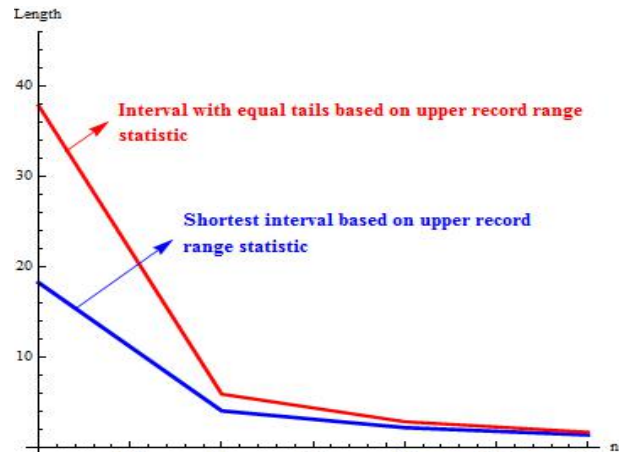


Fig. 2. Length's of the Shortest Interval and interval with equal tails Estimations based on upper record range statistic for 90% confidence.

under squared error loss function. This comparison is shown more vividly in figure 1. In table 2, Shortest interval confidences and their Lengths for records number 2, 3, 4, 5 and confidence ratio 90, 95, 99 levels have been obtained. The longer the "n", the shorter the interval distance. Table 3, shows interval with equal tails and their

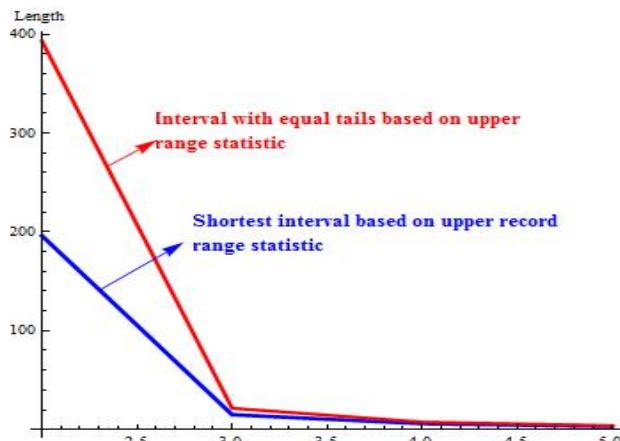


Fig. 3. Length's of the Shortest Interval and interval with equal tails Estimations based on upper record range statistic for 95% confidence.

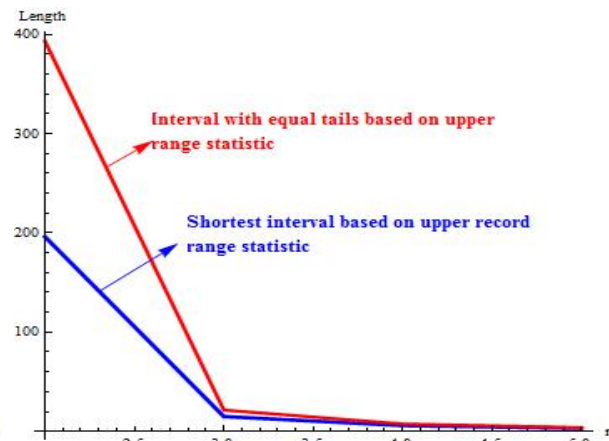


Fig. 4. Length's of the Shortest Interval and interval with equal tails Estimations based on upper record range statistic for 99% confidence.

Lengths for records number 2, 3, 4, 5 and confidence ratio of 90, 95, 99 levels. By comparing tables 2 and 3, the researcher reaches the point that shortest interval based on upper record range have the shorter length than the interval confidence with equal tails. This comparison has been done in figures 2, 3, 4 for different confidence levels.

REFERENCES

- Ahsanullah, M. 1990. Estimation of the Parameters of the Gumbel Distribution Based on m Record Values. Computational Statistics. Quarterly. 6:231-239.
- Ahsanullah, M. and Kirmani, SNUA. 1991. Characterizations of the Exponential Distribution through a Lower Records. Communications in Statistics-Theory and Methods. 20:1293-1299.
- Arnold, BC., Balakrishnan, N. and Nagaraja, HN. 1998. Records, Wiley, Canada.
- Ahmadi, J., Doostparast, M. and Parsian, A. 2005. Estimation and Prediction in a two Parameter Exponential Distribution based on k -record Values under LINEX loss Function. Communication in Statistics. Theory and Methods. 34:795-805.
- Balakrishnan, N. and Ahsanullah, M. 1978. Relations for Single and Product Moment of Record values from Exponential Distribution. Journal of Applied Statistical Science. 2:73-87.
- Balakrishnan, N., Ahsanullah, M. and Chan, PS. 1995. On the Logistic record values and associated Inference. Journal of Applied Statistical Science. 2:233-248.
- Feuerverger, A., Hall, P. 1998. On Statistical inference based on record Values. Extremes. 12:169-190.
- Lehmann, EL. and Casella, G. 1998. Theory of Point Estimation. Springer, New York, USA.
- Nagaraja, HN. 1988. Record values and related Statistics - a Review, Communications in Statistics - Theory and Methods. 17(2):2233-2238.
- Nevzorov, VB. 2001. Records: Mathematical Theory, American Mathematical Society, USA.
- Tate, RF. and Klett Source, GW. 1959. Optimal Confidence Interval for the Variance of a Normal Distribution. Journal of the American Statistical Association. 54:287:674-682.

Received: Dec 20, 2011; Accepted: April 3, 2012

Short Communication

STATISTICAL ANALYSIS OF MEDICAL DATA ON ANOREXIA NERVOSA PATIENTS

*JI Mbegbu¹, E Akpeli¹ and FO Chete²

¹Department of Mathematics, University of Benin, Benin City

²Department of Computer Science, University of Benin, Benin City, Nigeria

ABSTRACT

A sample of twenty anorexia nervosa patients on admission at Government Psychiatric Hospital, Uselu, Benin City were placed on antidepressant, vitamin and mineral supplements. After they were discharged from the hospital, an investigation was carried out to ascertain treatment effect of the drugs on the patients. On the assumption of normality of gain or loss in the body mass indices (BMI) of the patients, the null hypothesis of no treatment effect was rejected. The statistical results showed that the drugs yielded a significant treatment effect on the patients.

Keywords: Anorexia nervosa, antidepressant, body mass index, bootstrapping, null hypothesis, patients.

INTRODUCTION

Anorexia nervosa is an eating disorder characterized by refusal to maintain a healthy body weight, and an obsessive fear of gaining weight (Keys, 1972). It is a serious mental illness and the highest mortality rate of any psychiatric disorder. Keys (1972) expatiates that a person is underweight if his/her body mass index (BMI) is in the interval $[16\text{kg}/\text{m}^2, 18.5\text{kg}/\text{m}^2]$; normal weight if his/her BMI lies in the interval $[18.5\text{kg}/\text{m}^2, 25\text{kg}/\text{m}^2]$; and overweight if his/her BMI is in the interval $[25\text{kg}/\text{m}^2, \infty)$. Body mass index (BMI) of a patient is explained as the weight (in kilograms) of a patient divided by the square of his or her height (in metres). Medical data on the body mass indices of anorexia nervosa patients that were on admission at Government Psychiatric Hospital, Benin City, Nigeria and after discharge, were collected respectively for possible statistical investigation of treatment effect of drugs on the patient. In line with the works of Armitage and Berry (1994) and Altman (1991), the paired t-test statistic under the hypothesis of equal mean body mass indices for the patients on admission and after discharge from the hospital is most suited for the analysis of these data. The paired t-test statistic according to Sarmukaddam (2006) is applicable under the assumption that the data are quantitative, the distribution of the differences in body mass indices of patients on admission and after discharge is normal, and these differences are independent of each other.

Consequently, rejecting the null hypothesis of equal mean body mass indices (BMI) of patients on admission and after discharge from the hospital statistically implies no treatment effect of drugs on the patients.

MATERIALS AND METHODS

Methods

Let $[x_1, x_2, \dots, x_n]$ and $[x_1^*, x_2^*, \dots, x_n^*]$ be the body mass indices (BMI) of anorexia nervosa patients on admission and after discharge from the hospital respectively. Define the differences $d_i = x_i^* - x_i$, for $i = 1, 2, \dots, n$, which are assumed to be normally distributed with unknown mean μ_d and variance σ_d^2 .

Hence, under the null hypothesis of equal mean body mass indices, $\mu_d = \mu^* - \mu = 0$, the random variable

$$T = \frac{\bar{d}\sqrt{n}}{s_d} \quad (2.1)$$

has the t-distribution (Montgomery and Runger, 2003)

$$f(x) = \frac{\Gamma\left(\frac{n+1}{2}\right)}{\sqrt{\pi n} \Gamma\left(\frac{n}{2}\right) \left(\frac{x^2}{n} + 1\right)^{\frac{n+1}{2}}}, \quad -\infty < x < \infty \quad (2.2)$$

with $(n-1)$ degrees of freedom, where

μ^* = mean BMI of patients after discharge

μ = mean BMI of patients on admission

μ_d = mean difference in BMI

\bar{d} = estimate of μ_d

σ_d^2 = variance of differences in BMI

*Corresponding author email: odichet@yahoo.com

$$\begin{aligned}s_d^2 &= \text{estimate of } \sigma_d^2 \\n &= \text{sample size.}\end{aligned}$$

Let $t_{0.05,n-1}$ be the value of the random variable, T with $(n-1)$ degrees of freedom. Thus, $t_{0.05,n-1}$ is an upper tail 95 percent point of the t-distribution with $(n-1)$ degrees of freedom. Now, the decision to reject the null hypothesis of no treatment effect on the patients depends on whether (statistical rule) the value of the random variable, $T > t_{0.025,n-1}$ or $T < -t_{0.025,n-1}$.

Evidently, we have the statement of hypothesis

$$H_0 : \mu_d = \mu^* - \mu = 0 \quad (2.3)$$

$$H_1 : \mu_d = \mu^* - \mu \neq 0$$

and 95 percent confidence interval for the mean difference μ_d as

$$(\bar{d} - s_d t_{0.025,n-1}, \bar{d} + s_d t_{0.025,n-1}) \quad (2.4)$$

The statistics \bar{d} and s_d are obtained by creating 200 bootstrap samples of the differences d_i 's through bootstrap re-sampling approach. Bootstrapping according to Efron and Tibshirani (1993) is a computer based method for assigning measures of accuracy to sample estimates. This method according to Varian (2005) can be implemented by constructing a number of re-samples of the d_i 's, each of which is obtained by random sampling with replacement from the original data set, d_1, d_2, \dots, d_n (see Table 1)

Table 1. Bootstrapping Method.

Bootstrap Sample	Re-samples (differences, d_i)	Bootstrap estimates
1	$d_1^*, d_2^*, \dots, d_n^*$	$\hat{\mu}_d^1$
2	$d_1^*, d_2^*, \dots, d_n^*$	$\hat{\mu}_d^2$
3	$d_1^*, d_2^*, \dots, d_n^*$	$\hat{\mu}_d^3$
\vdots	$\vdots \quad \vdots \quad \vdots$	\vdots
200	$d_1^*, d_2^*, \dots, d_n^*$	$\hat{\mu}_d^{200}$

By bootstrapping method,

$$\bar{d} = \frac{1}{200} \sum_{i=1}^{200} \hat{\mu}_d^i \quad (2.5)$$

and

$$s_d = \sqrt{\frac{1}{199} \sum_{i=1}^{200} (\hat{\mu}_d^i - \bar{d})^2} \quad (2.6)$$

Data Collection

The body mass indices (BMI) of twenty (20) patients who were treated for anorexia nervosa on admission, and their body mass indices (BMI) after discharge from the hospital were recorded as shown in table 2.

Table 2. BMI of Anorexia nervosa Patients.

BMI of patients on Admission (kg/m^2)	16.84	16.26	14.33	14.30
	11.98	13.59	13.95	14.02
	12.22	12.00	16.05	15.86
	11.55	15.76	14.12	14.44
	18.12	12.30	15.25	
BMI of patients after discharge (kg/m^2)	24.03	18.50	16.61	16.57
	18.99	15.62	25.96	13.82
	21.09	21.38	13.17	17.32
	16.07	17.22	13.06	14.72
	21.16	18.92	18.01	

Source: Government Psychiatric Hospital, Benin City, Nigeria.

RESULTS AND DISCUSSION

The body mass indices's gain or loss for the patients is shown in table 3.

Table 3. BMI's Gain or Loss.

7.19	2.24	2.28	2.27	7.01
2.03	10.93	(-) 0.13	7.07	9.16
0.34	(-) 2.88	1.46	4.52	1.46
(-) 1.06	0.28	3.04	6.62	2.76

Bootstrapping the data set in table 3 generates the values of the statistics $\bar{d} = 3.33$ and $s_d = 3.61$ respectively.

Hence,

$$\bar{d} - s_d t_{0.025,19} = -4.23 \text{ and}$$

$$\bar{d} + s_d t_{0.025,19} = 10.89$$

The 95 percent confidence interval for the mean difference, μ_d is (-4.23, 10.89), and the value of random variable, T = 4.13. Since T > 2.093 we reject the null hypothesis, H_0 of no treatment effect on the basis of sample data. Statistically the confidence interval for μ_d is quite wide which evidently supports the formulation of the hypothesis since zero lies in the confidence interval.

CONCLUSION

The patients on admission that were placed on antidepressants, vitamins and mineral supplements responded positively to the treatment since the null hypothesis H_0 of no treatment effect was rejected.

Hence, on the basis of sample data we conclude in statistical terms that the drugs yielded a significant treatment effect on the patients.

REFERENCES

Sarmukaddam, SB. 2006. Fundamentals of Biostatistics. Jaypee Brothers Medical Publishers Ltd, New Delhi, India. 91-93.

Altman, DG. 1991. Practical Statistics for Medical Research. Chapman and Hall, London. 37-39.

Armitage, P. and Berry, G. 1994. Statistical Methods in Medical Research (3rd ed.). Blackwell Scientific Publications, Oxford. 112-113.

Efron, B. and Tibshirani, RJ. 1993. An Introduction to the Bootstrap. Chapman and Hall, New York, USA. 201-209.

Keys, A. 1972. Body Composition and its change with age and diet. Journal of Chronic Diseases. 25(6 & 7):329-342.

Montgomery, DC. and Runger, GC. 2003. Applied Statistics and Probability for Engineers (3rd ed.). John Wiley and Sons Inc., USA. 245-265.

Varian, H. 2005. Bootstrap Tutorial. Mathematics Journal. 9:768-775.

Received: Feb 10, 2012; Accepted: April 17, 2012

Short Communication

ON DEPENDENT ELEMENTS AND FREE ACTION OF DERIVATIONS IN SEMIPRIME Γ -RINGS

*Nishteman N Suliman¹ and Abdul-Rahman H Majeed²

¹Department of Mathematics, College of Education, Scientific Departments, Salahaddin University – Erbil

²Department of Mathematics, College of Science, Baghdad University, Iraq

ABSTRACT

In this paper we characterize a dependent element of a derivation on a semiprime Γ -ring M . It is shown that the dependent elements of a derivation d of a semiprime Γ -rings M are central, and it is proved that if a is a dependent element of a derivation d of M , then there exist ideals U and V of the semiprime Γ -ring M such that (i) $U \oplus V$ is an essential ideal of M . (ii) $d = 0$ on U , and $d(V) \subseteq V$ and (iii) the derivation d of the semiprime Γ -ring M is free action on V . Furthermore, some of results of free action for several mappings in prime and semiprime Γ -rings are given.

2000 Mathematics Subject Classification: 16W25, 16W10, 16N16.

Keywords: Prime Γ -ring, semiprime Γ -ring, derivation, dependent element free action.

Introduction

The notion of a Γ -ring was introduced by Nobusawa (1964) and generalized by Barnes (1966) as follows: Let M and Γ be two additive abelian groups. If for all $x, y, z \in M$ and $\alpha, \beta \in \Gamma$, the following conditions are satisfied

- (1) $x\alpha y \in M$,
- (2) $(x + y)\alpha z = x\alpha z + y\alpha z$,
- $x(\alpha + \beta)y = x\alpha y + x\beta y$,
- $x\alpha(y + z) = x\alpha y + x\alpha z$,

(3) $(x\alpha y)\beta z = x\alpha(y\beta z)$,

then M is called a Γ -ring (in the sense of Barnes, 1966). If these conditions are strengthened to

(1') $x\alpha y \in M$, and $\alpha\beta \in \Gamma$,

(2') same as (2),

(3') $(x\alpha y)\beta z = x(\alpha y\beta)z = x\alpha(y\beta z)$,

(4') $x\alpha y = 0$ for all $x, y \in M$ implies $\alpha = 0$,

we then have M a Γ -ring in the sense of Nobusawa (1964). We may note that it follows from (1) \rightarrow (3) that $0\alpha x = x0y = 0\alpha x = 0$, for all $x, y \in M$ and $\alpha \in \Gamma$.

Recall that a Γ -ring M is called a prime if for any two elements $x, y \in M$, $x\Gamma M\Gamma y = 0$ implies either $x = 0$ or $y = 0$, and M is called semiprime if $x\Gamma M\Gamma x = 0$ with $x \in M$ implies $x = 0$. Note that every prime Γ -ring is obviously semiprime. An additive mapping $d: M \rightarrow M$ is called a derivation if $d(x\alpha y) =$

$d(x)\alpha y + x\alpha d(y)$ for all $x, y \in M$ and $\alpha \in \Gamma$. An additive subgroup U of M is called a left (right) ideal of M if $M\Gamma U \subseteq U$ ($U\Gamma M \subseteq U$). If U is both left and right ideal of M , then we say U is an ideal of M . An ideal of M is said to be essential if it has non zero intersection with any non zero ideal of M . For a subset U of M , $\text{Ann}_l(U) = \{a \in M | a\Gamma U = \langle 0 \rangle\}$ is called the left annihilator of U . A right annihilator $\text{Ann}_r(U)$ can be defined similarly. It is known that the right and left annihilators of an ideal U of a semiprime Γ -ring M coincide, it will be denoted by $\text{Ann}(U)$ (Ztürk and Yazarli, 2007). It is easy to show that $U \cap \text{Ann}(U) = \{0\}$ and $U \oplus \text{Ann}(U)$ is an essential of the Γ -ring M . Following (Pual and Sabur, 2010) an element x of M is called nilpotent if for some $\gamma \in \Gamma$, there exists a positive integer $n = n(\gamma)$ such that $(x\gamma)^n x = 0$ and an ideal U of a Γ -ring M is called nilpotent if $(U\Gamma)^n U = 0$, where n is the least positive integer. Furthermore, M is said to be a commutative Γ -ring if $x\alpha y = y\alpha x$ for all $x, y \in M$ and $\alpha \in \Gamma$. The set $Z(M) = \{x \in M; x\alpha y = y\alpha x \text{ for all } x, y \in M \text{ and } \alpha \in \Gamma\}$ is called the center of M . The commutator $x\alpha y - y\alpha x$ will be denoted by $[x, y]_\alpha$. We will use for all $x, y, z \in M$ and $\alpha, \beta \in \Gamma$, the basic commutator identities:

$$[x\alpha y, z]_\beta = x\alpha[y, z]_\beta + [x, z]_\beta\alpha y + x[\alpha, \beta]_z y, \text{ and}$$
$$[x, y\alpha z]_\beta = y\alpha[x, z]_\beta + [x, y]_\beta\alpha z + y[\beta, \alpha]_x z,$$

*Corresponding author email: vananesh@gmail.com

Throughout this paper, consider the following assumption $x\alpha y\beta z = x\beta y\alpha z$, for all $x, y, z \in M$ and $\alpha, \beta \in \Gamma$ and it will be represented by (*). According to the assumption (*), the above two identities reduce to $[x\alpha y, z]_\beta = x\alpha[y, z]_\beta + [x, z]_\beta\alpha y$, and $[x, y\alpha z]_\beta = y\alpha[x, z]_\beta + [x, y]_\beta\alpha z$.

Laradji and Thaheem in (Laradji and Thaheem, 1998) defined the dependent element of a mapping f as follows: An element $a \in R$ is said to be a dependent element of a mapping $f: R \rightarrow R$ if $f(x)a = ax$ for all $x \in R$,

They studied the dependent elements of endomorphisms of semiprime rings and Vukman and Kosi-Ulbl in (Vukman and Kosi-Ulbl, 2004) studied dependent elements of various mappings related to derivations, automorphisms and generalized derivations on prime and semiprime rings. Several other authors have studied dependent elements in prime and semiprime rings (Faisal and Muhammad, 2009; Muhammad and Mohammad, 2008a; Hentzel *et al.*, 2011; Mohammad, and Muhammad, 2008b). Furthermore, a mapping $f: R \rightarrow R$ is said to be a free action on M if zero is the only dependent element of f .

In this paper analogous in (Laradji and Thaheem, 1998) we define a dependent element of a mapping f on a semiprime Γ -rings M as follows: An element $a \in M$ is said to be dependent element of a mapping $f: M \rightarrow M$ if $f(x)\alpha a = a\alpha x$ for all $x \in M$ and $\alpha \in \Gamma$. A mapping $f: M \rightarrow M$ is said to be free action on M if the only dependent element of f is zero. We investigate some properties and give some results of free action for mappings related to derivations on prime and semiprime Γ -rings M . For a mapping $f: M \rightarrow M$, $D(f)$ denotes the collection of all dependent elements of f .

1. Dependent elements on derivations

For proving the main results, we start by the following theorem:

Theorem 2.1. Let M be a semiprime Γ -ring satisfying (*) and $d: M \rightarrow M$ be a derivation of M . If $a \in D(d)$, then $a \in Z(M)$.

Proof. Suppose that $a \in D(d)$, that is $d(x)\alpha a = a\alpha x$, for all $x \in M$ and $\alpha \in \Gamma$. (2.1)

Replacing x by $x\gamma y$ in (2.1), we get

$$d(x)\gamma y\alpha a + x\gamma d(y)\alpha a = a\alpha x\gamma y, \text{ for all } x, y \in M \text{ and } \alpha, \gamma \in \Gamma. \quad (2.2)$$

Using (2.1) we get

$$d(x)\gamma y\alpha a = [a, x]_\alpha \gamma y, \text{ for all } x, y \in M \text{ and } \alpha, \gamma \in \Gamma. \quad (2.3)$$

Hence we obtain

$$d(x)\gamma y\alpha a\beta z = [a, x]_\alpha \gamma y\beta z, \text{ for all } x, y, z \in M \text{ and } \alpha, \beta, \gamma \in \Gamma. \quad (2.4)$$

Replacing y by $y\beta z$ in (2.3), we obtain

$$d(x)\gamma y\beta z\alpha a = [a, x]_\alpha \gamma y\beta z, \text{ for all } x, y, z \in M \text{ and } \alpha, \beta, \gamma \in \Gamma. \quad (2.5)$$

Subtracting (2.5) from (2.4), we have

$$d(x)\gamma y\beta[a, z]_\alpha = 0, \text{ for all } x, y, z \in M \text{ and } \alpha, \beta, \gamma \in \Gamma.$$

Replacing y by $a\delta y$ and using (2.1), we obtain

$$a\gamma x\delta y\beta[a, z]_\alpha = 0, \text{ for all } x, y, z \in M \text{ and } \alpha, \beta, \gamma, \delta \in \Gamma. \quad (2.6)$$

Hence we obtain

$$z\alpha a\gamma x\delta y\beta[a, z]_\alpha = 0, \text{ for all } x, y, z \in M \text{ and } \alpha, \beta, \gamma, \delta \in \Gamma. \quad (2.7)$$

Replacing x by $z\alpha x$ in (2.6), we get

$$a\gamma z\alpha x\delta y\beta[a, z]_\alpha = 0, \text{ for all } x, y, z \in M \text{ and } \alpha, \beta, \gamma, \delta \in \Gamma. \quad (2.8)$$

Subtracting (2.7) from (2.8), we obtain

$$[a, z]_\alpha \gamma x\delta y\beta[a, z]_\alpha = 0, \text{ for all } x, y, z \in M \text{ and } \alpha, \beta, \gamma, \delta \in \Gamma. \quad (2.9)$$

Hence we obtain $[a, z]_\alpha \gamma x\delta y\beta[a, z]_\alpha \gamma x = 0$, for all $x, y, z \in M$ and $\alpha, \beta, \gamma, \delta \in \Gamma$. By semiprimeness we have $[a, z]_\alpha = 0$, for all $z \in M$ and $\alpha \in \Gamma$. Hence $a \in Z(M)$.

Corollary 2.2. Let M be a semiprime Γ -ring satisfying (*) and $d: M \rightarrow M$ be a derivation on M . If $a \in D(d)$, then $d(x)\alpha a = 0$.

Proof. Let $a \in D(d)$, by Theorem 2.1 $a \in Z(M)$, that is $d(x)\alpha a = a\alpha x = x\alpha a$, for all $x \in M$ and $\alpha \in \Gamma$.

Replacing x by $x\beta y$, we get

$$\begin{aligned} x\beta y\alpha a &= d(x)\beta y\alpha a + x\beta d(y)\alpha a \\ &= d(x)\beta a\gamma y + x\beta d(y)\alpha a = d(x)\beta a\gamma y + x\beta a\gamma y, \text{ for all } x, y \in M \text{ and } \alpha, \beta, \gamma \in \Gamma. \end{aligned}$$

Being $a \in Z(M)$ the last relation implies that $d(x)\beta a\alpha y = 0$. By semiprimeness we get $d(x)\alpha a = 0$, for all $x \in M$ and $\alpha \in \Gamma$.

Corollary 2.3. Let M be a semiprime Γ -ring satisfying $(*)$ and $d: M \rightarrow M$ be a derivation on M . If $a \in D(d)$ then $d(a) = 0$.

Proof. Since $a \in D(d)$, by corollary 2.2 we get

$$\begin{aligned} d(x)\alpha a &= 0, \text{ for all } x \in M \\ \text{and } \alpha \in \Gamma. \end{aligned} \quad (2.10)$$

Replacing x by $d(x)$ in (2.10) we get

$$\begin{aligned} d(d(x))\alpha a &= 0, \text{ for all } x \in M \\ \text{and } \alpha \in \Gamma. \end{aligned} \quad (2.11)$$

From (2.10), we obtain $d(d(x))\alpha a = d(0) = 0$, which implies $d(d(x))\alpha a + d(x)\alpha d(a) = 0$, for all $x \in M$ and $\alpha \in \Gamma$. Using (2.11), we get $d(x)\alpha d(a) = 0$, for all $x \in M$ and $\alpha \in \Gamma$. Replacing x by $a\beta x$, we have $d(a)\beta x\alpha d(a) = 0$, for all $x \in M$ and $\alpha, \beta \in \Gamma$. By semiprimeness we get $d(a) = 0$.

Remark 2.4. Let M be a semiprime Γ -ring and U be a right ideal of M , then U is a semiprime subring of M and $Z(U) \subseteq Z(M)$.

Now we prove the main result in this section.

Theorem 2.5. Let M be a semiprime Γ -ring satisfying $(*)$ and $d: M \rightarrow M$ be a derivation on M . Let a be a dependent element of d . Then there exist ideals U and V of M such that

- (i) $U \oplus V$ is an essential ideal of M .
- (ii) $d = 0$ on U and $d(V) \subseteq V$.
- (iii) $D(d|_V) = \{0\}$, where $d|_V$ is restriction of d on V .

That is d free action on V .

Proof. (i) Since $a \in D(d)$, by Theorem 2.1 we have $a \in Z(M)$. Therefore

$a\alpha m = m\alpha a$, for all $m \in M$ and $\alpha \in \Gamma$,
that is $a\Gamma M = M\Gamma a$, and this implies $a\Gamma M$ is a two sided ideal of M .

Put $U = a\Gamma M$ and $V = \text{Ann}(U)$. Since $\text{Ann}(U)$ is an ideal of M , then V is an ideal of M , and $U \oplus V$ is essential of M .

(ii) By Corollary 2.2, Corollary 2.3 and Theorem 2.1 we have $d(x)\alpha a = 0$, $d(a) = 0$, and $a \in Z(M)$, for all $x \in M$, $\alpha \in \Gamma$. Thus $d(a\alpha x) = d(a)\alpha x + a\alpha d(x) = d(a)\alpha x + d(x)\alpha a = 0$, for all $x \in M$, $\alpha \in \Gamma$.

$d(x\alpha a) = d(x)\alpha a + x\alpha d(a) = 0$, and $d(x\alpha a\beta y) = d(x)\alpha a\beta y + x\alpha d(a)\beta y + x\alpha a\beta d(y) = x\alpha d(y)\beta a = 0$, for all $x, y \in M$, $\alpha, \beta \in \Gamma$. Hence $d = 0$ on U .

Now let $d(v) \in d(V)$, for $v \in V = \text{Ann}(U)$, thus $v\alpha a = 0$, for all $a \in U$. So $d(v\alpha a) = d(0) = 0$, and $v\alpha d(a) = 0$, since $a \in U$, and $d = 0$ on U . Then $d(v\alpha a) = d(v)\alpha a + v\alpha d(a)$, this implies that $d(v)\alpha a = 0$, that is $d(v) \in \text{Ann}(U) = V$.

(iii) Since V is an ideal of M , by Remark 2.4 we have $Z(V) \subseteq Z(M)$. Since $d(V) \subseteq V$ so $d|_V$ is a derivation on V . Now let $a \in V$ be a dependent element of $d|_V$ on V , then by Theorem 2.1 we have $a \in Z(V)$, and by Remark 2.4 we have $Z(V) \subseteq Z(M)$, that is $a \in Z(M)$. By Corollary 2.2 and Corollary 2.3 we have $d|_V(v)\alpha a = 0 = a\alpha d|_V(v)$ and $d|_V(a) = 0$.

Let $x \in M$, so $x\beta v \in V$. Thus $d(x\beta v)\alpha a = 0$, but $d(x\beta v)\alpha a = d(x)\beta v\alpha a + x\beta d(v)\alpha a$, this implies that $d(x)\beta v\alpha a = 0$.

Since $a \in Z(V)$, so $d(x)\beta a\alpha v = 0$, for all $x \in M$, $v \in V$ and $\alpha, \beta \in \Gamma$. By semiprimeness of V we get $d(x)\alpha a = 0$, and by definition we obtain $a\alpha x = 0$, for all $x \in M$ and $\alpha \in \Gamma$, then by semiprime of M we get $a = 0$. Hence $D(d|_V) = \{0\}$ on V .

2. Free actions of prime and semiprime Γ -rings

In this section we discuss free action for mappings related to derivations and we obtain some results. We start by the following lemma:

Lemma 3.1 (Chakraborty and Paul, 2010. Lemma 2.13). Let M be a 2-torsion free semiprime Γ -ring and suppose that $a, b \in M$. If $a\Gamma m\Gamma b + b\Gamma m\Gamma a = 0$ for all $m \in M$, then $a\Gamma m\Gamma b = b\Gamma m\Gamma a = 0$.

Theorem 3.2 (Pual and Sabur, 2010. Theorem 3.1). Let M be a prime Γ -ring and $U \neq 0$ be a right ideal of M . Suppose that $a \in U$, $(ay)^n a = 0$ for a fixed integer n , then M has non-zero nilpotent ideal.

Remark 3.3. Let M be a Γ -ring. If a is nilpotent, then $M\Gamma a$ is a nilpotent ideal of M . In a semiprime Γ -ring M , if a is nilpotent, then $a = 0$.

Theorem 3.4. Let M be a semiprime Γ -ring satisfying $(*)$ and $d: M \rightarrow M$ be a derivation. Then $\Phi: M \rightarrow M$ defined as $\Phi(x) = x\beta d(x)$ for all $x \in M$ and $\beta \in \Gamma$ is free action.

Proof: Suppose that $a \in D(\Phi)$, that is

$$\begin{aligned} \Phi(x)\alpha a &= a\alpha x \text{ for all } x \in M \\ \text{and } \alpha &\in \Gamma. \end{aligned} \quad (3.1)$$

Equivalently

$$\begin{aligned} x\beta d(x)\alpha a &= a\alpha x, \text{ for all } x \in M \\ \text{and } \alpha, \beta &\in \Gamma. \end{aligned} \quad (3.2)$$

Linearizing (3.2) with respect x we get

$$\begin{aligned} x\beta d(y)\alpha a + y\beta d(x)\alpha a &= 0, \text{ for all } x, y \in M \\ \text{and } \alpha, \beta &\in \Gamma. \end{aligned} \quad (3.3)$$

Replacing x and y by a , we obtain $2a\beta d(a)\alpha a = 0$, this implies that

$$\begin{aligned} 2a\alpha a &= 0, \text{ for all } x \in M \\ \text{and } \alpha &\in \Gamma. \end{aligned} \quad (3.4)$$

Replacing y by $x\alpha a$ in (3.3) we get

$$x\beta d(x)\alpha a a + x\beta x\alpha d(a)\alpha a + x\alpha a\beta d(x)\alpha a = 0, \text{ for all } x \in M \text{ and } \alpha \in \Gamma.$$

By using (3.2) we get

$$a\alpha x\alpha a + x\beta x\alpha d(a)\alpha a + x\alpha a\beta d(x)\alpha a = 0.$$

Replacing x by a we obtain $a\alpha a\alpha a + 2a\alpha a\beta d(a)\alpha a = 0$. By using (3.4) we get $a\alpha a\alpha a = 0$, since M is semiprime Γ -ring, then by Remark 3.3 we get $a = 0$.

Theorem 3.5. Let M be a 2-torsion free semiprime Γ -ring and $d: M \rightarrow M$ be a derivation. Then a mapping $\Phi: M \rightarrow M$ defined as $\Phi(x) = x\alpha d(x) + d(x)\alpha x$ for all $x \in M$ and a fixed $\alpha \in \Gamma$ is free action.

Proof: Suppose that $a \in D(\Phi)$, that is $\Phi(x)\alpha a = a\alpha x$ for all $x \in M$ and $\alpha \in \Gamma$, equivalently $x\alpha d(x) + d(x)\alpha x\}\alpha a = a\alpha x$, for all $x \in M$ and $\alpha \in \Gamma$. $\quad (3.5)$

Linearizing (3.5) with respect x we get

$$x\alpha d(y)\alpha a + y\alpha d(x)\alpha a + d(x)\alpha y\alpha a + d(y)\alpha x\alpha a = 0, \text{ for all } x, y \in M \text{ and } \alpha \in \Gamma. \quad (3.6)$$

Replacing x and y by a , and using (3.5) we obtain $2a\alpha a = 0$. $\quad (3.7)$

Since M is 2-torsion free semiprime Γ -ring, by Remark 3.3 we get $a = 0$.

Theorem 3.5. Let M be a prime Γ -ring satisfying $(*)$ and d, g and h be nonzero derivations of M . Then the mapping $\Phi: M \rightarrow M$ defined as $\Phi(x) = d(g(x)) + h(x)$ for all $x \in M$ is free action.

Proof: Suppose that $a \in D(\Phi)$, that is

$$\begin{aligned} \Phi(x)\alpha a &= a\alpha x \text{ for all } x \in M \\ \text{and } \alpha &\in \Gamma. \end{aligned} \quad (3.8)$$

Equivalently

$$\begin{aligned} (d(g(x)) + h(x))\alpha a &= a\alpha x. \\ \text{Replacing } x \text{ by } x\beta a \text{ we get} \\ (d(g(x\beta a)) + h(x\beta a))\alpha a &= a\alpha x\beta a. \end{aligned}$$

This implies that

$$\Phi(x)\beta a\alpha a + x\beta\Phi(a)\alpha a + g(x)\beta d(a)\alpha a + d(x)\beta g(a)\alpha a = a\alpha x\beta a.$$

By using (3.8) we obtain

$$x\beta a\alpha a + g(x)\beta d(a)\alpha a + d(x)\beta g(a)\alpha a = 0 \quad (3.9)$$

Replacing x by $y\gamma x$ and using (3.9) we obtain $g(y)\gamma x\beta d(a)\alpha a + d(y)\gamma x\beta g(a)\alpha a = 0$, for all $x, y \in M$ and $\alpha, \beta, \gamma \in \Gamma$. $\quad (3.10)$

Replacing y by a and x by $a\alpha x$ we obtain

$$g(a)\gamma a\alpha x\beta d(a)\alpha a + d(a)\gamma a\alpha x\beta g(a)\alpha a = 0, \text{ for all } x, y \in M \text{ and } \alpha, \beta, \gamma \in \Gamma.$$

By using Lemma 3.1 we conclude that $d(a)\gamma a\alpha x\beta g(a)\alpha a = 0$, and by the primeness of M , either $d(a)\alpha a = 0$ or $g(a)\alpha a = 0$.

If both are zero we get from (3.9) that is $x\beta a\alpha a = 0$ and by primeness we get $a\alpha a = 0$, then by Remark 3.3, $a = 0$.

If $d(a)\alpha a = 0$ and $g(a)\alpha a \neq 0$, then the relation (3.10) yields $d(y)\gamma x\beta g(a)\alpha a = 0$. By primeness and relation (3.9) $a = 0$.

If $g(a)\alpha a = 0$ and $d(a)\alpha a \neq 0$, the relation (3.10) yields $g(y)\gamma x\beta d(a)\alpha a = 0$, and by primeness and

relation (3.9), $a = 0$. So for any case we get $a = 0$, this implies that Φ is free action.

REFERENCES

Barnes, W. 1966. On the 5-Rings of Nobusawa. *Pacific J. Math.* 18(3):411-422.

Chakraborty, S. and Paul, AC. 2010. On Jordan Generalized k-Derivations of Semiprime Γ_N - Rings. *Bulletin of the Iranian Math. Soc.* 36(1):41-53.

Faisal, Al. and Muhammad, CH. 2009. Dependent Elements of Derivations on Semiprime Rings. *IJMMS*. :1-6.

Hentzel, L., Daif, MU., Tammam, EL. and Haetinger, CL. 2011. On Free Actions and Dependent Elements in Rings. *Algebra and its Applications*. 69-84.

Laradji, A. and Thaheem, AB. 1998. On Dependent Elements in Semiprime Rings. *Math. Japon.* 47(1):29-31.

Mohammad, SA. and Muhammad, CH^a. 2008. Dependent Elements of Left Centralizers of Semi-prime Rings. *The Arabian J for Science and Engineering*. 33(2A):313-319.

Muhammad, CH and Mohammad, SA. 2008^b. Free Action on Semiprime Rings. *Mathematica Bohemica*. 2 (133):197-208.

Nobusawa, N. 1964. On a Generlazetion of the Ring Theory. *Osaka J. Math.* 1:81-89.

Pual, A. and Sabur, M. 2010. Lie and Jordan Structure in Simple Gamma Rings. *J. of Physical Science*. 14:77-86.

Vukman, JO. and Kosi-Ulbl, IR. 2004. On Dependent Elements in Rings. *IJMMS*. 54:2895-2906.

Ztürk, MA and Yazarli, HA. 2007. Modules over the Generalized Centroid of Semiprime Gamma Rings. *Bull. Korean Math. Soc.* 44 (2):203-213.

Received: Dec 21, 2011; Accepted: April 18, 2012

Short communication

SHALLOW RESISTIVITY SURVEY FOR PROTECTION OF SUBMERGED FUEL TANKS FROM EXTERNAL CORROSION IN A COASTAL ENVIRONMENT, SOUTHEASTERN, NIGERIA

*Okiwel AA¹, Evans UF², Ekanem CH³ and Etim VB²

¹Department of Physics, University of Calabar

²Department of Science, Maritime Academy of Nigeria, Oron

³Department of Physics, Akwa Ibom State College of Education, Afaha Nsit, Nigeria

ABSTRACT

Geoelectrical resistivity soundings employing Schlumberger electrodes array was used to measure resistivity distributions of geomaterials in four fuel stations located in coastal environment within the Nigerian sector of the Niger Delta basin. The aim is to find alternative solution for the mitigation of external corrosion of buried storage fuel tanks. A maximum current electrodes spacing of 40m was used for the investigations. An average depth of 10m was penetrated by the current. Analyses of results show that the storage tank (station A) is within non-corrosive environment. The tank may eventually suffer corrosion attack due to the 132kV electrical power lines which is in close proximity to the fuel station. The other tanks (B, C, and D) are within corrosive environments but the tank at station C is at a higher corrosion risk. This is because of the presence of conductive clay in the area. Based on the low resistivity, sites for planting of protective anodes have been delineated to protect the storage tanks from external corrosion.

Keywords: Shallow, protection, submerged tanks, corrosion, environment.

INTRODUCTION

External corrosion of buried metallic structures such as storage tanks has been one of the most challenging tasks of the petroleum product marketers in Nigeria. Generally, subsurface geologic materials show variation in the concentration of electrolyte (groundwater and dissolved salt). These differences result in vertical and lateral variations in resistivities of the subsurface rocks. Subsurface resistivity variations have direct link with the corrosion potential of the subsurface which also varies laterally and vertically (SESCO, 2002). There is therefore, the need to study the corrosion behaviour of metals when exposed to various environments (Osarolube *et al.*, 2008). Submerged materials are at risk of forming anodic and cathodic regions with the electrolyte (corrosion cell) as they traverse geologic materials of different resistivities. The risk increases as the anodic area becomes relatively small with respect to the cathodic area (Stefler, 1980). It had been shown that the anodic area is developed within soil of low resistivity which normally accelerates the flow of electric current from the buried structure to the surrounding including the cathodic area of the structure; since current flow through the path of least resistance (USDD, 2004 and FHWA, 2000). Submerged structure that receives current becomes protected, while a structure that releases current tends to be sacrificed.

Attempt to protect materials from external corrosion had been by surface coating (painting or electroplating). The main idea of coating is to isolate the material from its environment (electrolyte), thereby maintaining an open circuit in the corrosion cell, which inhibits corrosion process. However, it had been shown that with the existence of holidays [coating defect] (Lilly *et al.*, 2007) there is no amount of coating that can guarantee total protection of a buried structure (Sheir, 1993 and Bird, 2001). This explains why the over dependence of Nigerian petroleum product marketers on surface coating as an ultimate means of external corrosion protection often fails. Such failure results in loss of assets and pollution of the environment including aquifers and other environmental disaster (Alawode and Ogunleye, 2011). A standard practice recommended by Zdunrk and Barlo (1992), Lisk (1992), NACE (2003), Khan (2002) and Wansah *et al.* (2008) has been supplementing surface coating with cathodic protection system. The first class information necessary for the design of a cathodic protection system is soil resistivity, which can be measured *on-line* or *off-line*. The on-line measurements require geoelectrical resistivity measurement, while the off-line involves laboratory analysis of soil samples. This study adopted the “online” (geoelectrical resistivity technique) to measure soil resistivity values near selected fuel stations in a coastal area, Uyo (Fig.1), Southeastern,

*Corresponding author email: okiwelu2000@yahoo.com

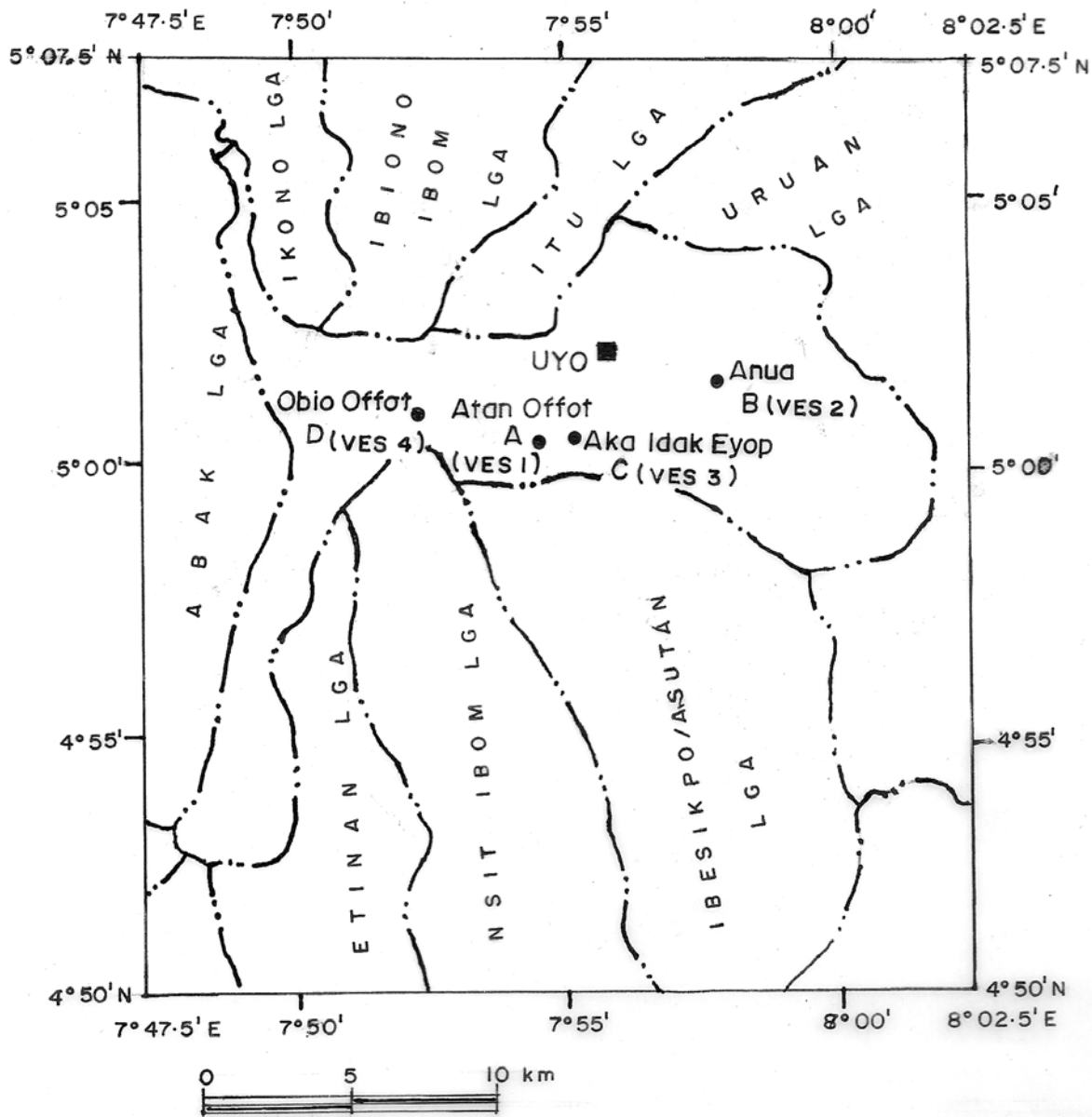


Fig. 1. Location map of the study area showing location of the tanks (A, B, C, D) and VES sounding locations at Uyo and Environs.

Nigeria in view of finding a lasting solution to underground fuel storage tank leakages. Geoelectrical resistivity soundings method have been found to be very useful for the investigation of soil corrosion of pipeline (Ekine and Emujakporue, 2010).

The study area is located in Southeastern Nigeria within Latitude $5^{\circ} 01'$ N- $5^{\circ} 05'$ N and longitude $7^{\circ} 45'$ E - $7^{\circ} 75'$ E. The tanks are located in Uyo (Fig.1) within the Niger Delta basin, Southeastern, Nigeria. The area is typical of the Niger Delta undulating plains with extensive near

shore sands of various grain sizes. The thickness of this sand increases towards the depocentre. The area is also noted for seasonal variation of rainfall. Monthly rainfall data shows that the average rainfall during the dry season is 65mm against 382mm during the rainy season. Previous study of the meteorology of the area reveals the air temperature to be 25.5°C in the rainy season and 30.1°C in the dry season (Gobo, 1998). The daily relative humidity ranges from 75% in the dry season to 96% in the rainy season.

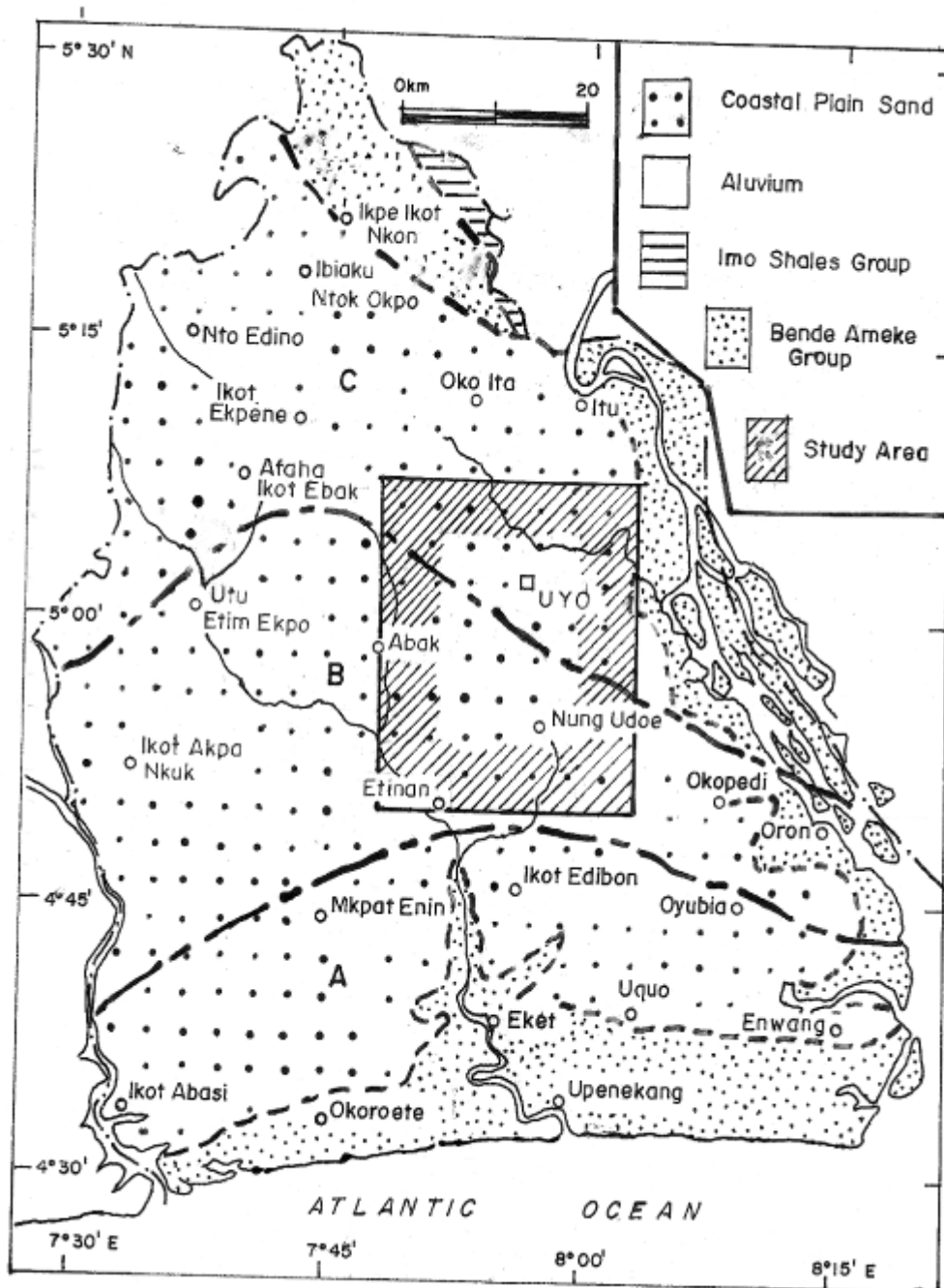


Fig. 2. Geologic map of Akwa Ibom State showing the study area.

The study area falls within the coastal plain sands of the deltaic depositional environment of the Niger Delta (Hospers, 1971; Onyeagocha, 1980; Kogbe and Buriollet, 1990) (see Fig. 2). The Benin Formation is the uppermost unit of the Niger Deltaic lithofacies and has clastic sedimentary rocks formed either as terrestrial or marine deposits (Reyment, 1965; Fetter, 1980). The sediments are predominantly sandy with minor shale intercalations. Onyeagocha (1980) describes the Benin Formation as a continental depositional environment having massive,

poorly sorted sands and sandstones with thin shales, clay, and gravel which grades downwards into the delta front Agbada lithofacies.

MATERIALS AND METHODS

The ABEM terrameter (model SAS 300) and its accessories arranged in the Schlumberger array were used for obtaining the vertical electrical sounding resistivity data over the four fuel tanks. The geometric array for this

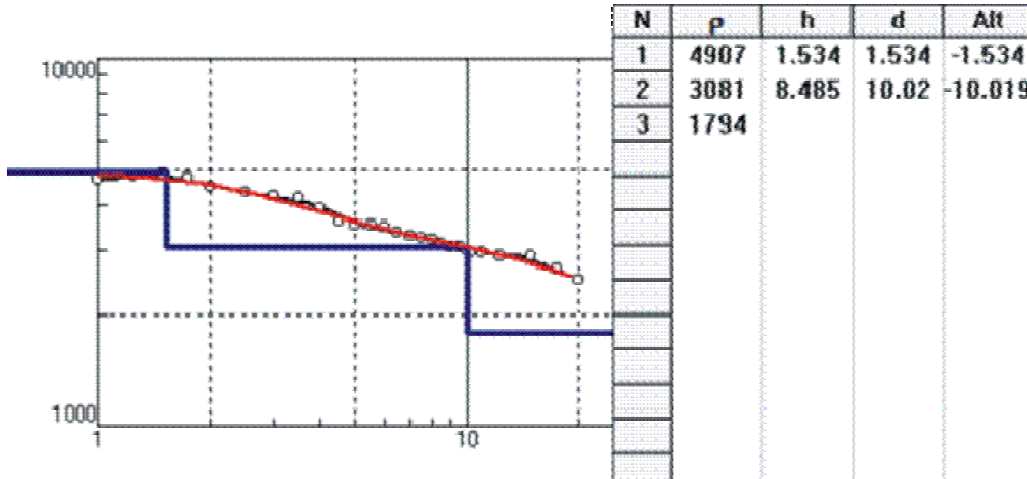


Fig. 3. Modelled VES curves at location A.

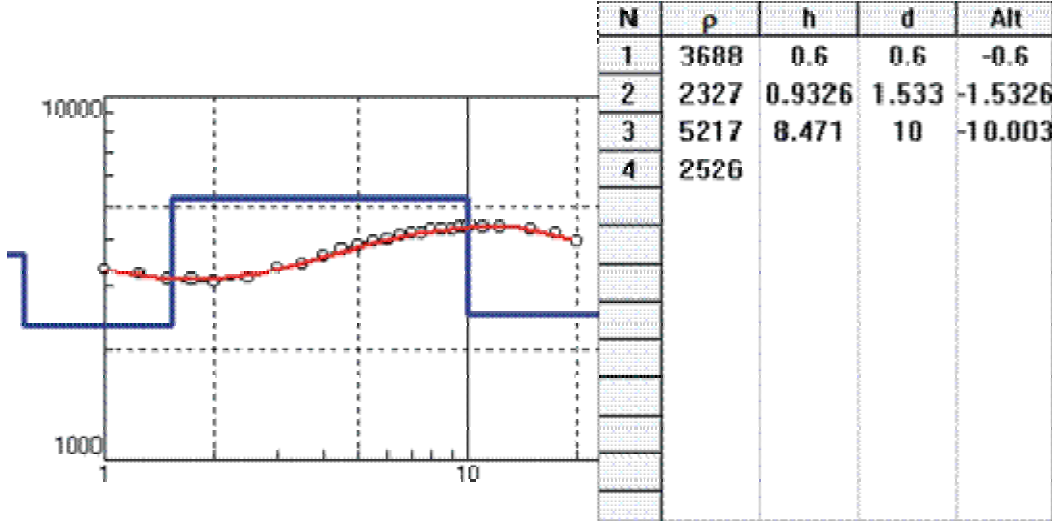


Fig. 4. Modelled VES curves at location B.

study is compatible to the software for the quantitative interpretation of field data. Hence, the conventional electrodes spacing used for vertical electrical sounding with Schlumberger array applied in groundwater investigations were modified so that it will be amenable to this study. This was necessary due to the shallow depth of burial and size (6.0m) of the buried fuel tanks. Thus, a maximum current electrodes separation of 40m was used for the study. A traverse of 5m away from the buried metallic structure and perpendicular to the structure was adopted to ensure that the structure does not contribute to the measured resistance. The K-factor for Schlumberger array enabled the calculation of the apparent resistivity from the measured resistances. For the purpose of quantitative interpretations, the apparent resistivity which is a function of current electrode spacing was modeled using IPI2win (computer software). The input parameters

for the modelling were apparent resistivity values, half the current electrodes spacing as well as the potential electrodes spacing. The software at first instance performed the forward modeling and the results were used for the inverse modeling which yielded the final parameters.

RESULTS AND DISCUSSION

The results of the inverse modeling indicate variation of earth resistivity with depth (Figs. 3-6). Geoelectrical layer parameters obtained from the models are presented in table 1. These resistivity values were correlated with the ANSI/AWWA (American National Standard Institute and American water works Association C-105) standard rating for soil corrosivity (Table 2) in order to infer the corrosivity at various stations. Results suggest that tank

Table 1. Summary of VES modelled data.

Station	ρ_1	ρ_2	ρ_3	ρ_4	h_1	h_2	h_3	d_1	d_2	d_3
A	4907	3081	1784	-	1.534	8.405	-	1.5	10.02	-
B	3688	2327	5217	2526	0.6	0.932	8.471	0.6	1.53	10
C	336	168.3	43.77	58.38	0.574	1.229	4.584	0.574	1.803	6.384
D	7186	7973	2222	29468	0.6	0.9326	8.471	0.6	1.533	10

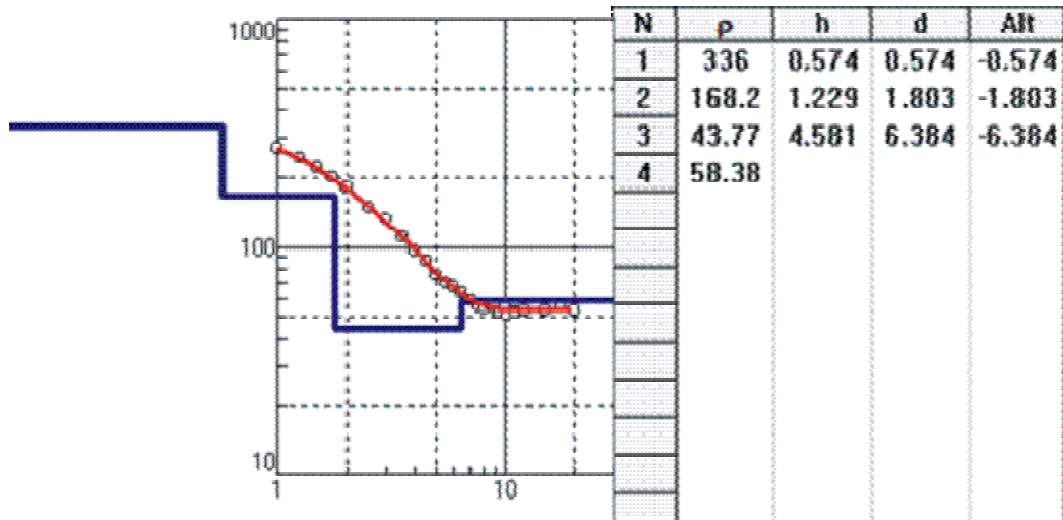


Fig. 5. Modelled VES curves at location C.

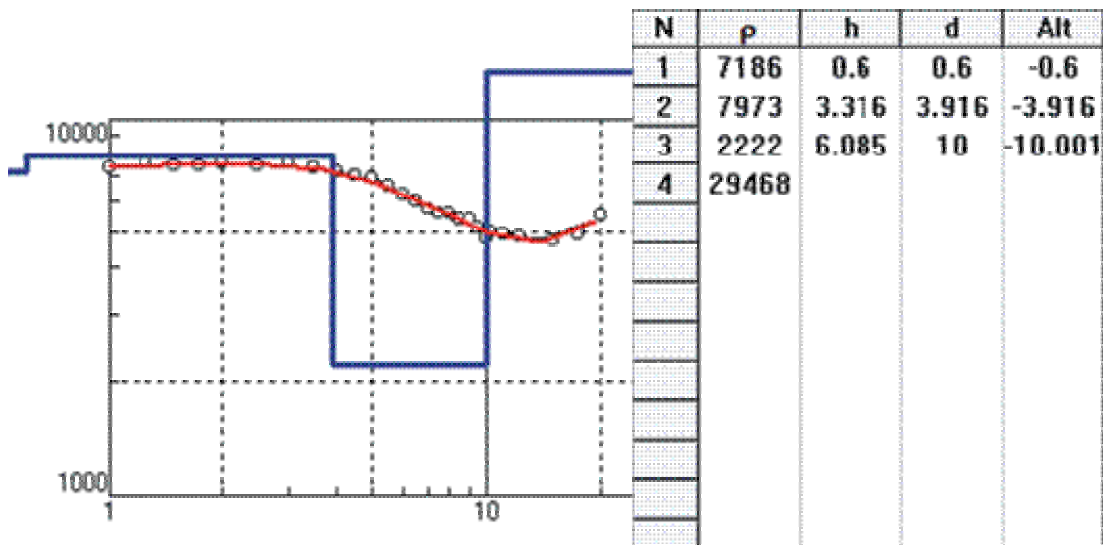


Fig. 6 Modelled VES curves at location D.

"A" is within high resistive ($1784\text{-}4907\Omega\text{m}$) earth materials which indicate non corrosive materials. The local geology at location "A" obtained from borehole log (Fig.7) shows medium grained sand as the host of the buried tank. Resistivity values obtained for locations "B" and "D" are ($2526\text{-}5217 \Omega\text{m}$) and ($2222\text{-}29468 \Omega\text{m}$)

respectively. However, at station "D" there is evidence of gravel deposit from the borehole log. The VES result at station C showed low resistivity ($43.77\text{-}336\Omega\text{m}$). The lithology log at this site reveals the presence of conducting clay; hence, the subsurface environment is described as being highly corrosive.

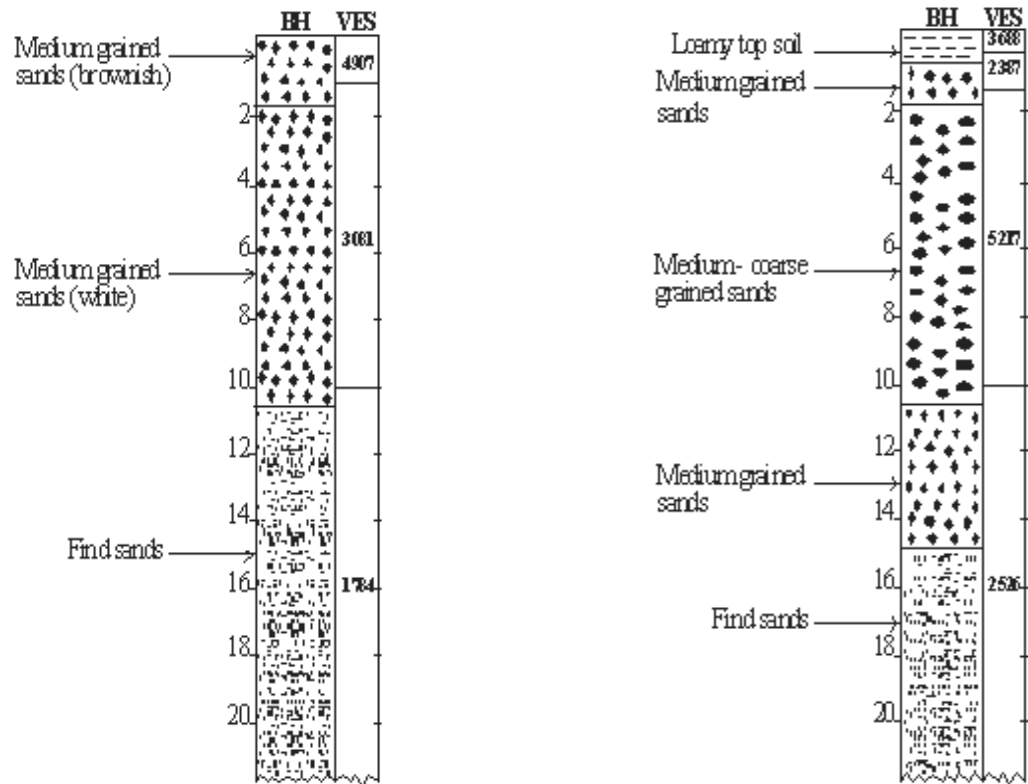


Fig. 7. Correlation of VES with borehole lithology log at location A.

Fig. 8. Correlation of VES with borehole lithology log at location B.

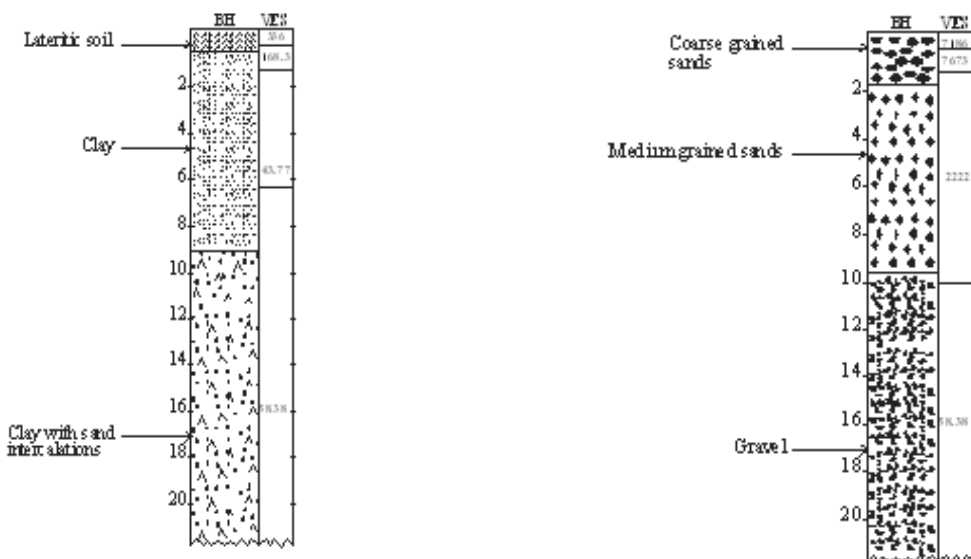


Fig. 9. Correlation of VES with borehole lithology log at location C.

Fig. 10. Correlation of VES with borehole lithology log at location D.

Table 2. Standard for soil corrosivity rating (ANSI/AWWA C-105).

$\rho(\Omega m)$	Corrosivity rating
>200	Essentially non-corrosive
100-200	Mildly corrosive
50-100	Moderately corrosive
30-50	Corrosive
10-30	Highly corrosive
<10	Extremely corrosive

Tank "A" may not be subjected to adverse subsurface conditions, since the resistivity range is not wide and the soil resistivity values are high. However, the tank could corrode due to stray current effect from 132KV power line in close proximity to the storage tank.

The subsurface corrosion at the submerged tank at site B is minor because the soil resistivity at shallow depth is not only high but of minor variation. This minor variation in resistivity makes the formation of cathodic and anodic part on the tank practically difficult.

Storage tank, D shows wide range variation in soil resistivity values with the least resistivity ($2222\Omega m$) at 1.533m depth. The segments of the tank exposed to the soil at this depth are anodic in the electrochemical circuit set up within the subsurface. Based on the principle of electrochemical corrosion, this tank segment will release electrons to protect adjacent segments of the tank exposed to high resistivity ($7186 - 29468\Omega m$) soil. Therefore, pitting type of corrosion may set in at depth with relatively low resistivity geologic materials. Correlations of VES results with the true subsurface conditions obtained from borehole lithology logs for the different locations of the storage tanks are presented in figures 7-10.

CONCLUSION

Geo-electrical resistivity method has been applied to solving environmental problem by providing primary information needed to protect submerged fuel tanks in the study area from external corrosion. From the combination of data obtained from VES modeled curves and borehole lithology log, the only fuel tank that may be free from severe external corrosion threat is the tank buried at location "B". The tank at location "A" is at risk bowing to the induced AC voltage from the 132kV high tension power line in the area. Tank at site "C" is exposed to highly corrosive environment; hence, the tank is under a severe threat. The wide range of resistivity at station "D" gives rise to external corrosion of the tank buried in the study area. A sacrificial anode cathodic protection system should be installed for fuel tank at sites A, C and D to mitigate external corrosion of the tanks and Soil

resistivity survey should always be carried out to identify potential corrosive geomaterials before establishing fuel stations. In addition, fuel tanks should not be buried close to stray current sources (such as high tensioned power lines).

REFERENCES

- Alawode, AJ. and Ogunleye, IO. 2011. Maintenance, Security and Environmental Implications of Pipeline Damage and Ruptures in the Niger Delta Region. Pacific Journal of Science and Technology. 12(1):565-573.
- Bird, AF. 2001. Corrosion Detection Interpretation and Repairs of Steel Pipelines. NACE International Conference Houston, Texas, USA.
- Ekine, AS. and Emujakporue, GO. 2010. Investigation of Corrosion of Buried Oil Pipeline by the Electrical Geophysical Methods. Journal of Applied Science and Environmental Management. 14 (1):63-65.
- Federal Highway Administration [FHWA]. 2000. Corrosion/ Degradation of Soil Reinforcements for Mechanically Stabilized Earth walls and Reinforced Soil Slopes. United States Department of Transport Publications.
- Fetters, CW. 1980. Applied Hydrology. Bell and Howell Company, Columbus, Ohio, USA. 224-421.
- Gobo, AE. 1998. Meteorology and Man's Environment. Ibadan: African-Link Books. 7:101-127.
- Hosper, J. 1971. Gravity field and the structure of the Niger Delta, Nigeria. Geological Society of America's Bulletin. 76:407-422.
- Khan, NA. 2002. Use of Electrical Resistivity Soil Corrosion Probes to Determine the Effectiveness of Cathodic Protection. NACE International Conference, Houston Paper No. 02104.
- Kogbe, CA. and Buriollet, PF. 1990. A Review of Continental Sediments in Africa. Journal of African Earth Sciences. 10:1-25.
- Lilly, MT., Ihekwoaba, SC., Ogaji, SOT. and Probert, SD. 2007. Prolonging the lives of Buried Crude-oil and Natural-gas Pipelines by Cathodic Protection. Applied energy. 84 (9):958-970.
- Lisk, I. 1992. The Use of Coatings and Polyethylene for Corrosion Protection. Water Online. American Water Works Association. 1-25.
- National Association of Corrosion Engineers Int. 2003. Cathodic Protection Training Manual. 6.1-6.10.
- Onyeagocha, AC. 1980. Petrography and Depositional Environment of the Benin Formation. Journal of Mining and Geology. 17 (2):147-151.

Osarolube, E., Owate, IO. and Oforka, NC. 2008. Corrosion Behaviour of Mild and High Carbon Steels in Various Acidic Media. *Scientific Research and Essay*. 3 (6):224-228.

Reyment, RA. 1965. Aspects of the Geology of Nigeria. Ibadan, University Press. 90-97.

Service Scolare (SESCO). 2002. Cathodic Protection Engineering. Tutorial Manual, Brook Park South Seminole Bartles Ville.

Sheir, LL. 1993. Corrosion Handbook. John Wiley and Sons, New York, USA. 345-401.

Stefler, FE. 1980. Accelerating Leak Rate in Ductile Cast Iron Water Mains Yields to Cathodic Protection. *Materials Performance*. 19 (10):10-15.

United State Department of Defense (USDD). 2004. Design: Electrical engineering: Cathodic protection Unified Facilities Criteria (UFC). 3:570-602.

Wansah, J., Obi, O., Osuji, R., Okeke, C. and Oparaku, O. 2008. Soil Resistivity Measurements for Pipeline Cathodic Protection Design. *Nigerian Journal of Solar Energy*. 19 (2):106-110.

Zdunrk, AD. and Barlo, TJ. 1992. Effect of Temperature on Cathodic Protection. Criteria Practical Manual. 31(11):22-27.

Received: Dec 26, 2011; Accepted: April 4, 2012